

Exploring the intraspecific variability of *Solanum lycopersicum* L. to identify potential tolerance traits to Ni and drought – the role of the antioxidant metabolism and detoxification strategies

Sofia Spormann

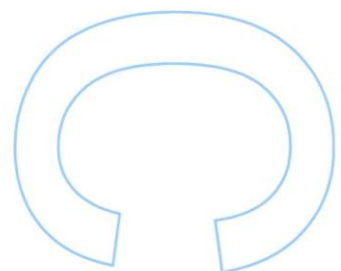
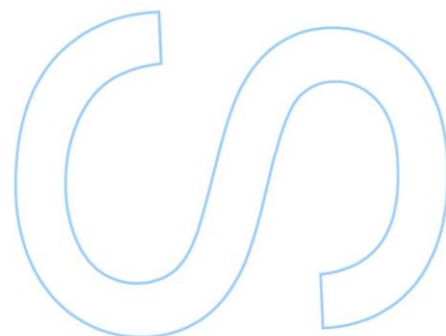
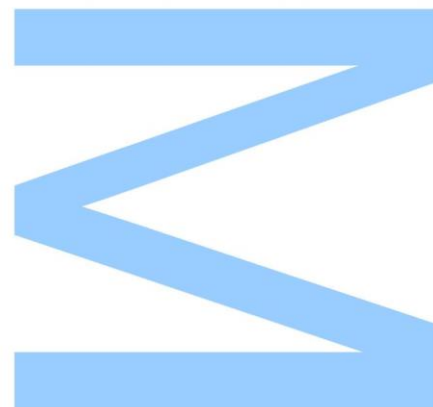
Mestrado em Biologia Funcional e Biotecnologia de Plantas
Departamento de Biologia
2020

Orientadora

Fernanda Fidalgo
Prof. Associada com Agregação, Faculdade de Ciências da Universidade do Porto

Coorientadora

Viviana Martins
Investigadora Júnior, Escola de Ciências da Universidade do Minho



Todas as correções determinadas pelo júri, e só essas, foram efetuadas.

O Presidente do Júri,

Porto, ____ / ____ / ____

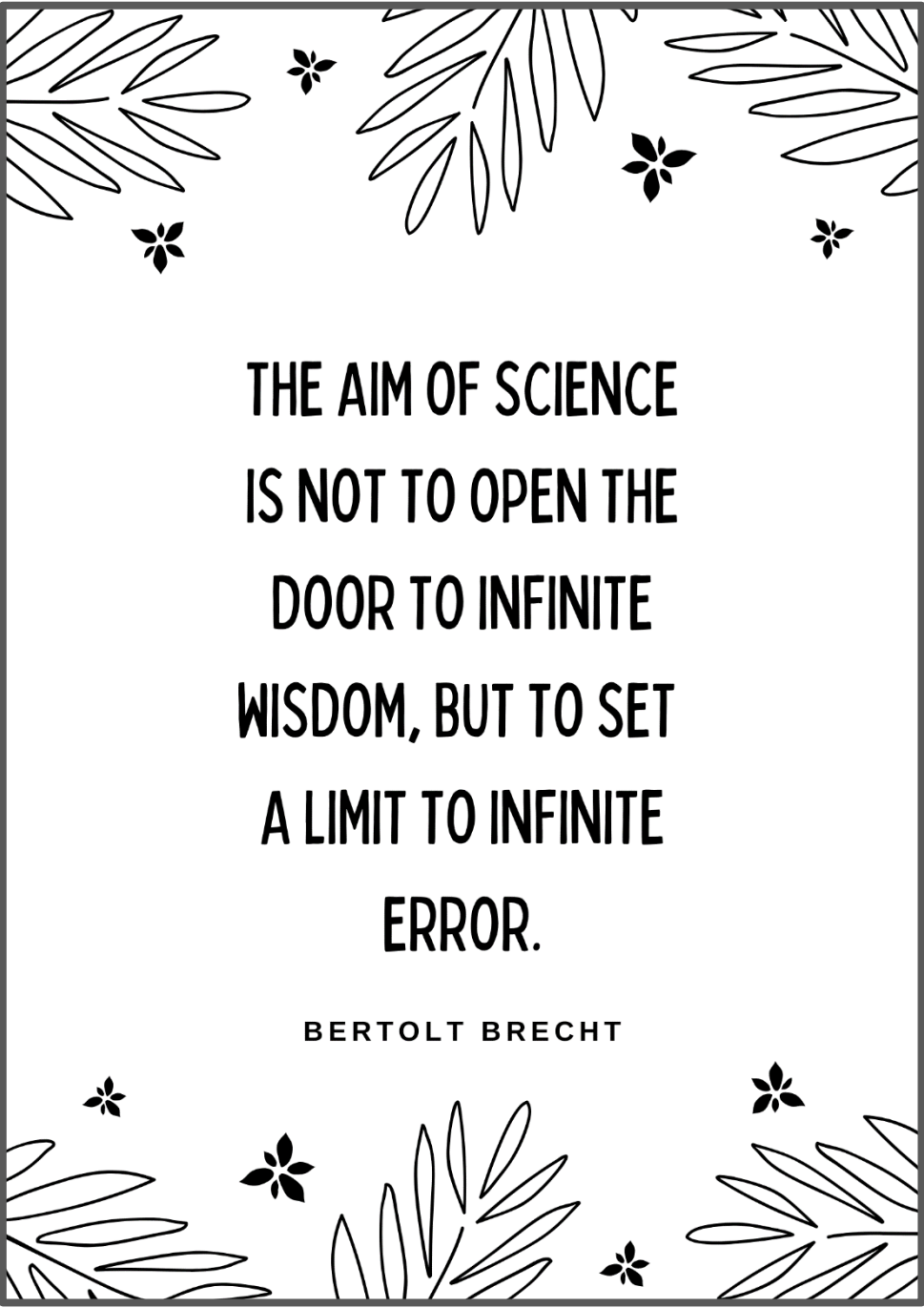
3

5

6

Para os meus avós, Lucinda e Antero.

Für meine Oma Karin und Siegfried.

A decorative border consisting of stylized leaves and small flowers, arranged in a repeating pattern around the central text.

**THE AIM OF SCIENCE
IS NOT TO OPEN THE
DOOR TO INFINITE
WISDOM, BUT TO SET
A LIMIT TO INFINITE
ERROR.**

BERTOLT BRECHT

For the elaboration of this master thesis, data present in the following scientific article and communications was used:

- Spormann, S., Soares, C., Teixeira, J., & Fidalgo, F. (2020). Polyamines as key regulatory players in plants under metal stress – a way for an enhanced tolerance. *Annals of Applied Biology*. (**Article in press**)
- Spormann, S., Soares, C. & Fidalgo, F (2020) Polyamines as key regulatory players in plants under metal stress. Summer School: Hands on Science for Sustainable Agrifood Production: From the Soil to the Fork., Porto, Portugal
- Spormann, S., Soares, C. & Fidalgo, F (2020) A comparative insight into the effects of combined drought and Ni stress between domestic and wild tomato species. IJUP 20 - Encontro de Jovens Investigadores da Universidade do Porto, Portugal.



Produção Agroalimentar
Sustentável
Centro de Investigação



Acknowledgments

Agradecimentos - Danksagung

Findado um ano tão atípico, tão repleto de obstáculos e com constantes ameaças à nossa saúde física e mental, como foi 2020, vejo que tive a sorte de permanecer relativamente saudável e rodeada de pessoas inspiradoras, amáveis e disponíveis para me ajudar. Sem elas, não teria sido capaz de escrever esta dissertação. A todas, o meu sincero **obrigada**.

Em primeiro lugar, gostaria de dirigir os meus especiais agradecimentos à pessoa que me tem orientado, sempre de perto, desde 2016. À professora Fernanda, deixo aqui o meu enorme **obrigada!** Foram a sua eloquência e dedicação com que leciona que, primeiramente, me cativaram pela área da fisiologia do stress. Agradeço-lhe a disponibilidade, a entrega e o rigor a que me habituou ao longo destes anos. Sei que ambas nutrimos a vontade de contribuir para o avanço desta área científica. Orgulho-me de poder partilhar isso consigo. Evidentemente, agradeço-lhe ainda as oportunidades de comunicação e publicação dos resultados que obtive, que sem dúvida serão determinantes para o meu futuro académico e profissional, e as correções e sugestões que fez à escrita desta dissertação. Por último, gostaria ainda de aproveitar a oportunidade para lhe dirigir, uma vez mais, os meus parabéns pelas conquistas profissionais e pessoais que alcançou nos últimos meses, apesar de todas as dificuldades que este ano lhe impôs, às quais pode acrescentar ainda o mérito na orientação e liderança de uma equipa de investigação extraordinariamente competente. É, sem dúvida, uma fonte de inspiração para todos os que a rodeiam.

Em segundo lugar, gostaria de agradecer, de uma forma muito especial, ao meu mentor e amigo Cris. Quem não te conhece, certamente não saberá o que é ser-se verdadeiramente entregue à ciência. Tens sido o meu maior conselheiro, que me tem acompanhado desde o início do meu percurso académico e que me tem motivado para me tornar numa cientista cada vez mais atenta, digna e confiante. Não te agradeço por seres meu amigo, porque sei que o és involuntariamente, mas agradeço-te por todo o apoio que me deste ao longo deste ano, principalmente no laboratório e na escrita da tese. Tem sido uma honra seguir os teus passos, ser contagiada pelo teu afeto à fisiologia vegetal e aprender a fazer ciência contigo. Não sei o que nos aguarda o futuro, mas sei que levarei comigo todos os teus ensinamentos e todos os conselhos, para onde quer que vá. Espero que saibas que independentemente do que fizer a partir de

agora, sem ti não teria chegado até aqui, por isso estarei para sempre em dívida contigo.

Muito, muito obrigada!

Agradeço, também, à minha coorientadora, Dra. Viviana Martins, pela atenção, disponibilidade e por todas as sugestões que contribuíram para a qualidade da presente dissertação. Nos poucos momentos que partilhámos, aprendi a executar diversas técnicas essenciais para o estudo de marcadores moleculares, retive apontamentos e dicas preciosos, que guardarei para o futuro! Agradeço-te ainda a cuidadosa análise aos resultados da expressão génica e também a atenção prestada na correção da escrita da tese. **Muito obrigada!**

À Dra. Inês Valente, gostaria também de expressar os meus sinceros agradecimentos pelo apoio à análise dos níveis de poliaminas. Graças à tua disponibilidade, pude acrescentar resultados que considero extremamente relevantes para o estudo aqui efetuado. **Obrigada!**

Ao Prof. Dr. Manuel Azenha, agradeço também a atenção prestada e o tempo que disponibilizou na quantificação do teor em Níquel nas amostras do presente estudo. Os resultados por si obtidos, a par das restantes análises, permitiram-me interpretar, de uma forma mais precisa, os efeitos observados. **Obrigada!**

Aos meus pais, Anja e Gil, gostaria de agradecer por se desafiarem, todos os dias, ano após ano, a serem os melhores pais do mundo. Obrigada por se manterem tão unidos na qualidade de pais. Obrigada por nunca esquecerem o que é ser jovem, por se porem no meu lugar e compreenderem tão bem o que sinto, por confiarem nos meus gostos, nas minhas escolhas e na importância do que faço. Reconheço a sorte e o privilégio que é ser vossa filha. Obrigada por me terem incentivado a questionar-me cada vez mais sobre a realidade que nos rodeia, a sonhar cada vez mais alto e a pensar cada vez mais fora da caixa, sem esquecer de onde venho nem do que sou feita. Espero continuar a dar-vos motivos de orgulho. Ich hab euch lieb! **Vielen Dank!**

Às manas, Clara e Maria, obrigada por confiarem em mim para vos guiar, por me terem ensinado a partilhar e a cuidar, por me desafiarem a ser um exemplo cada vez melhor para vocês. Obrigada por terem sempre umas palavrinhas de apoio na ponta da língua, e nunca me deixarem ficar triste sozinha. Obrigada por serem tão confiantes e determinadas nas vossas escolhas, por arriscarem e mostrarem ao mundo que são mulheres cheias de garra. São o maior motivo de orgulho da mana. **Obrigada!**

Ao meu avô Antero, a quem dedico esta tese, um enorme **obrigada!** As palavras não chegam para expressar a admiração e o afeto que sinto por si, e o quão grata sou

por ser a sua primeira neta. Obrigada por me mostrar, todos os dias, o que é o amor. Obrigada por continuar a ver a avó Lucinda como ela é, para além da doença. Por me recordar quem ela foi, quando eu já não consigo lembrar. Com o avô, aprendi que ser compreensivo, prestável e trabalhador são as bases para tudo na vida. Ao avô, que apesar da disparidade geracional, nunca julgou as escolhas dos netos e se mostrou sempre disponível para ajudar e aconselhar, um gigante **obrigada!** Para alguém a quem a ciência parece tão longínqua e, talvez até vã, é de admirar o respeito que nutre pela minha dedicação a esta área. O avô e a sua horta têm vindo a ser uma enorme fonte de inspiração ao longo do meu percurso académico. Com este e com trabalhos futuros espero, um dia, vir a contribuir para melhorar e tornar mais sustentável a produção agroalimentar, facilitando o trabalho também de pequenos produtores, como o avô. Espero que se orgulhe.

Ao João, meu amor, **obrigada**. Agradeço-te por estares sempre do meu lado, por confiares em mim, por conseguires colocar-te sempre tão bem na minha posição e me ajudares a manter-me otimista. Não te agradeço a amizade nem o companheirismo, mas agradeço-te todas as palavras, beijos e abraços de apoio que me permitiram concluir esta tese a tempo, orgulhosa e sã! Aos teus pais, que me acolhem sempre como se fosse da família, um beijo do tamanho do mundo, **obrigada!**

À Inês, uma irmã emprestada, muito obrigada por todo o apoio, não só ao longo deste ano, mas desde sempre. Obrigada por acreditares em mim e por estares sempre do meu lado. Tem sido um gosto crescer contigo. À Isabel, a Bióloga que me inspirou para seguir esta área, agradeço-te precisamente por isso, mas também por te preocupares e mostrares sempre tanto interesse no meu trabalho. Incentivas-me a dar o meu melhor. Muito **obrigada** por tudo!

Ao meu padrinho, Rui, e à minha afilhada, Mariana, agradeço por fazerem de mim uma pessoa melhor, por me mostrarem que as coisas boas da vida, são na verdade muito simples. 2020 foi bem mais suportável com as vossas visitas. Espero deixar-vos orgulhosos com este trabalho, e espero que não só enquanto cientista, mas também enquanto mulher, possa continuar a servir-vos de exemplo. Aos restantes membros da família, Rita, Diogo, Ana, Tina e Carlos, resta-me agradecer-vos por estarem sempre lá quando preciso, com uma palavra amiga para me reconfortar. Sou uma sortuda por ter uma família tão cheia como a nossa. **Obrigada por tudo!**

Agradeço ainda à Maria e ao Bruno, os amigos e colegas de equipa que tornaram o meu dia a dia no laboratório bastante mais divertido e o ano de 2020 um pouco mais suportável! Obrigada por me terem aceitado tão bem na equipa, por se terem mostrado

sempre tão disponíveis e por terem dispensado tanto tempo para me ajudarem no laboratório. Contem sempre comigo. Espero que gostem desta tese. **Obrigada!**

À Filipa, Margarida e Mafalda, agradeço-vos por se terem mantido sempre em contacto, por terem estado disponíveis para os meus desabafos, por me terem apaziguado as minhas angústias e todos os meus momentos de ansiedade ao longo deste ano. Sem o vosso apoio, facilmente me teria perdido em pensamentos negativos e contraproducentes. Olhando para trás, vejo que apesar de termos diferentes ritmos de trabalho e formas distintas de lidar com a pressão, a nossa união, compreensão mútua pelas emoções umas das outras, e o respeito pelo percurso individual de cada uma, ajudou-nos a todas. **Obrigada!** Tenho muito orgulho nas jovens cientistas em que as três se tornaram, e nas teses, artigos e apresentações que completaram ao longo deste ano. Espero poder continuar a crescer ao vosso lado enquanto cientista. Agora, depois de todos os desvairos de 2020, chega o momento para celebrarmos em conjunto.

À Rita, à Alexandra e a todos os outros amigos que me acompanharam, não só ao longo do meu percurso académico, mas também em casa, um enorme **obrigada!** Sem vocês, esta longa viagem não teria sido tão boa. Espero poder continuar a celebrar conquistas minhas e vossas, em conjunto. Adoro-vos a todos!

Perdoem-me o alemão nos seguintes parágrafos, mas não gostaria de deixar passar a oportunidade para agradecer também aos meus familiares maternos e amigos na Alemanha:

Ich möchte meiner Oma Karin und Siegfried danken, denen ich auch diese Arbeit widme. Vielen Dank, dass Ihr mich immer mit offenen Armen empfangen habt, dass Ihr nur einen Anruf entfernt seid, dass ihr immer wissen wolltet wie meine Woche war und immer Worte der Unterstützung und Ermutigung gefunden habt. Ich hoffe, Ihr seid stolz auf mich.

Meiner Patentante Franziska, meinem Onkel Jörg und meiner Tante Anja sowie Freunden, die bereits zur Familie gehören, Regina, Susanne und Christian, möchte ich für ihr stetes Interesse an meiner akademischen Karriere und die Begleitung auf meinem Lebensweg danken. Es ist gut zu wissen, dass ihr mir so nahe seid, trotz der Entfernung, die uns trennt. Wir sprechen selten, aber ich möchte sagen, dass ich Euch in meinem Herzen habe und dass ihr mich inspiriert habt, immer mein Bestes zu geben, besonders in diesem Jahr. Ich hoffe, dass wir weiterhin gemeinsam gute Erfolge feiern können. Ich empfinde für euch alle eine große Bewunderung.

Table of contents

Resumo	IX
Palavras-chave.....	X
Abstract.....	XI
Key-words	XII
List of figures	XIII
List of tables.....	XVIII
List of abbreviations.....	XIX
1. Introduction.....	1
1.1. GROWING CROPS UNDER A CHANGING ENVIRONMENT	1
1.2. DROUGHT: A THREAT TO AGRICULTURAL PRODUCTIVITY WORLDWIDE	2
1.2.1. Water stress induces physiological and biochemical disorders in plants ..	3
1.2.2. The challenge of inducing drought to plants in a laboratory	4
1.3. ENVIRONMENTAL CONTAMINATION BY HEAVY METALS (HM): NICKEL (Ni) AS A CASE-STUDY	5
1.3.1. Ni induces stress to crops and vegetables.....	6
1.3.2. Vacuolar sequestration of Ni – the perfect hideout!.....	8
1.3.3. Transport of HM through the tonoplast.....	9
1.4. RESEARCH ON ABIOTIC STRESS: DIFFERENCES BETWEEN SINGLE AND COMBINED STRESS APPROACHES	14
1.5. ABIOTIC STRESS-INDUCED REDOX DISORDERS: A SNEAK PEEK INTO OXIDATIVE STRESS AND ANTIOXIDANT (AOX) SYSTEM	16
1.5.1. The dual side of ROS: from bad guys to signaling rescuers.....	17
1.5.2. Plants' sophisticated AOX system – enzymatic and non-enzymatic mechanisms	19
1.5.2.1. Superoxide Dismutase (SOD).....	20
1.5.2.2. Ascorbate Peroxidase (APX)	21
1.5.2.3. Catalase (CAT).....	21
1.5.2.4. Proline (Pro)	22
1.5.2.5. Ascorbate - reduced (AsA) and oxidized (DHA) forms	23
1.5.2.6. Glutathione (GSH)	23
1.5.2.7. Tocopherols.....	24
1.5.2.8. Carotenoids (Car)	25
1.5.2.9. Phenolic Compounds.....	25
1.5.2.10. Polyamines (PAs).....	26
1.6. DROUGHT- AND Ni-INDUCED OXIDATIVE STRESS	32

1.7. IMPROVEMENT OF <i>Solanum lycopersicum</i> L. STRESS TOLERANCE – EXPLORING ITS INTRASPECIFIC DIVERSITY	34
2. Aims.....	39
3. Material and Methods	40
3.1. CHEMICALS AND SUBSTRATE	40
3.2. PLANT MATERIAL AND GROWTH CONDITIONS.....	40
3.3. NICKEL TOLERANCE SCREENING	40
3.3.1. Selection of Ni concentration – germination assay.....	40
3.3.2. Selection of tomato cultivars under Ni stress – germination assay.....	41
3.3.3. Selection of tomato cultivars under Ni stress – semi-hydroponic experiment.....	41
3.4. FINAL GROWTH TRIAL	42
3.5. QUANTIFICATION OF Ni CONTENT IN TISSUES.....	44
3.6. EVALUATION OF PHYSIOLOGICAL ENDPOINTS.....	44
3.6.1. Extraction and quantification of photosynthetic pigments.....	44
3.6.2. Extraction and quantification of soluble proteins	44
3.7. EVALUATION OF OXIDATIVE STRESS MARKERS.....	45
3.7.1. Quantification of lipid peroxidation (LP).....	45
3.7.2. Quantification of H ₂ O ₂	45
3.7.3. Quantification of O ₂ ⁻	46
3.8. ASSESSMENT OF THE ANTIOXIDANT DEFENSE MECHANISMS.....	46
3.8.1. Extraction and quantification of AOX metabolites	46
3.8.1.1. Proline (Pro)	46
3.8.1.2. Glutathione (GSH)	47
3.8.1.3. Ascorbate - reduced (AsA) and oxidized (DHA) forms	47
3.8.2. Extraction and quantification of AOX enzymes' activity.....	48
3.8.2.1. Superoxide Dismutase (SOD) activity assay.....	48
3.8.2.2. Catalase (CAT) activity assay.....	48
3.8.2.3. Ascorbate Peroxidase (APX) activity assay	49
3.9. EXTRACTION, DERIVATIZATION AND QUANTIFICATION OF POLYAMINES (PAs).....	49
3.10. ASSESSMENT OF THE EXPRESSION PROFILE OF Ni TRANSPORTERS.....	50
3.10.1. Computational identification and analysis of putative Ni transporters.....	50
3.10.2. Extraction of total RNA	51
3.10.3. cDNA synthesis	52
3.10.4. q-PCR amplification.....	53
3.11. STATISTICAL ANALYSIS.....	55
4. Results	56
4.1. ECOTOXICITY OF Ni TO CHERRY TOMATO PLANTS.....	56
4.2. EFFECTS OF Ni EXPOSURE ON DIFFERENT TOMATO CULTIVARS	57

4.3.	EFFECTS OF SINGLE AND COMBINED EXPOSURE TO Ni AND PEG-INDUCED DROUGHT ON <i>S. LYCOPERSICUM</i> CULTIVARS GN AND PC.....	59
4.3.1.	Biometric parameters and biomass production	60
4.3.2.	Relative water content	61
4.3.3.	Ni content in tissues.....	62
4.3.4.	Photosynthetic pigments.....	63
4.3.5.	Oxidative stress markers	63
4.3.5.1.	Reactive Oxygen Species (ROS).....	63
4.3.5.2.	Lipid Peroxidation (LP)	65
4.3.6.	Non-enzymatic components of the antioxidant (AOX) system.....	66
4.3.6.1.	Proline (Pro)	66
4.3.6.2.	Glutathione (GSH)	67
4.3.6.3.	Ascorbate - reduced (AsA) and oxidized (DHA) forms	68
4.3.7.	Enzymatic components of the antioxidant (AOX) system	70
4.3.8.	Levels of free polyamines (PAs)	71
4.4.	INVOLVEMENT OF METAL TRANSPORTERS IN THE RESPONSES OF GN AND PC PLANTS TO SINGLE AND COMBINED STRESS	74
4.4.1.	Computational analysis of metal transporters possibly involved in the detoxification of Ni	74
4.4.2.	Expression profile of selected metal transporters.....	80
5.	Discussion	87
5.1.	Ni TOXICITY DURING SEEDLING VS VEGETATIVE GROWTH IN DIFFERENT TOMATO CULTIVARS	87
5.2.	AN OVERVIEW OF GROWTH AND OVERALL PHYSIOLOGICAL PERFORMANCE OF TOMATO CULTIVARS GOLD NUGGET AND PURPLE CALABASH UNDER Ni- AND PEG-INDUCED STRESS.....	89
5.3.	PEEKING FOR TOLERANCE TRAITS THROUGH MARKERS OF OXIDATIVE STRESS AND ANTIOXIDANT DEFENSE	94
5.4.	THE ROLE OF PAs IN GN AND PC PLANTS UNDER SINGLE AND COMBINED STRESS.....	101
5.5.	EXPRESSION PROFILE AND INVOLVEMENT OF METAL TRANSPORTERS IN GN AND PC PLANTS UNDER SINGLE AND COMBINED STRESS.....	107
6.	Conclusions	113
7.	Future Perspectives.....	115
8.	References	117

Resumo

Devido às ameaças provocadas pela crescente urbanização e pelas alterações climáticas, é expectável que diversos fatores de stresse ambiental, como a seca e a contaminação dos solos por metais pesados, ocorram com cada vez maior intensidade e frequência, afetando significativamente o crescimento e produtividade vegetal. Assim, torna-se imperativo desenvolver ferramentas que garantam a produtividade das plantas sob condições adversas. Apesar das perdas de diversidade genética ao longo da domesticação do tomateiro (*Solanum lycopersicum* L.) ainda existem cultivares com diferentes sensibilidades a determinados stresses, incluindo a seca e a toxicidade induzida por metais. Uma vez que as culturas frequentemente estão expostas a mais do que um fator de stresse, este trabalho visa conhecer as respostas de diferentes cultivares de tomateiro à combinação da seca e excesso de Ni. As respostas bioquímicas, moleculares e fisiológicas das cultivares Gold Nugget (GN) e Purple Calabash (PC) foram comparadas, focalizando particularmente na homeostasia redox, sistema antioxidante (AOX), incluindo as poliaminas (PAs), e destoxificação de metais, em resposta ao stresse induzido pela exposição ao Ni 50 µM durante 20 dias, seca induzida por PEG durante 48 h, ou à combinação de ambas as condições. Além disso, foram avaliadas a absorção, acumulação e distribuição do Ni, juntamente com a análise transcricional de transportadores de metais. Relativamente às condições de stresse individuais, a exposição ao Ni causou mais efeitos prejudiciais às plantas do que a seca, em termos de inibição do crescimento, degradação de pigmentos fotossintéticos e acumulação de peróxido de hidrogénio (H₂O₂). O stresse combinado causou efeitos fisiológicos idênticos ao Ni, mostrando efeitos não aditivos. As plantas de tomate foram capazes de acumular a maior parte do Ni absorvido nos tecidos radiculares, especialmente na cultivar GN. As plantas de GN também mostraram uma ativação mais rápida do sistema AOX sob exposição ao Ni (através da acumulação de prolina, ascorbato e ativação das enzimas catalase (CAT), superóxido dismutase (SOD) e ascorbato peroxidase (APX), principalmente nos tecidos foliares), enquanto que as plantas de PC apenas induziram expressivamente as suas defesas AOXs perante o stresse combinado (através da acumulação de ascorbato, glutatona e ativação da SOD e APX, sobretudo nas raízes). Sob condições de stresse individual, os aumentos moderados de prolina poderão referir-se ao seu papel protetor, principalmente observado em plantas de GN, enquanto que, em condições de stresse combinado, a drástica acumulação de prolina pareceu impor-se como sinal de maior sensibilidade ao stresse, especialmente em plantas de PC. A acumulação de putrescina (Put), uma PA, também reconhecida como sinal de stresse, ocorreu nos tecidos foliares de ambas as

cultivares expostas ao Ni, enquanto que as raízes puderam manter uma maior razão de espermidina/Put, especialmente em plantas de PC. A expressão dos genes *ABCC5-18*, *MTP1* e *IREG2-like* em ambas as cultivares foi principalmente afetada pela exposição ao Ni, enquanto que a dos genes *CAX3* e *ABCB21* foi induzida exclusivamente pela condição de secura.

Globalmente, os resultados sugerem que as plantas de GN são capazes de se preparar mais rapidamente perante uma situação de stresse do que as plantas de PC, sobretudo na ativação de defesas AOX e expressão de genes envolvidos na detoxificação de metais, o que poderá ter facilitado a aclimação adicionalmente exigida pela co-exposição à secura. Espera-se que este estudo facilite a procura de variedades/espécies tolerantes a stresses abióticos e auxilie o desenvolvimento de ferramentas para melhorar a produtividade do tomateiro sob condições de stresse, através de *plant breeding* ou enxertia, a fim de promover práticas agrícolas mais sustentáveis e lucrativas.

Palavras-chave

alterações climáticas, tolerância ao stresse abiótico, tomateiro, variabilidade intraespecífica, stresse oxidativo, sistema antioxidante, poliaminas, transportadores de metais.

Abstract

Due to the increasing urbanization and climate change-related threats, abiotic stresses, such as drought and metal contamination, are expected to rise in intensity and frequency, delaying plant growth and productivity. Thus, it becomes imperative to find tolerance traits among wild species and varieties that could be used to enhance plant productivity under adverse conditions. Despite the loss of genetic diversity throughout the domestication of tomato plant (*Solanum lycopersicum* L.), there are still some tomato cultivars showing different sensitiveness to stress, including resilience towards drought and metal toxicity. As crops are almost permanently exposed to more than one stress factor under field conditions, this study aimed at providing functional and practical knowledge on the tolerance/susceptibility responses of different tomato cultivars to the combination of soil drought and excessive Ni. The biochemical, molecular, and physiological responses of the tomato cultivars Gold Nugget (GN) and Purple Calabash (PC) were compared, particularly focusing on the redox homeostasis, antioxidant (AOX) system, including polyamines (PAs), and metal detoxification, in response to single 50 μM Ni stress for 20 days, single PEG-induced drought for 48 h, or to the combination of both stresses. Moreover, metal uptake, accumulation and partition were evaluated, along with the transcript analysis of metal transporters. Regarding the single stress conditions, Ni single exposure caused more harmful effects to plants than PEG-induced drought, in terms of growth inhibition, degradation of photosynthetic pigments, and accumulation of hydrogen peroxide (H_2O_2). The combined stress caused identical effects as Ni stress on the overall plant physiology, showing non-additive effects. Tomato plants were able to restrain most of the absorbed Ni in root tissues, especially GN. Moreover, GN plants also displayed a prompter activation of the AOX system under single Ni stress (through accumulation of proline, ascorbate and activation of the enzymes catalase (CAT), superoxide dismutase (SOD) and ascorbate peroxidase (APX), mainly in shoots), while PC plants only had their AOX defenses induced upon combined stress conditions (through accumulation of ascorbate, glutathione and activation of SOD and APX, especially in the roots). Under single stress conditions, the moderate proline increases may have accounted for its protective role, mainly observed in GN plants, while under combined stress, the drastic proline accumulation resembled a signal of stress sensitivity, especially in PC plants. Putrescine (Put) accumulation, also recognized as a stress signal, occurred in the shoots of both cultivars under Ni stress, while roots tissues could maintain a higher spermidine/Put ratio, especially in PC plants. In general, the

expression of *ABCC5-18*, *MTP1* and *IREG2-like* in both cultivars was mainly affected by Ni, while that of *CAX3* and *ABCB21* was exclusively induced by drought.

Overall, results suggest that GN plants are more readily prepared than PC plants to activate AOX defenses, and adjust gene expression related to metal detoxification, when a stress condition is imposed, which may ease the further adjustments demanded by the co-exposure to drought. It is expected that this study will give relevant insights in the search for abiotic stress tolerant varieties/species and help to design new strategies to improve tomato plant tolerance to stress, through inexpensive breeding or grafting approaches, in order to promote a more sustainable and profitable agriculture.

Key-words

climate change, abiotic stress tolerance, tomato, intraspecific diversity, oxidative stress, antioxidant system, polyamines, metal transporters.

List of figures

Figure 1 Nickel uptake, transport, and detoxification in plants. Ni is absorbed by plants in the form of Ni²⁺, via the cation transport system or, through secondary active transport, when chelated to organic molecules. Most Ni is retained in the apoplast and in the vacuoles of the roots. Ni is translocated from roots to shoots through the transpiration stream, via xylem, which is regulated by metal-binding compounds. In stems and leaves, Ni is mainly directed to the vacuoles, cell walls and epidermal trichomes, associated with chelators. This schematic representation was adapted and modified from the figures present in reviews by Chen et al. (2009), Krämer et al. (2007), Sachan & Lal (2019), and Yusuf et al. (2014).

Figure 2 Enzymatic and non-enzymatic components of the plant antioxidant system. Adapted from Soares et al. (2019a).

Figure 3 Biosynthesis, back-conversion, and terminal catabolism of Put, Spd and Spm in plants. Adapted from Alcázar et al. (2006), Chen et al. (2019), Gill and Tuteja (2010b), Rangan et al. (2014), Todorova et al. (2014), and Yu et al. (2019).

Figure 4 The diverse roles of PAs in plants under HM stress.

Figure 5 A mechanistic model on how PAs mediate plant responses to metal stress.

Figure 6 Experimental setup and timeline of the final growth trial. Exposure to Ni started for plantlets of both cultivars on the 7th day of the trial, as represented in the highlighted scheme, above the timeline. For the following 16 days, the experimental setup consisted of only two treatments (CTL and Ni 50 µM) being applied to plants of the two different tomato cultivars (Gold Nugget and Purple Calabash). The stage of the trial in which all treatments were applied simultaneously, is highlighted in the grey rectangle from the last section of the timeline and is visually represented bellow. In this representation it is possible to distinguish the four different treatments (CTL; Ni 50 µM; 6 % PEG 6000; and 50 µM + 6 % PEG 6000) being applied to plants of the two different tomato cultivars (Gold Nugget and Purple Calabash).

Figure 7 Effects of increasing concentrations of Ni (0, 50, 150, 250 and 500 µM) on the radicle and hypocotyl growth of cherry tomato seedlings after a 5 day exposure under *in vitro* conditions. Different letters above bars of each tissue type represent significant differences at $p \leq 0.05$.

Figure 8 (a) Effects of 75 µM Ni on radicle growth of plantlets from 12 different tomato cultivars after a 5 day exposure under *in vitro* conditions. Different letters above bars indicate statistical differences for each cultivar between Ni-exposed plants and the respective control (0 µM Ni), at $p \leq 0.05$. (b) Growth inhibition percentages for each cultivar, written above the respective bars, placed from lowest to highest radicle growth inhibition.

Figure 9 Effects of 75 µM Ni on the growth of roots from 4 different tomato cultivars after a 15 day exposure under a semi-hydroponic system. Different letters above bars indicate statistical differences for each cultivar between Ni-exposed plants and the control (0 µM Ni), at $p \leq 0.05$.

Figure 10 Effects of 75 μM Ni on the biomass of roots (a) and shoots (b) from 4 different tomato cultivars after a 15 day exposure under a semi-hydroponic system. Different letters above bars indicate statistical differences for each cultivar between Ni-exposed plants and the respective control (0 μM Ni), at $p \leq 0.05$.

Figure 11 Effects of exposure to 50 μM Ni and/or 6 % (w/v) PEG 6000 on the length of roots (a) and shoots (b) of Gold Nugget and Purple Calabash tomato plants grown for 20 days under a semi hydroponic system. Colored bars refer to the 6 % (w/v) PEG 6000 treatment. Different lines on top of each sub chart represent significant differences between cultivars. Different letters above the bars of each cultivar represent significant differences between groups, at $p \leq 0.05$; lowercase and capital letters refer to GN and PC, respectively.

Figure 12 Effects of exposure to 50 μM Ni and/or 6 % PEG 6000 on the biomass of roots (a) and shoots (b) of Gold Nugget and Purple Calabash tomato plants grown for 20 days under a semi hydroponic system. Colored bars refer to the 6 % PEG 6000 treatment. Different lines on top of each sub chart represent significant differences between cultivars. Different letters above the bars of each cultivar represent significant differences between groups, at $p \leq 0.05$; lowercase and capital letters refer to GN and PC, respectively.

Figure 13 Effects of exposure to 50 μM Ni and/or 6 % PEG 6000 on the relative water content of roots (a) and shoots (b) of Gold Nugget and Purple Calabash tomato plants grown for 20 days under a semi hydroponic system. Colored bars refer to the 6 % PEG 6000 treatment. Different lines on top of each sub chart represent significant differences between cultivars. Different letters above the bars of each cultivar represent significant differences between groups, at $p \leq 0.05$; lowercase and capital letters refer to GN and PC, respectively.

Figure 14 Effects of exposure to 50 μM Ni and/or 6 % PEG 6000 on the Ni content of roots (a) and shoots (b) of Gold Nugget and Purple Calabash tomato plants grown for 20 days under a semi hydroponic system. Colored bars refer to the 6 % PEG 6000 treatment. Different lines on top of each sub chart represent significant differences between cultivars. Different letters above the bars of each cultivar represent significant differences between groups, at $p \leq 0.05$; lowercase and capital letters refer to GN and PC, respectively.

Figure 15 Effects of exposure to 50 μM Ni and 6 % PEG 6000 on the content of the photosynthetic pigments Chl (a) and Car (b) in the shoots of plants from the tomato cultivars Gold Nugget and Purple Calabash grown for 20 days under a semi hydroponic system. Colored bars refer to the 6 % PEG 6000 treatment. Different lines on top of each sub chart represent significant differences between cultivars. Different letters above the bars of each cultivar represent significant differences between groups, at $p \leq 0.05$; lowercase and capital letters refer to GN and PC, respectively.

Figure 16 Effects of exposure to 50 μM Ni and/or 6 % PEG 6000 on the levels of H_2O_2 in the roots (a) and shoots (b) of Gold Nugget and Purple Calabash tomato plants grown for 20 days under a semi hydroponic system. Colored bars refer to the 6 % PEG 6000 treatment. Different lines on top of each sub chart represent significant differences between cultivars. Different letters above the bars of each cultivar represent significant differences between groups, at $p \leq 0.05$; lowercase and capital letters refer to GN and PC, respectively.

Figure 17 Effects of exposure to 50 μM Ni and/or 6 % PEG 6000 on the levels of O_2^- in the roots (a) and shoots (b) of Gold Nugget and Purple Calabash tomato plants grown for 20 days under a semi hydroponic system. Colored bars refer to the 6 % PEG 6000 treatment. Different lines on top of each sub chart represent significant differences between cultivars. Different letters above the bars of each cultivar represent significant differences between groups, at $p \leq 0.05$; lowercase and capital letters refer to GN and PC, respectively.

Figure 18 Effects of exposure to 50 μM Ni and/or 6 % PEG 6000 on the levels of MDA in the roots (a) and shoots (b) of Gold Nugget and Purple Calabash tomato plants grown for 20 days under a semi hydroponic system. Colored bars refer to the 6 % PEG 6000 treatment. Different lines on top of each sub chart represent significant differences between cultivars. Different letters above the bars of each cultivar represent significant differences between groups, at $p \leq 0.05$; lowercase and capital letters refer to GN and PC, respectively.

Figure 19 Effects of exposure to 50 μM Ni and/or 6 % PEG 6000 on the levels of Pro in the roots (a) and shoots (b) of Gold Nugget and Purple Calabash tomato plants grown for 20 days under a semi hydroponic system. Colored bars refer to the 6 % PEG 6000 treatment. Different lines on top of each sub chart represent significant differences between cultivars. Different letters above the bars of each cultivar represent significant differences between groups, at $p \leq 0.05$; lowercase and capital letters refer to GN and PC, respectively.

Figure 20 Effects of exposure to 50 μM Ni and/or 6 % PEG 6000 on the levels of GSH in the roots (a) and shoots (b) of Gold Nugget and Purple Calabash tomato plants grown for 20 days under a semi hydroponic system. Colored bars refer to the 6 % PEG 6000 treatment. Different lines on top of each sub chart represent significant differences between cultivars. Different letters above the bars of each cultivar represent significant differences between groups, at $p \leq 0.05$; lowercase and capital letters refer to GN and PC, respectively.

Figure 21 Effects of exposure to 50 μM Ni and/or 6 % PEG 6000 on the activity of CAT in the roots (a) and shoots (b) of Gold Nugget and Purple Calabash tomato plants grown for 20 days under a semi hydroponic system. Colored bars refer to the 6 % PEG 6000 treatment. Different lines on top of each sub chart represent significant differences between cultivars. Different letters above the bars of each cultivar represent significant differences between groups, at $p \leq 0.05$; lowercase and capital letters refer to GN and PC, respectively.

Figure 22 Effects of exposure to 50 μM Ni and/or 6 % PEG 6000 on the activity of APX in the roots (a) and shoots (b) of Gold Nugget and Purple Calabash tomato plants grown for 20 days under a semi hydroponic system. Colored bars refer to the 6 % PEG 6000 treatment. Different lines on top of each sub chart represent significant differences between cultivars. Different letters above the bars of each cultivar represent significant differences between groups, at $p \leq 0.05$; lowercase and capital letters refer to GN and PC, respectively.

Figure 23 Effects of exposure to 50 μM Ni and/or 6 % PEG 6000 on the activity of SOD in the roots (a) and shoots (b) of Gold Nugget and Purple Calabash tomato plants grown for 20 days under a semi hydroponic system. Colored bars refer to the 6 % PEG 6000 treatment. Different lines on top of each sub chart represent significant differences between cultivars. Different letters above the bars of each cultivar represent significant differences between groups, at $p \leq 0.05$; lowercase and capital letters refer to GN and PC, respectively.

Figure 24 Effects of exposure to 50 μM Ni and/or 6 % PEG 6000 on the levels of Put in the roots (a) and shoots (b) of Gold Nugget and Purple Calabash tomato plants grown for 20 days under a semi hydroponic system. Colored bars refer to the 6 % PEG 6000 treatment. Different lines on top of each sub chart represent significant differences between cultivars. Different letters above the bars of each cultivar represent significant differences between groups, at $p \leq 0.05$; lowercase and capital letters refer to GN and PC, respectively.

Figure 25 Effects of exposure to 50 μM Ni and/or 6 % PEG 6000 on the levels of Spd in the roots (a) and shoots (b) of Gold Nugget and Purple Calabash tomato plants grown for 20 days under a semi hydroponic system. Colored bars refer to the 6 % PEG 6000 treatment. Different lines on top of each sub chart represent significant differences between cultivars. Different letters above the bars of each cultivar represent significant differences between groups, at $p \leq 0.05$; lowercase and capital letters refer to GN and PC, respectively.

Figure 26 Effects of exposure to 50 μM Ni and/or 6 % PEG 6000 on the ratio Spd / Put in the roots (a) and shoots (b) of Gold Nugget and Purple Calabash tomato plants grown for 20 days under a semi hydroponic system. Colored bars refer to the 6 % PEG 6000 treatment. Different lines on top of each sub chart represent significant differences between cultivars. Different letters above or within the bars of each cultivar represent significant differences between groups, at $p \leq 0.05$; lowercase and capital letters refer to GN and PC, respectively. The bar respective to the Spd / Put ratio in the roots of PC plants under single Ni-stress is intentionally represented as “limitless”, since Put levels in these tissues were untraceable.

Figure 27 Evolutionary analysis of 28 metal transporter protein sequences from tomato (SIABCC3-25, SIABCB21, SICAX3, SICAX3-like, SIIREG2-like, SIMTP1), rice (OsMTP1), tiny wild mustard (NgMTP1), grape-vine (VvCAX3), and Arabidopsis (AtABCC1-7, AtCAX2-4, AtMTP1, AtIREG2) plants by Maximum Likelihood method and JTT matrix-based model. The tree with the highest log likelihood is shown. The % of trees in which the associated taxa clustered together is shown next to the branches.

Figure 28 Effects of exposure to 50 μM Ni and/or 6 % PEG 6000 on the expression of *SIABCC5* in the roots (a) and shoots (b) of Gold Nugget and Purple Calabash tomato plants grown for 20 days under a semi hydroponic system. Colored bars refer to the 6 % PEG 6000 treatment. Different lines on top of each sub chart represent significant differences between cultivars. Different letters above the bars of each cultivar represent significant differences between groups, at $p \leq 0.05$; lowercase and capital letters refer to GN and PC, respectively.

Figure 29 Effects of exposure to 50 μM Ni and/or 6 % PEG 6000 on the expression of *SIABCC6* in the roots (a) and shoots (b) of Gold Nugget and Purple Calabash tomato plants grown for 20 days under a semi hydroponic system. Colored bars refer to the 6 % PEG 6000 treatment. Different lines on top of each sub chart represent significant differences between cultivars. Different letters above the bars of each cultivar represent significant differences between groups, at $p \leq 0.05$; lowercase and capital letters refer to GN and PC, respectively.

Figure 30 Effects of exposure to 50 μM Ni and/or 6 % PEG 6000 on the expression of *SIABCC16* in the roots (a) and shoots (b) of Gold Nugget and Purple Calabash tomato plants grown for 20 days under a semi hydroponic system. Colored bars refer to the 6 % PEG 6000 treatment. Different lines on top of each sub chart represent significant differences between cultivars. Different letters above the bars of each cultivar represent significant differences between groups, at $p \leq 0.05$; lowercase and capital letters refer to GN and PC, respectively.

Figure 31 Effects of exposure to 50 μM Ni and/or 6 % PEG 6000 on the expression of *SIABCC18* in the roots (a) and shoots (b) of Gold Nugget and Purple Calabash tomato plants grown for 20 days under a semi hydroponic system. Colored bars refer to the 6 % PEG 6000 treatment. Different lines on top of each sub chart represent significant differences between cultivars. Different letters above the bars of each cultivar represent significant differences between groups, at $p \leq 0.05$; lowercase and capital letters refer to GN and PC, respectively.

Figure 32 Effects of exposure to 50 μ M Ni and/or 6 % PEG 6000 on the expression of *SIACB21* in the roots (a) and shoots (b) of Gold Nugget and Purple Calabash tomato plants grown for 20 days under a semi hydroponic system. Colored bars refer to the 6 % PEG 6000 treatment. Different lines on top of each sub chart represent significant differences between cultivars. Different letters above the bars of each cultivar represent significant differences between groups, at $p \leq 0.05$; lowercase and capital letters refer to GN and PC, respectively.

Figure 33 Effects of exposure to 50 μ M Ni and/or 6 % PEG 6000 on the expression of *SICAX3* in the roots (a) and shoots (b) of Gold Nugget and Purple Calabash tomato plants grown for 20 days under a semi hydroponic system. Colored bars refer to the 6 % PEG 6000 treatment. Different lines on top of each sub chart represent significant differences between cultivars. Different letters above the bars of each cultivar represent significant differences between groups, at $p \leq 0.05$; lowercase and capital letters refer to GN and PC, respectively.

Figure 34 Effects of exposure to 50 μ M Ni and/or 6 % PEG 6000 on the expression of *SIIREG2-like* in the roots (a) and shoots (b) of Gold Nugget and Purple Calabash tomato plants grown for 20 days under a semi hydroponic system. Colored bars refer to the 6 % PEG 6000 treatment. Different lines on top of each sub chart represent significant differences between cultivars. Different letters above the bars of each cultivar represent significant differences between groups, at $p \leq 0.05$; lowercase and capital letters refer to GN and PC, respectively.

Figure 35 Effects of exposure to 50 μ M Ni and/or 6 % PEG 6000 on the expression of *SIMTP1* in the roots (a) and shoots (b) of Gold Nugget and Purple Calabash tomato plants grown for 20 days under a semi hydroponic system. Colored bars refer to the 6 % PEG 6000 treatment. Different lines on top of each sub chart represent significant differences between cultivars. Different letters above the bars of each cultivar represent significant differences between groups, at $p \leq 0.05$; lowercase and capital letters refer to GN and PC, respectively.

Figure 36 Overall physiological disturbances to Gold Nugget tomato plants caused by the exposure to PEG and Ni. Red or green arrows represent significant negative or positive alterations, respectively, in comparison to the CTL. Black symbols correspond to non-significant changes.

Figure 37 Overall physiological disturbances to Purple Calabash tomato plants caused by the exposure to PEG and Ni. Red or green arrows represent significant negative or positive alterations, respectively, in comparison to the CTL. Black symbols correspond to non-significant changes.

Figure 38 Changes in expression of genes encoding metal transporters conceivably involved in the detoxification of Ni in Gold Nugget plants caused by the exposure to PEG and Ni. Red or green arrows represent significant increases or decreases in gene expression, respectively, in comparison to CTL levels. Black symbols correspond to non-significant changes.

Figure 39 Changes in expression of genes encoding metal transporters conceivably involved in the detoxification of Ni in Purple Calabash plants caused by the exposure to PEG and Ni. Red or green arrows represent significant increases or decreases in gene expression, respectively, in comparison to CTL levels. Black symbols correspond to non-significant changes.

List of tables

Table 1 Examples of *S. lycopersicum* L. cultivars showing different sensitivity levels towards biotic and abiotic stresses

Table 2 List of primer sequences used in analysis of gene expression by qPCR.

Table 3 Effects of exposure to 50 μM Ni and 6 % PEG 6000 on the levels and ratios of total, reduced and oxidized (DHA) forms of AsA in the roots and shoots of plants from the tomato cultivars Gold Nugget and Purple Calabash grown for 20 days under a semi hydroponic system. For simplicity, reduced AsA was termed AsA. Results are expressed as mean ($\mu\text{mol g}^{-1}$ f. w.) \pm SD. Different lines underlying the concentrations in each cultivar represent significant differences between cultivars. Different letters above the bars of each cultivar represent significant differences between groups, at $p \leq 0.05$; lowercase and capital letters refer to GN and PC, respectively.

Table 4 Characterization of 13 genes and respective transcripts encoding metal transporters conceivably involved in the detoxification of Ni in tomato plants.

Table 5 Characterization of 13 metal transporter proteins conceivably involved in the detoxification of Ni in tomato plants.

List of abbreviations, acronyms, and symbols

¹ O ₂	singlet oxygen	CuDAO	Cu dependent amine oxidase
3Chl*	triplet Chl	DAO	diamine oxidase
ABC	ATP-binding cassette	DAP	1,3-diaminopropane
Abs	absorbance	dcSAM	decarboxylated S-adenosylmethionine
ADC	arginine decarboxylase	ddH ₂ O	sterile deionized water
AIH	agmatine iminohydrolase	DHA	dehydroascorbate
AOX	antioxidant	DHAR	dehydroascorbate reductase
APX	ascorbate peroxidase	DNS-Cl	dansyl chloride
AsA	ascorbate / reduced ascorbate	EDTA	ethylenediaminetetraacetic acid
BC	back-conversion	ETC	electron transport chain
BSA	bovine serum albumin	f. w.	fresh weight
Car	carotenoids	FAAS	flame atomic absorption spectroscopy
CAT	catalase	FAD	flavin adenine dinucleotide
CAX	cation exchanger	GABA	γ-aminobutyric acid
CC	climate change	GLDH	L-galactano-γ-lactone dehydrogenase
CDF	cation diffusion facilitator	GN	Gold Nugget
Chl	chlorophyll	GPOX	guaiacol peroxidase
CO ₂	carbon dioxide	GPX	glutathione peroxidase
CPA	N-carbamoylputrescine amidohydrolase	GR	glutathione reductase
CTL	control		

GS	glutathione synthetase	MPBQ	2-methyl-6-phytylbenzoquinol methyltransferase
GSH	glutathione	MS	Murashige and Skoog
GSSG	glutathione disulfide	MT	metallothioneins
GST	glutathione S-transferase	MTP	metal tolerance proteins
H ₂ O ₂	hydrogen peroxide	N ₂	nitrogen
HGA	homogentisic acid	NA	nicotianamine
His	histidine	NADPH	nicotinamide adenine dinucleotide phosphate
HM	heavy metals	NaN ₃	sodium azide
HNO ₃	nitric acid	NBDs	nucleotide-binding domains
HPLC	high performance liquid chromatography	NBT	nitroblue tetrazolium
HPLC-UV	HPLC with UV detection	NCBI	National Center for Biotechnology Information
HPPD	4-hydroxyphenylpyruvate dioxygenase	NiSO ₄ ·6H ₂ O	Nickel sulfate hexahydrate
HPT	homogentisate phytyltransferases	NO	nitric oxide
HS	Hoagland's nutrient solution	O ₂ ⁻	superoxide anion
HUGO	Human Genome Organization	·OH	hydroxyl radical
IREG	iron-regulated protein	P5C	Δ ¹ -pyrroline-5-carboxylate
IRT1	IRON REGULATED TRANSPORTER 1	P5CR	Δ ¹ -pyrroline-5-carboxylate reductase
JTT	Jones-Taylor-Thornton	P5CS	Δ ¹ -pyrroline-5-carboxylate synthetase
KI	potassium iodide	P680	PSII primary donor
LP	lipid peroxidation	PA	polyamine
MDA	malondialdehyde	PAO	polyamine oxidase
MDHAR	monodehydroascorbate reductase	PAR	photosynthetically active radiation

PC	Purple Calabash	SD	standard deviation
PCD	programmed cell death	SDG	Sustainable Development Goals
PDP	phytyl diphosphate	<i>SIEF1</i>	<i>S. lycopersicum</i> <i>ELONGATION FACTOR 1 – ALPHA</i>
PEG	polyethylene glycol	SN	supernatant
PK	potassium phosphate buffer	Spd	spermidine
PMSF	phenylmethylsulphonyl fluoride	SPDS	Spd synthase
POX	peroxidase	Spm	spermine
Pro	proline	SPMS	Spm synthase
PSI	photosystem I	TAE	tris-acetate-EDTA
PSII	photosystem II	TC	terminal catabolism
Put	putrescine	TCA	trichloroacetic acid
PVPP	polyvinylpyrrolidone	TMDs	transmembrane domains
qPCR	quantitative real-time polymerase chain reaction	UV	ultraviolet
ROS	reactive oxygen species	γ -ECS	γ -glutamyl-cysteinyl synthetase
RT	room temperature	YSL	YS1-like protein
RuBisCO	ribulose-1,5-bisphosphate carboxylase/oxygenase	ZAT	zinc transporter

1. Introduction

1.1. GROWING CROPS UNDER A CHANGING ENVIRONMENT

The debate around climate change (CC) has already shifted from whether it is happening to how to deal with it. According to roughly all predictions and reviews on the subject, in the next decades, the catastrophic effects of CC will become even more impactful on food production and quality (Stocker et al., 2001; FAO, 2008; Smith and Gregory, 2013; Lipper et al., 2014; Esham et al., 2017; Nazir et al., 2017; FAO, 2018a). These adverse effects arise as a consequence of the expected increased frequency of some abiotic stresses (IPCC, 2007; FAO, 2008; IPCC, 2014; FAO, 2018), along with the growing probability of pests and diseases (Ceccarelli et al., 2010). Continued emissions of greenhouse gases will rise annual temperatures and reduce water availability in important crop-growing regions (IPCC, 2007, 2014; Ainsworth & Ort, 2010; Nguyen et al., 2016). Changes in temperature, precipitation, soil moisture and salinity, along with the increased risk of storms, wildfires, pests and diseases and the implementation of water use restrictions, are expected to cause serious losses in agricultural productivity, especially in developing countries (Stocker et al., 2001; de la Peña and Hughes, 2007; Wassmann et al., 2009; FAO, 2018a; Amwata et al., 2019; Mersha and Leta, 2019). For an inclusive insight into the many challenges imposed by global warming and CC, the internationally renowned documentary films and series “Our Planet” (2019), “Before the Flood” (2016), “An Inconvenient Truth” (2006) and “Sustainable” (2016) are highly recommended, as they are scientifically supported by leading researchers in these fields. According to the FAO’s Work on CC (2018a), agriculture embraces about 26 % of all damage caused by CC in developing countries, placing food production at risk in regions where food availability is already scarce. The effects of CC on food production have already affected people’s lives in recent years. Around 2.5 billion people in rural areas of developing countries depend directly on agriculture for their earnings. Their vulnerability to adverse climatic conditions in a changing environment, along with higher and more volatile food prices, could explain the recent and alarming rise in the global number of hungry people (from 17 million up to 821 million in 2017) (FAO, 2008; FAO, 2018a).

Furthermore, agriculture is also part of the CC problem, contributing directly to the global warming effect with approximately 20 % of the annual global emission of greenhouse gases, and indirectly through changes in land use, such as deforestation and soil erosion (Aydinalp and Cresser, 2008; FAO, 2018a). However, as mentioned above, while no other sector is more vulnerable to drastic shifts in weather conditions,

agriculture is not only a contributor to CC, but one of the most affected by it. In this sense, it becomes imperative for governments and plant scientists to find effective and low-cost ways, by which agriculture could transform from being part of the CC problem to become part of its solution. Only in this way, it will be possible to sustain food production on an overpopulated planet, nurturing a healthy and peaceful lifestyle for all human beings around the world. Fortunately, climate action in agriculture has finally become a priority to many countries. In fact, over 90 % of commitments under the Paris Agreement include decisions for the agricultural sector (FAO, 2018a) and the problems around agriculture and food production are addressed in all of the 17 Sustainable Development Goals (SDG) for the 2030 Agenda, covering important actions to end poverty and hunger, as well as responding to CC and sustaining natural resources. According to Olesen et al. (2011), farmers across Europe are currently adapting to CC, mainly by changing the timing of cultivation and selecting different crop species and cultivars. Although other traditional agricultural practices, such as tillage and irrigation, alleviate stresses due to salinity or drought, the development of stress tolerant cultivars is considered detrimental to achieve higher yields in stressful environments (Foolad, 2007). In order to ensure the food supply needed to meet the demand of a growing world population, plant researchers have been putting effort into the development of new strategies for agricultural adaptation, damage mitigation and stress resilience, so that plants can cope with the harmful effects of CC (Ceccarelli et al., 2010; Lipper et al., 2014). Among these, are the adoption of varieties more resilient to metal stress, salinity, heat, and/or drought, to replace the most common susceptible cultivars of crops and vegetables. For a few plants, tolerant varieties, obtained through breeding, grafting and genetic engineering approaches, are already being cultivated at large scales (Ashraf & Harris, 2005; Bitá & Gerats, 2013; Ceccarelli et al., 2010; Joseph & Jini, 2011; Vinocur & Altman, 2005).

1.2. DROUGHT: A THREAT TO AGRICULTURAL PRODUCTIVITY WORLDWIDE

CC is projected to aggravate conditions of high temperatures and drought in the Mediterranean Basin, western USA, southern Africa, north-eastern Brazil, southern and eastern Australia and south-east Asia, reducing the hydropower potential, water availability and crop productivity in these already vulnerable regions (IPCC 2007, 2014; Nguyen et al., 2016). Water availability is one of the major limitations for plant productivity (Nguyen et al., 2016). The occurrence of drought is being considered the worldwide key threat for a wide range of biological, agronomical, industrial and socioeconomical practices, particularly food production (Hanjra and Qureshi, 2010). Currently, 36% of the

world population lives in regions where water is a limited resource (Safriel and Adeel, 2005). Agriculture is a major user of fresh water worldwide, accounting for up to 90% of total water consumption in some regions (FAO, 2008; Hoekstra and Mekonnen, 2012). Given the current trend in annual water usage, it is expected that, by 2030, it will rise to 6.9 trillion m³, being 40 % more than what can be provided by natural water supplies (Gilbert, 2010). Water use for crop cultivation is soon approaching its planetary limits (Bodner et al., 2015), and the area of drylands and arid soils is expanding, which will probably aggravate the losses in agricultural productivity (Rosenzweig et al., 2001; Stocker et al., 2001; FAO, 2008; FAO, 2018a).

1.2.1. Water stress induces physiological and biochemical disorders in plants

When plants are exposed to significant periods of drought, they enter the stage of water stress, impairing growth, development, yield and ultimately leading to plant death (Bodner et al., 2015). Drought alone induces a range of physiological and biochemical responses in plants, including reductions in carbon dioxide (CO₂) assimilation rates, transpiration and net photosynthesis, damage to the photosynthetic machinery, reduced chlorophyll (Chl) fluorescence, stomatal closure, along with higher accumulation of ROS, osmoprotectors and antioxidants (AOXs) involved in stress tolerance (Basha et al., 2015; Bodner et al., 2015; Brdar-Jokanovic and Zdravkovic, 2015; Farooq et al., 2009; George et al., 2013; Kumar et al., 2017; Sánchez-Rodríguez et al., 2010; Shinozaki and Yamaguchi-Shinozaki, 2007; Zgallai et al., 2005). The stomatal closure and consequent reduced transpiration raises internal plant temperatures, which could, in turn, exacerbate the effects of the frequently simultaneous exposure of plants to heat stress (Rosenzweig et al., 2001; Zandalinas et al., 2018). The most noticeable effect of drought is the delayed growth and wrinkle of plants' aerial parts, leading to a reduced leaf area, lower photosynthetic efficiency and lower production of fruits and seeds (Bodner et al., 2015). Water stressed plants are also more prone to fall and break under strong winds and the effects of drought on plants can exacerbate soil erosion, affecting future crop productivity (Rosenzweig et al., 2001). Prolonged and/or intense water stress finally decreases cell membrane stability leading to irreversible damage (Bodner et al., 2015). Osmotic adjustment is a key response of plants to maintain cell turgor under drought conditions, by lowering internal osmotic potential, increasing the water potential gradient to soil and thereby maintain water uptake and expansive growth for a longer time (Farooq et al., 2009). Furthermore, osmotic adjustment enhances root elongation in dry soil (Bodner et al., 2015). In fact, the ability of continued elongation of roots under water stress has been

suggested as an important indicator of drought resistance in tomato plants (Kulkarni and Deshpande, 2007). The effects of drought on plants' redox homeostasis will be discussed in more detail in section 1.6.

Overall, besides the direct, additive and long-lasting impacts of drought events in plants, it has also been noticed that this condition increases the vulnerability of crop systems to other types of abiotic stressors, particularly to coexistent CC-related threats, such as high temperatures, high solar irradiance and strong winds, soil erosion and waterlogging, as well as to biotic stresses caused by pests and diseases, whose life-cycles and geographical distributions are also being affected by CC (Rosenzweig et al., 2001). Therefore, new strategies of adaptation to the changes in rainfall patterns and to enhance water-use efficiency on cropping systems that could help reduce the negative impact on food production must be developed in the coming decades (Bodner et al., 2015). Although countries must make investments individually, worldwide collaboration of governments, organizations, scientists, and individuals is needed to address these issues on a global basis. The forthcoming strategies should focus on agricultural and biotechnological research, as well as on the investment in new technologies that can reduce or avoid the impacts of water scarcity (Takle and Hofstrand, 2015).

1.2.2. The challenge of inducing drought to plants in a laboratory

Although numerous studies have already been set to assess the effects of drought on tomato cultivars, water stress has often been imposed by suppressing the irrigation in hydroponic systems (Çelik et al., 2017; Zhou et al., 2019), which means that not only would these plants be exposed to drought, but probably also to nutritional imbalances, that could be just as responsible for the observed and reported physiological damages as the water deficit per se. These limitations are recurrent in experimental setups which aim to simulate drought under controlled conditions, and the difficulty of adequately controlling the water potential in the root microenvironment has driven the drought stress research to the development of new approaches (Osmolovskaya et al., 2018). Currently, the use of biologically inert polymeric osmolytes is considered preferable and advantageous (Cui et al., 2019), and most drought stress models are now using the high-molecular-weight osmolyte polyethylene glycol (PEG) with an average molecular weight of 6000 Da, as an osmoticum added to the watering solution (George et al., 2013; Meng et al., 2016; Kumar et al., 2017; Osmolovskaya et al., 2018). This approach simulates drought by applying osmotic stress to plants (Cui et al., 2019). Similar events occur in natural soils with low water availability, as the solutes become more concentrated (Osmolovskaya et al., 2018). Molecules of PEG 6000 can effectively decrease the water

potential of the medium, being large enough not to be absorbed by plants (Saint-Claire, 1976; Carpita et al., 1979; Osmolovskaya et al., 2018). The use of low molecular weight PEG (such as 4000 Da) in these types of experiments can lead to its absorption and accumulation in plant roots, which might result in plant injury. Because PEG 6000 does not enter the apoplast, water is withdrawn from the cells. Therefore, this PEG solution mimics dry soil more closely than interrupted irrigation or than solutions of lower molecular osmoticum (Verslues et al., 1998; Cui et al., 2019).

Cultivated tomato varieties are generally sensitive to PEG 6000-induced water stress, presenting considerable physiological changes under PEG treatments, including during seed germination, seedling emergence, vegetative growth, and reproduction (Foolad, 2007). The decline in growth under water stress induced by PEG has been reported in different crops, including tomato cultivars (George et al., 2013). Significant decreases in germination percentage and rate, root and shoot length as well as dry weight have been observed in tomato plants under increasing PEG 6000 concentrations (Abdelrahem and Ahmed, 2007; Kulkarni and Deshpande, 2007; Aazami et al., 2010; Shamim et al., 2014; Brdar-Jokanovic and Zdravkovic, 2015; Kumar et al., 2017). The induction of oxidative stress and the activation of the AOX defenses has also been reported in several plants under PEG-induced drought, including tomato (Türkan et al., 2005; Laxa et al., 2019).

1.3. ENVIRONMENTAL CONTAMINATION BY HEAVY METALS (HM): NICKEL (Ni) AS A CASE-STUDY

The increasing rate of urbanization and industrialization worldwide, alongside the fast population growth, are the main contributors to the anthropic sources of HM in the environment. Alarming levels of these chemicals are currently present in several environmental matrices, including soils and water used in agricultural fields (Nagajyoti et al., 2010). Although HM occur naturally due to weathering processes and geological activity, and despite their important roles on soil composition and nutrient cycles, they can be easily found in soils at much higher levels than expected, imposing toxicological risks to both eco- and agrosystems. As a part of a gigantic vicious circle, agriculture itself is also partly responsible for the HM soil contamination, as a result of the extensive use of limes, manure, sewage sludge, polluted irrigation waters and metal-based fungicides and fertilizers. Because of these procedures, agriculture is now a significant source of metals, such as cadmium (Cd), chromium (Cr), nickel (Ni), lead (Pb) and zinc (Zn) in soils. As HM are non-biodegradable compounds, their overuse and long-term

accumulation in the fields exacerbate their threats to the growth and productivity of crops and vegetables (Nagajyoti et al., 2010). Although several studies have been set out to find solutions to prevent environmental contamination by HM and to reduce the agronomic damage from this type of pollution (Baker et al., 1994; Clemens, 2001; Giordani et al., 2005; Vinocur and Altman, 2005; Shah and Nongkynrih, 2007; Chen et al., 2009), the levels of HM in the environment are still expected to rise in the next decades (Bradl, 2005; Nagajyoti et al., 2010) and the conventional outdoors agricultural facilities are not technologically prepared to overcome their effects, imposing serious risks to local crop yield and food production.

Ni is the 24th most abundant element on earth's crust and, as a transition state element, has various oxidation states (-1, +1, +2, +3 and +4), but its divalent (Ni^{2+}) state is the most stable form in environment and biological systems (Yusuf et al., 2011). Along with other HM, like Zn, copper (Cu), manganese (Mn), Pb, Cr, and Cd, Ni is a non-biodegradable, inorganic chemical element with a density higher than 5 g cm^{-3} , that over threshold concentrations possess cytotoxic and genotoxic effects on both plants and animals (Sachan and Lal, 2017). As a HM, Ni occurs naturally in the soil crust; however, several anthropogenic activities, such as burning of fossil fuels, use and discharge of electric batteries, industrial and municipal waste treatment, smelting, metal mining, overuse of fertilizers and herbicides, metallurgic and electroplating industries, increase its concentration to toxic levels in the environment (Ameen et al., 2019). To date, Ni has already been found in polluted soils at levels as high as 26.4 g kg^{-1} , much higher than its general range between 3 and 1000 mg kg^{-1} worldwide, with a mean value of 22 mg kg^{-1} in natural soils (Ameen et al., 2019; Chen et al., 2009).

1.3.1. Ni induces stress to crops and vegetables

Ni bioavailability depends not only on the Ni form and concentration, but also on the presence of organic matter, other HM, and on the pH level of the soil or growth medium. Ni absorption rate is reduced for higher pH levels, since this promotes the formation of less soluble Ni complexes, and, on the contrary, is accelerated when the medium is slightly acidic (Chen et al., 2009; Yusuf et al., 2011; Ameen et al., 2019). As represented in **Fig. 1**, Ni enters plants mainly through the root system, directly by passive diffusion into the apoplast, and then symplastically through H^+ -ATPase pump/channel into the vascular tissues (Chen et al., 2009; Sachan & Lal, 2017; Seregin & Kozhevnikova, 2006). Ni is transported to the upper parts of the plant through the xylem tissue, in the form of complexes with several chelates, by using the transpiration stream (see **Fig. 1**) (Ameen et al., 2019; Chen et al., 2009; Sachan & Lal, 2017; Seregin & Kozhevnikova, 2006).

Amino acids, organic acids and peptides are common examples of Ni-chelating agents, which help assuring that Ni reaches the most distant parts of the plant without being trapped in the cell walls of the xylem bundle (Ameen et al., 2019). Once inside the cells, Ni can seriously damage the phospholipid membranes and organelle structure, and therefore its chelation in the cytosol is a very important mechanism of metal-stress tolerance. The main metal chelators in plants are metallothioneins (MT), phytochelatins, organic acids, such as malic acid, citric acid and oxalic acid, and amino acids, such as histidine (His) and nicotianamine (NA) (Chen et al., 2009; Clemens, 2001; Krämer et al., 1996; Sachan & Lal, 2017). Additionally, the reactive oxygen species (ROS) scavenging molecules polyamines (PAs), which will be later discussed in section 1.5.2.10, can also be produced in response to Ni stress, perhaps, acting as Ni chelating agents (Hasanuzzaman et al., 2019; Shevyakova et al., 2008). Since Ni is taken up as a divalent cation, its absorption in high concentrations decreases the uptake of other divalent cations, which share the same type of carriers, such as Mg^{2+} , Fe^{2+} , Mn^{2+} , Cu^{2+} , and Zn^{2+} , leading to deficiencies in other essential nutrients (Palacios et al., 1998).

When exposed to higher levels of Ni, plants exhibit visible signs of metal-induced toxicity, such as the inhibition of seed germination, significant decreases in root and apical growth, decreased dry weights of roots and shoots, reduced leaf area and Chl content, impaired photosynthesis and sugar transport, induction of chlorosis, necrosis and wilting, increased levels of lipoxygenase activity and of malondialdehyde (MDA), ROS and proline (Pro) (Ameen et al., 2019; Balaguer et al., 1998; Chen et al., 2009; Kumar et al., 2015; Palacios et al., 1998; Rehman et al., 2016; Sachan & Lal, 2017; Yusuf et al., 2011). These signs are thought to be the consequences of two main physiological disturbances: i) interference of Ni with the uptake of other essential nutrients and ii) Ni-induced oxidative stress (Chen et al., 2009; Yusuf et al., 2011). The toxicity imposed by exposure to Ni is not equally harmful for all plant species. In fact, the critical toxicity levels of Ni differ from more than 10 mg kg^{-1} dry mass in sensitive species and 50 mg kg^{-1} dry mass in moderately tolerant species, to levels as high as $1,000 \text{ mg kg}^{-1}$ dry mass in Ni hyperaccumulator plants, such as *Alyssum* and *Noccaea* species (Yusuf et al., 2011). In this sense, Ni-tolerant plants appear as attractive sources of new agronomic tools and biotechnological applications. According to Sachan & Lal (2019), understanding the biochemical machinery responsible for Ni tolerance in hyperaccumulator plants, is a very important starting point to develop tolerant plants suitable for cultivation in Ni-contaminated soils.

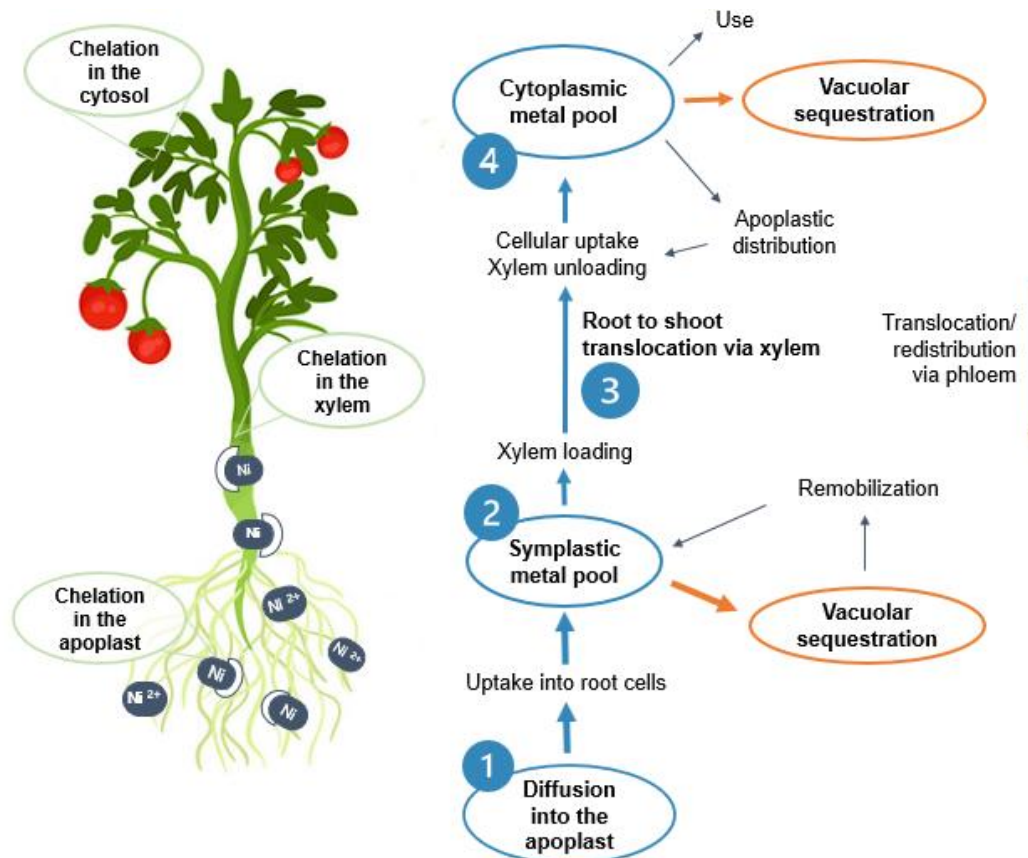


Figure 1 Ni uptake, transport, and detoxification in plants. Ni is absorbed by plants in the form of Ni^{2+} , via the cation transport system or, through secondary active transport, when chelated to organic molecules. Most Ni is retained in the apoplast and in the vacuoles of the roots. Ni is translocated from roots to shoots through the transpiration stream, via xylem, which is regulated by metal-binding compounds. In stems and leaves, Ni is mainly directed to the vacuoles, cell walls and epidermal trichomes, associated with chelators. This schematic representation was adapted and modified from the figures present in reviews by Chen et al. (2009), Krämer et al. (2007), Sachan & Lal (2019), and Yusuf et al. (2014).

1.3.2. Vacuolar sequestration of Ni – the perfect hideout!

The activation of specific defense systems leads to the production of stress signals that initiate biochemical adjustments. Under Ni stress, various attempts to neutralize its action take place at the cellular level (Ameen et al., 2019). As mentioned above, one of the first mechanisms of Ni detoxification is its chelation with amino acids, organic acids, or peptides (**Fig. 1**). In plant cells, chelating agents buffer the cytosolic metal concentrations, delivering the essential metal ions to specific cytosolic proteins and organelles and regulating the detoxification and storage of excess metal, mainly through vacuolar sequestration (Clemens, 2001). Saito et al. (2010) showed that Ni-tolerant tobacco cell lines accumulated more Ni than the wild type cells. These authors reported that Ni tolerant cells accumulated less Ni in the cytosol, that 95% of vacuolar Ni was in the form of Ni-citrate complexes, and that approximately 60 % of the total His and citrate were found inside the vacuoles, in the form of such Ni chelates, while free Ni was virtually

absent. These findings agreed with previous observations by Krämer et al. (2000) in the hyperaccumulator tiny wild mustard *Noccaea goesingensis* (formerly known as *Thlaspi goesingense*), which possess the ability to store high amounts of Ni into its vacuoles, mainly chelated to citrate. The efficient chelation of Ni, along with the abundant presence of efficient carriers in the tonoplast, could present the distinctive adaptations of these species towards metal stress. Depending on the nutritional status of the plant, HM accumulated in the vacuoles may be either re-exported to support the growth of new organs, or they can remain stored during the entire lifetime of the plant (**Fig. 1**) (Martinoia, 2018). Previous studies have demonstrated that Ni accumulates more in roots than in shoots of several plants, including tomato (Kazemi, 2012; Sachan & Lal, 2017). Vacuolar sequestration of Ni explains why over 50 % of absorbed Ni accumulates in the roots of most plants, hampering the passage of this HM to aerial organs (Chen et al., 2009). Additionally, during the apoplastic transport of Ni in root tissues, the cell wall can also function as an important chelator of this toxic metal (Mozafari et al., 2013). In stems and leaves, Ni is mainly redirected to the vacuoles, cell walls and epidermal trichomes, being bonded to chelators, such as NA, His, citrate, organic acids and proteins, such as permeases, MT, metallochaperones and YS1-like proteins (YSLs) (Chen et al., 2009). The level of Ni chelation and vacuolar sequestration depends mainly on the amount of Ni, exposure time and plant species (Ameen et al., 2019).

The transport and accumulation into the vacuoles are the final steps in the detoxification of potentially toxic chemicals, HM, and metalloids in plants. Accumulation of HM in the vacuoles depends on the presence and activity of carriers residing in the tonoplast (Clemens, 2001). This is the case of primary active transporters, such as P-type ATPases and ATP-binding cassette (ABC) transporters, requiring ATP hydrolysis, and secondary active antiporters, such as iron-regulated protein (IREG), cation exchanger (CAX) and transmembrane pH gradient (Krämer et al., 2007). Ni enters vacuoles against an electrochemical gradient, though the action of efflux tonoplast transporters (Krämer et al., 2007).

1.3.3. Transport of HM through the tonoplast

The ABC superfamily is one of the largest protein groups within the kingdoms of archaea, eubacteria and eukarya (Andolfo et al., 2015). ABC proteins have been initially reported as membrane-anchored transporters, but other types of ABC proteins with distinctive functions and structures have been identified, including antigen partners, gene regulators, ion channel partners, and ribosome manipulators (Kang et al., 2011; Pang et al., 2013). Regardless of their different functions, every ABC contains at least one

conserved domain of ATPase, which acts as an energy provider. The canonical architecture of ABC transporters comprises two transmembrane domains (TMDs) and two cytosolic nucleotide-binding domains (NBDs) (Rees et al., 2009; Andolfo et al., 2015; Ofori et al., 2018). The two NBDs bind and hydrolyze ATP to generate energy, which leads to conformational changes in the TMDs creating an opening through which the substrate passes. The position of the TMDs ensures the unidirectional transport of the substrate (Rees et al., 2009). Full-size ABC transporters have this typical four domain structure, while ABC transporters with only one TMD and one NBD are called half-size (Ofori et al., 2018). ABC transporters participate in the detoxification of various kinds of biotic or abiotic stresses and hormone signaling. Following the designation rules proposed by the Human Genome Organization (HUGO), ABC proteins were classified in eight subfamilies, ABCA to ABCI (Andolfo et al., 2015; Ofori et al., 2018). Plants, however, do not have any member of the ABCH subfamily. Plants have twice as many ABC proteins as animals, which is thought to be a consequence of adaptations to the several stresses they face under the constraints of their sessile nature (Ofori et al., 2018). Subfamilies E and F, having only two NBD domains, are soluble proteins and do not act as transporters, but their NBDs bind to those of other ABC proteins, possibly regulating their activity (Andolfo et al., 2015; Ofori et al., 2018). Subfamilies ABCA-D and G-H contain membrane anchored transporters with “forward” or “reverse TMD-NBD orientation”, respectively (Andolfo et al., 2015). Plant ABC transporters participate in the transport of secondary metabolites, phytohormones and HM (Ofori et al., 2018). The class C of ABC transporters is, to date, the only class of putative tonoplast-localized ABC transporters (Martinoia, 2018). It has been reported that one of the main roles of ABCC transporters is the transport of HM conjugates with phytochelatins and glutathione (GSH) into the vacuoles of plant cells (Hwang et al., 2016; Martinoia, 2018). This is thought to be an efficient and stress-inducible mechanism for the detoxification of HM after their chelation in the cytosol (Clemens, 2001). Members of the ABCC subfamily are also responsible for the accumulation of anthocyanin in the vacuoles of maize and grape plants, and transport of phytates in *Arabidopsis thaliana*, rice and maize and of folates and Chl catabolites in *A. thaliana* plants (reviewed by Ofori et al., 2018). In the case of HM, the AtABCC3 and AtABCC6 are Cd-inducible and are involved in the transport and detoxification of phytochelatin-Cd conjugates into the vacuoles of *A. thaliana* plants exposed to toxic levels of this HM (Brunetti et al., 2015).

The antiporters of the CAX family are also located in the tonoplast and have been implicated in the vacuolar and cytosolic pH regulation and in the transport of transition metals (Krämer et al., 2007; Martinoia, 2018). CAX transporters can be found in all living

organisms except for mammals and insects (Pittman and Hirschi, 2016; Martinoia, 2018). Initially, CAX antiporters were identified as calcium (Ca) antiporters (Pittman et al., 2011), but later studies have reported that some CAX members can also deliver other divalent cations to the vacuoles, such as Cd, Mn and Zn (reviewed by Martinoia, 2018). The substrate specificity of many CAX proteins was shown to be determined by just one or two amino acid residues (Shigaki et al., 2003; Martinoia, 2018). The latest reviews suggest that, due to their broad substrate specificity, members of the CAX family play important roles in the detoxification of many HM (Martinoia et al., 2007). Research has shown that enhanced expression of CAX genes can provide HM tolerance in plants, increasing the vacuolar sequestration of metals like Cd, Mn, and Zn (reviewed by Pittman and Hirschi, 2016). Studies with *A. thaliana* plants have also shown that the depletion of CAX2 causes higher sensitivity to Mn, Zn and Fe stress and leads to higher accumulation of these HM in the seeds (reviewed by Martinoia, 2018). Another study revealed that the expression of CAX4 is induced in cells of the root apex and lateral root primordia of *A. thaliana* plants under high levels of Ni or Mn or when Ca is depleted (Mei et al., 2009). Furthermore, increased levels of CAX4 led to an increased sequestration of Ca²⁺ and Cd²⁺ into the vacuoles of *A. thaliana* plants (Mei et al., 2009).

Within the ZIP metal transporter family of plants, the first member to be identified was the IRON REGULATED TRANSPORTER 1 (IRT1) in *A. thaliana*, which was initially identified as an iron (Fe) efflux integral membrane protein, with a metal-binding domain, involved in the uptake of Fe from the soil (Eide et al., 1996; Guerinot, 2000; Bughio et al., 2002). To date, other IRT1-like Fe transporters have been isolated. In tomatoes, for instance, these IRT1-like transporters are referred to as SIIREGs (Merlot et al., 2014) or SIIRTs (Eckhardt et al., 2016). In *A. thaliana*, the genes *IRON REGULATED1* and *2* (*IREG1* and *IREG2*), which are co-regulated with *AtIRT1*, have been shown to have a broader specificity for substrates, transporting Ni, Zn, Mn, Cd and cobalt (Co). *AtIREG2* protein, (also known as Solute carrier family 40 member 2, Iron-regulated transporter 2 or Ferroportin-2), has been shown to be responsible for the sequestration of excess Ni in the vacuoles, under conditions of Fe deficiency, displaying increased tolerance to this HM (Schaaf et al., 2006). Moreover, a study by Morrissey et al. (2009) also revealed a role for *AtIREG2* for vacuolar sequestration of Co and for *AtIREG1* in regulating the root-to-shoot translocation of this metal. Besides *A. thaliana*, the involvement of Fe regulated transporters in the detoxification of HM has also been assessed for other plants species. For example, Yokosho et al. (2016) have reported that the tonoplast protein *FeIREG1* was responsible for Al detoxification through sequestration in the root vacuoles of buckwheat plants. In fact, the expression of *FeIREG1* was inducible by the high levels of

Al, representing a fine-tuned regulation of Al homeostasis. Bughio et al. (2002) found that the expression of *OsIRT1* is limited to the root tissues and can be induced under both Fe- and Cu-deficiency, suggesting that *OsIRT1* is not only involved in the uptake of Fe but also in regulating the homeostasis of Cu, and potentially other HM, which have not been evaluated yet. Additionally, the insertion and expression of tomatoes' *SIIRT1* and *SIIRT2* was found to complement metal uptake-deficient yeast mutants, not only in the transport of Fe but also of other HM, being the transient expression of *SIIRT1* in yeast strongly enhanced by Fe starvation (Eckhardt et al., 2016). Merlot et al. (2014) have also identified PgIREG2 as a vacuolar Ni transporter in the hyperaccumulator species *Psychotria gabriellae*. Interestingly, these authors have also found that IREG2's expression was much higher in *P. gabriellae* than in its close relative *P. semperflorens*, a non-hyperaccumulator plant. In this sense, differences in expression of this gene, or homologous genes in other plants, could represent differences in terms of metal tolerance. Although the reports on the induction of *IRT1-like* gene expression in the presence of HM seem contradictory, being this expression stimulated by both the excess of some HM, and by the deficiency of others, in the case of Ni, the common response is an increased expression of *IRT1-like* genes, associated with detoxification strategies, suggesting that Ni uptake and vacuolar sequestration is induced by Ni stress (Merlot et al., 2014; Nishida et al., 2012).

Persans et al. (2001) were the first to isolate and characterize the metal tolerance proteins (MTPs) in the hyperaccumulator plant *Noccaea goesingensis*, as putative vacuolar metal ion transport proteins, members of the cation-efflux family, also known as cation diffusion facilitator (CDF) family (Delhaize et al., 2003). Eukaryotic proteins of the CDF family share an N-terminal signature sequence, which is specific to the family, six transmembrane domains, a C-terminal cation efflux domain, and an intracellular His-rich domain, which is absent in the prokaryotic CDF members. In a genome-wide study, Mäser et al. (2001) identified eight genes in *A. thaliana* encoding proteins with homology to members of the CDF family, which were initially designated AtMTP1 (previously known as zinc transporter (ZAT)), AtMTPa1 - 2, AtMTPb and AtMTPc1 - 4. Nonetheless, all of these AtMTPs proteins lack the His-rich domain, and four (AtMTPc1-4) showed poor conservation of the N-terminal signature sequence and/or C-terminal cation efflux domain (Delhaize et al., 2003; Mäser et al., 2001). The overexpression of *AtMTP1* (*ZAT*) conferred increased resistance to excess Zn and higher ability to accumulate Zn in the roots of *A. thaliana* plants, although the expression of this gene was not Zn-inducible (reviewed by Mäser et al., 2001). With the discovery of new *A. thaliana* genes that encode CDF proteins, and to simplify their nomenclature, *AtMTPs* have been renamed

to *AtMTP1 – 12* (Delhaize et al., 2003). As a result of their phylogenetic relationships with *AtMTP1* (*ZAT*), three other proteins from the *A. thaliana* CDF family, *AtMTP2*, *AtMTP3*, and *AtMTP4*, were also described as Zn transporters and now *AtMTP8 - 11* are the new designations for the previously named *AtMTPc1 – 4* (Delhaize et al., 2003). Persans et al. (2001) have described MTPs as being responsible for the accumulation of metal ions within shoot vacuoles of *A. thaliana*. Accordingly, as reviewed by Ameen et al. (2019), the overproduction of the MTP1 tonoplast protein in *N. goesingensis*, is behind its ability to accumulate high levels of metal inside the vacuoles, conferring a higher tolerance to Ni, Co, and Cd. In fact, the transient expression of *NgMTP1t2* (*TgMTP1t2*), which represents an alternatively spliced transcript of *NgMTP1* (*TgMTP1*), complemented the Ni-sensitive mutant phenotypes in yeast (Persans et al., 2001; Mäser et al., 2001). In rice plants, the expression of *OsMTP1* has been reported to be induced by the exposure to Zn, Cd, Cu, and Fe, and increased the tolerance of *cot1*, *yfc1*, and *smf1* yeast mutants to Zn, Cd, and Ni, respectively (Ricachenevsky et al., 2013). Several reports have also suggested a role of MTPs in conferring tolerance to excess Mn (Delhaize et al., 2003; Delhaize et al., 2007; Chen et al., 2013). In fact, Delhaize et al. (2003) showed that the *AtMTP8 – 11* clustered with the *ShMTP1 - 4* as a major group, separated from the Zn transporters *AtMTP1 – 4*. Additionally, Delhaize et al. (2003; 2007) have reported that the *ShMTP1* from the tropical legume *Stylosanthes hamata*, and the *AtMTP11* (previous *AtMTPc4*) from *A. thaliana*, were shown to confer Mn tolerance to yeast and plants through the vacuolar sequestration of this HM. The transient expression in yeast of a homologous rice gene encoding a specific transporter of Mn, *OsMTP8.1*, also enhanced the tolerance to Mn by increasing its accumulation in the vacuoles (Chen et al., 2013). Besides their role in alleviating the toxic effects of excessive HM, MTPs are also important for the development of wealthy seeds. As reviewed by Ricachenevsky et al. (2013), during the development of barley grains, the expression of *HvMTPs* is enhanced in the cells of the aleurone layer and embryo, where it is involved in the transport and accumulation of Zn in the vacuoles of the endosperm cells. In rice grains, a similar tonoplast localized *OsMTP1* transports Zn, Co, Fe, Cd, and Ni. Like other cation efflux transporters, the selectivity of MTPs towards certain metal ions seems to be dependent on key residues in the amino acid sequences of these proteins (Ricachenevsky et al., 2013).

The functional characterization of most of these proteins in tomato plants still lacks experimental validation, which is why most transporters identified in protein databases are still predicted sequences from the genomic sequences. However, given the homologies between these protein sequences with those of other species, which

have already been described for their involvement in the detoxification of HM, it is becoming increasingly clear that an improved production and activity of these transporters could represent a crucial response of plants to HM-induced toxicity, especially considering that micronutrient transporters often have a broad substrate specificity, being usually capable of transporting different metals or metal conjugates (Ricachenevsky et al., 2013).

1.4. RESEARCH ON ABIOTIC STRESS: DIFFERENCES BETWEEN SINGLE AND COMBINED STRESS APPROACHES

According to the forecasted CC, drought, high temperatures, strong radiation, elevated CO₂ levels and salinity are the main environmental changes that are expected to become common coincident abiotic stressors, especially in the Mediterranean basin and in arid and semi-arid regions of the world, where they will affect numerous important cultures of crops and vegetables (Ragab and Prudhomme, 2002; IPCC, 2014; Rivero et al., 2014; Minhas et al., 2017; Zandalinas et al., 2018). Besides, as mentioned before, agricultural soils are also getting increasingly polluted with toxic HM, from geogenic, but also, and most critically, from expanding anthropogenic sources (Nagajyoti et al., 2010; Minhas et al., 2017).

In the last decades, research on plant's responses towards abiotic stress has been intensively focused on individual stress conditions, such as drought, salinity, or heat. However, in the field, crops and vegetables are usually subjected to an array of different abiotic stresses combined (Mittler, 2006; Suzuki et al., 2014). Recent findings have shown that the molecular, biochemical, and physiological processes activated in plants exposed to one single abiotic stress are distinctive of those in plants exposed to more than one stress at the same time (Mittler, 2006; Suzuki et al., 2014; Zandalinas et al., 2018). When exposed to combined abiotic stresses, plants trigger unique molecular and metabolic responses, which cannot be extrapolated from the well-known adjustments triggered by each stress alone (Mittler, 2006). Furthermore, the co-occurrence of different abiotic stresses results in more complex plant responses, as combined stresses induce different, and sometimes opposing, signaling pathways, which may interact, aggravate, or inhibit each other (Mittler, 2006; Suzuki et al., 2014; Zandalinas et al., 2018). One of the current challenges in this research field is to add more realistic insights into the physiology of open-field crops and vegetables, under present and future scenarios of CC, which could open new doors to the development of more efficient stress avoidance and tolerance strategies. Considering that the most vulnerable farmers are

often threatened by multiple environmental shifts affecting their cultures with several stress factors, the development of broader crop protection strategies is needed (Ahuja et al., 2010). Gene responses induced by multiple environmental stresses are being identified and present a valuable starting point (Ahuja et al., 2010; Rasmussen et al., 2013). Additionally, understanding the consequences of combined stress factors on plant metabolism, particularly, on photosynthesis, oxidative metabolism, and the activity of antioxidant mechanisms, could help find specific molecular targets to be used in breeding, grafting or genetic engineering strategies that could confer tolerance to combined stresses. Cairns et al. (2013) and Rizhky et al. (2002; 2004) have reported that maize, tobacco, and *A. thaliana* plants, respectively, revealed differences on plant physiology, growth and productivity, under combined drought and heat stress when compared to each of these stresses individually (reviewed by Zandalinas et al., 2018). According to them, the tolerance to combined drought and heat stress must also be genetically distinct from tolerance to each individual stresses (Cairns et al., 2013). These results strongly suggest that the combination of drought and heat results in the activation of unique genetic programs. Additionally, studies regarding combined exposure of plants to environmental changes and soil pollutants have revealed that both additive and contrasting effects can appear (Mittler, 2006; Suzuki et al., 2014; Zandalinas et al., 2018). HM stress is commonly reported to cause a higher detrimental effect on plant growth when combined with other abiotic stresses (de Silva et al., 2012; Suzuki et al., 2014). For example, in an experiment by Ain et al. (2016), plants under salinity stress exposed to Ni showed an aggravation of the HM's toxic effects (Ameen et al., 2019). Regarding drought, for the same HM, Ameen et al. (2019) elucidated that the availability of Ni to plants could be impaired under water stress, leading to Ni deficiency, or reducing its toxicity, when present in high concentrations in the soil. However, contrasting conclusions were taken from findings by de Silva et al. (2012), whose experiments revealed that the exposure to combined drought and Ni reduced the growth of red maple in an additive manner by decreasing the content of Chl and altering the xylem structure and hydraulic conductivity. The Ni-induced harmful effects on Chl seem to be maintained under combined exposure to other abiotic stresses, particularly when those stressors alone also cause damage to the photosynthetic apparatus (Suzuki et al., 2014). As reviewed by Mittler (2006), the combined exposure of plants to heat and salinity and/or HM stress is also likely to induce an aggravation of the responses to each stressor, since the increased transpiration caused by heat could result in an enhanced uptake of salt and/or HM from the soil.

Although there is already a significant body of research regarding the interactions between different stresses (Mittler, 2006; Suzuki et al., 2014), the reported effects are not always consistent (e. g. combined drought and Ni stress, mentioned before), since the interaction between two stresses depends not only on the intensity, time and mode of exposure to each stress, but also on the plant species, among other factors. Therefore, it should be noted that there is still a huge gap of knowledge about the effects that the future climate will have on crops and vegetables (not to mention the different cultivars of each), being urgent to investigate in depth the combined effects of the main stresses, using the most realistic approaches of exposure (Zandalinas et al., 2018).

1.5. ABIOTIC STRESS-INDUCED REDOX DISORDERS: A SNEAK PEEK INTO OXIDATIVE STRESS AND ANTIOXIDANT (AOX) SYSTEM

Plants have developed many ways to sense and manage abiotic stresses. Due to their sessile nature, plants, unlike animals, are unable to avoid unfavorable environmental conditions; however, they have developed a number of anatomical, developmental, biochemical, physiological and molecular adaptations and acclimation processes which allow them to strive and counteract the negative effects of such conditions (Taiz and Zeiger, 2012). Plant responses to abiotic stresses can either be stress inducible or continuously present, forging the functioning and shape of plants as we know them. The morphological, biochemical, and molecular adjustments to environmental stimuli are mainly stress inducible, being dependent on the rapid activation of signaling cascades (Mignolet-Spruyt et al., 2016; Vinocur & Altman, 2005). One well-known response to abiotic stress is the induction of oxidative stress. Although specific plant responses can be triggered under certain stressful conditions, the induction of oxidative stress is common to practically all types of stress (Gill and Tuteja, 2010a; Sharma et al., 2012; Soares et al., 2019a).

Although molecular oxygen is relatively unreactive, its natural and continuous reduction during aerobic cell metabolism leads to the production of reactive species (Choudhury et al., 2017; Mittler, 2017; Soares et al., 2019a). Approximately 1–2 % of the total oxygen consumed by plants is used to generate ROS (Bhattacharjee, 2005; Das and Roychoudhury, 2014). Indeed, plant metabolism relies on the continuous production and removal of ROS, such as singlet oxygen ($^1\text{O}_2$), hydrogen peroxide (H_2O_2), and the radicals superoxide anion (O_2^-) and hydroxyl radical ($\cdot\text{OH}$), which all occur in plant cells as by-products of metabolic pathways in the mitochondria, chloroplasts, peroxisomes,

and cytosol (Mittler, 2002; Mittler et al., 2011; Foyer and Noctor, 2013; Mittler, 2017; Soares et al., 2019a).

1.5.1. The dual side of ROS: from bad guys to signaling rescuers

In contrast with atmospheric oxygen, ROS can oxidize several molecules, including proteins, nucleic acids, and lipids, leading to the oxidative destruction of the cell (Mittler, 2002). For this reason, a tight control of ROS levels is required to sustain the well-functioning of the cells. The balance between ROS production and scavenging can sometimes be disturbed as a result of the activation of signaling cascades, which take place when plants go through abiotic stresses, such as exposure to water deficit, intensive radiation, extreme temperatures, flooding, and pollution (Mittler, 2017; Soares et al., 2019a; Verma et al., 2019). Upon such disturbances, the levels of ROS in the cytosol and inside organelles can rapidly achieve levels that become harmful to the cellular homeostasis. Such rapid production of ROS is called an oxidative burst and their impacts on DNA, RNA, protein, and membrane oxidation and damage are collectively known as oxidative stress (Mittler, 2002; 2017; Soares et al., 2019a).

The first ROS to be formed is usually $O_2^{\cdot-}$. It is mainly produced in the complexes I and III of the mitochondria and in the photosystems I and II (PSI and PSII) of the chloroplasts due to partial reduction of dioxygen (O_2) or as a result of transfer of energy to O_2 , but it can also be produced in peroxisomes, glyoxysomes, and even in the cell wall (Sharma et al., 2012; Das and Roychoudhury, 2014; Soares et al., 2019a). Normally, during non-cyclic electron transport chain (ETC), the interaction of cytochrome c oxidase with O_2 generates H_2O . However, occasionally, O_2 reacts with the different components of the ETC to give rise to $O_2^{\cdot-}$ (Das and Roychoudhury, 2014; Soares et al., 2019a). Having a short half-life of 1 - 1000 μs and low mobility, $O_2^{\cdot-}$ is considered only moderately reactive, but its powerful reducing ability allows it to undergo further reactions and generate more toxic ROS, such as $\cdot OH$ and 1O_2 , through the Haber-Weiss reaction (Halliwell, 2006; Sharma et al., 2012; Das and Roychoudhury, 2014; Soares et al., 2019a).

The most reactive and toxic ROS, $\cdot OH$, is formed from $O_2^{\cdot-}$ and H_2O_2 through the Fe catalyzed Haber–Weiss reaction. At neutral pH, $\cdot OH$ can damage different organelles, through lipid peroxidation (LP), protein damage and membrane destruction. Its formation is subject to inhibition by superoxide dismutase (SOD, EC 1.15.1.1) and catalase (CAT, EC 1.11.1.6), which limit the availability of $O_2^{\cdot-}$ and H_2O_2 , respectively. Since there is no

existing enzymatic mechanism to scavenge this toxic radical, the excess accumulation of $\cdot\text{OH}$ usually causes cell death.

$^1\text{O}_2$ is the most atypical ROS, since it is generated by the energy transference from triplet Chl (3Chl^*), carbonyls or excited PSII primary donor (P680) to O_2 , independently of electron transfer (Soares et al., 2019). Its production is induced under strong light and/or low CO_2 assimilation rates. $^1\text{O}_2$ can cause severe damages to both PSI and PSII, presenting a serious threat to the entire photosynthetic system (Sharma et al., 2012; Das and Roychoudhury, 2014; Soares et al., 2019a). Although its short half-life (3 μs), $^1\text{O}_2$ quickly diffuses and affects a broad range of targets, including proteins, pigments, nucleic acids, and lipids (Das and Roychoudhury, 2014). Much of the oxidative inactivation, caused by over-excitation of the photosynthetic ETC and induced loss of PSII activity is caused by $^1\text{O}_2$ (Foyer, 2018).

The moderately reactive H_2O_2 is formed in ETCs of chloroplast, mitochondria, endoplasmic reticulum, and plasma membrane, as well as during β -oxidation of fatty acid and photorespiration, when O_2^- undergoes both univalent reduction as well as protonation and can be easily dismutated to H_2O_2 , under low pH conditions, or through a thylakoid Cu/Zn-SOD catalyzed reaction (Soares et al., 2019a). H_2O_2 is moderately reactive, is easily diffused across membranes, because it does not have any unpaired electrons, and has the longest half-life (1 ms) when compared to other ROS, triggering oxidative stress far from its site of production (Sharma et al., 2012). Within the Haber-Weiss process, the last step, known as Fenton reaction, comprises the H_2O_2 -induced oxidation of Fe^{2+} , resulting in the production of $\cdot\text{OH}$, a far more damaging ROS. H_2O_2 is now starting to be considered as a secondary messenger, due to its involvement in the activation of a large number of signaling pathways, both involved in the triggering of acclimation responses to stress, as well as in physiological processes, regulating senescence, photorespiration and photosynthesis, stomatal aperture, cell cycle, growth and development (Gill and Tuteja, 2010a). Notwithstanding, in high levels, H_2O_2 exerts toxic effects on plant cells, leading to LP, and programmed cell death (PCD). H_2O_2 can oxidize cysteine or methionine residues and thiol groups of enzymes as well as thiolate residues of transcription factors, inactivating them (Gill and Tuteja, 2010a; Sharma et al., 2012). The levels of this ROS must be kept under control by the activity of AOX enzymes such as dismutases, reductases and peroxidases, in order to prevent oxidative stress (Halliwell, 2006).

In recent years, it has become evident that besides their toxic potential, ROS also play an important signaling role in plants (Das and Roychoudhury, 2014). Indeed, plants

master redox control, using ROS and AOXs to control almost every aspect of their physiology (Foyer and Noctor, 2013). Despite their harmful effects, in homeostatic concentrations, ROS function as signaling agents, important for numerous metabolic processes, including the regulation of responses to environmental stresses (Gill and Tuteja, 2010a; Mittler, 2017). ROS can act as signals through chemical reactions with specific residues of target proteins, such as cysteine residues, leading to covalent protein modifications. Another primary target of ROS are low-molecular-weight thiols, such as GSH. ROS sensors activate signaling cascades that can ultimately affect gene expression. Alternatively, ROS are also capable of oxidizing the components of signaling pathways, affecting them directly or change gene expression by targeting and modifying the activity of transcription factors (Apel and Hirt, 2004). According to Foyer and Noctor (2013), a cell is to be considered as a group of sections, each of which can differently generate and accumulate ROS, as well as AOXs, and proteins susceptible to oxidation and reduction in a way that causes activation of signaling pathways. Therefore, the accumulation of ROS in specific cellular compartments is a very important aspect of their signaling role. The rate of ROS diffusion and reactivity, removal and perception in different cellular compartments, and the integration of ROS-dependent signals determines the overall response of the cell to environmental stimuli (Mittler, 2017). For example, upon an oxidative burst, H_2O_2 and $O_2^{\cdot-}$ accumulate on the extracellular matrix, oxidizing the apoplastic face of the plasma membrane, which generates a redox gradient across the membrane, regulating proteins at the cell surface, such as receptors and ion channels that initiate a cascade of signaling pathways (Foyer and Noctor, 2013).

1.5.2. Plants' sophisticated AOX system – enzymatic and non-enzymatic mechanisms

In order to prevent oxidative-induced damages, plant cells need to balance the levels of ROS, by the action of a powerful AOX system, which includes enzymatic and non-enzymatic mechanisms for ROS scavenging and/or neutralization (Sharma et al., 2012). The enzymatic component of plant's AOX system includes enzymes with strong scavenging activity, such as SOD, CAT, ascorbate peroxidase (APX, EC 1.11.1.11), glutathione peroxidase (GPX; EC 1.11.1.9), glutathione reductase (GR, EC 1.8.1.7), glutathione S-transferase (GST; EC 2.5.1.18), guaiacol peroxidase (GPOX, EC 1.11.1.7), monodehydroascorbate reductase (MDHAR; EC 1.6.5.4) and dehydroascorbate reductase (DHAR; EC 1.8.5.1) (**Fig. 2**) (Soares et al., 2019a). Additionally, other smaller molecules are also essential players in the AOX system, either due to their osmoprotective potential, scavenging activity and/or membrane stabilizing abilities. These include osmoprotectants such as sorbitol, mannitol and Pro, being the

latest also an important ROS scavenger, along with ascorbate, GSH, α -tocopherol, carotenoids (Car), flavonoids and PAs (**Fig. 2**) (Groppa et al., 2003; Gill and Tuteja, 2010a; Gill and Tuteja, 2010b; Das and Roychoudhury, 2014; Soares et al., 2019a). In the following topics some of the most relevant components of the AOX machinery will be briefly described, mostly based on some noteworthy reviews written by Gill and Tuteja (2010a; 2010b), Halliwell (2006), Mittler (2002), Sharma et al. (2012) and Soares et al. (2019a). The reading of these review articles is highly encouraged for a more comprehensive insight into the functioning and regulation of plant's AOX system.

ANTIOXIDANT SYSTEM	
<i>Enzymatic component</i>	<i>Non-enzymatic component</i>
<ul style="list-style-type: none"> • SOD • APX • CAT • GR • MDHAR • DHAR • GST • GPX • GPOX 	<ul style="list-style-type: none"> • Ascorbate • Proline • Glutathione • α-Tocopherol • Carotenoids • Phenolic compounds • Polyamines • Sugars • Cysteine • Methionine • Dehydrins • Annexins

Figure 2 Enzymatic and non-enzymatic components of the plant AOX system. Adapted from Soares et al. (2019a).

1.5.2.1. Superoxide Dismutase (SOD)

The AOX enzyme SOD catalyzes the reaction in which O_2^- is dismutated in to H_2O_2 and molecular oxygen. By doing so, SOD has a pivotal role in the detoxification of ROS, affecting the levels of both O_2^- and H_2O_2 and preventing the oxidative damage associated to high levels of O_2^- . Because of its action in O_2^- removal, SOD is also an indirect controller of the production of $\cdot OH$, through the Haber-Weiss reaction, mentioned before. In plants, SOD functions as a metalloenzyme that can be classified in three

classes, depending on the ion it bears in its active center: Cu/Zn-SOD, Mn-SOD and Fe-SOD (Gill and Tuteja, 2010a; Sharma et al., 2012; Soares et al., 2019a). Having two metallic ions in its center, the most abundant isoform, Cu/Zn-SOD, has a different structure and behaves distinctively of the other SOD types. This isoenzyme is found in the cytosol, apoplast, chloroplasts and peroxisomes, while the Mn-SOD is essentially present in the mitochondrial matrix, and the Fe-SOD is coupled to the thylakoid membranes of the chloroplasts (Gill and Tuteja, 2010a).

1.5.2.2. Ascorbate Peroxidase (APX)

APX is regarded as the most ubiquitously distributed AOX enzyme in plant cells. As a member of the class I super family of heme peroxidases, this enzyme is regulated by redox signals and uses two molecules of ascorbic acid (AsA) to reduce H_2O_2 to H_2O with a parallel generation of two molecules of MDHA (Gill and Tuteja, 2010a; Sharma et al., 2012; Soares et al., 2019a). APX activity is greatly dependent on AsA availability (Soares et al., 2019), pointing out the importance of AsA regeneration, through the AsA-GSH cycle, which will be later discussed. APX has a much higher affinity for H_2O_2 , even at low levels, than other H_2O_2 -detoxifying enzymes, such as CAT. Considering the differences on the amino acid sequences, there have been identified five different APX isoenzymes, each with a specific subcellular localization in plant cells. APX isoforms can be cytosolic, stromal, thylakoidal, mitochondrial or peroxisomal. The isoenzymes of APX present inside organelles scavenge the H_2O_2 produced within these organelles, whereas the cytosolic APX removes the levels of H_2O_2 present in the cytosol or apoplast. Although the biological functions of organelle-specific APX are still being discovered, most researchers agree that the cytosolic forms of APX are the ones more involved in the H_2O_2 scavenging response under oxidative stress, while the isoenzymes of APX from chloroplasts are mainly integrated in the homeostatic H_2O_2 signaling pathways (Soares et al., 2019). Extensive research has reported that the activity of APX usually increases in response to abiotic stresses, such as drought, salinity, chilling, metal toxicity, and ultraviolet (UV) irradiation (Sharma et al., 2012). However, in different approaches, stressors such as UV-B and salinity have also been reported to inhibit APX activity (Soares et al., 2019). Nevertheless, the fact that this enzymes' activity is modulated in response to abiotic stress makes it a good cellular indicator of the induction of AOX responses.

1.5.2.3. Catalase (CAT)

CAT, the first AOX enzyme to be discovered and described (Sharma et al., 2012), is a tetrameric heme-containing enzyme responsible for catalyzing the dismutation of H_2O_2 into H_2O and O_2 . This enzyme is mostly found in the peroxisomes, whose aerobic metabolism comprise the main sources of H_2O_2 in plant cells. CAT scavenges the H_2O_2 produced during photorespiratory oxidation and β -oxidation of fatty acids that occur inside this organelle (Halliwell, 2006; Gill and Tuteja, 2010a; Soares et al., 2019a). The confinement of CAT to the sinks of H_2O_2 is thought to be a way of limiting the diffusion of this ROS across the cell (Soares et al., 2019). Contrarily to other H_2O_2 -degrading enzymes, CAT does not require any reducing equivalent, and due to its incredibly fast turnover rate (much higher than APX), CAT occupies a central role in the H_2O_2 scavenging process. In fact, CAT is able to reduce 6 million molecules of this ROS per minute (Gill and Tuteja, 2010a; Soares et al., 2019a). Nevertheless, when compared to APX, CAT presents a much lower affinity for H_2O_2 , which explains why this enzyme's activity is only efficient under high levels of H_2O_2 (Mittler, 2002; Soares et al., 2019a). The different affinities of APX and CAT for H_2O_2 suggest that while CAT might be responsible for the prevention and removal of excess ROS during stress, APX is probably implicated in the regulation of the homeostatic levels of H_2O_2 , to ensure its role as a signaling agent (Mittler, 2002).

1.5.2.4. Proline (Pro)

The osmolyte Pro has been shown to accumulate in the cytosol and vacuoles of plant cells during abiotic stresses such as drought, salinity, extreme temperatures, HM exposure and UV radiations. Pro acts as an excellent osmolyte, maintaining cell turgor through osmotic adjustment and protecting proteins, DNA and membranes against the oxidative damages caused by ROS (Gill and Tuteja, 2010a; Miller et al., 2010; Hayat et al., 2012; Das and Roychoudhury, 2014; Soares et al., 2019a). Pro is synthesized from glutamate via the intermediate Δ^1 -pyrroline-5-carboxylate (P5C), a pathway catalyzed by two enzymes, Δ^1 -pyrroline-5-carboxylate synthetase (P5CS, EC not assigned) and Δ^1 -pyrroline-5-carboxylate reductase (P5CR, EC 1.5.1.2) (Gill and Tuteja, 2010a). The increased biosynthesis (or reduced degradation) of Pro induced by stress, allows it to act as an AOX agent, being able to quench 1O_2 , scavenge $\cdot OH$ and bind to redox-active metal ions (Gill and Tuteja, 2010a; Miller et al., 2010; Soares et al., 2019a). Besides, during Pro biosynthesis, the reduction of glutamate by nicotinamide adenine dinucleotide phosphate (NADPH) increases $NADP^+$ availability, which is required to relieve PSI over-reduction, alleviate cytoplasmic acidosis, and to prevent the breakdown of redox-

sensitive pathways during stress. In this way, Pro also has an indirect role to protect photochemical efficiency of PSI and II (Miller et al., 2010).

1.5.2.5. Ascorbate - reduced (AsA) and oxidized (DHA) forms

AsA, usually referred to as vitamin C, has an important AOX role in plant cells, serving as an electron donor to a wide range of enzymatic and non-enzymatic reactions. AsA is mainly produced by plant cells through the Smirnoff-Wheeler pathway, catalyzed by L-galactano- γ -lactone dehydrogenase (GLDH, EC 1.3.2.3) in the mitochondria, being the remainder generated from D-galacturonic acid. It has been reported that approximately 90 % of the AsA pool is concentrated in the cytosol and apoplast, but significantly high levels have been found in the chloroplasts, while lower levels can also occur in the mitochondria, peroxisome, and vacuole. Under normal conditions, the main content of AsA is found in its reduced form, whose pool is maintained due to MDHAR and dehydroascorbate reductase DHAR activities, enzymes both belonging to the AsA-GSH cycle. AsA is oxidized in two successive steps, starting with oxidation into MDHA via APX. If MDHA is not reduced immediately again to AsA by MDHAR, it is spontaneously converted into dehydroascorbate (DHA), which, then, can only be reduced back to AsA by DHAR, at the expense of GSH (Soares et al., 2019). AsA has been reported to prevent photo-oxidation by pH-mediated regulation of the PSII activity but, given its strong ROS scavenging activity, AsA is also an important line of defense against oxidative stress, membrane and Chl degradation and loss of CO₂ assimilation (Das & Roychoudhury, 2014). By directly interacting with ¹O₂, O₂⁻ and ·OH, AsA, counteracts ROS toxic effects, and, while also acting as an electron donor for APX catalytic activity to reduce H₂O₂ content and generate MDHA. Besides, AsA, in association with other AOXs, can regenerate α -tocopherol from its α -tocopheroxyl radical state (Munné-Bosch and Alegre, 2003; Das and Roychoudhury, 2014; Soares et al., 2019a). However, under stressful conditions, in the presence of high H₂O₂ levels, AsA might act as pro-oxidant, stimulating the Fenton reaction, which generates high levels of ·OH, contributing to the enhancement of oxidative stress.

1.5.2.6. Glutathione (GSH)

GSH is a tripeptide found abundantly in its reduced form in all cell compartments, such as cytosol, chloroplasts, endoplasmic reticulum, vacuoles, and mitochondria. This non-protein thiol is an efficient scavenger of excessive O₂⁻, ·OH and H₂O₂ (Gill and Tuteja, 2010a; Miller et al., 2010; Sharma et al., 2012). Through its involvement in the reduction of DHA, GSH also contributes to the AOX system, regenerating, as previously

mentioned, the powerful AOX, AsA. The biosynthesis of GSH occurs in the cytosol and chloroplasts by compartment specific isoforms of the enzymes γ -glutamyl-cysteinyl synthetase (γ -ECS; EC 6.3.2.2) and glutathione synthetase (GS; EC 6.3.2.3) (Gill and Tuteja, 2010a; Miller et al., 2010; Sharma et al., 2012; Soares et al., 2019a). GSH can bump into multiple reactions, ending up producing glutathione disulfide (GSSG) (two GSH molecules linked by a disulfide bond). It has been reported that under severe stresses, the GSH:GSSG ratio usually declines, increasing cells' vulnerability to oxidation. In this sense, a healthy balance between the levels of GSH and GSSG is essential to maintain the cellular redox homeostasis (Gill and Tuteja, 2010a; Sharma et al., 2012; Soares et al., 2019a). Moreover, GSH is a precursor of phytochelatin, which in turn, play an important role in controlling the levels of free HM. Besides, and elevated GSH concentration has been reportedly correlated with the ability of plants to endure metal-induced oxidative stress (Gill and Tuteja, 2010a).

1.5.2.7. Tocopherols

Tocopherols, lipid-soluble amphipathic molecules with vitamin E functions (Munné-Bosch and Alegre, 2002), are produced from homogentisic acid (HGA) and phytyl diphosphate (PDP). At least five enzymes are engaged in the biosynthesis of tocopherols: 4-hydroxyphenylpyruvate dioxygenase (HPPD, EC 1.13.11.27), homogentisate phytyltransferases (HPT, EC 2.5.1.115), 2-methyl-6-phytylbenzoquinol methyltransferase (MPBQ MT, EC 2.1.1.295), tocopherol cyclase (EC 5.5.1.24) and γ -tocopherol methyltransferase (EC 2.1.1.95) (Munné-Bosch and Alegre, 2002; Gill and Tuteja, 2010a; Soares et al., 2019a). Out of the four isomers of tocopherols found in plants (α -, β -, γ -, and δ -), α -tocopherol is the most abundant and the one with the highest AOX activity (Munné-Bosch and Alegre, 2002; Gill and Tuteja, 2010a; Soares et al., 2019a). Being mainly localized in the thylakoid membrane of chloroplasts, α -tocopherol protects the structure and function of PSII by physically quenching and chemically reacting with ROS present in the chloroplasts. Several plants have been reported to increase their levels of α -tocopherol under abiotic stress (Soares et al., 2019a). According to Munné-Bosch and Alegre (2002), α -tocopherol neutralizes the ROS 1O_2 through a mechanism of energy transference, generating by-products such as quinones and epoxides, including α -tocopherol quinone, which also exhibits AOX properties and seems to be involved in the PSII energy dissipation. The reaction of α -tocopherol with peroxy radicals, which are responsible for LP, produces tocopheroxyl radicals, which can then be integrated in the AsA-GSH cycle, restoring the levels of α -tocopherol (Soares et al., 2019a). In chloroplasts, α -tocopherol helps to prevent oxidative stress and

preserves the integrity of the membranes (Munné-Bosch and Alegre, 2002; Soares et al., 2019a). Furthermore, recent studies have suggested that the functions of α -tocopherol surpass its AOX action. Its involvement in the regulation of phytohormones, indicates that α -tocopherol might interact with other important modules of signal transduction pathways (Munné-Bosch and Alegre, 2002; Soares et al., 2019a).

1.5.2.8. Carotenoids (Car)

Car are an extensive group of pigments found in plants and microorganisms, which serve an important function as photoprotectors, either by dissipating the excess energy or by scavenging of ROS (Gill and Tuteja, 2010a; Sharma et al., 2012; Soares et al., 2019a). In photosynthetic organs, these low-molecular-weight metabolites quench the $^3\text{Chl}^*$ and excited Chl molecules to inhibit the production of $^1\text{O}_2$, protecting the photosynthetic machinery and inhibiting LP. These lipid soluble AOX play many functions in plant metabolism, including the response to oxidative stress. The three main functions of Car in plants are the absorption of light between 400 and 550 nm and their transfer to the Chl, AOX protection of the photosynthetic apparatus and a structural role for PSI assembly and thylakoid membrane stabilization. Besides, Car, along with their by-products, are also crucial to modulate the production of two phytohormones, strigolactones and abscisic acid (ABA), serving as their precursors. The levels of Car, along with Chl, have been reported to decrease under abiotic stresses such as metal stress. Nonetheless, high levels of Car, mainly β -carotenes, have been found to improve the acclimation of plants under adverse conditions (Sharma et al., 2012).

1.5.2.9. Phenolic Compounds

Another group of AOX metabolites are members of the phenolic compounds, which include flavonoids, tannins, hydroxycinnamate esters, and lignin (Sharma et al., 2012). Flavonoids usually accumulate in the plant vacuole as glycosides, but they also occur in cell walls and sub-cellular compartments such as chloroplasts, endoplasmic reticulum, nucleus and as exudates on the surface of leaves and other aerial plant parts (Gill and Tuteja, 2010a; Soares et al., 2019a). Based on their chemical structure, flavonoids can be classified as anthoxanthins, flavanones, flavanonols, flavans and anthocyanidins (Gill & Tuteja, 2010b). Flavonoids have many well-studied functions in plants, from pigmentation of flowers, fruits, and seeds, protection against UV light, signaling functions in plant-microbe interaction and pathogen attack, pollen germination, to a powerful AOX role under oxidative stress (Gill and Tuteja, 2010a; Sharma et al., 2012; Soares et al., 2019a). The AOX power of flavonoids is due to their capacity to scavenge ROS, such as

$^1\text{O}_2$ and H_2O_2 , to serve as substrate for different peroxidases and to inhibit LP by trapping the alkoxy radical (Sharma et al., 2012). In plant vacuoles, flavonoids play a central role in the detoxification of H_2O_2 , through the peroxidase-flavonoid-ascorbate system (Gill and Tuteja, 2010a).

1.5.2.10. Polyamines (PAs)

PAs are small molecular mass polycations, containing two or more amino groups (Kusano et al., 2008). These ubiquitous molecules can be found either in free, covalently conjugated, or non-covalently conjugated forms (reviewed by Chen et al., 2019 and Rangan et al., 2014). The key plant PAs, putrescine (Put; diamine), spermidine (Spd; triamine) and spermine (Spm; tetramine), which have been recently recognized as members of the non-enzymatic AOX system, are involved in the regulation of plant growth, development and many basic cellular processes, including DNA replication, transcription, translation, cell proliferation, modulation of enzyme activities, cellular cation-anion balance and membrane stability (Gill and Tuteja, 2010b; Todorova et al., 2014). Because of their hormone-like, acid neutralizing and AOX properties, as well as for their membrane and cell wall stabilizing abilities, PAs play important roles in regulating embryogenesis, organogenesis, seed germination, flowering, PCD, stress tolerance and foliar senescence (Alcázar et al., 2006; Gill & Tuteja, 2010b; Yu et al., 2019). Superior PAs, such as Spd and Spm, have been described to act mainly as ROS scavenging agents and as membrane protectors. Recent evidence strongly suggests that, under oxidative stress, PAs prevent toxic damages induced by ROS (Soares et al., 2019a), not only by modifying the AOX system, given their recognized ability to interact with enzymes, but also by modulating ROS production and scavenge. In fact, as will be discussed later, despite the $\cdot\text{OH}$ and $^1\text{O}_2$ scavenging ability of PAs, it should be noted that their metabolism also implies the generation of H_2O_2 (Alcázar et al., 2006; Groppa and Benavides, 2008; Gill and Tuteja, 2010b; Sánchez-Rodríguez et al., 2016; Soares et al., 2019; Yu et al., 2019).

As represented in **Fig. 3**, the diamine Put is the first PA to be formed and is the central product in the PAs biosynthetic pathway, serving as a precursor to Spd and Spm (Chen et al., 2019; Rangan et al., 2014). PAs biosynthesis starts mainly from arginine (Arg), which is converted to Put via agmatine by three sequential reactions catalyzed by arginine decarboxylase (ADC, EC 4.1.1.19), agmatine iminohydrolase (AIH, EC 3.5.3.12) and N-carbamoylputrescine amidohydrolase (CPA, EC 3.5.1.53). The freshly formed Put serves as the precursor for other PAs by the action of the enzymes Spd synthase (SPDS, EC 2.5.1.16) and Spm synthase (SPMS, EC 2.5.1.22), which form Spd

and Spm by the sequential addition of aminopropyl groups to Put and Spd, respectively, being these residues gradually provided by methionine, such as decarboxylated S-adenosylmethionine (dcSAM) (**Fig. 3**) (Alcázar et al., 2006; Rangan et al., 2014; Chen et al., 2019). It is known that the catabolism of PAs depends mainly on the action of two types of amine oxidases (reviewd by Wang et al., 2019 and Yu et al., 2019). The ones responsible for Put oxidation (as well as for the oxidation of cadaverine) are called diamine oxidases or Cu dependent amine oxidases (DAO/CuAO), which have a high affinity for diamines, being able to catabolize their oxidation at the primary amino group. DAOs need to bind to Cu or pyridoxal phosphate as cofactors, and their catabolic activity leads to the formation of 4-aminobutanal (which spontaneously cyclizes to Δ^1 -Pyrroline), H_2O_2 , and NH_3 . The second type of amine oxidase is called flavin dependent polyamine oxidases (PAO). These are responsible for oxidizing Spd and Spm, along with their derivatives, at the secondary amino group (Wang et al., 2019; Yu et al., 2019) (**Fig. 3**). PAOs link to flavin adenine dinucleotide (FAD) as a cofactor, and are predominantly found in monocot species, while dicots are usually richer in DAOs (Chen et al., 2019; Rangan et al., 2014). PAOs can be divided into two functionally different groups, as is demonstrated in **Fig. 3**. The first group catalyzes the oxidation and decomposition of Spd and Spm producing H_2O_2 , 1,3-diaminopropane (DAP), and 4-aminobutanal or N-(3-aminopropyl)-4-aminobutanal, whether it refers to Spd or Spm catabolism, respectively. This class of PAOs are usually referred to as terminal catabolism-type PAOs (TC-type PAOs). The second class of PAOs is involved in a process called PA back-conversion, in which the oxidation of Spm leads to Spd and Spd to Put, in a reverse PA synthesis reaction, which produces 3-aminopropanal and H_2O_2 (Wang et al., 2019). Then again, these PAOs are called back-conversion-type (BC-type PAOs). Following a similar distribution pattern as the two types of DAOs, TC-type PAOs, involved in the oxidation and decomposition of PAs, are also located to the apoplast, while the BC-type PAOs are usually present intracellularly, in the peroxisomes (Wang et al., 2019). The compartmentalization of PAs could play a significant role in regulating the rate of their catabolism, since DAOs and PAOs have a well-defined pattern of distribution, which could be related to specific physiological processes (eg lignification or suberization responses in the apoplast) (Rangan et al., 2014), through the production of H_2O_2 , which is a widely recognized signaling molecule with important functions in cell wall maturation processes and stress responses (Mittler, 2017; Yu et al., 2019).

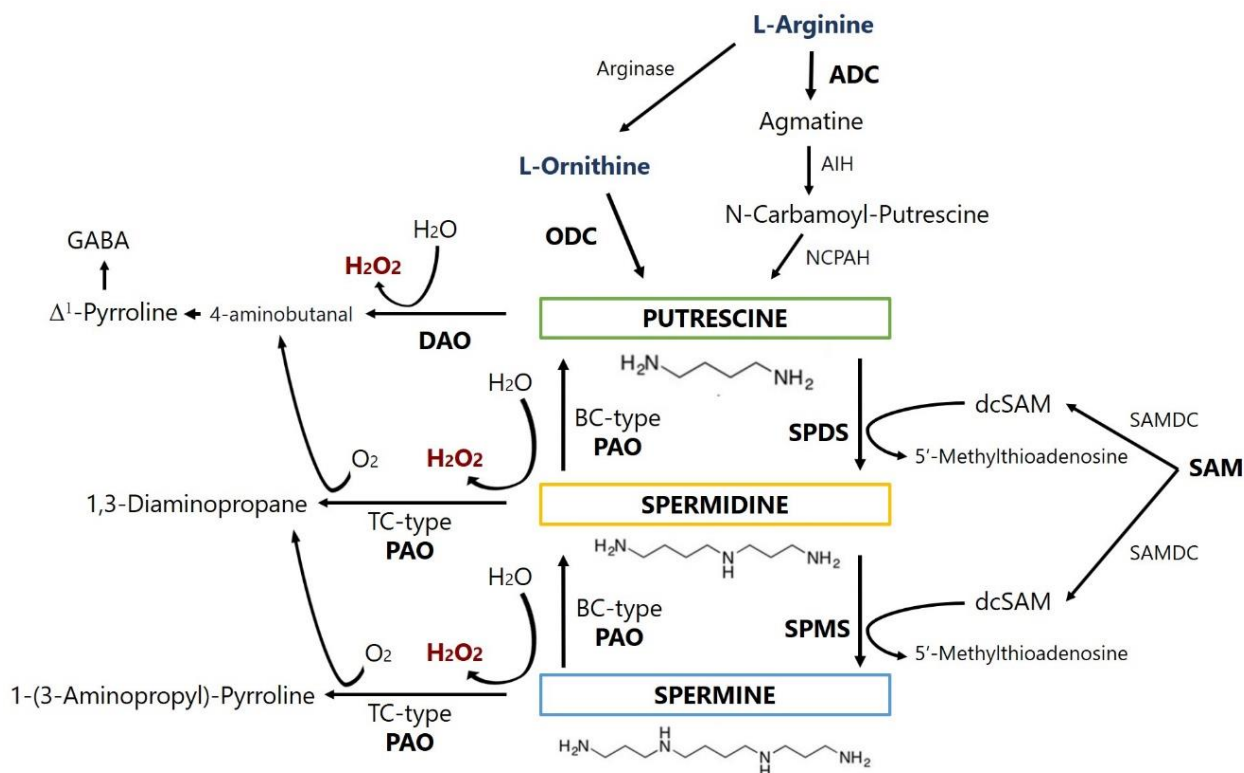


Figure 3 Biosynthesis, back-conversion, and terminal catabolism of Put, Spd and Spm in plants. Adapted from Alcázar et al. (2006), Chen et al. (2019), Gill and Tuteja (2010b), Rangan et al. (2014), Todorova et al. (2014), and Yu et al. (2019).

Recent studies have indicated that plant PAs are involved in the acquisition of tolerance to abiotic stresses. Ranging from transgenic approaches, where genes involved in PAs metabolism are silenced or overexpressed, to the exogenous application of these polycations, the important role of PAs in the defense of plants against drought (Hassan, Ali, & Alamer, 2018), salt (Baniasadi et al., 2018), temperature (Jing et al., 2020) and metals (Hasanuzzaman et al., 2019; Nasibi et al., 2013; Pathak, 2018) has been recently highlighted. Within this matter, the accumulation of PAs under stress, as well as their protective role, are of particular interest, given the recognized abilities of these molecules to improve plant tolerance. PAs in combination with brassinosteroids can also modulate the levels of AOXs like GSH, AsA, Pro and glycine-betaine and the activities of enzymes like GR, SOD, CAT, APX and peroxidase (POX, EC 1.11.1.1), having possible implication on stress tolerance (Rangan et al., 2014). Additionally, PAs have been shown to be produced as a response to HM stress, perhaps, acting as chelating agents or by inducing the production of other chelating agents. In this manner, it is thought that PAs can help plants to transport and detoxify phytotoxic metals, such as Ni and Cd (Shevyakova et al., 2008; Tajti et al., 2017). Further details on the interaction of PAs and metals are discussed at the end of the present section and illustrated in **Fig. 5**.

Although in some cases higher levels of PAs in the cells are correlated to higher stress tolerance (Hasanuzzaman et al., 2019; Tajti et al., 2018), this relationship should not be so simplistically generalized. The three main plant PAs appear to have different functions under abiotic stress. On sensitive plant species, Put content usually increases quickly to changes in the environment, which reflects in a decreased $(\text{Spm} + \text{Spd}) / \text{Put}$ ratio, being these changes usually accompanied by the generation of ROS, which, altogether, is considered as a stress signal (Groppa and Benavides, 2008; Zhao and Yang, 2008; Paul et al., 2018). In contrast, stress-tolerant species and cultivars are usually able to maintain higher levels of Spd and Spm under stress, while Put levels remain relatively low, which could imply their higher resilience (Sánchez-Rodríguez et al., 2016). Liu et al. (2004) reported that PEG-induced water stress significantly increased the levels of Spd and Spm levels in leaves of a drought-tolerant cultivar of *Triticum aestivum*, whereas a drought-sensitive cultivar showed a significant increase of free-Put level. The authors also suggested that Spd, Spm and Put facilitated the osmotic stress tolerance of wheat seedlings. Excessive Put accumulation in cells under stress can cause serious negative effects, such as the depolarization of membranes, leading to potassium leakage, tissue necrosis, and protein loss, especially in leaf tissues. On the other hand, Spd and Spm have anti-senescence effects under stress, being crucial for preserving the integrity of thylakoid membranes (Zhao et al., 2008). A more precise relationship between PAs levels and stress tolerance has been suggested, in which increases in the $(\text{Spm} + \text{Spd}) / \text{Put}$ ratio are behind the resistance to abiotic stresses such as drought and HM-stress (Wang et al., 2007; Zhao and Yang, 2008; Sánchez-Rodríguez et al., 2016), although this logic cannot be applied to every species or stress factor. For instance, according to Do et al. (2013), in rice plants under control conditions, Put is the predominant PA, followed by free Spd and Spm. However, under drought stress, Put levels decrease and Spm becomes the most prominent PA. In wheat, the cell wall-bound PAO was upregulated under Aluminum (Al) toxicity, leading to a higher generation of H_2O_2 . In contrast, the PAO activity was markedly inhibited by exogenous Put application, and subsequently reduced H_2O_2 accumulation in roots under Al stress, suggesting that Put plays an important protective role against Al-induced oxidative stress via inhibiting the PAO activity with lower H_2O_2 production (Yu et al., 2018). In accordance to this, it has been further reported that tomato PAOs respond to a variety of abiotic stresses (heat, wound, cold, drought, salt and metal toxicity), ROS, phytohormones, as well as other PAs, implying that tomato PAOs possibly have various functions in stress tolerance. Regarding the PAs biosynthetic pathway, a gene expression analysis revealed that the ADC-dependent PAs biosynthesis responds much more strongly to stress than the ODC pathway (Berberich et al., 2015; Do et al., 2013).

Despite the important roles PAs have as intermediate signalling agents in a wide range of metabolic chains, including those related to nitric oxide (NO), ABA, γ -aminobutyric acid (GABA) and ethylene, the overaccumulation of these aliphatic molecules in plant cells under stress can also directly control the maintenance of the redox homeostasis, by preventing the occurrence of oxidative stress, as pointed out in **Fig. 4** (Groppa and Benavides, 2008; Gill and Tuteja, 2010b; Todorova et al., 2014; Soares et al., 2019a). Being part of the non-enzymatic component of the plant AOX system, their ameliorating effects on ROS overaccumulation is much likely related to their chemical features, combining their acid-neutralizing anionic/cationic-binding properties (Gupta et al., 2013). However, as reviewed by Minocha et al. (2014), the exact points of interaction between PAs and ROS are far to be completely understood and remain as one of the most curious and complex biochemical phenomena occurring in plant cells. This fog of knowledge that hangs over the interaction of PAs with ROS arises mainly from the fact that, if on the one hand, PAs can directly eliminate ROS, such as $^1\text{O}_2$ and $\cdot\text{OH}$, on the other hand, their catabolism results in the production of oxidative species, namely H_2O_2 (Minocha et al., 2014). Still, the great majority of studies dealing with PAs and stress-exposed plants unequivocally elucidates the powerful action of these compounds as AOX, which can simultaneously act as radical scavengers, membrane stabilizers and inhibitors of LP (Alcázar et al., 2006; Groppa and Benavides, 2008; Gill and Tuteja, 2010b; Gupta et al., 2013; Sánchez-Rodríguez et al., 2016; Yu et al., 2019). However promising these findings are, the roles of PAs and the activation of PAs metabolism in plants for the abiotic stress tolerance is just beginning to be understood. A lot of effort is still required to uncover in detail the molecular mechanisms behind the protective roles of Spd, Spm and Put in abiotic stress tolerance.

The metabolism of PAs can also be affected by HM, both at the level of synthesis and catabolism (**Fig. 5**). Metal stress promotes the activity of the ADC, SPDS and SPMS enzymes, increasing the levels of Put in cells, which act as a signal, accusing the presence of a stress factor, and, consequently, enhancing the biosynthesis of the other PAs, Spd and Spm. PA catabolism is also enhanced in plants under metal-stress due to the increased activity of the DAO and PAO enzymes, resulting in a higher production of GABA and H_2O_2 . Eventually, high levels of PAs lead to the activation of AOX defenses, either through H_2O_2 -mediated signaling, by direct scavenging of toxic ROS, interaction with AOX enzymes and/or protection of molecules from oxidation. The hypothesis that PAs form direct chelates with HM has also been incorporated in the mechanistic model illustrated in **Fig. 5**, although further studies are required to confirm this role. Still, it is

known that the PA-induced enhancement of GSH content leads to a higher biosynthesis of phytochelatin-conjugates, which accelerates HM-detoxification.

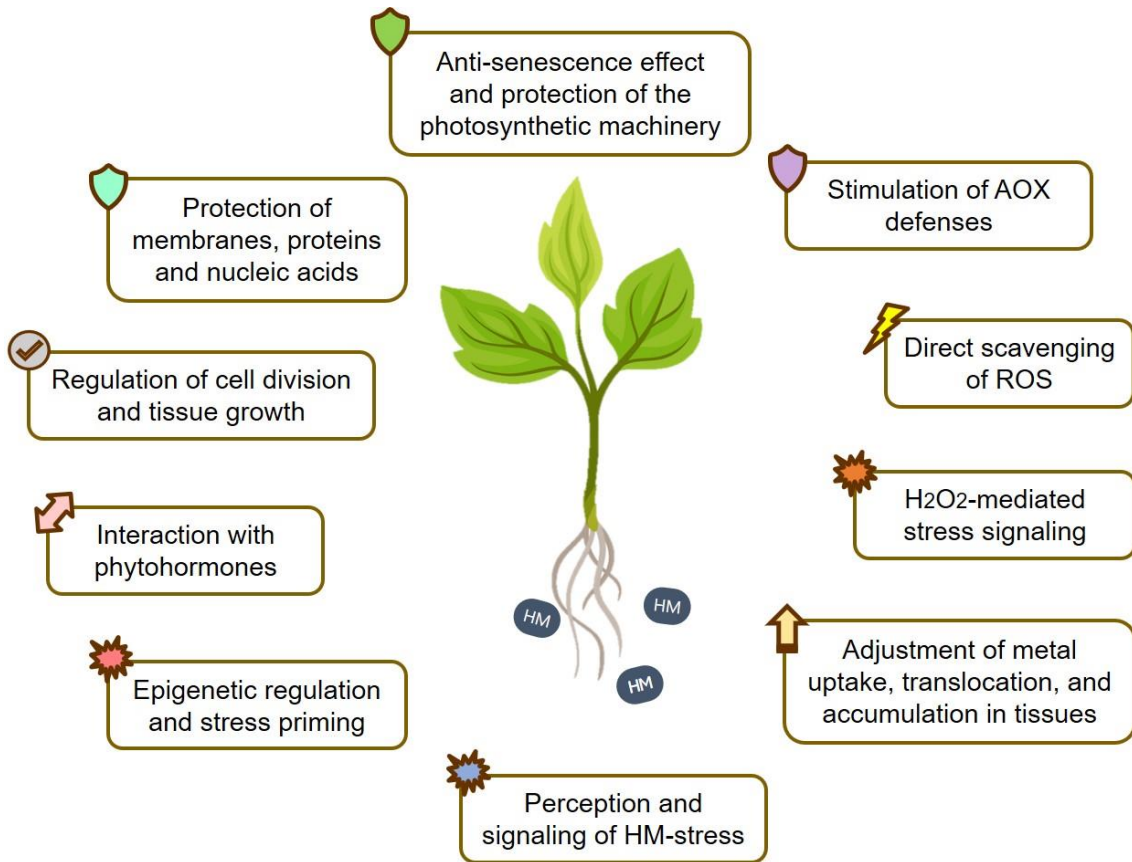


Figure 4 The diverse roles of PAs in plants under HM stress.

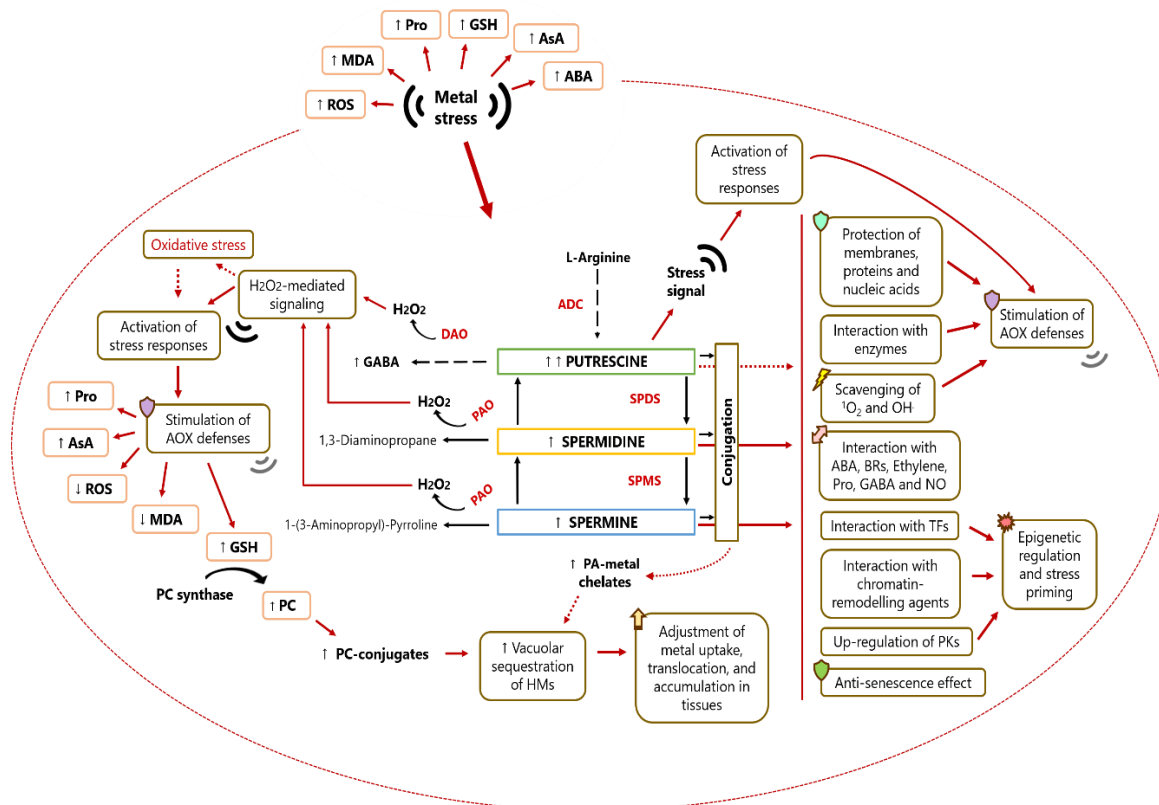


Figure 5 A mechanistic model on how PAs mediate plant responses to metal stress

1.6. DROUGHT- AND Ni-INDUCED OXIDATIVE STRESS

Similarly to other oxidative stress-inducing factors, stress imposed by drought and/or Ni activates cellular responses in plants, such as stress response protein production, up-regulation of AOX compounds and accumulation of compatible solutes (Kumar et al., 2012; Zhou et al., 2019). Both the effects of water stress and the exposure to contaminant levels of Ni in soil can trigger imbalances in the homeostasis and distribution of ions in the cell, leading to the overproduction of ROS and consequent oxidation and denaturation of functional and structural proteins (Chen et al., 2009; Farooq et al., 2009; Ameen et al., 2019).

Drought causes significant reductions in growth and harvestable yield of practically all crops and vegetables. Declines in photosynthesis as well as stomatal conductance, efficiency of PSII, activity of ribulose-1,5-bisphosphate carboxylase/oxygenase (RuBisCO, EC 4.1.1.39), Chl content, and leaf water potential have also been reported for several species (Farooq et al., 2009; Suzuki et al., 2014). Under water-stress, stomatal closure decreases the availability of CO₂ and leads to an increase of internal temperature. The negative effects of drought on the photosynthetic apparatus and on the cellular structure and functioning are usually aggravated when drought is combined

with other environmental stressors, such as heat, UV, salinity, HM, etc. (Suzuki et al., 2014). Plant cells produce high levels of ROS under drought stress, leading to enhanced LP of membranes, oxidation of DNA, RNA, and proteins (Jaleel et al., 2009). Chloroplasts, mitochondria, and peroxisomes are the sources as well as first targets of oxidative damage under drought stress. The accumulation of Pro, β -carotenes, α -tocopherol, AsA, GSH, PA, citrulline and several AOX enzymes, including SOD, APX and CAT, is essential to sustain the cellular functioning under drought. Phytohormones such as salicylic acid, auxins, gibberellins, cytokinin and abscisic acid also modulate plant responses towards drought (Farooq et al., 2009; Jaleel et al., 2009). Plants can endure drought stress by conserving cell and tissue water by osmotic adjustment, by scavenging ROS through the activity of the AOX defense system, and by keeping the cell membranes stabilized (Farooq et al., 2009; Suzuki et al., 2014). In tomato plants under water-stress the activity of AOX enzymes SOD, POX and polyphenol oxidases (PPO) only increased in the early stages of drought, but then decreased when plants were exposed to prolonged or severe water-stress (Tahi et al., 2008). This is similar to findings reviewed by Yordanov et al. (2000), in which severely drought-exposed pea plants showed declined activity of all AOX enzymes. Moreover, Fazeli et al. (2007) observed that the ability of stimulating the activity of AOX enzymes under drought stress is a sign of higher tolerance. Differences have been observed in the performance of plants from the same species plants, but of different varieties under water stress. This has been the case of sesame and tomato plants (Fazeli et al., 2007; Sánchez-Rodríguez et al., 2010). The criteria used in both studies to label each variety as tolerant or sensitive include the levels of ROS, degree of LP, activity of AOX enzymes and accumulation of low molecular weight molecules, such as Pro, phenolic compounds and quaternary ammonium compounds (Fazeli et al., 2007; Sánchez-Rodríguez et al., 2010). The results obtained in these two assessments reveal interesting differences among cultivars of the same species in terms of sensitivity to drought, contributing with the validation of specific criteria to be used for selecting cultivars in improvement strategies to create drought-tolerant varieties.

Although Ni is a redox-inactive metal and cannot be directly responsible for generating ROS, excessive Ni accumulation in plants reduces the efficiency of AOX mechanisms, delaying the scavenging potential of AOX enzymes and inducing the depletion of non-enzymatic AOX (Chen et al., 2009; Ameen et al., 2019). Interestingly, in some cases, the activity of AOX enzymes have been reported to increase in response to Ni-induced oxidative stress (Kumar et al., 2012). Exposure of wheat plants to high levels of Ni (200 μ M) has been reported to reduce the fresh weight (f. w.) of shoots,

induce LP of membranes, accumulation of ROS and Pro, but decreased the activity of the AOX enzymes SOD and CAT (Gajewska et al., 2006). In plants of the Ikram tomato cultivar, the activities of AOX enzymes like APX and GPX were enhanced under severe Ni stress conditions, while the activity of CAT seemed to be downregulated in the shoots (Kumar et al., 2015). Since SODs and CATs are metalloenzymes containing Fe, Cu or Zn (Chen et al., 2009), the interference of Ni with the uptake of other micronutrients could explain decreased biosynthesis and activity of these enzymes (Gajewska et al., 2006; Kumar et al., 2015). In fact, the negative effects of Ni on modulating the activity of Fe AOX enzymes (Fe-SOD and CAT) is corroborated by Sachan and Lal (2017). Similarly, in barley plants, Ni stress (200 and 400 μM) also inhibited the growth of both roots and leaves, increased levels of H_2O_2 , and led to the accumulation of Pro in roots, while LP was only detected in leaves (Kumar et al., 2012). Nevertheless, the activity of the AOX enzymes GPX, APX, SOD and GR increased in leaves and roots of barley plants under Ni stress, and the activity of CAT in roots remained unchanged, while markedly increasing in leaves (Kumar et al., 2012). Thus, the AOX enzyme's activities do not seem to be equally altered in response to Ni and seem to depend on the duration and means of exposure to Ni, as well as on plant species.

1.7. IMPROVEMENT OF *Solanum lycopersicum* L. STRESS TOLERANCE – EXPLORING ITS INTRASPECIFIC DIVERSITY

Tomato (*Solanum lycopersicum* L.) is one of the most important horticultural crops worldwide, as well as one of the best models for stress physiology studies (Gerszberg et al., 2015). Tomato production and consumption are constantly rising, not only due to its commercialization as a fresh product, but also processed as juices, soups, sauces, or powder concentrates. Tomato ranks 7th in global crop production after maize, rice, wheat, potatoes, soybeans, and cassava, being the most produced vegetable in the world. Tomatoes' worldwide production reaches more than 182 million tons on a cultivated area of almost 4.8 million hectares in 2018 (FAO, 2018b). Over the years, assemblages of the germplasm of the Solanaceae species and *ex situ* plant collections of tomatoes have been greatly used by breeders and scientists for improving the quality and yield of commercial tomato cultivars (Bai and Lindhout, 2007; Gerszberg et al., 2015). Tomato is widely cultivated as a typical horticultural crop in Mediterranean regions, where it requires regular irrigation during the spring and summer (Maggio and Saccardo, 2008). According to present and future climatic predictions for the Mediterranean basin, summer precipitation is projected to decrease by up to 45 %, impairing groundwater recharge in one of the most already water-stressed regions of the planet (IPCC 2007, 2014). Hence,

tolerance to drought has become a priority to plant breeders and geneticists to improve the performance of crops and vegetables in the fields, including tomato (Maggio and Saccardo, 2008). The expanding knowledge regarding physiological stress responses in different species and cultivars of tomato could allow for essential progress in the development of superior tomato cultivars, with improved stress tolerance.

During the domestication of modern tomato cultivars, genetic bottlenecks occurred in the *S. lycopersicum* L. genome, causing a significant loss of its genetic diversity, including of genes related to environmental stress tolerance (Bai and Lindhout, 2007; Foolad, 2007; Bauchet and Causse, 2012). Developing highly productive cultivars of crops and vegetables frequently implies a substantial loss of genetic diversity, as seed companies continuously limit the genetic pool used for breeding programs. This effect of genetic erosion is gradual and possibly irreversible (Fita et al., 2015). The loss of genetic diversity within the top cultivars of crops drops the opportunities to find new sources of variation to help them cope with future challenges (Esquinas-Alcázar, 2005; Fita et al., 2015). Presumably, as a consequence, the most common varieties of tomato been found to be rather susceptible to extreme environmental conditions and soil pollutant contaminations (Foolad, 2007), which forces growers to increasingly invest in crop protection, leading to a greater demand for faster and less expensive biotechnological solutions.

Despite the low genetic diversity among the most common “elite” tomato cultivars, there are other varieties within this species, about which little is known, or newly obtained cultivars from the most recent breeding approaches that have not yet been subjected to such intense selective pressures, and therefore could still present efficient stress-coping mechanisms, regardless of their reduced productivity (Hussain et al., 2015). Overall, there are hundreds of tomato cultivars available, displaying a large panoply of morphological, physiological and molecular adjustments to abiotic stresses (Bauchet and Causse, 2012; Causse et al., 2013; Gerszberg et al., 2015). As part of the attempt to ensure long term crop’s productivity and food safety, the assessment of the genetic diversity of crops in the search for tolerance traits is becoming an appealing strategy for the biotechnological improvement of economically important cultivars (Zamir, 2001; Atwell et al., 2014). Over the years, nearly all tomato-breeding programs led to the development of high-quality cultivars with high yield potential under non-stressful conditions, adapted to the demands of the market. However, during this time, less efforts have been put into creating abiotic stress-resistant cultivars and capable of adjusting to CC and environmental contamination (Bai and Lindhout, 2007). Recent breeding

approaches have focused attention on inducing crosses between wild and cultivated species of tomato. This type of breeding approaches has been responsible for the introgression of novel genetic variation in the offspring. Consequently, the genetic diversity of modern cultivars could be considerably widened in a near future, perhaps even leading to the appearance of characteristics of resilience to a wider range of abiotic stressors (Zamir, 2001; Bai and Lindhout, 2007).

Taking advantage from this new and unknown diversity, it becomes important to get some insights into the stress responses of these cultivars towards specific environmental conditions in order to explore and identify potential tolerance mechanisms that do not occur in industrial tomato cultivars. In this sense, the development of improved selection techniques and accurate criteria to identify these superior genotypes and associated tolerance traits is crucial for the effective screening of cultivars and varieties (de la Peña and Hughes, 2007). Some tomato cultivars have already been labeled as “tolerant” for their capability to survive under conditions that caused physiological damages to common tomato plants (Shamim et al., 2014). A list of examples of tomato cultivars and their respective categorization in terms of tolerance to stress is compiled in **Table 1**. For instance, the cultivars SV 7631TD and Brickyard are reportedly more tolerant to the tomato chlorotic spot tospovirus than the Sanibel cultivar (Zhang et al., 2019). George et al. (2013) and Kumar et al. (2017) compared the sensitivity of different tomato cultivars towards PEG-induced drought. The Walter, Punjab Chuhara, Kurihara, EC-620428, EC-620360, EC- 620427, EC-620557, and Arka Saurabh cultivars showed a better growth performance under PEG exposure when compared to 9 other tomato varieties (George et al., 2013; Kumar et al., 2017). Concerning drought stress, Çelik et al. (2017) also found that X5671R plants were less sensitive than 5MX12956, and Aghaie et al. (2018) clustered the cultivars Y-Falat, Punta Banda and Quine as drought tolerant, in contrast to the highly sensitive Early Orban, Roma and Cal J. Additionally, according to Abdul-Baki (1991) and Firon et al. (2006), Fresh Market 9, Saladette, Processor 40, Solar Set, Hazera 3018 and Hazera 3042 are considered heat-tolerant cultivars, while Campbell 28, Duke, Flora-Dade, Long Keeper and Hazera 3017 are referred to as heat-sensitive. Nevertheless, the stress tolerance does not only depend on the genotype of the plant, but also on the type of stress, intensity, and time of exposure, as well as on the influence of other environmental factors. Additionally, the methods and criteria used for the selection of cultivars can also impact the accuracy of their classification in terms of tolerance degree (Shamim et al., 2014). Insights on the coping mechanisms towards specific abiotic stresses have already been revealed for these and many other cultivars (George et al., 2013; Hussain et al., 2015; Çelik et al., 2017; Kumar et al., 2017). Similarly

to other types of oxidative stress-inducing factors, the rapid activation of efficient AOX mechanisms and expression of stress-induced genes, as well as improved detoxification strategies for organic pollutants and HM could be behind a higher stress resilience towards drought or HM stress (Treviño and O’Connell, 1998; Dixit et al., 2001; Iannelli et al., 2002; Albaladejo et al., 2015; Branco-Neves et al., 2017).

Table 1 Examples of *S. lycopersicum* L. cultivars showing different sensitivity levels towards biotic and abiotic stresses

Cultivar	Type of stress	Sensitivity	Reference
SV 7631TD Brickyard Sanibel	Tomato Chlorotic Spot Tospovirus	tolerant tolerant sensitive	Zhang et al. (2019)
9086 Roma Sitara TS-01 pak0010990 CLN-2123A Picdeneato 0.006231 7035 42-07 17883 BL-1176-Riostone-1-1 Marmande 17882	Cd Stress	less sensitive less sensitive less sensitive less sensitive less sensitive less sensitive less sensitive sensitive sensitive sensitive sensitive sensitive	Hussain et al. (2015)
Fresh Market 9 Saladette Processor 40 Solar Set Duke Flora-Dade Long Keeper Campbell 28	Heat Stress	tolerant tolerant tolerant tolerant sensitive sensitive sensitive sensitive	Abdul-Baki et al. (1991)
Hazera 3018 FLA 7156 Hazera 3042 Saladette NC 8288 Grace Hazera 3017	Heat Stress	tolerant tolerant tolerant tolerant sensitive sensitive sensitive	Firon et al. (2006)
Walter Punjab Chuhara Kurihara Money maker T-4 Tom-Round Feston Ratan	PEG - induced drought	tolerant tolerant tolerant most sensitive sensitive sensitive sensitive sensitive	George et al. (2013)

Indian Nagina		sensitive sensitive	
EC-620428 EC-62042 Arka Saurabh EC-620360 EC-620557 Arka Rakshak US-440 NS-516	PEG - induced drought	less sensitive less sensitive less sensitive less sensitive less sensitive sensitive sensitive sensitive	Kumar et al. (2017)
X5671R 5MX12956	Drought stress	less sensitive sensitive	Çelik et al. (2017)
Y-Falat Punta Banda Quine 111-Falat Rio Grande Better Boy Caribou CH-Falat Has2274 Korall Khorram Early Orbana Roma Cal J	Drought stress	tolerant tolerant tolerant moderately tolerant moderately tolerant moderately tolerant moderately tolerant moderately tolerant moderately tolerant sensitive sensitive sensitive highly sensitive highly sensitive highly sensitive	Aghaie et al. (2018)

2. Aims

It is well known that both the exposure to water deficit, including through PEG-induced drought approaches, and to toxic levels of Ni can induce detrimental changes in the growth and physiological performance of plants (Chen et al., 2009; Ameen et al., 2019). Tomato's responses to each of these stressors have been assessed in detail over the past decades, as it has been frequently used as a model plant for physiological studies. Nevertheless, taking a more realistic approach, research on the physiology of plants under stress is beginning to address studies of combined stress (Ameen et al., 2019), and much remains to be revealed regarding the effects of simultaneous exposure to adverse weather conditions and exposure to HM soil pollution on field crops and vegetables, including tomato cultivars. Bearing this in mind, the main goal of this work was to assess the physiological responses to the combination of excess nickel (Ni) and PEG-induced drought of different tomato cultivars and then, evaluate the physiological potential within the most tolerant one to enhance the resilience of common tomato plants under abiotic stress. For this purpose, the following questions were raised:

- 1) How will different cultivars of *S. lycopersicum* be affected by the isolate and simultaneous exposure to drought and Ni stress?
- 2) What are the biochemical and molecular basis of these physiological damages?
- 3) Is the intraspecific variability among different tomato cultivars enough to find differences in terms of tolerance to water deficit and Ni stress?
- 4) If so, what are the main mechanisms behind a higher resilience to these stressors?

3. Material and Methods

3.1. CHEMICALS AND SUBSTRATE

Nickel (II) sulfate hexahydrate ($\text{NiSO}_4 \cdot 6\text{H}_2\text{O}$) and polyethylene glycol 6000 (PEG 6000) were purchased from BDH[®] (BDH Chemicals Ltd., England) and Sharlau[®] (Sharlab S. L., Spain), respectively, as powders. Murashige and Skoog (MS) culture media containing Gamborg B5 vitamins was purchased from Duchefa Biochemie[®] (Duchefa Biochemie B.V., The Netherlands). The test substrate used in the growth trials was expanded perlite (3-6 mm), originated from volcanic silicates, purchased from SIRO (Sistemas Integrados de Reciclagem Orgânica, Leal & Soares, S.A., Portugal).

3.2. PLANT MATERIAL AND GROWTH CONDITIONS

Seeds of different cultivars of *Solanum lycopersicum* L. were obtained from Vilmorin[®] (Vilmorin Iberica S.A., Spain), Sementes Vivas[®] (Living Seeds – Sementes Vivas S.A., Portugal) and Flora Lusitana (Flora Lusitana Lda., Portugal). Before sowing, seeds of each variety were surface sterilized with 70 % (v/v) ethanol and 20 % (v/v) commercial bleach, for 10 and 7 min, respectively, followed by three series of rinsing with sterile deionized water (ddH_2O). For germination assays, seeds were incubated in a growth chamber with controlled conditions of temperature (24 °C), photoperiod (16 h light/8 h dark) and light (photosynthetically active radiation – PAR: $60 \mu\text{mol m}^{-2} \text{s}^{-1}$). Concerning the semi-hydroponic experiments, plants were grown under the same controlled conditions, but light intensity was scaled up to $120 \mu\text{mol m}^{-2} \text{s}^{-1}$.

3.3. NICKEL TOLERANCE SCREENING

3.3.1. Selection of Ni concentration – germination assay

A series of sequential concentrations of $\text{NiSO}_4 \cdot 6\text{H}_2\text{O}$, ranging from 0 to 500 μM , was applied to seeds of the cherry cultivar of *S. lycopersicum*, in a Petri dishes' germination assay, giving rise to the following treatments: 0, 50, 150, 250 and 500 μM . The maximum concentration of Ni was chosen based on previous bibliographic reports (Freeman et al., 2004; Gajewska et al., 2006; Gomes-Junior et al., 2006; Uruç Parlak, 2016; Ameen et al., 2019) and on the environmental relevancy. Recent findings of metal-polluted agricultural soils and irrigation waters have reported Ni occurrence at concentrations as high as 26 g kg^{-1} and 0.3 mg L^{-1} , respectively (Kumar et al., 2015; Ameen et al., 2019). In a semi-hydroponic system, the exposure of plants to 500 μM $\text{NiSO}_4 \cdot 6\text{H}_2\text{O}$ through

irrigation, leads to an accumulation of Ni in the substrate in a concentration of approximately 40 mg kg^{-1} .

After sterilization, cherry tomatoes' seeds were placed in Petri dishes with half strength MS solidified culture medium, supplemented or not with the different concentrations of Ni. For each concentration of Ni, as well as for the control (CTL; $0 \mu\text{M}$), three biological replicates were considered, with 10 seeds each. Then, seeds were placed to germinate for 5 days at $24 \text{ }^\circ\text{C}$ in a growth chamber, under a photoperiod of 16 h light / 8 h dark and a light intensity of $60 \mu\text{mol m}^{-2} \text{ s}^{-1}$. Afterwards, germination rate and the length of both hypocotyl and radicle were recorded.

3.3.2. Selection of tomato cultivars under Ni stress – germination assay

Twelve different tomato cultivars were screened for their response to Ni stress in a germination assay. Seeds of the tomato cultivars Ace VF, Agora, Black Cherry, Calabash Rouge, Cherry, Chico III, Coração-de-boi, Gold Nugget, Moneymaker, Purple Calabash, Pusa Ruby and San Manzano were surface sterilized as described in section 3.2 and placed in Petri dishes with half strength MS solidified medium, supplemented or not with $75 \mu\text{M NiSO}_4 \cdot 6\text{H}_2\text{O}$. The selection of this concentration was based on the previous experiment. Plates containing approximately 20 seeds each were placed in a growth chamber, at $24 \text{ }^\circ\text{C}$, under a photoperiod of 16 h light / 8 h dark. After 5 days, germination rate and radicle length were recorded. For each species and treatment, two biological replicates (plates) were considered.

3.3.3. Selection of tomato cultivars under Ni stress – semi-hydroponic experiment

Four of the twelve tomato cultivars were selected for further screenings based on their differences in early growth performance just after seed germination under Ni stress. For this purpose, the seedlings of *Solanum lycopersicum* cultivars Ace VF, Gold Nugget, Moneymaker and Purple Calabash were transferred to plastic pots containing approximately 100 g of perlite moistened with ddH₂O and were allowed to grow for 15 days in a growth chamber as previously described. During this time, plants of all cultivars were watered with half strength Hoagland's nutrient solution (HS; Taiz et al., 2014), supplemented or not with $75 \mu\text{M NiSO}_4 \cdot 6\text{H}_2\text{O}$. For each cultivar and treatment (CTL and $75 \mu\text{M NiSO}_4 \cdot 6\text{H}_2\text{O}$), two replicates (pots) were considered, with four plants each. After 15 days, plants were collected, cleansed, and measured in terms of f. w. and total length

of roots and shoots. The growth inhibition percentages were compared with one another, allowing to choose two from these four cultivars for the final experimental trial.

3.4. FINAL GROWTH TRIAL

Focusing on the contrasting patterns of growth under Ni stress, the two cultivars of *Solanum lycopersicum* L. Gold Nugget and Purple Calabash (Vilmorin®) were selected for the final growth trial, aiming to compare the tolerance response of both cultivars to contaminant levels of Ni, simulated drought and to the combination of both stressors. During the entire trial, plants of both cultivars were equally treated in terms of stress exposure and growth conditions. Once again, considering the results from preliminary assays and the fact that the exposure to 75 μM of Ni still caused a significant loss of biomass production, which would be required for future assessments, the concentration of $\text{NiSO}_4 \cdot 6\text{H}_2\text{O}$ was ultimately adjusted to 50 μM (corresponds to approximately 0.4 mg $\text{NiSO}_4 \cdot 6\text{H}_2\text{O}$ kg^{-1} substrate), and plants were exposed to this heavy metal (HM) through the watering solution in a semi-hydroponic system. After seed germination, Gold Nugget and Purple Calabash plantlets grew separately for 20 days in a growth chamber as described earlier. During the first 48 h, plants of both cultivars were irrigated with half strength HS, and in the 16 days afterwards, the watering solution for plants from the Ni treatment was supplemented with 50 μM $\text{NiSO}_4 \cdot 6\text{H}_2\text{O}$. After 16 days of Ni exposure, half the pots from the CTL and Ni stress treatments of each cultivar were randomly separated from the remainder and started to be subjected to a treatment of simulated moderate drought, by adding 6 % PEG 6000 to their respective watering solution, as represented in the image below (**Fig. 6**). For each cultivar and treatment (CTL; 50 μM $\text{NiSO}_4 \cdot 6\text{H}_2\text{O}$; 6 % PEG-induced drought; and combination of 50 μM $\text{NiSO}_4 \cdot 6\text{H}_2\text{O}$ and 6 % PEG-induced drought), 8 replicates (pots) were considered, with five plants each. Details on the experimental design can be found in **Fig. 6**.

After 48 h of the first PEG 6000 administration, plants of all treatments were collected, measured for total root and shoot length, and f. w. of shoots and roots, separately. A portion of fresh material of each replicate was immediately used for the biochemical quantification of O_2^- , while the remainder material was frozen and grinded in liquid nitrogen (N_2) and stored at -80°C to be used for further biochemical and molecular analyses. Four independent assays were carried out to obtain enough biomass to perform all the biochemical and molecular procedures. On the last repetition of this trial, roots and shoots were weighted before and after drying to determine the relative water content.

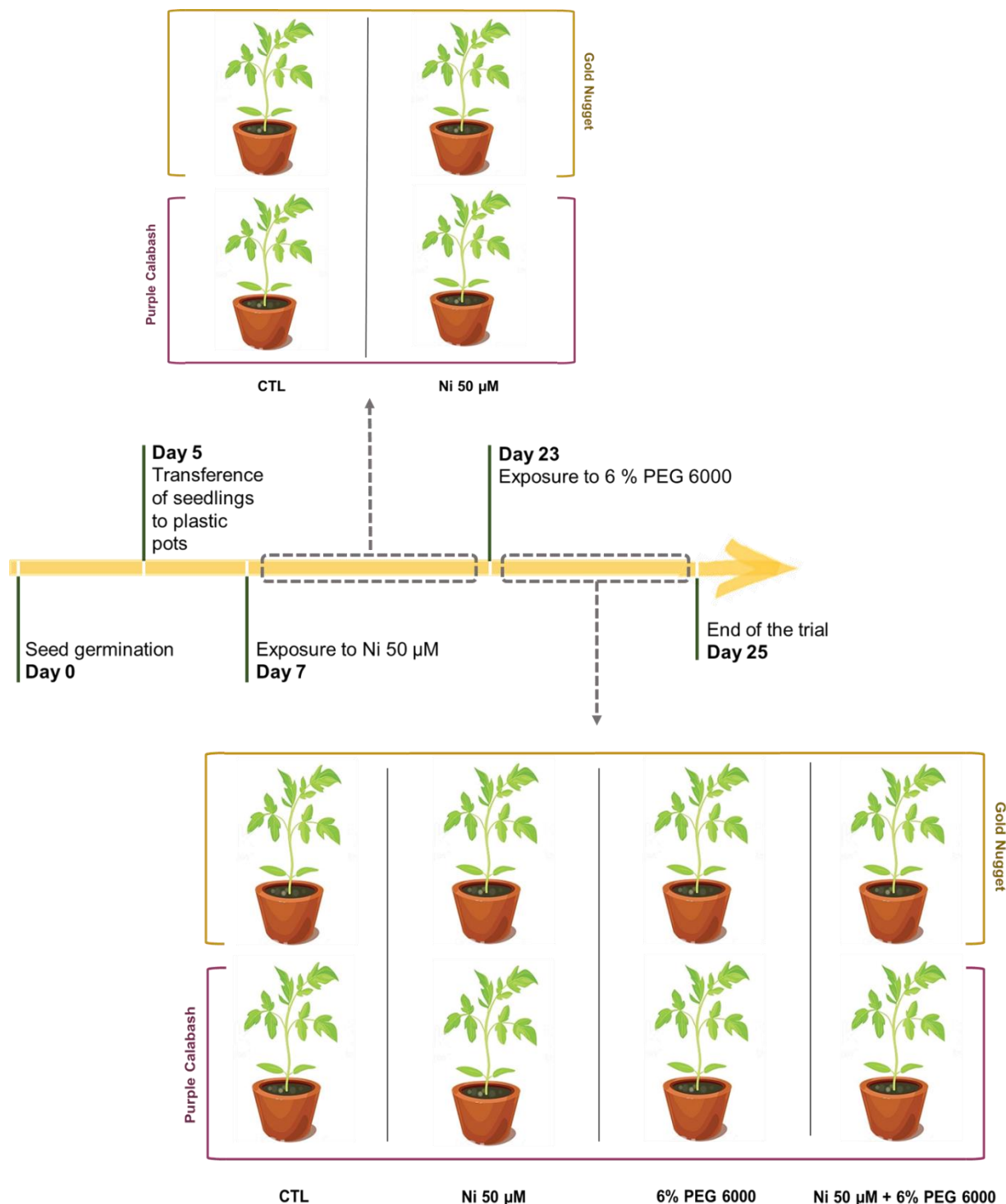


Figure 6 Experimental setup and timeline of the final growth trial. Exposure to Ni started for plantlets of both cultivars on the 7th day of the trial, as represented in the highlighted scheme, above the timeline. For the following 16 days, the experimental setup consisted of only two treatments (CTL and Ni 50 µM) being applied to plants of the two different tomato cultivars (Gold Nugget and Purple Calabash). The stage of the trial in which all treatments were applied simultaneously, is highlighted in the grey rectangle from the last section of the timeline and is visually represented below. In this representation it is possible to distinguish the four different treatments (CTL; Ni 50 µM; 6% PEG 6000; and 50 µM + 6% PEG 6000) being applied to plants of the two different tomato cultivars (Gold Nugget and Purple Calabash).

3.5. QUANTIFICATION OF Ni CONTENT IN TISSUES

Ni stressed plants were analyzed for the quantification of Ni content in the tissues in comparison to non-Ni stressed plants. Roots and shoots were separately dried in a VENTI-Line® oven (VWR International, LLC.) for a few days at 60 °C (until constant weight was recorded). The dried material was crushed with an ultracentrifuge mill at 8000 rpm. Three sub-samples (0.3 - 0.5 g) were obtained for each treatment and cultivar by cone and quartering sub-sampling. The samples and two analytical blanks were digested in a microwave oven with 4 mL supra pure concentrated nitric acid (HNO₃) and 2 mL H₂O₂ at 30 %. The digestion proceeded at 800 W for 10 min, followed by 5 min at 1000 W and a cooling period of 15 min. Each clear solution obtained was quantitatively transferred to 50 mL volumetric flasks. The analysis was performed by flame atomic absorption spectroscopy (FAAS), operated at the optical and flame parameters recommended for the instrument used (Perkin Elmer, AAnalyst 200). Calibration was performed with an external standard (in 0.5 % suprapure HNO₃) in the following range: 10-100 µg L⁻¹.

3.6. EVALUATION OF PHYSIOLOGICAL ENDPOINTS

3.6.1. Extraction and quantification of photosynthetic pigments

The extraction and quantification of Chl and Car were performed on shoot samples of all treatments, according to methods described by Lichtenthaler (1987). Frozen aliquots of approximately 200 mg f. w. were grinded in 14 mL of 80 % (v/v) acetone and centrifuged for 10 min at 1 400 g. After collecting the supernatant (SN), the absorbance (Abs) at 470, 647 and 663 nm was recorded and the concentrations of Chl a and b and Car were calculated according to the following equations (Lichtenthaler, 1987):

- Chl a (mg L⁻¹) = 12.25 x Abs (663 nm) – 2.79 x Abs (647 nm)
- Chl b (mg L⁻¹) = 21.50 x Abs (647 nm) – 5.10 x Abs (663 nm)
- Car (mg L⁻¹) = [1000 x Abs (470 nm) – 1.82 x Chl a – 85.02 x Chl b] / 198

Finally, results were expressed as mg g⁻¹ f. w..

3.6.2. Extraction and quantification of soluble proteins

Total soluble proteins were extracted, on ice, from frozen samples of roots and shoots (ca. 200 mg) in 1.5 mL of extraction buffer containing: 100 mM potassium phosphate buffer (PK; pH 7.3); 1 mM ethylenediaminetetraacetic acid (EDTA), for protection against

metallic peroxidases; 8 % (v/v) glycerol, which was used as a cryoprotectant to increase protein stability; 1 mM phenylmethylsulphonyl fluoride (PMSF), a protease inhibitor; 5 mM AsA; and 2 % (w/v) polyvinylpyrrolidone (PVPP), which inhibits phenolic compounds from inactivating enzymes. Samples were homogenized in the Bead Mill Homogenizer BEAD RUPTOR 12 from Omni International Inc., using 5 beads per tube. Between each homogenizing cycle, tubes were incubated for 1 min on ice to prevent overheating of the samples. Then, the extracts were centrifuged at 16 000 g for 25 min at 4 °C. The resulting SN was then used to quantify the total soluble proteins, and to measure the activity of three AOX enzymes, as described in sections 3.6.2 and 3.8.2, respectively.

The total soluble proteins were quantified according to Bradford (1976), by measuring the Abs at 595 nm. Total protein content was calculated based on a calibration curve, using standard samples of different known concentrations of bovine serum albumin (BSA), and expressed in mg g⁻¹ f. w..

3.7. EVALUATION OF OXIDATIVE STRESS MARKERS

3.7.1. Quantification of lipid peroxidation (LP)

The membrane damage was assessed in terms of LP, by quantifying the levels of MDA, according to Heath and Packer (1968). Frozen aliquots of roots and shoots of approximately 200 mg were homogenized in 1.5 mL of 0.1 % (w/v) trichloroacetic acid (TCA). Extracts were centrifuged at 10 000 g for 5 min. Afterwards, 1 mL of 0.5 % (w/v) thiobarbituric acid (TBA) in 20 % (w/v) TCA was added to 250 µL of SN. In parallel, a blank tube was prepared, replacing the SN with 250 µL of 0.1 % (w/v) TCA. Tubes were incubated at 95 °C for 30 min and subsequently cooled on ice for 15 min before a final centrifugation (10 000 g; 15 min). Afterwards, the Abs of each sample was recorded at 532 and 600 nm. The obtained Abs values at 600 nm were subtracted to the ones at 532 nm, to minimize unspecific turbidity effects. The MDA content, expressed as nmol MDA g⁻¹ f. w., was determined using the extinction coefficient of 155 mM⁻¹ cm⁻¹.

3.7.2. Quantification of H₂O₂

The assessment of H₂O₂ levels was performed according to Alexieva et al. (2001), following the same extraction method as for the evaluation of LP, summarized in the previous paragraph. Following the 5 min centrifugation (10 000 g; 4 °C) of the extracts, 250 µL of SN were added to 250 µL of 100 mM PK buffer (pH 7.0) and 1 mL of 1 mM potassium iodide (KI), in triplicate. Tubes were vortexed and then, incubated at room

temperature (RT), for 1 h, in the dark. A blank tube was also prepared, replacing the SN with 250 μL of 0.1 % (w/v) TCA. Afterwards, the Abs of each sample was recorded at 390 nm. The levels of H_2O_2 were quantified considering an ϵ value of $0.28 \mu\text{M}^{-1}\text{cm}^{-1}$ and expressed as $\text{nmol H}_2\text{O}_2 \text{ g}^{-1} \text{ f. w.}$.

3.7.3. Quantification of O_2^-

The content of O_2^- was spectrophotometrically evaluated according to the procedures described by Gajewska and Skłodowska (2007), through the reduction of the nitroblue tetrazolium (NBT) reagent from Alfa Aesar (Thermo Fisher Scientific, Germany). Small freshly-cut fragments of leaves and roots (ca. 300 mg) were immersed and incubated in 3 mL of a solution composed of 0.01 M sodium phosphate buffer (pH 7.8), 0.05 % (w/v) NBT and 10 mM sodium azide (NaN_3) for 60 min, under constant shaking, in the dark. Posteriorly, 2 mL of this reaction solution were collected and transferred to new tubes which were incubated for 15 min at 85°C . After cooling on ice, tubes were vortexed and briefly centrifuged (15 s; maximum speed), before recording the Abs of the SN at 580 nm. The levels of O_2^- , represented by the reduction of the NBT, were expressed as the Abs $580 \text{ nm h}^{-1} \text{ g}^{-1} \text{ f. w.}$.

3.8. ASSESSMENT OF THE ANTIOXIDANT DEFENSE MECHANISMS

3.8.1. Extraction and quantification of AOX metabolites

3.8.1.1. Proline (Pro)

Pro levels were quantified according to a protocol described by Bates et al. (1973). Frozen aliquots of roots and shoots (ca. 200 mg) were homogenized on ice using a mortar, pestle, and quartz sand, in 1.5 mL of 3 % (w/v) sulfosalicylic acid. The homogenates were centrifuged at 500 g for 10 min. For each sample, each of three replicates of 200 μL of SN were combined with 200 μL of glacial acetic acid and 200 μL of acid ninhydrin. All reaction mixtures were incubated at 96°C for 1 h and then cooled on ice. For Pro extraction, 1 mL of toluene was added to each tube, and tubes were vortexed for 15 s. After total separation of phases, the Abs of the upper pink phase was recorded at 520 nm, using toluene as blank. The Pro content was estimated through a calibration curve, obtained by different solutions of known concentration of Pro. Results were expressed as $\mu\text{g g}^{-1} \text{ f. w.}$.

3.8.1.2. Glutathione (GSH)

The levels of GSH were evaluated following procedures optimized by Soares et al. (2019b), using the same SN as for the Pro assessment, described in the previous paragraph. After centrifugation at 500 g for 10 min, each of three replicates of 50 µL of SN were added to 200 µL of H₂O and 750 µL of a reaction mixture containing 100 mM PK buffer (pH 7.0), 1 mM EDTA and 0.1 M 5,5'-dithiobis-(2-nitrobenzoic acid) (DTNB; Ellman's Reagent). Tubes were vortexed and incubated at RT in the dark for 10 min. Afterwards, the Abs was recorded at 412 nm. The levels of GSH were calculated according to this: $\text{GSH } (\mu\text{mol/L}) = (\text{Abs } 412 \text{ nm} - 0,0002) / 0,0008$ and the results were expressed in $\mu\text{mol GSH g}^{-1} \text{ f. w.}$.

3.8.1.3. Ascorbate - reduced (AsA) and oxidized (DHA) forms

Quantification of ascorbate was based on the methods described by Gillespie and Ainsworth (2007). Frozen aliquots of roots and shoots of approximately 200 mg were homogenized in 1.5 mL of 6 % TCA (w/v) at 4 °C, using 5 beads per tube, in the BEAD RUPTOR 12. Between each homogenizing cycle, tubes were incubated for 1 min on ice to prevent overheating of the samples. The homogenates were centrifuged for 10 min (15 000 g, at 4 °C) and then the SN was collected. For total ascorbate quantification, 100 µL of SN were added 50 µL of 75 mM PK buffer (pH 7.0) and 50 µL of 10 mM 1,4-dithiothreitol (DTT), for a complete reduction of all ascorbate [AsA + DHA] present in the sample. This mixture was vortexed and incubated at RT for 10 min. Then, 50 µL of 0.5 % (w/v) N-ethylmaleimide (NEM) were added to remove excess DTT. To assess the levels of AsA (reduced), 100 µL of SN were mixed with 50 µL of 75 mM PK buffer (pH 7.0) and 100 µL of ddH₂O (to replace the volume of DTT and NEM that had been previously added to the other tubes for total ascorbate quantification). Subsequently, 750 µL of a reaction mixture containing 10 % (w/v) TCA, 43 % (v/v) H₃PO₄, 4 % (w/v) 2,2'-bipyridine (BIP) and 3 % (w/v) FeCl₃ were added to all tubes (for total ascorbate and AsA quantification). This reaction mix was carefully prepared by adding the reagents gradually, to avoid the formation of precipitates. All samples were incubated at 37 °C for 1 h. After incubation, the Abs were recorded at 525 nm. The concentrations of total and reduced AsA were calculated from a calibration curve previously prepared with solutions of known AsA concentration. The levels of DHA were calculated by subtracting the levels of its reduced form from the total ascorbate level. Results were expressed in $\mu\text{mol AsA / DHA g}^{-1} \text{ f. w.}$.

3.8.2. Extraction and quantification of AOX enzymes' activity

As previously mentioned, the protein extracts obtained in 3.6.2 for the quantification of total soluble proteins, were also further used for the assessment of the enzymatic activities of SOD, CAT and APX. In the case of SOD, 300 μL of protein extract were complexed with 10 μL of 0.3 mM NaN_3 .

3.8.2.1. Superoxide Dismutase (SOD) activity assay

The total activity of SOD (E.C. 1.15.1.1) was spectrophotometrically quantified, based on the inhibition of the photochemical reduction of NBT at 560 nm (Donahue et al., 1997). A reaction mix was prepared in separate consisting of 50 mM PK buffer (pH 7.8), 0,1 mM EDTA, 13 mM methionine and 75 μM NBT. The volume of complexed extract containing exactly 30 μg of protein was mixed with 2.8 mL of this reaction mix, 30 μL of 2 μM riboflavin and 50 mM PK buffer (pH 7.8) to a final volume of 3 mL, in triplicate. The reaction started upon adding the riboflavin. Tubes were quickly shaken and incubated for 10 min at RT, under exposure to 6 fluorescent 8 W lamps. A blank tube was prepared under the same conditions, replacing the protein extract with 100 mM PK buffer (pH 7.3). After incubation, the Abs of all tubes, including the blank, was recorded at 560 nm. SOD activity was determined in terms of NBT reduction, following these calculations:

- % oxidized NBT = $\text{Abs. (sample)} / \text{Abs. (blank)} \times 100$
- % NBT reduction = $100 - \% \text{ oxidized NBT}$

The activity of SOD was expressed according to Beauchamp and Fridovich (1971) as units of SOD mg^{-1} protein, in which one unit of SOD corresponds to the amount of enzyme needed to inhibit the photochemical reduction of NBT by 50 %.

3.8.2.2. Catalase (CAT) activity assay

The total activity of CAT (E.C. 1.11.1.6) was also spectrophotometrically assayed following a procedure described by Soares et al. (2018), based on methods of Aebi (1984). This evaluation was performed in a 96-well UV microplate, in a final volume of 200 μL , in which 20 μL of protein extract were added to 160 μL of 50 mM PK buffer (pH 7.0) and 20 μL of 100 mM H_2O_2 . After mixing for 5 s, the rate of H_2O_2 consumption was recorded in the high-quality monochromatorbased UV/VIS spectrophotometer Multiskan GO[®] (Thermo Fisher Scientific) at 240 nm, every 5 s, for a total of 40 s. The activity of CAT was calculated on SkanIt[®] software (Thermo Fisher Scientific) and was expressed

in terms of H_2O_2 consumption, considering an ϵ value of $39.4 \text{ mM}^{-1} \text{ cm}^{-1}$, as $\text{nmol of H}_2\text{O}_2 \text{ min}^{-1} \text{ mg}^{-1}$ of protein.

3.8.2.3. Ascorbate Peroxidase (APX) activity assay

Similarly to CAT's, the activity of APX (EC 1.11.1.11) was also assessed spectrophotometrically using Miltiskan GO[®] in a 96-well UV microplate, through the oxidation of AsA, following the methods of Murshed et al. (2008). In each well, 20 μL of protein extract were combined with 170 μL of 50 mM PK buffer (pH 7.0) supplemented with 0.6 mM AsA, and the reaction started upon adding 10 μL of 254 mM H_2O_2 . After agitating for 5 s, the variations in Abs at 290 nm were recorded every 5 s, for a total of 40 s. The total activity of APX, measured by the potential to reduce AsA into DHA, was calculated on SkanIt[®] using an ϵ value of $0.49 \text{ mM}^{-1} \text{ cm}^{-1}$ and expressed in $\mu\text{mol of DHA min}^{-1} \text{ mg}^{-1}$ of protein.

3.9. EXTRACTION, DERIVATIZATION AND QUANTIFICATION OF POLYAMINES (PAs)

PAs were extracted from frozen aliquots of roots and shoots (ca. 200 mg). Samples were homogenized in 1.5 mL 1 % TCA (w/v) at 4 °C in the BEAD RUPTOR 12, using 5 beads per tube. The extracts were kept on ice for 1 h before a 30 min centrifugation at 4 °C (20 000 g). Since PAs are not detectable at the visible or ultraviolet (UV) wavelengths, and do not exhibit fluorescence either, chemical derivatization is usually applied for their analysis by high performance liquid chromatography (HPLC) (La Torre et al., 2010). The pre-column derivatization reaction was carried out according to adapted methods described by Cai et al. (2010), in triplicate, by adding 300 μL of SN to 100 μL of 1 M carbonate buffer (pH 10.6) and 100 μL of 1 % (w/v) dansyl chloride (DNS-Cl) reagent (Alfa Aesar, Germany) prepared in acetonitrile, which forms stable and colored compounds that can be detected at the UV and visible spectrum (La Torre et al., 2010). This mixture was incubated for 45 min at 60 °C. After incubation, the tubes were left at RT to cool down before adding 10 μL of 15 % formic acid. This blend was centrifuged for 3 min (10 000 g) and the SN was collected to injection vials for the quantitative analysis.

The dansyl derivates from tomato samples were analyzed in a HPLC-UV system (Ultimate 3000, Thermo Scientific, Waltham, Massachusetts, EUA) and separated using a Gemini C₁₈ column (150 x 4.6 mm; 5 μm) from Phenomenex (Torrance, CA) by HPLC with UV detection (HPLC-UV) with the column temperature at 25 °C. Sample injection volume was 20 μL at a flow rate of 0.5 mL min^{-1} . The chromatographic mobile phase for

elution consisted of a gradient established between 0.1 % formic acid in 20 mM ammonium acetate (A) and acetonitrile (B). The separation was achieved by using a gradient starting at 90 % solution A / 10 % solution B and followed by an increase of B, reaching 100 % at 58 min. An isocratic regime of 100 % acetonitrile was maintained from 58 to 63 min, and the initial conditions were restored between 68 and 78 min. Three calibration curves were made using extracts of standard solutions of Put, Spd, and Spm. The individual PAs in samples were quantified by the external standard method using the calibration curves of commercial standards purchased from Merck (Darmstadt, Germany). Data analysis was made with the Chromeleon® software (version 7.2.9, Thermo Scientific, Waltham, Massachusetts, USA).

3.10. ASSESSMENT OF THE EXPRESSION PROFILE OF Ni TRANSPORTERS

3.10.1. Computational identification and analysis of putative Ni transporters

Several metal transporters from the tomato proteome were identified as being possibly involved in the vacuolar sequestration of Ni, as part of a mechanism of HM detoxification. Thirteen tomato proteins were selected either based on previous references regarding their location to the roots and function as vacuolar carriers, or by comparing with very similar and fully characterized vacuolar metal transporters from other plant species, whose involvement in the detoxification of HM was demonstrated. The protein sequences of several metal transporters reportedly involved in the sequestration of HM in *A. thaliana*, *O. sativa*, *H. vulgare*, and *N. goesingense*, were retrieved from the databases: GenBank® (Benson et al., 2013), accessible through the National Center for Biotechnology Information (NCBI, U.S. National Library of Medicine), Sol Genomics Network (Fernandez-Pozo et al., 2015), and Ensembl Plants® (Howe et al., 2020). Given the fact that they had been previously characterized for their function and involvement in the detoxification of HM, these sequences were used as queries for BLASTP search against the tomato genome, with an E value threshold of $<10^{-21}$ in the above-mentioned databases. Upon each BLASTP search, the tomato protein exhibiting the highest blasting score, query coverage, E value and maximum identity % of its amino acidic sequence was selected for further analysis. Some of the proteins reported by Ofori et al. (2018) could be found amongst the BLASTP top hitting results, which confirmed their homology, and functional resemblance, with the annotated vacuolar metal carriers.

The protein sequences from the 13 tomato proteins selected in this study were submitted to a multiple sequence alignment using the Muscle algorithm from the software MEGA X: Molecular Evolutionary Genetics Analysis across computing platforms (version 10.1.8) (Kumar et al., 2018), along with 15 sequences from previously characterized homologous proteins in other species, which had been used as blasting queries in the search of the tomato transporters. An amino acid sequence similarity tree of the aligned metal transporter protein sequences was inferred by using the Maximum Likelihood method and Jones-Taylor-Thornton (JTT) matrix-based model (Jones et al., 1992) and analyzed in MEGA X (Kumar et al., 2018). Bootstrap values from 1000 replicates were used (Felsenstein, 1985). Branches corresponding to partitions reproduced in less than 50 % bootstrap replicates are collapsed. The percentage of replicate trees in which the associated sequences clustered together in the bootstrap test (1000 replicates) are shown next to the branches (Felsenstein, 1985). Initial tree(s) for the heuristic search were obtained automatically by applying Neighbor-Join and BioNJ algorithms to a matrix of pairwise distances estimated using the JTT model, and then selecting the topology with superior log likelihood value. This analysis involved 28 amino acid sequences. There were a total of 1753 positions in the final dataset. Evolutionary analyses were conducted in MEGA X (Kumar et al., 2018).

The 13 selected tomato proteins were then described not only in terms of size, domains, protein structure, topology and predicted subcellular location, but also for their encoding mRNA and DNA sequences, which were characterized in terms of length, position and orientation of each locus in the genome. This information is presented separately in **Tables 4** and **5** from the **Results** and could be found either in the GenBank, Sol Genomics Network, and/or Ensembl Plants and UniProt® / UniParc (The UniProt Consortium, 2019) databases. The subcellular locations of the proteins were retrieved from the databases Plant-mPLoc (Chou and Shen, 2010) and LocTree3 (Goldberg et al., 2014). Sequences of the transcripts of each gene were retrieved from the Sol Genomics Network database and used to design a respective set of primers to be used in a quantitative real-time polymerase chain reaction (qPCR) assessment to compare the levels of expression of each gene in the different tissues of the two tomato cultivars, under Ni and/or drought stress.

3.10.2. Extraction of total RNA

Total RNA was extracted from frozen samples (ca. 300 mg) of roots and shoots. Samples were homogenized in 1.5 mL of the ready-to-use phenolics solution NZYol (NZYTech, Lda. – Genes and Enzymes, Portugal), at RT by vortexing in 4 cycles of 10 s. RNA

extraction procedure was then performed according to optimized methods by Martins et al. (2014a; 2014b) and to the NZYol manufacturer's protocol. RNA extracts were centrifuged for 10 min (12 000 g, at 4 °C) and the SN was collected and incubated at RT for 5 min. 300 µL of chloroform were added to the SN and this mixture was vigorously shaken for 15 s by hand. Tubes were incubated at RT for 2 to 3 min and centrifuged for 15 min (12 000 g, at 4 °C). The colorless upper aqueous phase of the SN (containing RNA) was carefully collected to new tubes and the RNA therein was precipitated by adding 750 µL of cold isopropyl alcohol. Samples were incubated at -20 °C for 10 min, and then centrifuged at 4 °C for 10 min (12 000 g). The SN was discarded, and the RNA pellet left at the bottom of the tube was washed in 75 % (v/v) ethanol in two consecutive resuspensions followed by 5 min centrifugations (12 000g, at 4 °C). The final pellet was air-dried for 10 min. Afterwards, the RNA pellet was resuspended in 40 µL of RNase-free water and kept on ice until usage. The RNA was then purified using the GRS Total RNA kit - Plant from GRiSP® (GRiSP Research Solutions, Portugal), according to the manufacturer's protocol, in a series of resuspensions, incubations and brief flow-through centrifugations (16 000 g) following the kit instructions. The purified RNA samples were eluted in RNase-free water and collected to new RNase-free tubes, which were used right after for RNA quantification and then kept at -80 °C until further use. RNA levels were determined using a DS-11 Microvolume Abs Spectrophotometer from DeNovix® (DeNovix Inc., USA) at 260 nm, and results were expressed in terms of ng µL⁻¹ (data not shown). Purity ratios were also determined by dividing the Abs at 260 nm with the Abs values at 280 and 230 nm, which measured the residual proteins and phenolics, respectively. To evaluate the integrity and purity of the extracted RNA, samples were submitted to an electrophoresis run for the identification of rRNA subunits (data not shown). A 1 % (w/v) agarose gel was prepared in 0.5x tris-acetate-EDTA (TAE) buffer and stained with 1x Xpert Green DNA Stain dye (GRiSP). Each well received a total amount of 350 ng of RNA, as well as 1.6 µL of Bromophenol Blue loading dye (Thermo Fisher Scientific) and RNase-free water up to a final volume of 10 µL. The gel was electrophoresed at 5-6 V/cm until the bromophenol blue (the faster-migrating dye) had migrated 3/4 the length of the gel. The gel was then observed in an UV transilluminator.

3.10.3. cDNA synthesis

The extracted mRNA was converted to cDNA by reverse transcription using the Xpert cDNA Synthesis Kit (GRiSP), following the manufacturer's protocol. Briefly, 1 µL of a dNTP mix (10 mM each) was combined with 1 µL of 10 µM oligo(dT) primers, RNase-free water and 1 µg of template RNA, to a final volume of 14.5 µL. This mix was heated

at 65 °C for 5 min and then placed on ice for 2 min. A solution containing 4 µL of reaction buffer, 0.5 µL of RNase inhibitor and 1 µL of Xpert RTase was added to the previous mix. Samples were incubated at 50 °C for 25 min and then at 85 °C for 5 min. The cDNA was then diluted 10x in nuclease-free ddH₂O and stored at -20 °C.

3.10.4. q-PCR amplification

The qPCR was performed in 96-well plates on the CFX96 Touch Real-Time PCR Detection System® (Bio-Rad Laboratories, Inc.) using the Xpert Fast SYBR 2X Master mix (uni) Blue (GRiSP Research Solutions), which contains the fluorescent DNA binding protein SYBR Green. For each sample, three technical replicates of qPCR reactions were performed using 5 µl of this Master Mix, 0,3 µL of each primer, 1 µl of cDNA and nuclease-free ddH₂O to a final volume of 10 µl. Aliquots from the same cDNA sample were used with all primer sets in each experiment. The following cyclers conditions were used: an initial step of 2 min at 95 °C followed by 45 cycles of 5 s at 95 °C, 20 s at 55 °C and 20 s at 72 °C. Fluorescence was measured at the end of each amplification cycle. Primers were designed with the aid of QuantPrime© (<https://quantprime.mpimp-golm.mpg.de> Universität Potsdam) to anneal specifically with each candidate gene (Arvidsson et al., 2008). The set of primers used for each gene is listed in **Table 2**. The specificity of PCR was checked through dissociation curves at the end of each qPCR reaction, by heating the amplicons from 65 °C to 95 °C with increments of 0.5 °C for 5 s.

Primer efficiency was assessed by performing qPCR reactions with different dilutions of the same cDNA sample. In rows of four wells, each primer pair was tested for its ability to amplify 1 µL of cDNA diluted 10x, 20x, 40x or with no dilution (1x). In parallel, for each gene, one well was left without cDNA, to assess the occurrence of primer dimers. Primer efficiency was calculated in the CFX Manager Software 3.1 (Enke, 2016). A regression line was generated by calculating the C_q standard curve data points. The slope (m) of the standard curve was used to estimate the PCR amplification efficiency: $[10^{(-1/m)}] - 1$ (data not shown).

In qPCR experiments, gene expression was normalized to the transcript levels of *S. lycopersicum* *ELONGATION FACTOR 1 – ALPHA* (*SIEF1*; NCBI/GenBank Database accession no. XM_004240531), used as reference gene. Data were analyzed using CFX Manager Software 3.1® (Bio-Rad Laboratories, Inc.) according to the $\Delta\Delta C_q$ method (Livak and Schmittgen 2001).

Table 2 List of primer sequences used in analysis of gene expression by qPCR.

	Transcript ID	Primer sequences	
SIABCC3	Solyc03g117540.2.1	Fwd. 5'-CAAGATGCGGCTGTTGTCATCC- 3'	Rev. 5'-TTTCCTTCTCGTCACTGCTCGAC- 3'
SIABCC5	Solyc07g065320.2.1	Fwd. 5'-TTCCATCCGTGGACGATAGAGC- 3'	Rev. 5'-GCAGTTTCCCTCAAGTCACATGC- 3'
SIABCC6	Solyc08g006880.2.1	Fwd. 5'-TGGAGCAGTACCAGGTTTCCAG- 3'	Rev. 5'-CACCGAGAGACCTTCAACCATC- 3'
SIABCC14	Solyc00g283010.1.1	Fwd. 5'-TCATCGAGGTTGCTGAAGGAAGAG- 3'	Rev. 5'-AAAGCCAGCTGTTAGAGCAAATCC- 3'
SIABCC15	Solyc11g065710.1.1	Fwd. 5'-TAAGGTCTTAACGCTGACAACAGG- 3'	Rev. 5'-TGAAGAGCCATTGCCTTGTTAGAG- 3'
SIABCC16	Solyc11g065720.1.1	Fwd. 5'-GTGCAAACAAACCACCCTCTACC- 3'	Rev. 5'-GGTCGCGAATTTCCACTTTGCC- 3'
SIABCC17	Solyc12g036150.1.1	Fwd. 5'-TGGCCATCATCAGGGTTCAT- 3'	Rev. 5'-AGCATGCTCGATTTTCCAGC- 3'
SIABCC18	Solyc12g036140.1.1	Fwd. 5'-GCAAGAGCACCAACAAGATGTAAC- 3'	Rev. 5'-CCTCCCAAAGCATCTTTGTACCTC- 3'
SIABCC25	Solyc12g036160.1.1	Fwd. 5'-AAGCATTAGAGCGGGCACACTTG- 3'	Rev. 5'-CAGCATCTAGACCGAAGGTACTION- 3'
SIIREG2-like	Solyc10g076280.1.1	Fwd. 5'-CGGGTTAGGAAGCACCTATTTCCAC- 3'	Rev. 5'-GTGCTCATCGTTGCAGAGTCTAAG- 3'
SIMTP1	Solyc07g007060.1.1	Fwd. 5'-AGCCGACACCATCACCATAATGAG- 3'	Rev. 5'-ACAGTGTTGTCAGCGTCGTGTG- 3'
SICAX3	Solyc09g005250.2.1	Fwd. 5'-AGCCACTCTGGCTACAGGTTTG- 3'	Rev. 5'-TGCCTTCTCACTGTGTCCAATG- 3'
SIABCB21	Solyc03g114950.2.1	Fwd. 5'-TGCCATGGATTCCCTGATGCAAG- 3'	Rev. 5'-GTGTTGCGGCTCTTGACTGTTG- 3'
SIEF1	Solyc06g005060.3.0	Fwd. 5'-TGGCCCTACTGGTTTGACACTION- 3'	Rev. 5'-CACAGTTCACTTCCCCTTCTTCTG- 3'

3.11. STATISTICAL ANALYSIS

The final growth trial of the present study was set up as a randomized factorial block design, considering four biological replicates (CTL, Ni, PEG, Ni + PEG) for each cultivar (Gold Nugget and Purple Calabash), summing up a total of eight biological replicates. Results were expressed as mean \pm standard deviation (SD). After checking the homogeneity of variances (Levene's test), data from biometric and biochemical analyses were first subjected to a three-way analysis of variance (ANOVA), with cultivar, Ni, and PEG, separately as fixed main factors, followed by two-way ANOVAs for each cultivar with Ni and PEG as fixed main factors. Whenever significant differences were found ($p \leq 0.05$), Tukey's *post-hoc* test was used to compare individual means. All statistical procedures were performed in GraphPad Prism® 8 (version 8.0.2 (263), GraphPad Software Inc., USA).

4. Results

4.1. ECOTOXICITY OF Ni TO CHERRY TOMATO PLANTS

Aiming to evaluate the effects of Ni on the growth of tomato plants, preliminary assays were performed to select the most appropriate concentrations of $\text{NiSO}_4 \cdot 6\text{H}_2\text{O}$ to be used in a final growth trial, where the combination of Ni and water stress (drought) will be studied on different tomato cultivars. First, the germination rate and seedling growth responses were assessed in one of the most common *S. lycopersicum* cultivars – cherry tomato. Seeds were exposed to increasing concentrations of $\text{NiSO}_4 \cdot 6\text{H}_2\text{O}$, from 0 to 500 μM , in Petri dishes containing half strength MS culture media. After a 5 day germination period, plantlets revealed a significant decrease in radicle and hypocotyl growth for all Ni concentrations above 50 μM , when compared to seedlings from the control (CTL; 0 μM Ni) treatment (**Fig. 7**), although the germination rate was not affected by any level of Ni-stress (data not shown). Plantlets exposed to 150, 250 or 500 μM Ni showed growth inhibition ranging from 76 % to 92 % in the radicle, and between 28 and 52% in the hypocotyl, when compared with the CTL (0 μM Ni) (**Fig. 7**).

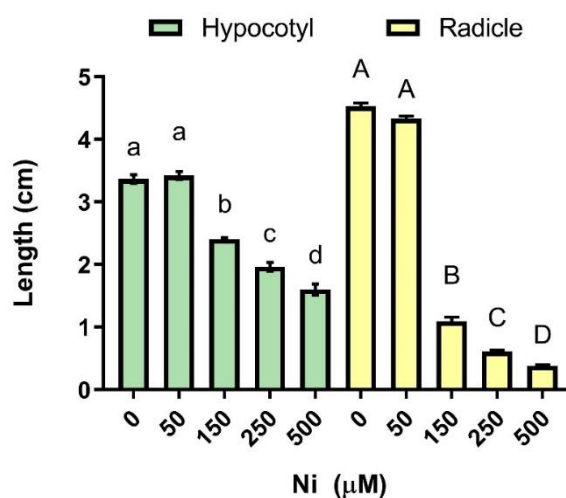


Figure 7 Effects of increasing concentrations of Ni (0, 50, 150, 250 and 500 μM) on the radicle and hypocotyl growth of cherry tomato seedlings after a 5 day exposure under *in vitro* conditions. Different letters above bars of each tissue type represent significant differences at $p \leq 0.05$.

Given the observed abrupt growth loss and considering the contrasting results obtained in this first trial between the concentrations of 50 μM and 150 μM Ni, a new assay was carried out using 75 μM $\text{NiSO}_4 \cdot 6\text{H}_2\text{O}$, to screen tomato cultivars with potential differences in Ni sensitivity.

4.2. EFFECTS OF Ni EXPOSURE ON DIFFERENT TOMATO CULTIVARS

The screening of tomato cultivars was divided in two parts: first, a wider short-term assay was carried out under *in vitro* conditions, comparing the germination and seedling growth performance of twelve tomato cultivars for 5 days. For this assay, the following cultivars were used: Ace VF, Agora, Black Cherry, Calabash Rouge, Cherry, Chico III, Coração-de-boi, Gold Nugget, Moneymaker, Purple Calabash, Pusa Ruby and San Manzano. After 5 days, the germination rate was 100 % for all treatments and cultivars, while the root length of plantlets from all cultivars was significantly affected by the exposure to Ni at 75 μ M. Radicle growth inhibition varied from 38 %, for Ace VF, to 70% for Gold Nugget (**Fig. 8**). During seedling development, the tomato cultivars Gold Nugget and Purple Calabash seemed to be the most affected by Ni-stress, while the cultivars Moneymaker and Ace VF stood out as the least affected (**Fig. 8**).

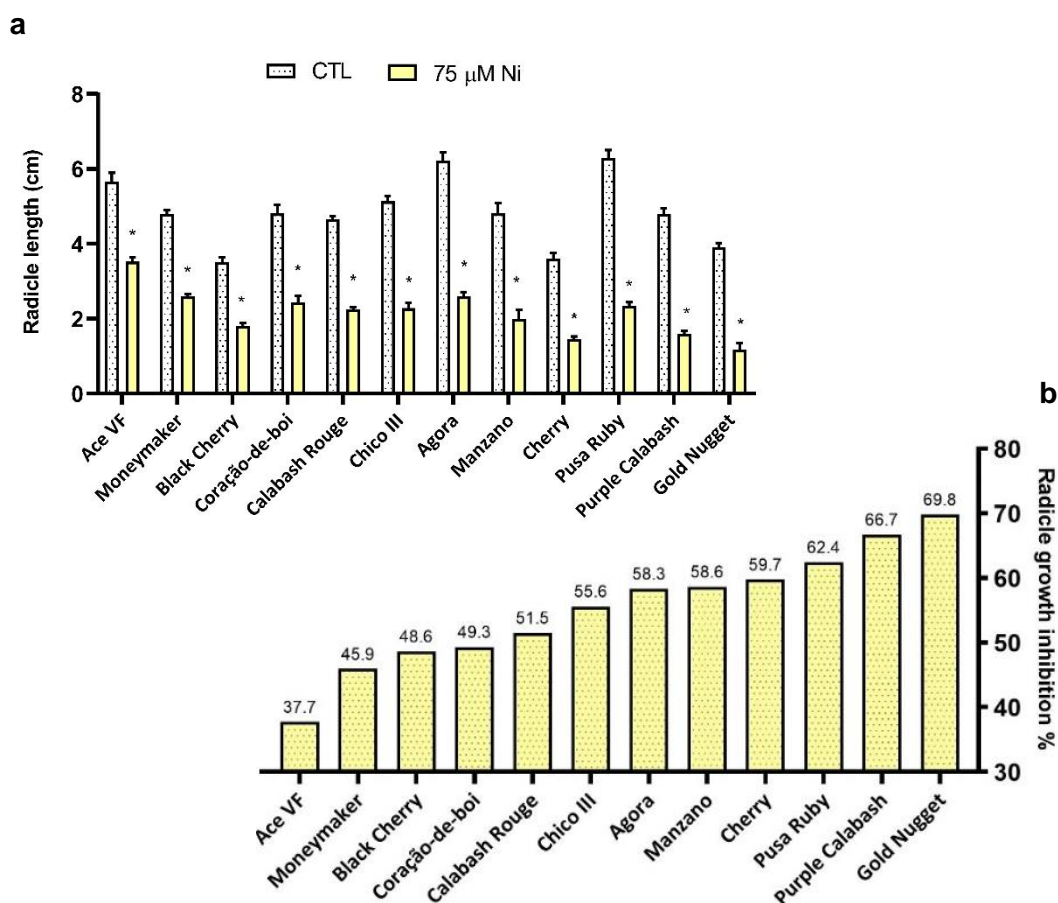


Figure 8 (a) Effects of 75 μ M Ni on radicle growth of plantlets from 12 different tomato cultivars after a 5 day exposure under *in vitro* conditions. * above bars indicate statistical differences for each cultivar between Ni-exposed plants and the respective control (0 μ M Ni), at $p \leq 0.05$. (b) Growth inhibition percentages for each cultivar, written above the respective bars, placed from lowest to highest radicle growth inhibition.

Aiming to discern whether the sensitivity patterns recorded in the Petri dishes' assay were observed in advanced growth stages, the two apparently more tolerant cultivars (Ace VF and Moneymaker) and the two more sensitive ones (Gold Nugget and Purple Calabash) were selected to be used in a second trial. For this purpose, plantlets grew for 15 days in plastic pots in a semi-hydroponic system. As can be seen (**Fig. 9 and 10**), the growth of plants from all four cultivars was significantly affected by the exposure to 75 μM Ni. Surprisingly, the lowest root growth inhibition was observed in plants of Gold Nugget (41 % - root length; 56 % - biomass production), followed by Ace VF and Moneymaker cultivars, whose exposure to Ni led to a loss of 44 % in terms of root length, and about 65 %, in terms of f. w. (**Fig. 9 and 10**). The roots of Purple Calabash continued to exhibit the highest sensitivity to Ni, being its growth reduced by 48 % in length, and 66 % in f. w., when compared to the respective CTL (**Fig. 9 and 10**).

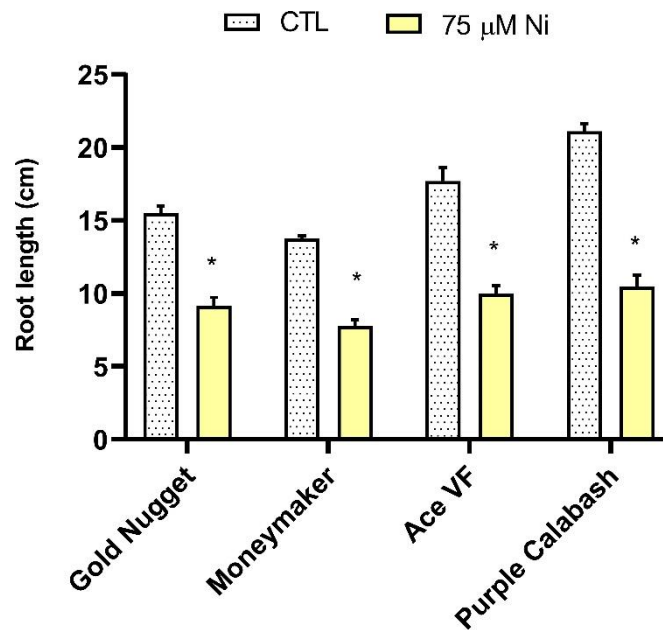


Figure 9 Effects of 75 μM Ni on the growth of roots from 4 different tomato cultivars after a 15 day exposure under a semi-hydroponic system. * above bars indicate statistical differences for each cultivar between Ni-exposed plants and the control (0 μM Ni), at $p \leq 0.05$.

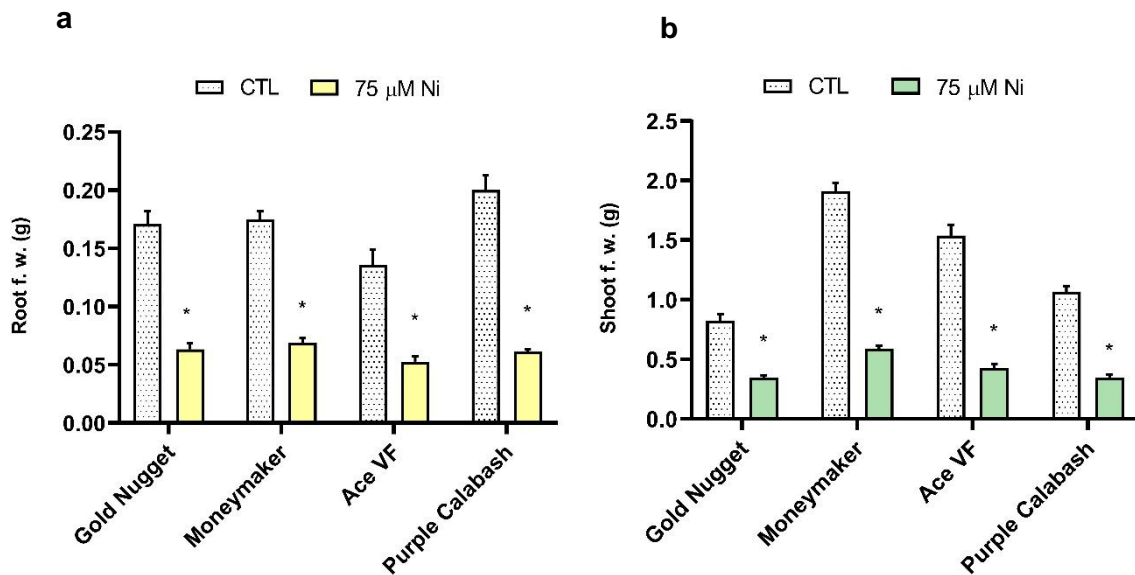


Figure 10 Effects of 75 µM Ni on the biomass of roots (a) and shoots (b) from 4 different tomato cultivars after a 15 day exposure under a semi-hydroponic system. * above bars indicate statistical differences for each cultivar between Ni-exposed plants and the respective control (0 µM Ni), at $p \leq 0.05$.

Since the main goal of this study was to evaluate the effects of stress on plant growth during its vegetative stage, and not during germination, the selection of tomato cultivars to be used on the final trial was based on the later results, despite the different sensitivity patterns observed during seedling development. Thus, the cultivars Gold Nugget and Purple Calabash were the ones selected for further analysis. For simplicity, these cultivars will be referred to as GN and PC, respectively, hereafter. Although the four tomato cultivars tested in the trial with perlite did not show the same level of sensitivity to Ni, it could be generally observed that exposing any of these plants to the concentration of 75 µM Ni for 15 days in perlite still affected tomato plant growth quite severely and caused yellowing and wilting of leaves.

4.3. EFFECTS OF SINGLE AND COMBINED EXPOSURE TO Ni AND PEG-INDUCED DROUGHT ON *S. LYCOPERSICUM* CULTIVARS GN AND PC

In the final trial, the plant growth of the two contrasting cultivars GN and PC, was compared, not only for their physiological performance under 50 µM Ni-stress or short-term water stress induced by the osmolyte PEG 6000, but also for their ability to cope with the simultaneous exposure to both stressors.

4.3.1. Biometric parameters and biomass production

Results referring to organ elongation and biomass production are presented in **Fig. 11 and 12**. Tomato plants from GN and PC cultivars grown under 50 μM Ni-stress exhibited a similar pattern of root length inhibition (**Fig. 11a**). PEG-induced drought did not seem to influence the length of roots, but the exposure to Ni led to reductions in root length by 43 % for GN and 57 % for PC plants. The Ni and PEG combination treatment affected the length of roots to a similar extent as single Ni-stress, with inhibitions in the range of 60 % for both cultivars, when compared to their CTL plants (**Fig. 11a**). The length of shoots in plants of the GN cultivar was significantly higher than that of PC plants, under CTL conditions (**Fig. 11b**). Under PEG-induced drought or Ni-stress, both cultivars had their shoot lengths significantly reduced by approximately 20 % and 70 %, respectively, in comparison to their CTL plants. The length of shoots was not further decreased in plants under combined stress, being similar to those under single Ni-stress (**Fig. 11b**).

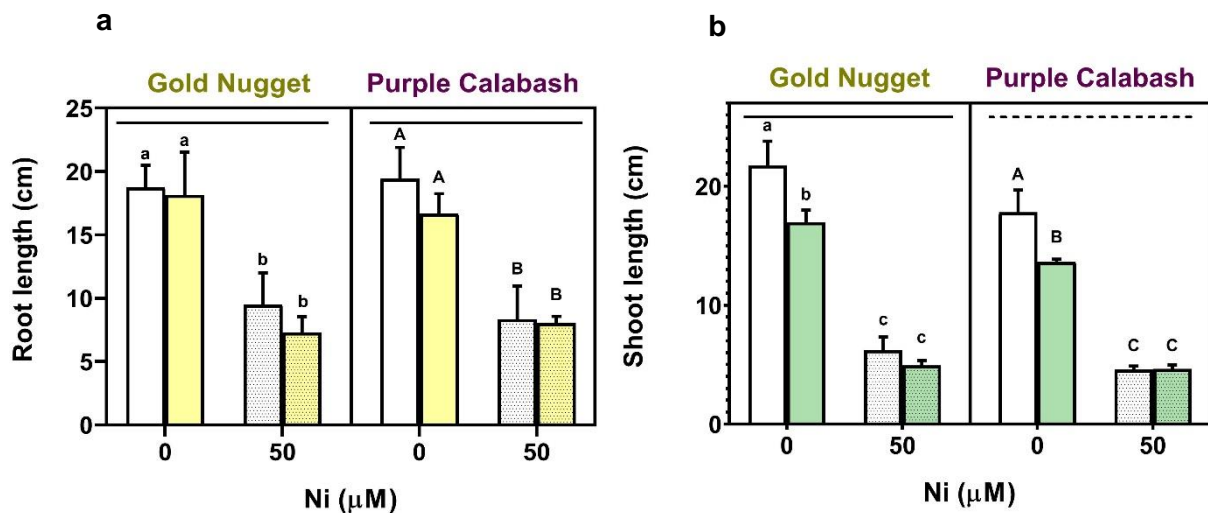


Figure 11 Effects of exposure to 50 μM Ni and/or 6 % (w/v) PEG 6000 on the length of roots (a) and shoots (b) of Gold Nugget and Purple Calabash tomato plants grown for 20 days under a semi hydroponic system. Colored bars refer to the 6 % (w/v) PEG 6000 treatment. Different lines on top of each sub chart represent significant differences between cultivars. Different letters above the bars of each cultivar represent significant differences between groups, at $p \leq 0.05$; lowercase and capital letters refer to GN and PC, respectively.

The biomass of roots was differentially affected in the two cultivars, although both witnessed sharp reductions in terms of root f. w. under Ni exposure (83 % for GN and 87 % for PC), independently of drought co-presence (94 % for GN and PC). When PEG 6000 was applied alone, a less severe inhibition of root biomass production was found in both cultivars (23 % for GN and 31 % for PC) (**Fig. 12a**). Concerning shoots, the two cultivars had identical patterns of biomass production (**Fig. 12b**). Similar reductions in f. w. were recorded for both cultivars under PEG and Ni-stress. The exposure to Ni, both individually or in combination with PEG, caused biomass reductions of 84 % and 93 %

for GN and 88 % and 91 % for PC shoots, in comparison to the respective CTL, while the PEG-induced stress alone only decreased the biomass of GN and PC shoots by 40 % and 32 %, respectively (**Fig. 12b**). Such sharp reductions in the growth of shoots in both cultivars were also accompanied by the gradual appearance of chlorotic spots and interveinal yellowing of leaves (data not shown).

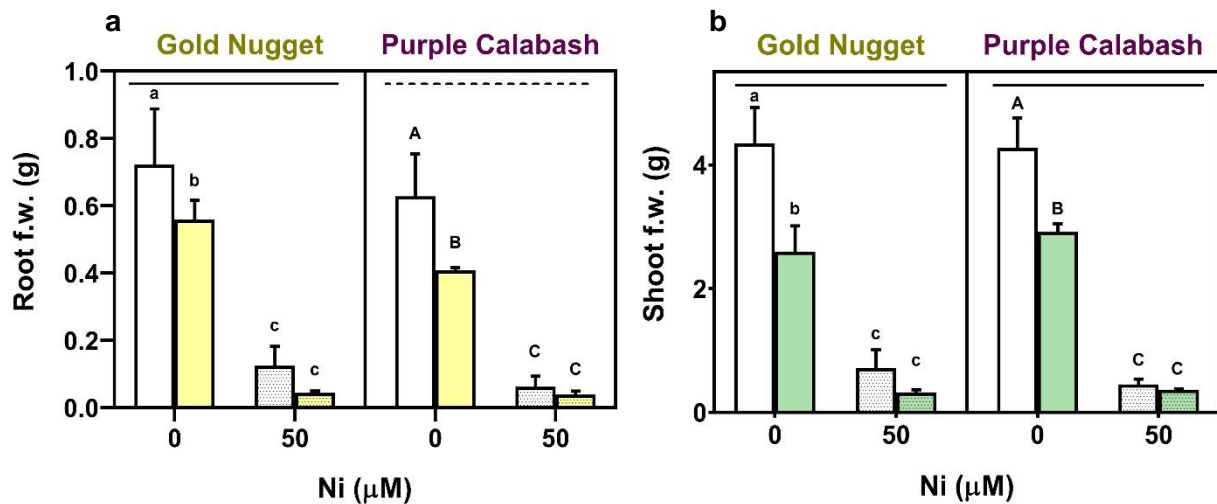


Figure 12 Effects of exposure to 50 µM Ni and/or 6 % PEG 6000 on the biomass of roots (a) and shoots (b) of Gold Nugget and Purple Calabash tomato plants grown for 20 days under a semi hydroponic system. Colored bars refer to the 6 % PEG 6000 treatment. Different lines on top of each sub chart represent significant differences between cultivars. Different letters above the bars of each cultivar represent significant differences between groups, at $p \leq 0.05$; lowercase and capital letters refer to GN and PC, respectively.

4.3.2. Relative water content

The water content in leaves and shoots of tomato plants was assessed in terms of percentage (%) of the total f. w.. The relative water content was similar in the roots of both cultivars under CTL conditions (**Fig. 13a**). Roots from GN and PC plants under Ni-stress alone did not suffer significant losses in terms of this parameter, in comparison to the respective CTL. The exposure to single PEG-induced stress, however, caused a significant decline in PC roots water content by 3 %, but not in the roots of GN (**Fig. 13a**). On the other hand, the combined stress treatment caused the water content in GN roots to drop 6 % but did not affect the water content in the roots of PC (**Fig. 13a**).

The relative water content in the shoots under CTL conditions was slightly higher in PC plants than in GN (**Fig. 13b**). In shoots of PC plants, the exposure to Ni reduced the relative water content by 3 %, both alone and in combination with simulated drought. Curiously, the drought treatment alone did not affect the relative water content in the shoots of this cultivar. In GN shoots, similarly to the roots, the relative water content was only significantly affected by the condition of combined stress, in which it dropped 3 % (**Fig. 13b**).

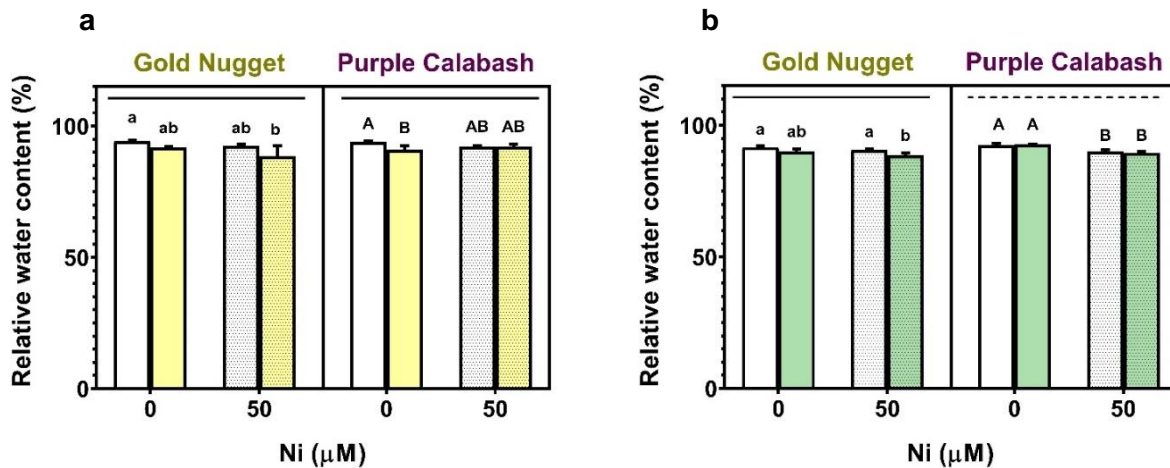


Figure 13 Effects of exposure to 50 μM Ni and/or 6 % PEG 6000 on the relative water content of roots (a) and shoots (b) of Gold Nugget and Purple Calabash tomato plants grown for 20 days under a semi hydroponic system. Colored bars refer to the 6 % PEG 6000 treatment. Different lines on top of each sub chart represent significant differences between cultivars. Different letters above the bars of each cultivar represent significant differences between groups, at $p \leq 0.05$; lowercase and capital letters refer to GN and PC, respectively.

4.3.3. Ni content in tissues

As expected, Ni content was enhanced in the tissues of plants from both cultivars under Ni exposure. GN plants were able to accumulate higher levels of Ni than PC (**Fig. 14**). In plants of the PC cultivar, the combination of Ni-stress with PEG exposure did not alter the accumulation of this HM in neither the roots nor the shoots. In GN, however, the combined stress further increased the uptake and accumulation of Ni from the substrate (**Fig. 14**). Ni levels increased much more in the root tissues (**Fig. 14a**, 42- to 49-fold increases) than in the shoots of both cultivars (**Fig. 14b**, 6 to 7-fold increases).

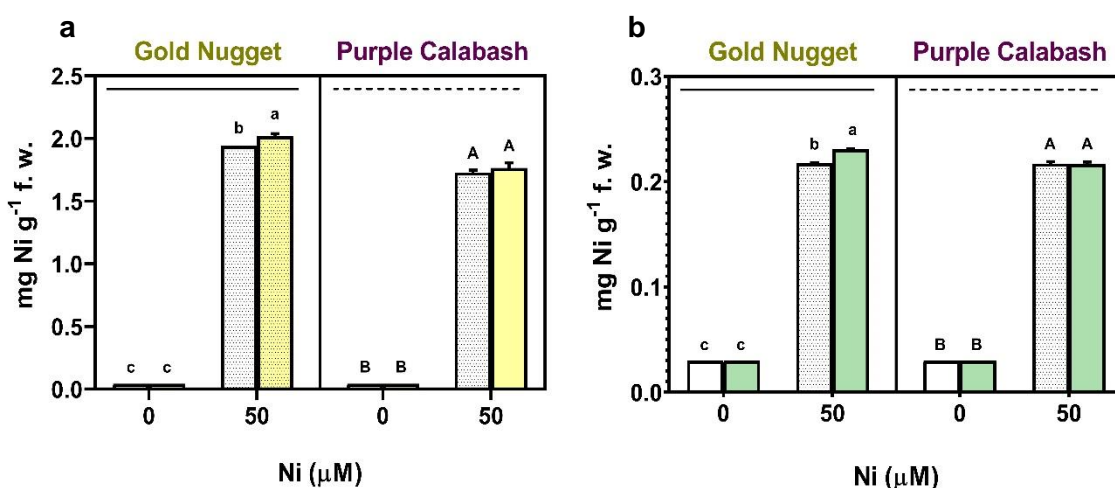


Figure 14 Effects of exposure to 50 μM Ni and/or 6 % PEG 6000 on the Ni content of roots (a) and shoots (b) of Gold Nugget and Purple Calabash tomato plants grown for 20 days under a semi hydroponic system. Colored bars refer to the 6 % PEG 6000 treatment. Different lines on top of each sub chart represent significant differences between cultivars. Different letters above the bars of each cultivar represent significant differences between groups, at $p \leq 0.05$; lowercase and capital letters refer to GN and PC, respectively.

4.3.4. Photosynthetic pigments

As can be observed, leaves of PC plants had less 35 % Chl content and less 37 % Car than the leaves of GN plants under homeostatic conditions (**Fig. 15**). Under single Ni-stress, the levels of photosynthetic pigments decreased by approximately 40 % in plants of both cultivars, while in combination with the drought treatment, GN leaves suffered sharper reductions of Chl and Car, by 60 % and 64 %, respectively; in PC leaves, these pigments were only diminished by 43 % and 50 %, respectively (**Fig. 15**). Interestingly, although there were no significant changes in the levels of pigments in GN leaves under single exposure to PEG 6000, when compared to the CTL, PEG-treated plants of the PC cultivar showed a demarked increase in the accumulation of these pigments, in the range of 70 % (**Fig. 15**).

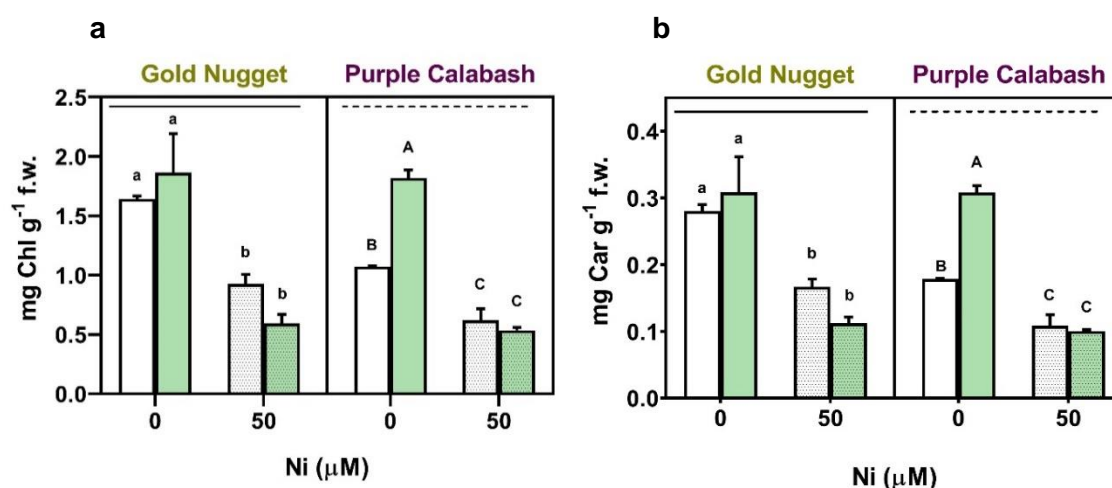


Figure 15 Effects of exposure to 50 μM Ni and 6 % PEG 6000 on the content of the photosynthetic pigments Chl (a) and Car (b) in the shoots of plants from the tomato cultivars Gold Nugget and Purple Calabash grown for 20 days under a semi hydroponic system. Colored bars refer to the 6 % PEG 6000 treatment. Different lines on top of each sub chart represent significant differences between cultivars. Different letters above the bars of each cultivar represent significant differences between groups, at $p \leq 0.05$; lowercase and capital letters refer to GN and PC, respectively.

4.3.5. Oxidative stress markers

4.3.5.1. Reactive Oxygen Species (ROS)

The levels of H_2O_2 and $O_2^{\cdot -}$ were assessed in the roots and shoots of both cultivars under all treatments. The basal levels of H_2O_2 in the roots and shoots of PC plants were considerably lower than those in GN plants under CTL conditions (**Fig. 16**). In the roots of GN plants, the concentration of this ROS was only significantly increased under combined stress (by 72 %), although there was a tendency to increase under Ni-stress alone (by 40 %) and to decrease under drought (by 30 %) (**Fig. 16a**). The same pattern was observed for PC plants, although in this cultivar's roots the levels of H_2O_2 increased

more due to the exposure to Ni, both as a single stressor and in combination with PEG (by 100 % and 129 %, respectively). The single exposure to PEG did not affect the levels of H₂O₂ in PC roots (**Fig. 16a**). In the GN leaves, these relatively higher levels of H₂O₂ were also somewhat sustained in plants under simulated drought and combined stresses but increased by 56 % in the shoots of GN plants exposed to single Ni-stress (**Fig. 16b**). In PC shoots, PEG treatment did not affect the levels of H₂O₂, but these were 1.3 and 1.7-fold higher in plants under single Ni- and combined stress, respectively (**Fig. 16b**).

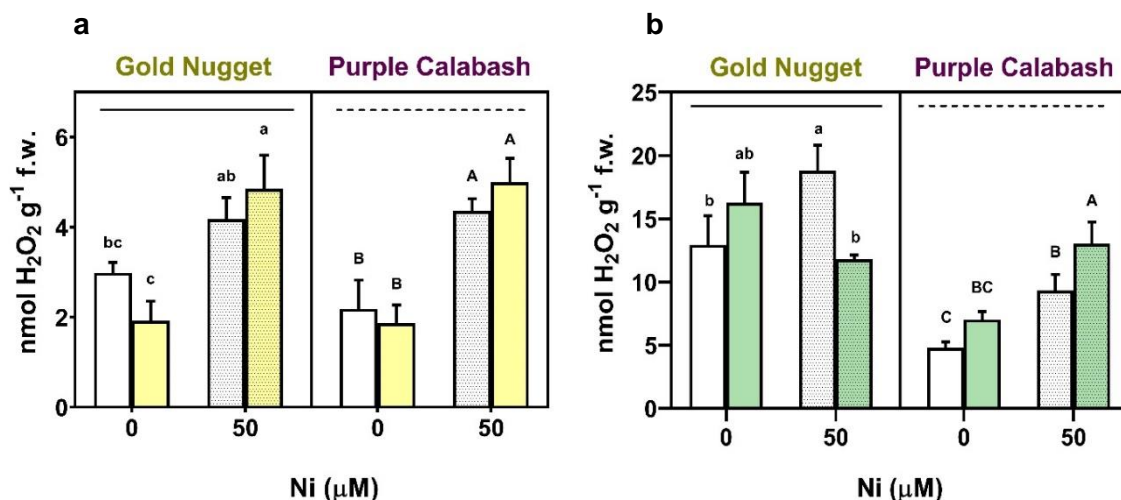


Figure 16 Effects of exposure to 50 μM Ni and/or 6 % PEG 6000 on the levels of H₂O₂ in the roots (a) and shoots (b) of Gold Nugget and Purple Calabash tomato plants grown for 20 days under a semi hydroponic system. Colored bars refer to the 6 % PEG 6000 treatment. Different lines on top of each sub chart represent significant differences between cultivars. Different letters above the bars of each cultivar represent significant differences between groups, at $p \leq 0.05$; lowercase and capital letters refer to GN and PC, respectively.

The two cultivars showed differences in O₂⁻ accumulation under CTL conditions and upon stress exposure. Under CTL conditions, GN plants had higher levels of this ROS in the roots but lower levels in the shoots, when compared to PC plants (**Fig. 17**). The accumulation of O₂⁻ in the roots of GN and PC plants under stress followed a different pattern than that of H₂O₂ (**Fig. 17a**). No significant increases were detected in the levels of O₂⁻ in the roots of both cultivars under any type of stress, in comparison to CTL plants. In fact, the levels of O₂⁻ were even lowered by 64 % and 46 % in the roots of GN and PC exposed to single Ni-stress, respectively (**Fig. 17a**). For the GN cultivar, the levels of O₂⁻ were also reduced by 34 % and 45 % in response to the PEG treatments, single and combined, respectively (**Fig. 17a**). In the shoots, however, the levels of this ROS were increased in response to stress (**Fig. 17b**). The levels of O₂⁻ in the shoots of GN plants under Ni-stress alone were identical to CTL, but under single or combined PEG-induced stress, these levels increased by 129 % and 175 %, respectively (**Fig. 17b**). Differently, the shoots of PC plants suffered an increased accumulation of

O_2^- under all stress treatments, by 103 % in plants under drought, 138 % under Ni-stress alone, and 172 % under combined Ni and osmotic stress (**Fig. 17b**).

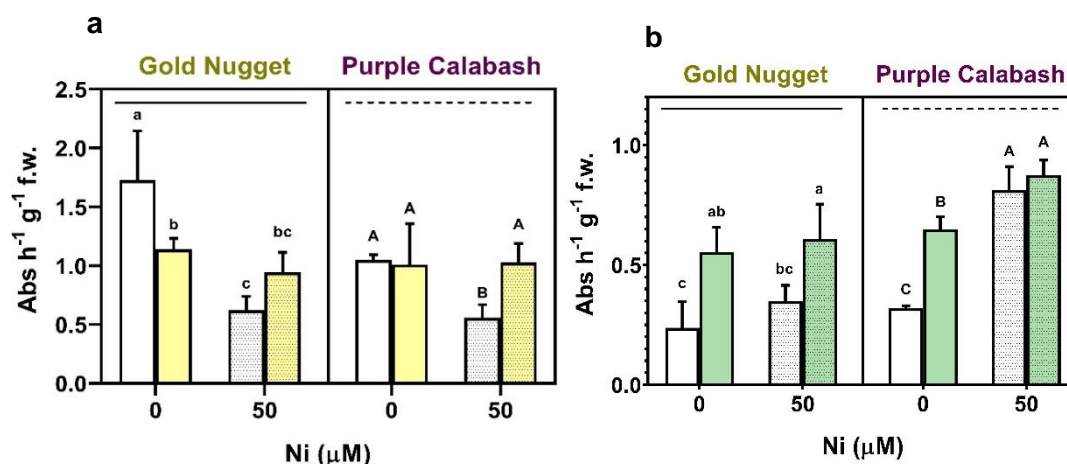


Figure 17 Effects of exposure to 50 μM Ni and/or 6 % PEG 6000 on the levels of O_2^- in the roots (a) and shoots (b) of Gold Nugget and Purple Calabash tomato plants grown for 20 days under a semi hydroponic system. Colored bars refer to the 6 % PEG 6000 treatment. Different lines on top of each sub chart represent significant differences between cultivars. Different letters above the bars of each cultivar represent significant differences between groups, at $p \leq 0.05$; lowercase and capital letters refer to GN and PC, respectively.

4.3.5.2. Lipid Peroxidation (LP)

The levels of MDA, one of the final products of polyunsaturated fatty acids peroxidation in the cells, and so a LP marker, were found to be significantly higher (by 55 %) in the roots of GN plants under CTL conditions when compared to those of PC plants (**Fig. 18a**). Although the degree of LP showed an odd tendency to decrease in the roots of GN plants exposed to single Ni-stress (by 60 %), the levels of MDA were increased by 63 % in roots under combined exposure (**Fig. 18a**). For PC, single Ni-stress did not influence the MDA levels in roots, being the exposure to PEG 6000, alone or combination with the HM, the responsible factor for increasing the degree of LP (by 60 % and 50 %, respectively, over the CTL) (**Fig. 18a**). Regarding shoots, GN plants under CTL conditions had 38 % less MDA than the PC cultivar. Curiously, in the shoots of GN plants, exposure to isolated stresses did not affect MDA levels and the combined stress condition even caused a 42 % reduction (**Fig. 18b**). In PC plants, the foliar levels of MDA were also found to be unchanged in response to Ni-stress and reduced by approximately 40 % in plants exposed to PEG treatments, independently of Ni co-exposure (**Fig. 18b**).

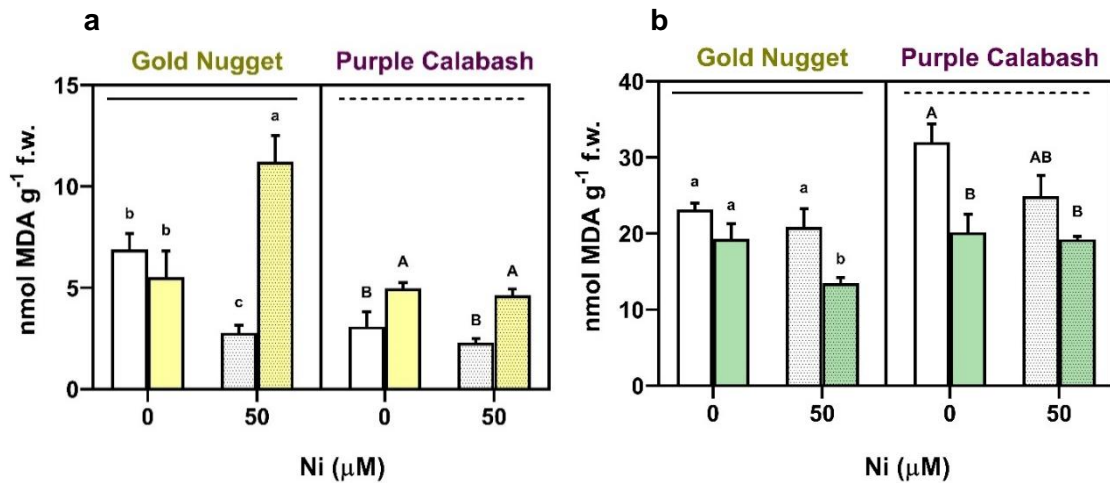


Figure 18 Effects of exposure to 50 μM Ni and/or 6 % PEG 6000 on the levels of MDA in the roots (a) and shoots (b) of Gold Nugget and Purple Calabash tomato plants grown for 20 days under a semi hydroponic system. Colored bars refer to the 6 % PEG 6000 treatment. Different lines on top of each sub chart represent significant differences between cultivars. Different letters above the bars of each cultivar represent significant differences between groups, at $p \leq 0.05$; lowercase and capital letters refer to GN and PC, respectively.

4.3.6. Non-enzymatic components of the antioxidant (AOX) system

4.3.6.1. Proline (Pro)

Despite the similarity between the two cultivars in terms of Pro accumulation under combined stresses, PC plants accumulated Pro in roots and shoots to a much higher extent than GN plants (**Fig. 19**). For the single stress treatments, no differences were observed in the levels of Pro in the roots of both cultivars, when compared to the CTL plants. However, Pro content was found to be acutely enhanced in the roots of both cultivars under combined exposure to Ni and PEG, by as much as 23-fold in GN roots and 58-fold in PC roots, when compared to the levels of the CTL plants (**Fig. 19a**). Concerning shoots, GN plants increased Pro accumulation by 9-fold in response to Ni-stress, being this effect even more evident upon the combination of Ni and drought (14-fold), in comparison to the CTL; PC shoots also showed a trend to increase Pro levels under Ni-stress alone, reaching statistical significance in response to the combination of both stressors (60-fold increase in relation to CTL) (**Fig. 19b**).

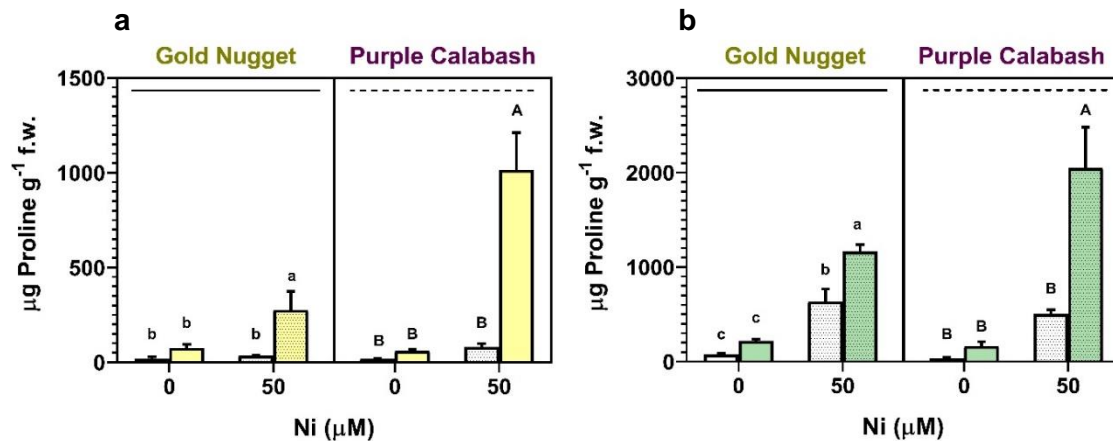


Figure 19 Effects of exposure to 50 µM Ni and/or 6 % PEG 6000 on the levels of Pro in the roots (a) and shoots (b) of Gold Nugget and Purple Calabash tomato plants grown for 20 days under a semi hydroponic system. Colored bars refer to the 6 % PEG 6000 treatment. Different lines on top of each sub chart represent significant differences between cultivars. Different letters above the bars of each cultivar represent significant differences between groups, at $p \leq 0.05$; lowercase and capital letters refer to GN and PC, respectively.

4.3.6.2. Glutathione (GSH)

The pattern of GSH production and accumulation seemed to be alike in plants from both cultivars. As illustrated in **Fig. 20a**, roots of both cultivars significantly enhanced GSH accumulation upon the combined exposure to drought and Ni; however, under single stress exposure, either Ni or PEG-induced drought, only an apparent trend was found. In what regards the aerial parts, in shoots of GN plants no significant differences were observed in the levels of GSH for any stress treatment, despite of the apparent increase of GSH in response to Ni single and co-exposure (**Fig. 20b**). In the case of PC, treatment with Ni alone was the only treatment causing a significant increase of GSH in the shoots (by 185 %), though this AOX also showed a tendency to increase under combined stress conditions.

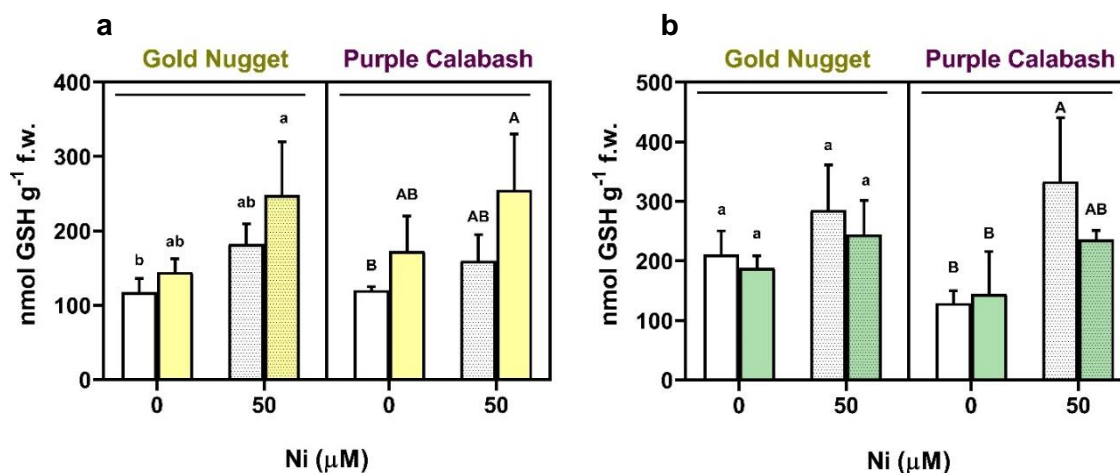


Figure 20 Effects of exposure to 50 μM Ni and/or 6 % PEG 6000 on the levels of GSH in the roots (a) and shoots (b) of Gold Nugget and Purple Calabash tomato plants grown for 20 days under a semi hydroponic system. Colored bars refer to the 6 % PEG 6000 treatment. Different lines on top of each sub chart represent significant differences between cultivars. Different letters above the bars of each cultivar represent significant differences between groups, at $p \leq 0.05$; lowercase and capital letters refer to GN and PC, respectively.

4.3.6.3. Ascorbate - reduced (AsA) and oxidized (DHA) forms

Results concerning total, reduced and oxidized AsA (DHA) are compiled in **Table 3**. In the shoots of both cultivars, almost no significant differences were found in the relative or absolute levels of AsA in plants under stress, when compared to their respective CTL, except for the levels of reduced AsA in PC shoots, which were increased in response to Ni (1.4 fold). Although the results do not allow to identify the factor cultivar as a source of variation, it is possible to observe that the levels of AsA were generally higher in GN shoots under CTL conditions, than in PC, and that, although there are no significant differences between stress treatments, exposure to Ni and/or PEG caused a slight increase in DHA content (and total AsA) in PC plants, to levels similar to those from GN shoots. Despite the lack of variation in AsA levels in the shoots between treatments for each cultivar, the relative content of reduced AsA was much higher in the shoots of GN than in the shoots of PC, and consequently, the AsA / DHA and AsA / Total ratios were also higher for GN than for PC plants, regardless of stress conditions. Under CTL conditions, GN plants also had slightly higher absolute levels of total AsA and DHA than the shoots of PC. The levels of total and oxidized AsA, however, tended to increase in PC plants under stress, to levels as high as those of GN plants, although no significant variation could be found between treatments.

In the case of roots, the absolute levels of AsA were similar for plants of both cultivars under CTL condition but showed different responses to stress. Exposing GN plants to PEG 6000 was responsible for a sharp increase in the DHA levels in the roots

of this cultivar, being this effect even more noticeable for the combined stress condition (6-fold) than for the single exposure (4-fold) in relation to the CTL. This increase was also observed in the roots of PC, but to a much smaller extent (1.6-fold for single PEG treatment and 2.3-fold for combined stress). The levels of reduced AsA were also enhanced by exposure to both stress factors, especially in response to Ni toxicity (over 1-fold) and in combination with drought (over 1.4-fold). For GN, the ratios AsA/DHA and AsA/Total in Ni-exposed plants were found to be identical to those of the CTL but were reduced under drought. The DHA/Total ratio, on the other hand, was enhanced in the roots of plants exposed to PEG 6000, and slightly decreased in those under Ni-stress alone.

Table 3 Effects of exposure to 50 μM Ni and 6 % PEG 6000 on the levels and ratios of total, reduced and oxidized (DHA) forms of AsA in the roots and shoots of plants from the tomato cultivars Gold Nugget and Purple Calabash grown for 20 days under a semi hydroponic system. For simplicity, reduced AsA was termed AsA. Results are expressed as mean ($\mu\text{mol g}^{-1}$ f. w.) \pm SD. Different lines underlying the concentrations in each cultivar represent significant differences between cultivars. Different letters above the bars of each cultivar represent significant differences between groups, at $p \leq 0.05$; lowercase and capital letters refer to GN and PC, respectively.

		Gold Nugget				Purple Calabash			
		CTL	6 % PEG 6000	50 μM Ni	50 μM Ni + 6 % PEG 6000	CTL	6 % PEG 6000	50 μM Ni	50 μM Ni + 6 % PEG 6000
Shoots	Total	0.88 \pm 0.30 a	0.80 \pm 0.15 a	0.93 \pm 0.28 a	0.87 \pm 0.18 a	0.43 \pm 0.11 A	0.79 \pm 0.39 A	1.04 \pm 0.26 A	0.93 \pm 0.33 A
	DHA	0.30 \pm 0.23 a	0.34 \pm 0.14 a	0.28 \pm 0.04 a	0.29 \pm 0.15 a	0.19 \pm 0.08 A	0.56 \pm 0.37 A	0.63 \pm 0.30 A	0.60 \pm 0.34 A
	AsA	0.59 \pm 0.09 a	0.46 \pm 0.02 a	0.64 \pm 0.25 a	0.57 \pm 0.02 a	0.24 \pm 0.05 B	0.24 \pm 0.03 B	0.41 \pm 0.07 A	0.34 \pm 0.03 AB
	AsA / Total	0.70 \pm 0.15 a	0.59 \pm 0.11 a	0.68 \pm 0.07 a	0.68 \pm 0.12 a	0.57 \pm 0.12 A	0.34 \pm 0.12 A	0.41 \pm 0.13 A	0.39 \pm 0.13 A
	DHA / Total	0.30 \pm 0.15 a	0.41 \pm 0.11 a	0.32 \pm 0.07 a	0.32 \pm 0.12 a	0.43 \pm 0.12 A	0.66 \pm 0.12 A	0.59 \pm 0.13 A	0.61 \pm 0.13 A
	AsA / DHA	2.89 \pm 1.87 a	1.54 \pm 0.75 a	2.29 \pm 0.78 a	2.56 \pm 1.77 a	1.48 \pm 0.77A	0.54 \pm 0.26 A	0.76 \pm 0.35 A	0.69 \pm 0.34 A
Roots	Total	0.22 \pm 0.03 c	0.57 \pm 0.11 b	0.46 \pm 0.03 b	0.89 \pm 0.13 a	0.25 \pm 0.02C	0.44 \pm 0.03 B	0.43 \pm 0.10 B	0.69 \pm 0.06 A
	DHA	0.06 \pm 0.03 b	0.30 \pm 0.07 a	0.10 \pm 0.03 b	0.44 \pm 0.10 a	0.09 \pm 0.04 B	0.23 \pm 0.03 A	0.09 \pm 0.08 B	0.30 \pm 0.06 A
	AsA	0.16 \pm 0.01 d	0.27 \pm 0.05 c	0.36 \pm 0.00 b	0.45 \pm 0.03 a	0.16 \pm 0.01 D	0.21 \pm 0.01 C	0.34 \pm 0.02 B	0.39 \pm 0.05 A
	AsA / Total	0.73 \pm 0.09 a	0.48 \pm 0.06 b	0.78 \pm 0.04 a	0.50 \pm 0.04 b	0.66 \pm 0.10 AB	0.48 \pm 0.02 B	0.81 \pm 0.13 A	0.57 \pm 0.07 B
	DHA / Total	0.27 \pm 0.09 b	0.53 \pm 0.06 a	0.22 \pm 0.04 b	0.50 \pm 0.04 a	0.34 \pm 0.10 AB	0.52 \pm 0.02 A	0.19 \pm 0.13 B	0.43 \pm 0.07 A
	AsA / DHA	3.07 \pm 1.65 ab	0.91 \pm 0.19 b	3.72 \pm 0.85 a	1.03 \pm 0.18 b	2.14 \pm 0.99 AB	0.93 \pm 0.07 B	6.19 \pm 3.75 A	1.37 \pm 0.43 AB

4.3.7. Enzymatic components of the antioxidant (AOX) system

The activity levels of the enzymes CAT, APX and SOD were measured to assess the induction of AOX defenses in response to stress. A very similar pattern of activity was observed for the three enzymes (**Fig. 21-23**). In the case of roots, the activity of CAT in roots under stress remained similar to that of the CTL, in both cultivars (**Fig. 21a**). APX also showed a weak response to stress in the roots of GN, but had its activity somewhat enhanced in the roots of PC plants. In these tissues and comparing to PC CTL plants, APX was more activated in the presence of Ni-stress (by 120 % for single, and by 111 % for combined stress), than under PEG 6000 (by 55 %) (**Fig. 22a**). SOD activity, on the other hand, even decreased in GN roots under single exposure to PEG 6000 (by 36 %) and in PC plants under combined stress (by 33 %) (**Fig. 23a**).

Despite the lack of variation in the activities of CAT, APX or SOD in the roots of plants under PEG and/or Ni-induced stresses, these AOX enzymes were strongly stimulated by single exposure to Ni in the shoots of GN plants (6-fold rise for CAT, 5-fold for APX, and 3-fold for SOD) (**Fig. 21-23b**). Nevertheless, the co-exposure of GN plants to Ni and water deficit seemed to reduce the total activity of these AOX enzymes back to the CTL levels. Single drought stress also tended to increase the activity of these three enzymes in the shoots of GN, but to a much lower extent than Ni-stress. In the case of PC, such increase of activity in response to Ni-stress was not observed for any of the enzymes assessed (**Fig. 21-23b**). Actually, neither CAT or APX activity levels changed in shoots of PC plants (**Fig. 21-22b**), and SOD was only significantly enhanced in response to the combined stress (135 %), in relation to the respective CTL (**Fig. 23b**).

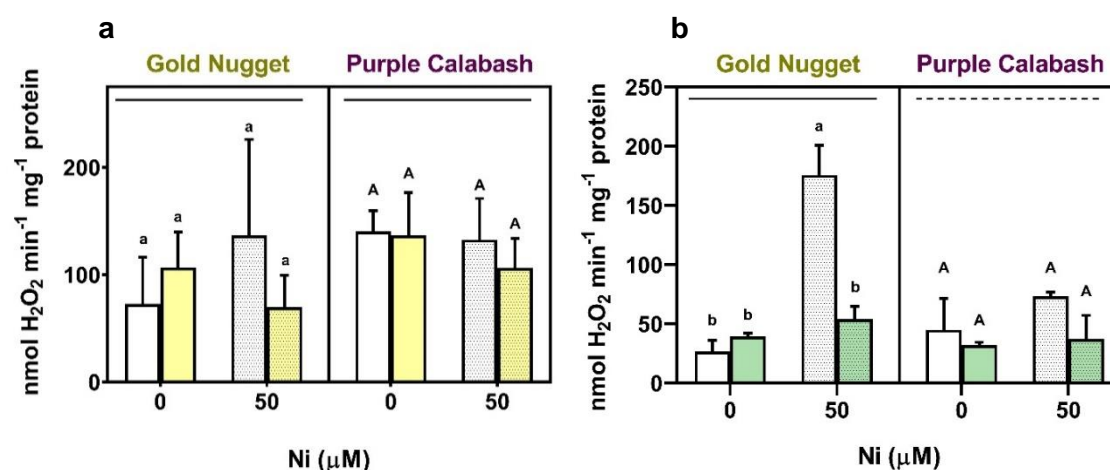


Figure 21 Effects of exposure to 50 μM Ni and/or 6 % PEG 6000 on the activity of CAT in the roots (a) and shoots (b) of Gold Nugget and Purple Calabash tomato plants grown for 20 days under a semi hydroponic system. Colored bars refer to the 6 % PEG 6000 treatment. Different lines on top of each sub chart represent significant differences between cultivars. Different letters above the bars of each cultivar represent significant differences between groups, at $p \leq 0.05$; lowercase and capital letters refer to GN and PC, respectively.

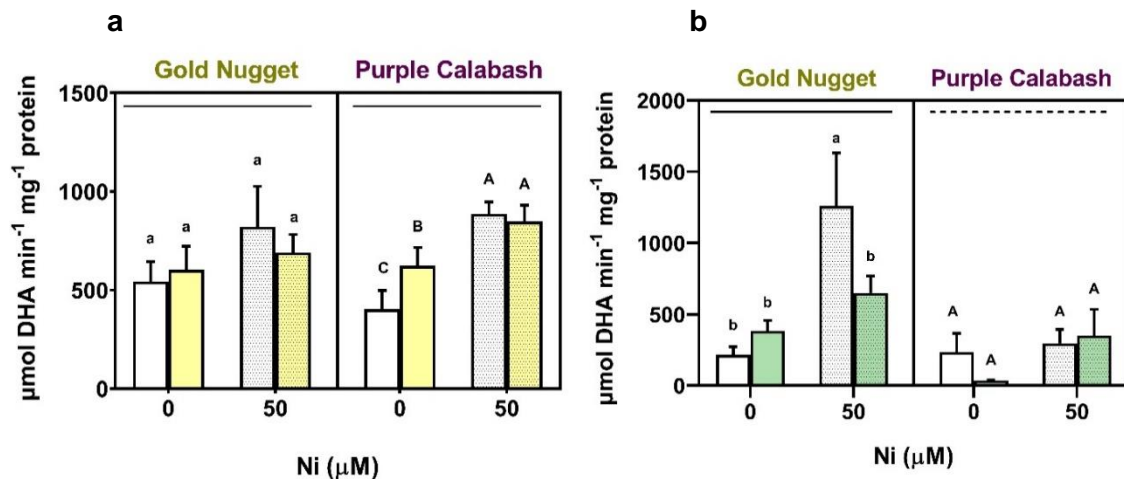


Figure 22 Effects of exposure to 50 μM Ni and/or 6 % PEG 6000 on the activity of **APX** in the roots (a) and shoots (b) of Gold Nugget and Purple Calabash tomato plants grown for 20 days under a semi hydroponic system. Colored bars refer to the 6 % PEG 6000 treatment. Different lines on top of each sub chart represent significant differences between cultivars. Different letters above the bars of each cultivar represent significant differences between groups, at $p \leq 0.05$; lowercase and capital letters refer to GN and PC, respectively.

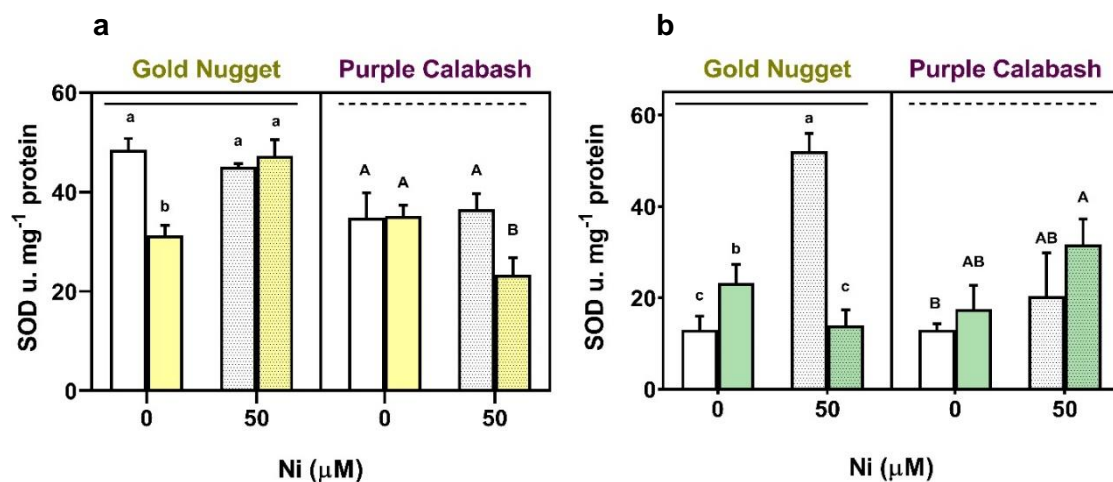


Figure 23 Effects of exposure to 50 μM Ni and/or 6 % PEG 6000 on the activity of **SOD** in the roots (a) and shoots (b) of Gold Nugget and Purple Calabash tomato plants grown for 20 days under a semi hydroponic system. Colored bars refer to the 6 % PEG 6000 treatment. Different lines on top of each sub chart represent significant differences between cultivars. Different letters above the bars of each cultivar represent significant differences between groups, at $p \leq 0.05$; lowercase and capital letters refer to GN and PC, respectively.

4.3.8. Levels of free polyamines (PAs)

The levels of the three main plant PAs – Put, Spd and Spm – were assessed by HPLC-UV to evaluate the effects of Ni and drought on inducing their production or depletion as free biogenic amines (Fig. 24-26). Different patterns of Put accumulation were observed in the roots and shoots between the two selected tomato cultivars.

Overall, Spm could not be detected in any tissue of either cultivars (data not shown). GN plants exhibited higher levels of Put under CTL conditions, in both organs analyzed (**Fig. 24**). In shoots, both the single Ni and the combined treatments caused significant enhances in the levels of Put, from 116 % to 155 % in GN shoots, and from 151 % to 184 % in shoots of PC. Moreover, GN shoots under single PEG treatment also witnessed an increase in the levels of Put, by 133 % over the CTL (**Fig. 24b**). In roots, although the Put was not changed in response to the drought treatment, the single exposure to Ni was found to oddly decrease Put, by 64 % in the cultivar GN and at levels that were untraceable by HPLC-UV in the cultivar PC (**Fig. 24a**). Due to the sharp reductions in the levels of Put, the Spd / Put ratio was significantly increased in the roots of both cultivars in response to the single Ni treatment (**Fig. 26a**). In the shoots, Put variations caused this ratio to decrease in GN in an identical way for all stress treatments, and to decrease more markedly in PC shoots under combined stress (**Fig. 24b**).

Comparing to Put, the levels of Spd were less affected in response to both stress factors, but, overall, Spd was the most abundant PA in roots of both cultivars (**Fig. 25a**). Specifically regarding Spd, this PA's levels were significantly enhanced in roots under Ni-stress alone for PC, with rises over 50 %, or in combination with water deficit in GN, with an increase of 40 % (**Fig. 25a**). In shoots, levels of Spd were also much higher than those of Put in both cultivars under CTL conditions, but the exposure to stress caused shoot Put levels to increase to concentrations higher than those of Spd (**Fig. 25b**).

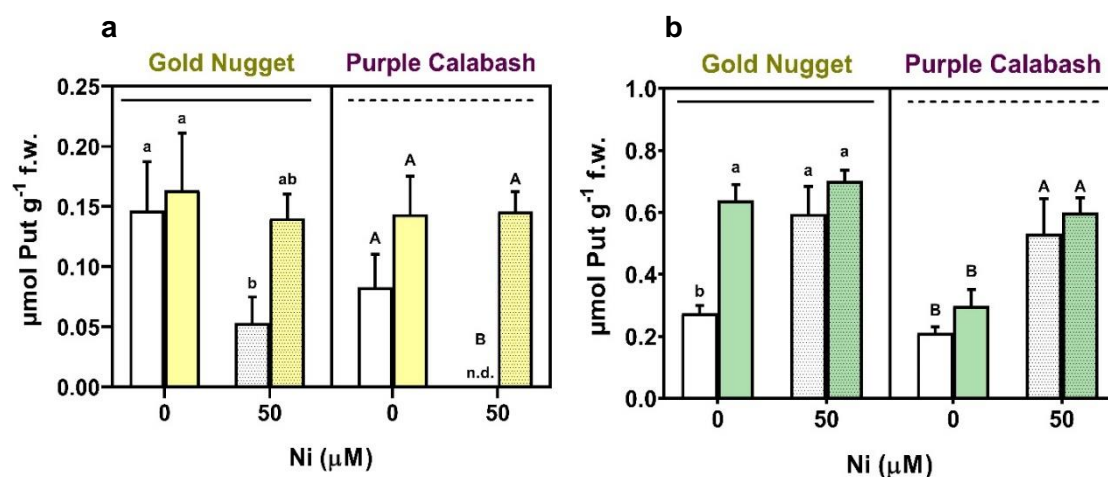


Figure 24 Effects of exposure to 50 μM Ni and/or 6 % PEG 6000 on the levels of Put in the roots (a) and shoots (b) of Gold Nugget and Purple Calabash tomato plants grown for 20 days under a semi hydroponic system. Colored bars refer to the 6 % PEG 6000 treatment. Different lines on top of each sub chart represent significant differences between cultivars. Different letters above the bars of each cultivar represent significant differences between groups, at $p \leq 0.05$; lowercase and capital letters refer to GN and PC, respectively.

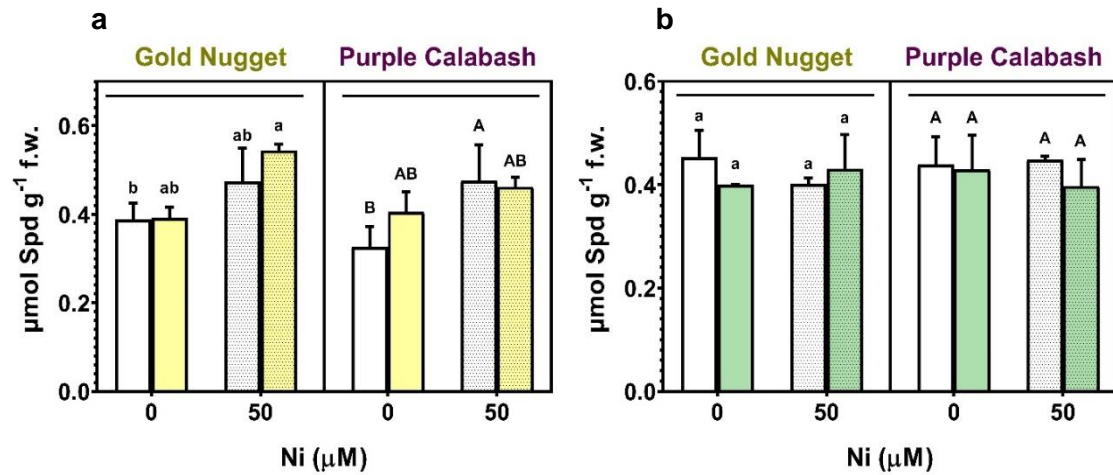


Figure 25 Effects of exposure to 50 μM Ni and/or 6 % PEG 6000 on the levels of Spd in the roots (a) and shoots (b) of Gold Nugget and Purple Calabash tomato plants grown for 20 days under a semi hydroponic system. Colored bars refer to the 6 % PEG 6000 treatment. Different lines on top of each sub chart represent significant differences between cultivars. Different letters above the bars of each cultivar represent significant differences between groups, at $p \leq 0.05$; lowercase and capital letters refer to GN and PC, respectively.

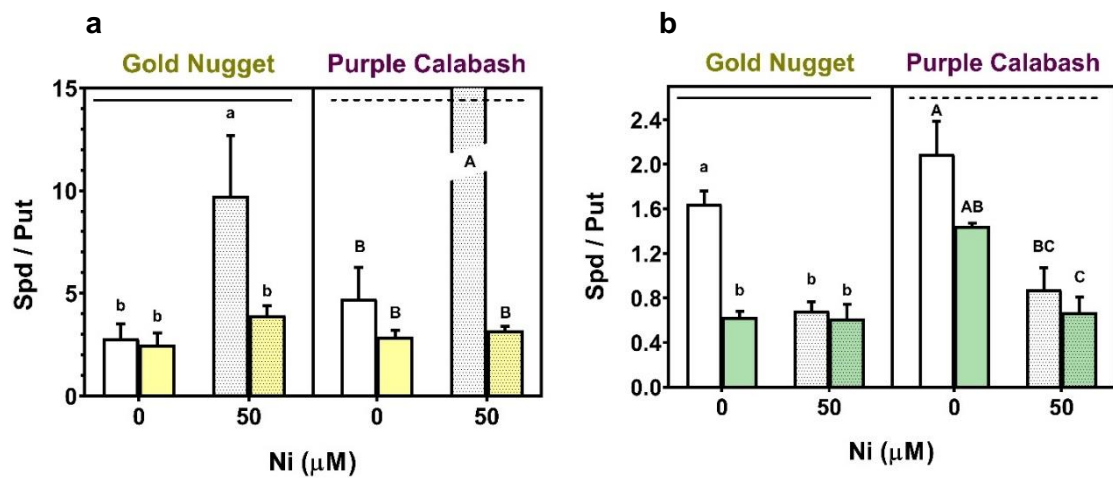


Figure 26 Effects of exposure to 50 μM Ni and/or 6 % PEG 6000 on the ratio Spd / Put in the roots (a) and shoots (b) of Gold Nugget and Purple Calabash tomato plants grown for 20 days under a semi hydroponic system. Colored bars refer to the 6 % PEG 6000 treatment. Different lines on top of each sub chart represent significant differences between cultivars. Different letters above or within the bars of each cultivar represent significant differences between groups, at $p \leq 0.05$; lowercase and capital letters refer to GN and PC, respectively. The bar respective to the Spd / Put ratio in the roots of PC plants under single Ni-stress is intentionally represented as “limitless”, since Put levels in these tissues were untraceable.

4.4. INVOLVEMENT OF METAL TRANSPORTERS IN THE RESPONSES OF GN AND PC PLANTS TO SINGLE AND COMBINED STRESS

4.4.1. Computational analysis of metal transporters possibly involved in the detoxification of Ni

Several metal transporters from the tomato proteome were identified as being possibly responsible for carrying Ni into the plant vacuoles or cell walls under Ni-stress, contributing for the detoxification of this HM. These transporters were selected based on: i) evidence found for homologue transporters in other plant species, ii) their affinity to HM and HM-conjugates, iii) their vacuolar and/or cellular membrane localization, iv) their stress-responsive accumulation. As mentioned in section 1.3.3, members of the *ABC* gene family such as *AtABCC3*, *AtABCC6*, *AtABCB27*, and *HvMDR2*, have been reported to transport HM into the vacuoles of plant cells, mainly in the form of conjugates with phytochelatins and GSH. Most tomato ABC transporters have been identified in a genome-wide analysis by Ofori et al. (2018). From all the 26 ABCC transporters therein identified, 9 were chosen for the transcriptomic analysis in the present study (*SIABCC3*, 5, 6, 14-18, and 25). The selection criteria used was based on the predicted high levels of expression in the roots, according to Ofori et al. (2018), as well as on the similarity with ABCC transporters from other species, whose involvement in the detoxification of HMs had been previously suggested. All these 9 ABCC transporters from tomato had been reported to be strongly and/or solely expressed in roots (Ofori et al., 2018). Since it is considered that most HM detoxification occurs in the root tissues of plants (Chen et al., 2009; Sachan & Lal, 2017), the expression patterns of the selected transcripts could provide some information on the responses of tomato plants to HM stress and on their ability to overcome it, despite the post-translational mechanisms that are involved in the regulation of transporter activity.

The same line of thought was used in the selection of the *SIABCB21* transporter, also identified by Ofori et al. (2018) as being strongly expressed in the roots, which shares a high similarity with the transporters *AtABCB27* and *HvMDR2*, involved in the transport and vacuolar sequestration of Al and Fe, in *A. thaliana* and in *H. vulgare*, respectively. The putative transporters *SIIREG2*-like, *SIMTP1*, and *SICAX3* (**Table 4**) are not yet validated in nucleotide databases, and have not yet been characterized in tomato plants, but the predicted sequences of these proteins, and consequently, of their corresponding mRNAs and genomic sequences, could be found amongst the top hits upon a simple

protein BLAST of known metal transporters from other plant species against the tomato genome, using NCBI's BLAST resource. The selection of these three putative transporters was based on the highest *blasting* scores, query coverage, E values and maximum identity % of their aminoacidic sequences, when compared with characterized homologues in *Arabidopsis thaliana*, *Oryza sativa*, *Vitis vinifera*, and *Noccaea goesingense* (OsMTP1, NgoesMTP1, AtCAX4, AtCAX2, VvCAX3, and AtIREG2). Moreover, by *blasting* the sequences of known vacuolar metal transporters from the ABC family, such as AtABCC3 and 6, AtABCB27, and HvMDR2, against the tomato proteome, the nine previously selected transporters from Ofori's list have resulted in very high hits, confirming their homology and accurate classification as vacuolar metal transporters, which highlights their utility for further analysis. The protein sequences, predicted genes, and mRNAs encoding for these 13 metal transporter proteins from *S. lycopersicum* were characterized for their gene, transcript and protein lengths, locus position and orientation in the genome, as well as protein size, topology, and subcellular location (**Tables 4 and 5**). All 13 *loci* listed therein can be found either on NCBI's, Ensembl Plants and/or Sol Genomics Network databases with the IDs presented in the first columns of **Table 4**.

Although a lot of information could be found in these three different databases, some aspects were found to be incoherent, and require further clarification. The 9 transporters listed by Ofori et al. (2018) were all recognizable with the IDs therein mentioned in the databases Sol Genomics Network and Ensembl Plants, except for SIABCC17 and SIABCB21, whose supposed IDs Solyc12g036150.1 and Solyc03g114950.2 (Ofori et al., 2018) cannot be found on Ensembl Plants. In this database, each transcript is usually shown with redirecting links to their respective pages on NCBI and UniProt, which simplifies the search for the corresponding protein, alternative transcripts, and gene sequences. In the case of ABCC17 and ABCB21 the NCBI and UniProt sites had to be found through a BLASTP, using the query protein sequence made available on Sol Genomics Network.

SIABCC14 is another exception, since the Ensembl Plants' page referring to its transcript (Solyc00g283010.2), although existent, did not show any redirecting links to NCBI or UniProt entries. This could either mean that there is still no annotation for this protein on NCBI and/or UniProt or, if there is one, the Ensembl Plant's page is not yet updated. Nonetheless, upon running a BLASTP using the query sequence of the SIABCC14 protein (from Sol Genomics Network) against the tomato proteome, the top hit result was the same protein as the one linked on the Ensembl Plant's page of SIABCC15: (ABC transporter C family member 10-like [*Solanum lycopersicum*],

XP_004253519.1), exhibiting the highest score, a 98% query cover, null E value, and 100% identity. In fact, the loci page associated to the ABCC15 protein annotation on NCBI has information on the gene that encodes the ABCC14 protein. This gene is, actually, referred to as ABC transporter C family member 14 (Gene ID 101254291) but is “also known as *SIABCC14*; *SIABCC15*”. It appears that *SIABCC14* and *SIABCC15* could be very similar variants of the same protein and are therefore encoded by the same gene and transcript, although this would be in disagreement with the fact that there were two different transcript annotations found on Ensembl Plants and Sol Genomics Network databases. However, given that the annotation for *SIABCC14* gene on both databases reveals an “unknown location” of the chromosome, it is possible that these annotations for the *SIABCC14* are incorrect.

Another interesting finding was that the records of *ABCC17*, *18* and *25* found on NCBI's GenBank database are all transcript variants (X8, X2, and X9, respectively) of the same gene called *ABC transporter C family member 17* or *ABC transporter C family member 12-like*, Gene ID: 101254459. For most transcripts (*SIABCC3*, *5*, *6*, *16*, *18* and *25*), the redirecting links found on each one's Ensemble Plant's page were directly used to identify the corresponding NCBI and UniProt annotations of proteins, transcripts and genes from the proteins listed by Ofori et al. (2018).

Table 4 Characterization of 13 genes and respective transcripts encoding metal transporters conceivably involved in the detoxification of Ni in tomato plants.

	Gene ID (SolGenomics)	Gene ID (EnsemblPlants)	Gene ID (NCBI)	Chromosome (according to NCBI)	Gene Size (bp)	Position (Mb)	Orientation	Exons	Transcript accession (NCBI)	Transcript ID (Sol Genomics)	Transcript ID (EnsemblPlants)	mRNA Size (bp)
SIABCC3	Solyc03g117540.2	Solyc03g117540.3	101250391	3	21367	68148307 - 68169673	Forward	36	XM_004236397.2	Solyc03g117540.2.1	Solyc03g117540.3.1	4687
SIABCC5	Solyc07g065320.2	Solyc07g065320.3	101253706	3	5825	67266327 - 67260503	Reverse	10	XM_010325975.3	Solyc07g065320.2.1	Solyc07g065320.3.1	4992
SIABCC6	Solyc08g006880.2	Solyc08g006880.3	101253706	8	28285	1450840 - 1422556	Reverse	28	XM_004244484.4	Solyc08g006880.2.1	Solyc08g006880.3.1	5501
SIABCC14	Solyc00g283010.1	Solyc00g283010.2	101254291	"Unplaced Scaffold"	2099	2149 - 51	Reverse	3	XM_004253471.3	Solyc00g283010.1.1	Solyc00g283010.1.1	1920
SIABCC15	Solyc11g065710.1	Solyc11g065710.2	101254291	"Unplaced Scaffold"	2099	2149 - 51*	Reverse*	3*	XM_004253471.3	Solyc11g065710.1.1	Solyc11g065710.1.1	1920*
SIABCC16	Solyc11g065720.1	Solyc11g065720.2	101261391	11	12789	51571867 - 51584656	Forward	9	XM_019210874.2	Solyc11g065720.1.1	Solyc11g065720.2.1	2201
SIABCC17	Solyc12g036150.1	not found	101254459	12	67973	45100977 - 45168949	Forward	27	XM_026028594.1	Solyc12g036150.1.1	not found	5233
SIABCC18	Solyc12g036140.1	Solyc12g036140.2	101254459	12	67973	45100977 - 45168950	Forward	27	XM_026028599.1	Solyc12g036140.1.1	Solyc12g036140.1.1	5233
SIABCC25	Solyc12g036160.1	Solyc12g036160.2	101254459	12	67973	45100977 - 45168951	Forward	27	XM_010315881.3	Solyc12g036160.1.1	Solyc12g036160.1.1	5233
SIABCB21	Solyc03g114950.2	not found	101258351	3	5538	66295821 - 66301358	Forward	17	NM_001324295.1 (XM_004236014)	Solyc03g114950.2.1	not found	2332
SIIREG2-like	Solyc10g076280.1	Solyc10g076280.2	101267281	10	7909	59290400 - 59298308	Forward	8	XM_004249661.4	Solyc10g076280.1.1	Solyc10g076280.2.1	2117
SIIMTP1	Solyc07g007060.1	Solyc07g007060.2	101249377	7	3896	1840444 - 1836549	Reverse	4	XM_004242652.3	Solyc07g007060.1.1	Solyc07g007060.2.1	1833
SICAX3	Solyc09g005250.2	Solyc09g005250.3	101254519	9	3901	195467 - 191567	Reverse	11	XM_026032900.1	Solyc09g005250.2.1	Solyc09g005250.3.1	1734

Table 5 Characterization of 13 metal transporter proteins conceivably involved in the detoxification of Ni in tomato plants.

	PROTEIN ID			SIZE		PROTEIN TOPOLOGY				PREDICTED SUBCELLULAR LOCATION		
	NCBI	UniProtKB	UniParc	Protein Size (aa)	Protein Mass (Da)	Reported Protein Topology	Aramemnon	UniParc	Plant-mPLoc	LocTree		
SIABCC3	XP_004236445.1	K4BLQ6	UPI00027676B1	1481	165348	(TMD-NBD)×2	2 predicted TMD and 2 predicted ATP-binding domains 14 predicted α-helix TM spans	2 predicted TMD and 2 predicted NBD	cell membrane	plasma membrane		
SIABCC5	XP_010324277.1	A0A3Q7HIQ0	UPI00032533A5	1505	167508	(TMD-NBD)×2	2 predicted TMD and 2 predicted ATP-binding domains 15 predicted α-helix TM spans	2 predicted TMD and 2 predicted NBD	cell membrane	plasma membrane		
SIABCC6	XP_004244532.1	A0A3Q7HKB1	UPI000276C241	1626	182173	(TMD-NBD)×2	2 predicted TMD and 2 predicted ATP-binding domains 14 predicted α-helix TM spans	2 predicted TMD and 2 predicted NBD	vacuole	vacuolar membrane		
SIABCC14	XP_004253519.1	K4AS31	UPI0002763706	645	72305	TMD-NBD	data not found	1 predicted TMD and 1 predicted NBD	cell membrane / cytoplasm	chloroplast		
SIABCC15	XP_004253519.1	K4D911	UPI0002769AFF	772	87027	TMD-NBD	1 predicted TMD and 1 predicted ATP-binding domain 5 predicted α-helix TM spans	1 predicted TMD and 1 predicted NBD	cell membrane	plasma membrane		
SIABCC16	XP_019066419.2	A0A3Q7IYA4	UPI0002769B00	664	73123	TMD-NBD	1 predicted TMD and 1 predicted ATP-binding domain 7 predicted α-helix TM spans	1 predicted TMD and 1 predicted NBD	cell membrane	vacuolar membrane		
SIABCC17	XP_0258884379.1	K4DE72	UPI000276A01C	373	41662	TMD-NBD	data not found	1 predicted TMD and 1 predicted NBD	vacuole	vacuolar membrane		
SIABCC18	XP_0258884384.1	K4DE69	UPI000276A019	377	43662	reverse orientation NDB-TMD	data not found	data not found	vacuole	vacuolar membrane		
SIABCC25	XP_010314183.1	K4DE73	UPI000276A01D	232	26504	NBD	data not found	1 predicted NBD and 1 unknown domain	vacuole	vacuolar membrane		
SIABCB21	NP_0013111224 (XP_004236062)	A0A3Q7FSS8	UPI00027685AD	638	68342	TMD-NBD	1 predicted TMD and 1 predicted ATP-binding domain 6 predicted α-helix TM spans	1 predicted TMD and 1 predicted NBD	cell membrane	vacuolar membrane		
SIIREG2-like	XP_004249709.2	K4D1X0	UPI0002769BFE	498	55282	1 Ferroportin-1 domain and 10 TMD	1 predicted Ferroportin-1 domain	1 predicted major facilitator superfamily domain (Ferroportin-1)	cell membrane	plasma membrane		
SIMTP1	XP_004242700.1	A0A3Q7H487	UPI000FD0EB75	389	43091	6 TMD and amino and a carboxy cytoplasmic termini	1 predicted cation efflux family domain	1 predicted cation efflux cytoplasmic domain	vacuole	vacuolar membrane		
SICAX3	XP_025888685.1	K4CQ15	UPI000276AF22	380	41711	6 TMD, 1 acidic motif and 1 calcium domain	1 predicted mitochondrial carrier protein domain 2 predicted α-helix TM spans	6 predicted TMD (within a mitochondrial carrier domain)	mitochondria	chloroplast membrane		

Moreover, the 13 aminoacidic sequences of tomato transporters were aligned along with 15 more sequences from previously characterized homologous proteins from other plant species, using the Muscle algorithm on MEGA X. Then, they were phylogenetically analyzed using the Maximum Likelihood method and JTT matrix-based model (**Fig. 27**). Phylogeny analysis revealed that the MTP and CAX transporters formed two isolated clusters within a distinct group from all others in the phylogenetic tree. The tomato MTP1 sequence was more similar to the MTP1 from *O. sativa* than to those from *N. goesingensis* or *A. thaliana*. The sequence of the tomato CAX3 transporter selected for further gene expression analysis in this study was found to be more similar to the CAX3 from grapevine and CAX4 from Arabidopsis than to the tomato transporter SICAX3-like, which clustered with CAX2 from Arabidopsis. A different branch in the phylogenetic tree contained the sequences of IREG and ABC family members. The two IREG sequences from tomato and Arabidopsis formed an early branch, separating them from the ABC-type transporters. The ABCB21 sequence was isolated from the other ABCs, forming an individual branch. Within the ABCC subfamily members, SIABCC3 disjointed from the remainder, suggesting a putative functional divergence from the other tomato ABCC transporters. The SIABCC6, 17, 18, and 25 were found to be more closely related to the ABCC1 and 2 from *A. thaliana*. In turn, SIABCC5 clustered more closely with AtABCC3, 6 and 7 than with AtABCC5 or other tomato sequences. The sequences from SIABCC14 and 15 were also closer to these three Arabidopsis transporters, than to AtABCC4 or SIABCC16.

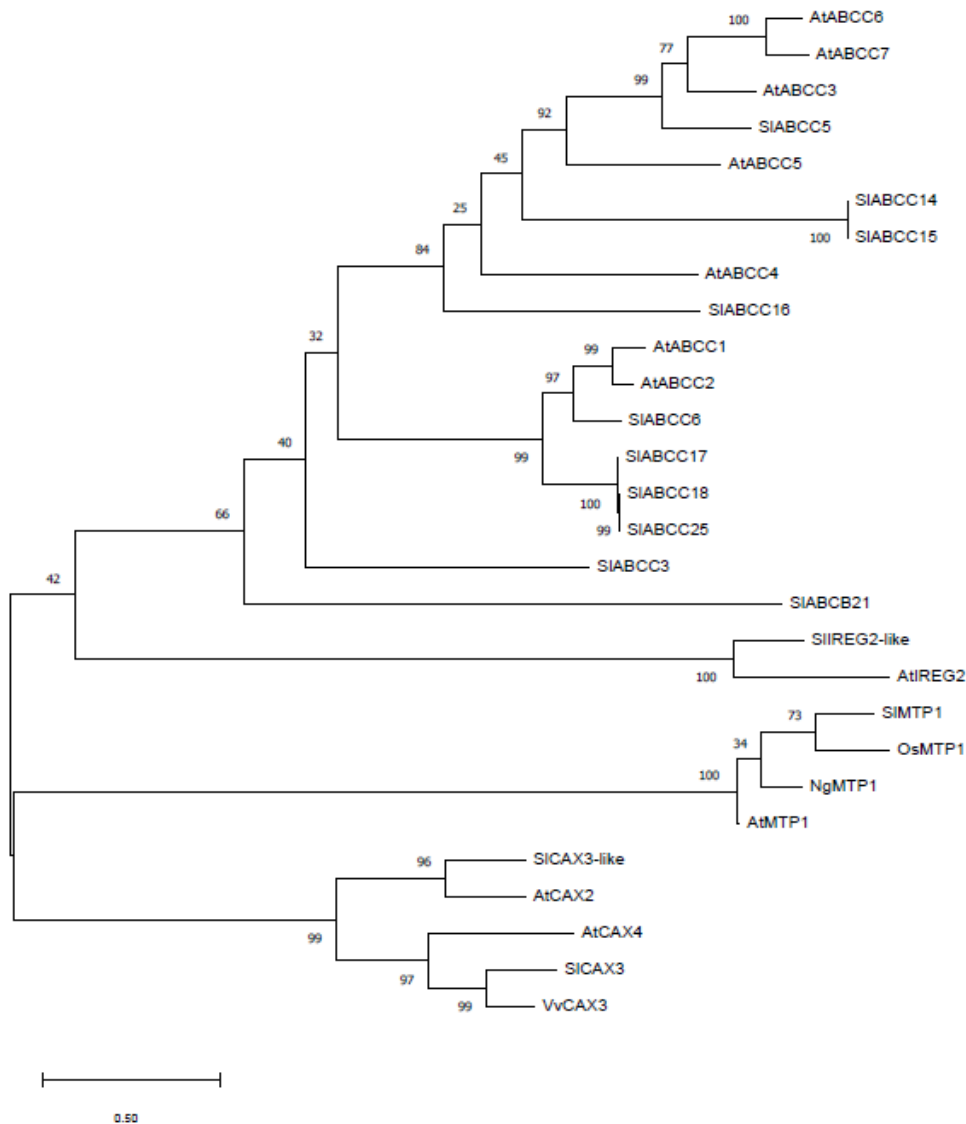


Figure 27 Evolutionary analysis of 28 metal transporter protein sequences from tomato (SIABCC3-25, SIABCB21, SICAX3, SICAX3-like, SIIREG2-like, SIMTP1), rice (OsMTP1), tiny wild mustard (NgMTP1), grape-vine (VvCAX3), and Arabidopsis (AtABCC1-7, AtCAX2-4, AtMTP1, AtIREG2) plants by Maximum Likelihood method and JTT matrix-based model. The tree with the highest log likelihood is shown. The % of trees in which the associated taxa clustered together is shown next to the branches.

4.4.2. Expression profile of selected metal transporters

The expression of the tomato genes encoding the metal transporters ABCC5, ABCC6, ABCC16, ABCC18, ABCB21, CAX3, IREG2-like and MTP1 was assessed by real-time qPCR. Transcript levels of the other 5 previously characterized transporters could not be evaluated due to the low primer efficiencies and time constraints.

Results showed that the expression profiles of most genes varied according to the cultivar and tissue. Under CTL conditions, the most expressed gene in the roots of PC was SIABCC6 and in GN was SIABCC5, while the genes SIABCC5 and SIMTP1 prevailed to similar extents in the leaves of the GN cultivar, and SIABCC18, along with

SICAX3, were the most expressed in PC shoots. The expression of *SIABCC5* was 2.7-fold higher in the roots of PC under drought stress, when compared to CTL plants, but not as much under Ni-stress, and was slightly reduced in the combination treatment (**Fig. 28a**). In GN roots, this transcript was more abundant in CTL plants than in stressed plants, having declined by 77 % in response to the combination of the stress factors (**Fig. 28a**). In GN shoots, the levels of *SIABCC5* expression enhanced 2.6-fold by single Ni-stress and also slightly by single PEG treatment (1.7-fold), but not in response to the combined stresses (**Fig. 28b**). In the shoots of PC, no statistically significant changes were observed in the expression of *SIABCC5* in any stress condition, although there was a noticeable decline of 54 % in plants stressed with Ni alone and a tendential increase of 34-37 % in plants subject to single or combined drought stress (**Fig. 28b**).

The transcript levels of *ABCC6* only seemed to be disturbed in PC roots under single Ni-stress, upon which they sharply increased by 4.5-fold (**Fig. 29a**). In all the other samples, expression levels were not significantly affected, although in the shoots of GN plants there was a visible trend of increased expression in response to the single Ni and drought stresses (**Fig. 29b**).

The expression of *ABCC16* in the roots was rather different in plants of the two cultivars (**Fig. 30a**). The basal levels of expression under control conditions were higher for GN roots than for PC roots. Moreover, in GN roots, the expression of this gene was significantly enhanced in response to single Ni-stress (1.5-fold) and drought stress (2-fold), but not when plants were subject to combined stresses (**Fig. 30a**). As for PC plants, the expression of this gene in the roots was not significantly affected by any treatment, although the levels were apparently higher in plants under single stress (**Fig. 30a**). In the shoots of GN plants, there was a similar trend of increased expression under single stress, although not significant. In PC shoots, the levels of this transcript were not detected upon drought stress but were slightly higher in plants subject to combined stresses than in CTL plants (**Fig. 30b**).

The regulation pattern of *ABCC18* expression was also different in the two cultivars. The basal levels of *ABCC18* expression under CTL conditions were much higher in GN roots than in PC roots. In GN roots, *ABCC18* transcripts were unchanged in response to PEG but were 1.3-fold more abundant under Ni-stress, when compared to the CTL (**Fig. 31a**). Interestingly, despite being upregulated by Ni-stress, this transcript was not detected in the roots of GN plants exposed to both stresses simultaneously. On the other hand, in the roots of PC, there was an overall drastic upregulation in *ABCC18* expression, especially in plants under single PEG-induced drought (~ 35-fold higher than

in the CTL) (**Fig. 31a**). The opposite effect was observed in the shoots of this cultivar, where, although no significant changes could be reported, there was a visible downregulation trend of ~ 80 % upon Ni and drought stress. In the shoots of GN, variations in the expression of *ABCC18* were not statistically significant, but this transcript was undetected in the shoots of plants under single Ni-stress (**Fig. 31b**).

The expression of *SIACB21* declined in GN roots in response to Ni-stress but increased in GN shoots under single PEG exposure, while in PC plants the single PEG treatment increased *SIACB21* transcripts by 1.3- and 2.3-fold in roots and shoots, respectively (**Fig. 32**). Additionally, GN plants under single Ni-stress had slightly higher levels of *ABCB21* transcripts in the shoots than control plants, but a downregulation was observed in PC shoots in the same conditions (**Fig. 32b**). In both cultivars, drought seemed to be the main factor responsible for inducing the expression of *ABCB21*, and not Ni.

The expression of *CAX3* was similarly influenced in the roots of both cultivars. Both in GN and PC roots under combined stress had around 60 % less *CAX3* transcripts than their respective CTL plants (**Fig. 33a**). In the shoots, however, stress induced by Ni did not affect *CAX3* expression, as the only significant change was the enhancement in response to PEG-induced stress, far more noticeable in GN (increased by 4.3-fold) than in PC plants (increased only by 1.4-fold) (**Fig. 33b**).

The levels of *IREG2*-like transcripts were differentially affected in roots and shoots of the two cultivars. In GN roots, the fluctuations were not statistically significant but the expression of *IREG2-like* was somewhat upregulated in GN plants under single Ni-stress (by 1.2-fold) (**Fig. 34a**). Although expression levels in GN roots were generally higher than in PC, the enhancement caused by single Ni treatment was much more emphasized in the later cultivar (4.1-fold) (**Fig. 34a**). In shoots, major differences in expression were only detected in the GN cultivar, for plants under single drought (increased 5 x) and single Ni-stress (increased 3.7-fold) (**Fig. 34b**).

The *MTP1* gene's expression was higher in GN plants than in PC plants under CTL conditions (**Fig. 35**). Relatively high levels of expression were observed in the roots of both cultivars under drought stress alone, but, in response to Ni-stress, this transcript was 35 % less abundant in GN roots under single Ni-stress and around 70 % lower in the roots of both cultivars under combined stresses, when compared to the levels of their respective CTL plants (**Fig. 35a**). The expression of this gene was unchanged in the shoot tissues of PC plants, despite stress exposure. In the shoots of GN plants, the

expression of *MTP1* was upregulated by 1.6-fold due to single Ni-stress, when compared to the levels in the shoots from CTL or any other treatment (Fig. 35b).

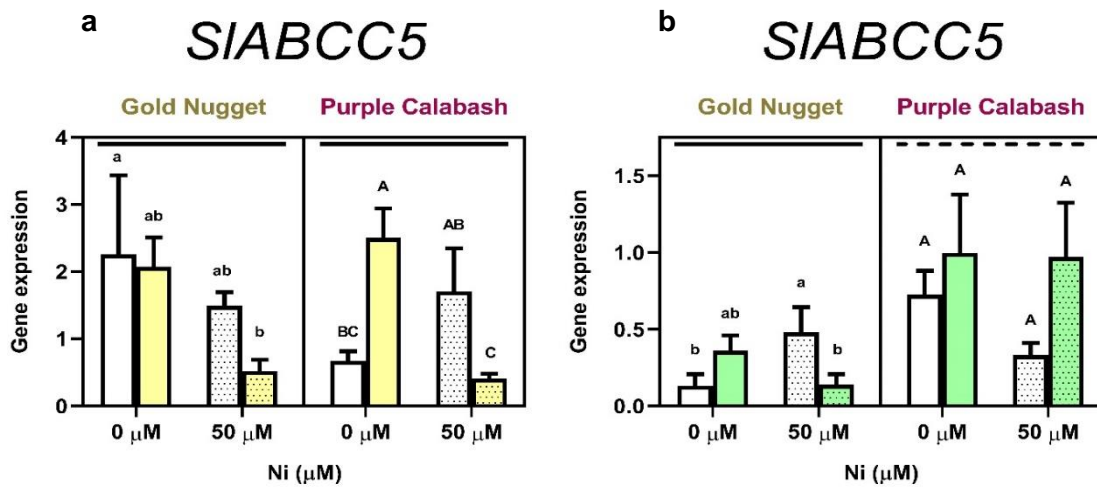


Figure 28 Effects of exposure to 50 μM Ni and/or 6 % PEG 6000 on the expression of *SIABCC5* in the roots (a) and shoots (b) of Gold Nugget and Purple Calabash tomato plants grown for 20 days under a semi hydroponic system. Colored bars refer to the 6 % PEG 6000 treatment. Different lines on top of each sub chart represent significant differences between cultivars. Different letters above the bars of each cultivar represent significant differences between groups, at $p \leq 0.05$; lowercase and capital letters refer to GN and PC, respectively. Expression of *SIABCC5* was normalized to the transcript levels of *SIEF1* (internal standard).

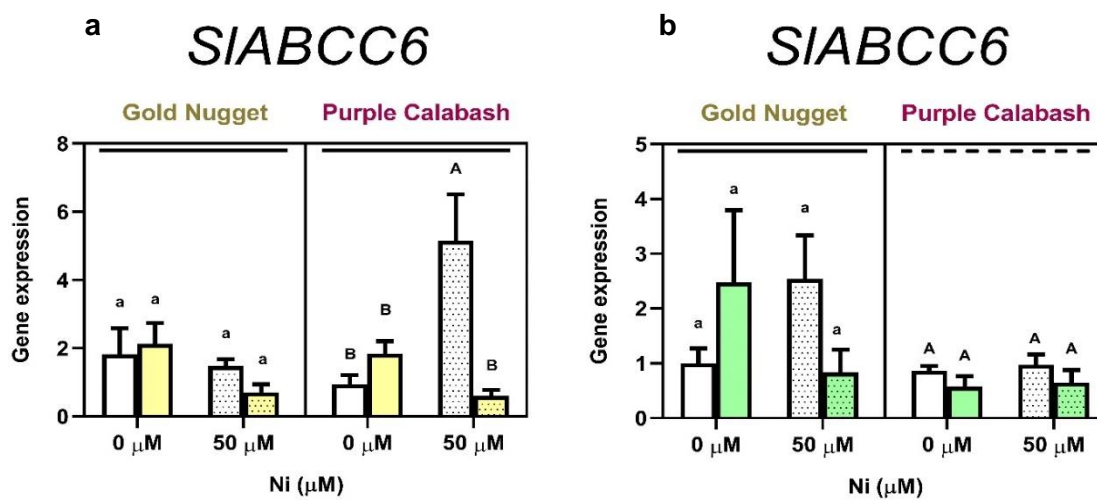


Figure 29 Effects of exposure to 50 μM Ni and/or 6 % PEG 6000 on the expression of *SIABCC6* in the roots (a) and shoots (b) of Gold Nugget and Purple Calabash tomato plants grown for 20 days under a semi hydroponic system. Colored bars refer to the 6 % PEG 6000 treatment. Different lines on top of each sub chart represent significant differences between cultivars. Different letters above the bars of each cultivar represent significant differences between groups, at $p \leq 0.05$; lowercase and capital letters refer to GN and PC, respectively. Expression of *SIABCC6* was normalized to the transcript levels of *SIEF1* (internal standard).

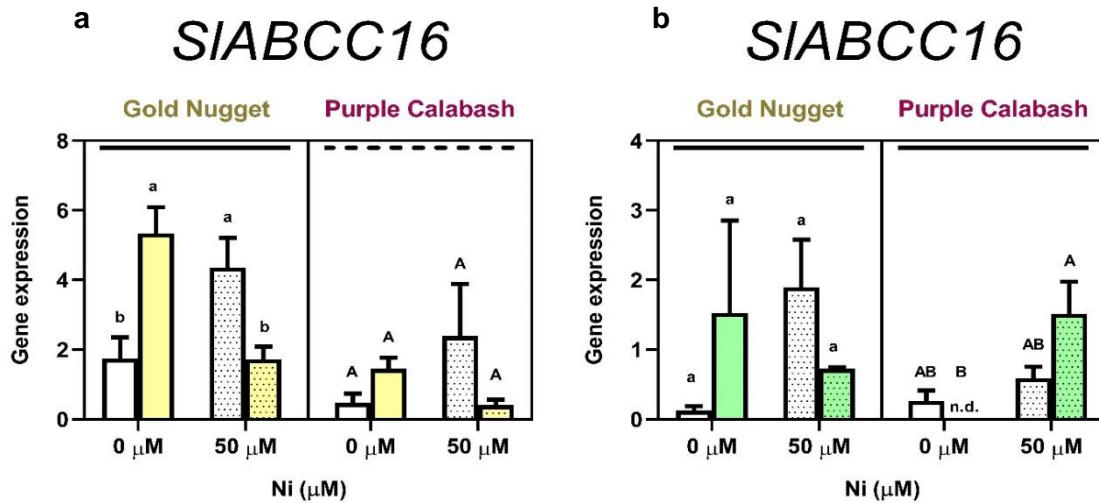


Figure 30 Effects of exposure to 50 μM Ni and/or 6 % PEG 6000 on the expression of *SIABCC16* in the roots (a) and shoots (b) of Gold Nugget and Purple Calabash tomato plants grown for 20 days under a semi hydroponic system. Colored bars refer to the 6 % PEG 6000 treatment. Different lines on top of each sub chart represent significant differences between cultivars. Different letters above the bars of each cultivar represent significant differences between groups, at $p \leq 0.05$; lowercase and capital letters refer to GN and PC, respectively. Expression of *SIABCC16* was normalized to the transcript levels of *SIEF1* (internal standard).

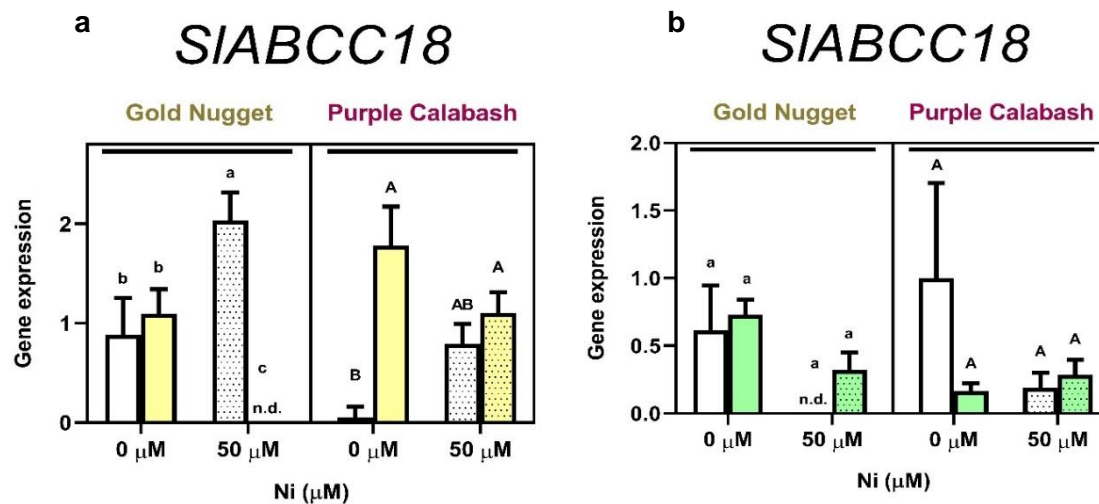


Figure 31 Effects of exposure to 50 μM Ni and/or 6 % PEG 6000 on the expression of *SIABCC18* in the roots (a) and shoots (b) of Gold Nugget and Purple Calabash tomato plants grown for 20 days under a semi hydroponic system. Colored bars refer to the 6 % PEG 6000 treatment. Different lines on top of each sub chart represent significant differences between cultivars. Different letters above the bars of each cultivar represent significant differences between groups, at $p \leq 0.05$; lowercase and capital letters refer to GN and PC, respectively. Expression of *SIABCC18* was normalized to the transcript levels of *SIEF1* (internal standard).

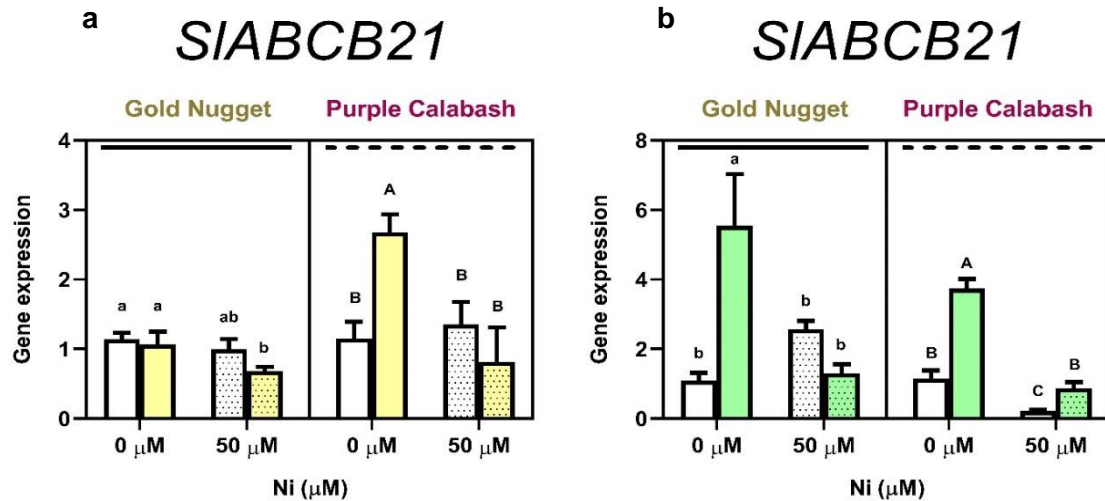


Figure 32 Effects of exposure to 50 μM Ni and/or 6 % PEG 6000 on the expression of *SIABC21* in the roots (a) and shoots (b) of Gold Nugget and Purple Calabash tomato plants grown for 20 days under a semi hydroponic system. Colored bars refer to the 6 % PEG 6000 treatment. Different lines on top of each sub chart represent significant differences between cultivars. Different letters above the bars of each cultivar represent significant differences between groups, at $p \leq 0.05$; lowercase and capital letters refer to GN and PC, respectively. Expression of *SIABC21* was normalized to the transcript levels of *SIEF1* (internal standard).

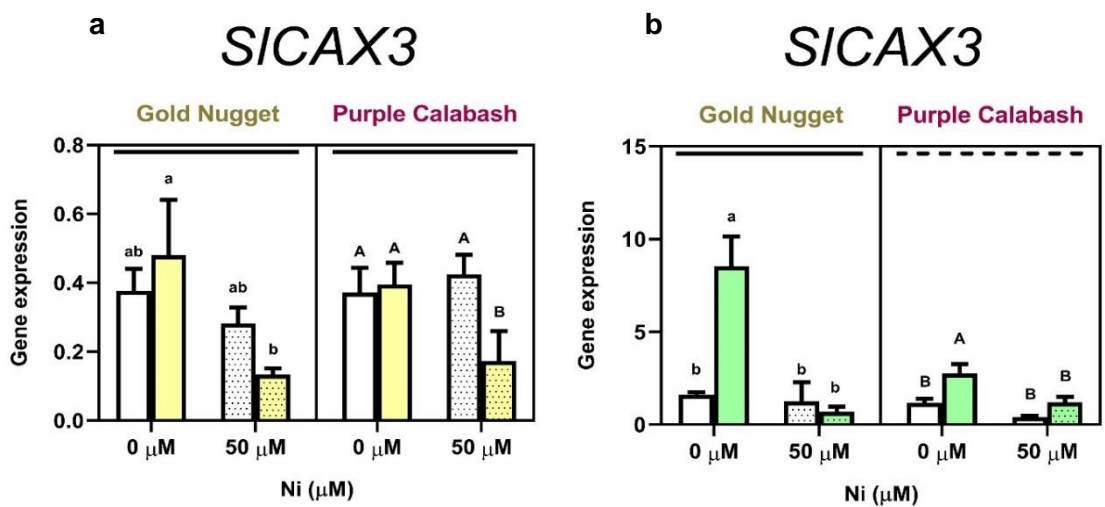


Figure 33 Effects of exposure to 50 μM Ni and/or 6 % PEG 6000 on the expression of *SICAX3* in the roots (a) and shoots (b) of Gold Nugget and Purple Calabash tomato plants grown for 20 days under a semi hydroponic system. Colored bars refer to the 6 % PEG 6000 treatment. Different lines on top of each sub chart represent significant differences between cultivars. Different letters above the bars of each cultivar represent significant differences between groups, at $p \leq 0.05$; lowercase and capital letters refer to GN and PC, respectively. Expression of *SICAX3* was normalized to the transcript levels of *SIEF1* (internal standard).

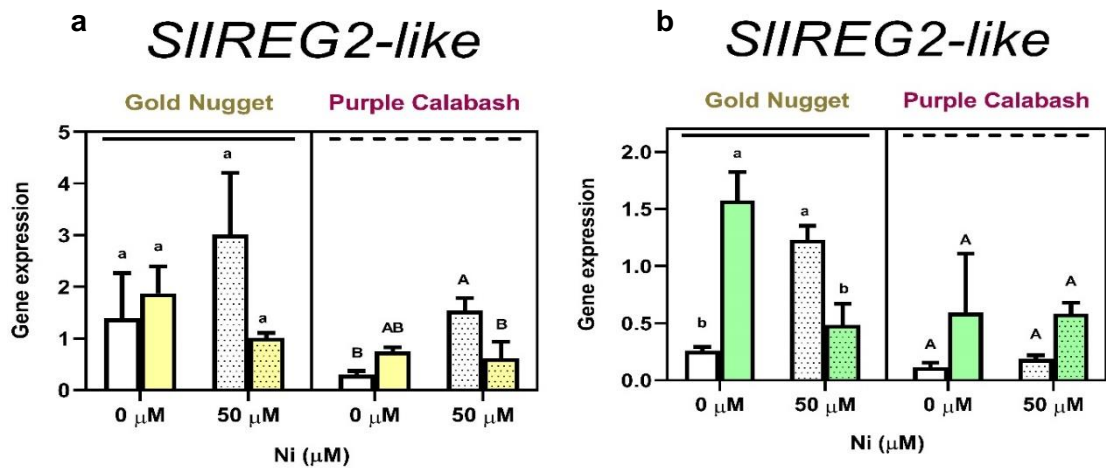


Figure 34 Effects of exposure to 50 μM Ni and/or 6 % PEG 6000 on the expression of *SIIREG2-like* in the roots (a) and shoots (b) of Gold Nugget and Purple Calabash tomato plants grown for 20 days under a semi hydroponic system. Colored bars refer to the 6 % PEG 6000 treatment. Different lines on top of each sub chart represent significant differences between cultivars. Different letters above the bars of each cultivar represent significant differences between groups, at $p \leq 0.05$; lowercase and capital letters refer to GN and PC, respectively. Expression of *SIIREG2-like* was normalized to the transcript levels of *SIEF1* (internal standard).

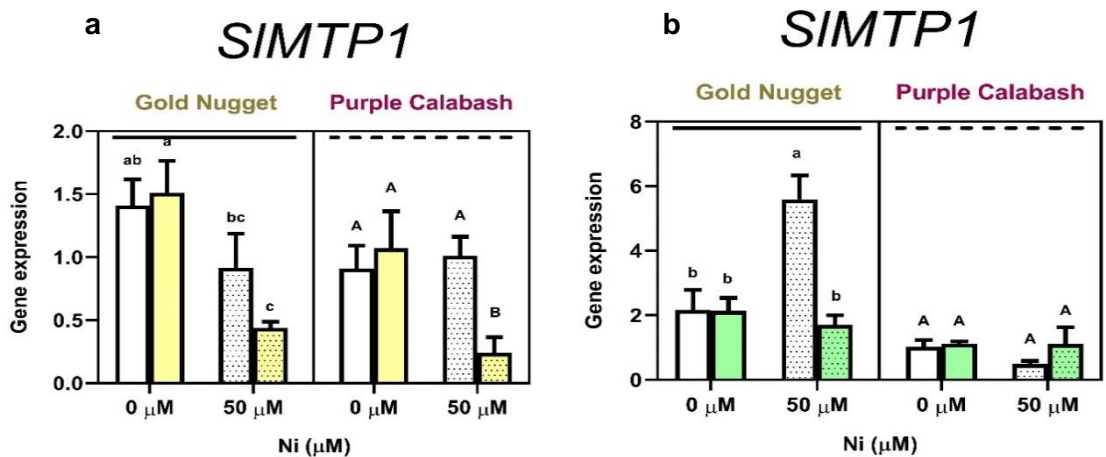


Figure 35 Effects of exposure to 50 μM Ni and/or 6 % PEG 6000 on the expression of *SIMTP1* in the roots (a) and shoots (b) of Gold Nugget and Purple Calabash tomato plants grown for 20 days under a semi hydroponic system. Colored bars refer to the 6 % PEG 6000 treatment. Different lines on top of each sub chart represent significant differences between cultivars. Different letters above the bars of each cultivar represent significant differences between groups, at $p \leq 0.05$; lowercase and capital letters refer to GN and PC, respectively. Expression of *SIMTP1* was normalized to the transcript levels of *SIEF1* (internal standard).

5. Discussion

Facing CC-related issues, along with the impacts of an increasingly contaminated land, is not an easy task for farmers nor for plant scientists. Efforts should then be reinforced to understand the consequences of the exposure of crops to multiple stresses. However, up to date, not much is known regarding the crosstalk between drought and metals, especially Ni, in agronomically-relevant species. Therefore, the main goal of this study was to compare, in terms of growth, Ni accumulation and homeostasis, and physiological performance, the responses of two tomato cultivars, potentially differing in metal tolerance, to the combined action of Ni and water deficit conditions. Starting by discussing growth-related endpoints and physiological indicators, this study further explores the regulation of the redox homeostasis, PA metabolism and Ni detoxification pathways in shoots and roots of *S. lycopersicum* plants.

5.1. Ni TOXICITY DURING SEEDLING VS VEGETATIVE GROWTH IN DIFFERENT TOMATO CULTIVARS

Prior to the main experiment, where the impacts of the co-exposure to Ni and drought were assessed, a series of preliminary assays were performed to optimize the Ni concentration. Cherry tomato plants showed to be progressively affected by increasing Ni concentration to levels above 50 μM . Actually, although germination rate was not affected by Ni, the radicle growth was severely affected by 150, 250 and 500 μM Ni. As a matter of fact, this apparent lack of sensitiveness of seeds during germination in exposure to contaminants has been discussed (Seregin and Kozhevnikova, 2006; Akinci and Akinci, 2010; Soares et al., 2016a). For seed germination to be affected by Ni exposure, this HM must pass through several layers of protective seed coats in order to reach the embryogenic tissues and hamper the development of the embryo (Seregin and Kozhevnikova, 2006; Akinci and Akinci, 2010; Soares et al., 2016a). Therefore, it is not surprising that this parameter did not change in response to any of the tested concentrations of Ni. Similarly, Soares et al. (2016a), when exploring the phytotoxicity induced by Ni nanomaterials, also reported germination index as a not sensitive exposure biomarker. Despite of that, in what concerns seedling growth, there were abrupt differences between the effects on radicle growth inhibition between 50 and 150 μM Ni. In this sense, the preliminary assays were carried out with a Ni exposure level of 75 μM .

In order to screen potential differences in Ni tolerance between different commercial varieties of *S. lycopersicum*, seeds of twelve cultivars were germinated and grown in Petri dishes exposed to 75 μM Ni for 5 days. Previous studies had shown that tomato performance under HM exposure can substantially vary according not only to the metal treatment (concentration, exposure conditions and duration), but also to plant features, including the genotype (Piotto et al., 2018). However, to the best of our knowledge, no study has been conducted so far to explore the intraspecific variability of *S. lycopersicum* against Ni-induced stress. As shown in our results, the exposure of multiple tomato cultivars to 75 μM Ni majorly compromised seedlings' radicle growth of all tested genotypes; however, different inhibition ranges were detected between 38% (Ace VF) and 70% (GN), suggesting the existence of a different response between different cultivars of *S. lycopersicum*. As Petri dish assays do not mimic a real scenario of soil contamination, another preliminary assay was performed in which 4 cultivars (the two supposedly more tolerant – Ace VF and Moneymaker – and sensitive – PC and GN) were grown under a semi-hydroponic system, using perlite as substrate, for 15 days under 75 μM Ni. Interestingly, the results were quite contrasting with those obtained for the *in vitro* assay, with GN standing out not as the most sensitive cultivar, but rather as one of the most tolerant, especially in what regards shoot biomass. Contrarily, this was not observed for PC, as the growth of this cultivar was still severely affected in the vegetative growth stage. Thus, in the present study, the seedling development of GN tomato plants was found to be more affected by 75 μM Ni in culture media than the growth of these plants exposed to the same concentration of Ni in a semi-hydroponics system. In fact, GN was the cultivar to show highest radicle growth inhibition during the 5 days assay *in vitro* trial, but then was the one that could maintain a higher root length and shoot f. w. on the 15 day Ni exposure trial. On the other hand, PC plants continued to exhibit a higher sensitivity to this HM, retaining high root growth inhibitions both at seedling and adult stages. The means by which Ni affects plants are different during germination and vegetative growth, which explains why growth inhibition are different during seedling or vegetative growth. In seeds exposed to Ni, the activities of amylase, protease and ribonuclease enzymes can be downregulated, retarding germination and seedling growth (Sethy and Ghosh, 2013). Ni also affects the digestion and mobilization of food reserves in the seeds (Sethy and Ghosh, 2013). Moreover, although seeds are well protected from environmental contaminants and disturbances, the growth of seedlings as soon as they emerge, is considered as the most vulnerable stage in the life of plants (Facelli, 2008). However, in plantlets, opposed to seedlings, several more sophisticated defensive mechanisms against Ni toxicity take place, as plants are more able to control the uptake, translocation and accumulation of Ni in tissues, and can

actively induce the production of AOXs and chelating agents in a much more efficient way than seeds can. Regardless of the contrasting growth performances of these two different cultivars, 75 μM Ni exposure still severely impaired the development of plants from both tomato cultivars. For this reason, as previously mentioned, 50 μM was the concentration chosen for the final growth trial.

5.2. AN OVERVIEW OF GROWTH AND OVERALL PHYSIOLOGICAL PERFORMANCE OF TOMATO CULTIVARS GOLD NUGGET AND PURPLE CALABASH UNDER Ni- AND PEG-INDUCED STRESS

Upon adjustment of Ni concentration to 50 μM , plants grown in perlite for 20 days under Ni stress still exhibited severe growth inhibitions, identical to those observed for the 75 μM concentration. Contrarily to what had been observed in cherry tomato seedlings that germinated under this Ni concentration and showed no negative effects, adult GN and PC tomato plants had their total length and biomass production significantly affected. This data, along with that obtained in the preliminary assays, agree with previous findings (Baccouch et al., 1998; Balaguer et al., 1998; Palacios et al., 1998; Madhava Rao and Sresty, 2000; Maksimović et al., 2007; Kumar et al., 2012; Shahid et al., 2018; Ameen et al., 2019). It should be noted, however, that the appropriateness of the 50 μM Ni concentration used in the last trial of this study was compromised by the choice of only perlite as substrate. Even though several studies have reported that perlite can effectively absorb HM (Alkan and Doğan, 2001; Mathialagan and Viraraghavan, 2002; Sari et al., 2007; Silber et al., 2012), the bioavailability of these elements in soilless systems is usually much higher than in natural soils (Ali and Shakrani, 2011). In this sense, although the Ni concentration tested in the present work was representative of that found in actual polluted soils and was in accordance with results from the preliminary assays, the use of perlite probably led to much more drastic effects in GN and PC plant growth than what would have been expected.

Fig. 36 and **37** sum up the observed effects of Ni, PEG-induced drought, and combined stress to GN and PC tomato plants, respectively, on growth, pigments, oxidative stress markers, AOX defenses, and PAs.

Overall, the toxic pattern of Ni was identical between both cultivars, although different inhibition values were recorded. In GN and PC plants, the growth of shoots was more affected than the growth of roots, with broad reductions in the range of 70 % for shoots and 50 % for roots elongation. Yet, the toxic effects of Ni were generally more accentuated in PC than in GN plants. The observed inhibition of growth and biomass

production in tomato plants exposed to Ni were fairly expected outcomes, since these are typical symptoms of metal toxicity and have been widely reported in many physiological assessments to plants under HM stress, including Ni (reviewed by Chen et al., 2009). From previous works on the induction of Ni stress to plants, it is possible to acknowledge that the concentrations in which Ni becomes phytotoxic are rather species- or variety-specific but also differ according to the life stage of the plant. Ni can affect plant growth at different dimensions, being able to inhibit not only cell division, but also cell elongation (Yusuf et al., 2011). Regarding the particularly distinct response between root and shoot tissues, the relatively better performance of the root tissues disagrees with what had been reported by Baccouch et al. (1998), Palacios et al. (1998), Parida et al., (2003), and Gajewska et al. (2006). These authors had witnessed that Ni stress reduced root growth more significantly than the growth of leaves in maize, Marmande tomato, fenugreek, and wheat plants, respectively, a response which all authors correlated with the higher accumulation of Ni in root tissues of these plants. However, in the present study, similarly to findings in Rambo tomato plants by Balaguer et al. (1998), root growth was not as affected as the growth of shoots, despite accumulating more Ni. Soares et al. (2016b; 2018) also observed a higher accumulation of Ni in the roots than in shoots of *S. nigrum* and *H. vulgare*. Ahmad et al. (2011) had already stated that the rate of uptake and root-to-shoot translocation of Ni varied depending on plant species, but it seems that cultivars of the same species can also have distinct patterns of Ni distribution in the tissues. As it was observed root-to-shoot translocation of Ni occurred, leading to enhanced levels of Ni in the shoots exposed to this HM, though the accumulation of Ni was still 10-fold higher in the roots than in the shoots. GN plants were also able to accumulate higher levels of Ni in their tissues, when compared to PC, especially in the roots, without apparently suffer a much more pronounced effect, suggesting a potential higher tolerance than PC.

The inhibition of growth caused by Ni, especially in the aboveground tissues, is thought to be a consequence of several disturbances: i) the interference with the uptake of water and essential nutrients; ii) the compromised efficiency of the photosynthetic machinery, by reducing leaf area and degrading or inhibiting the production of photosynthetic pigments; iii) the induction of oxidative stress (as discussed in section 5.3). In fact, it has been reported that Ni stress reduced the accumulation of N, K, Zn, Mn, Cu, Fe, and Ca (Ahmad et al., 2011; Hussain et al., 2015), and negatively affected photosynthesis-related traits, both in terms of Chl content and fluorescence parameters, photosynthetic activity, stomatal conductance, and intercellular CO₂ (Baccouch et al., 1998; Rahman et al., 2005; Gajewska et al., 2006; Pietrini et al., 2015; Soares et al.,

2016b; Soltani Maivan et al., 2017; Shahid et al., 2018). Although only tenuous variations were observed in terms of water content, this parameter seemed to be more affected by Ni stress than by the drought treatment, in GN and PC shoots. Rucińska-Sobkowiak (2016) reviewed the effects that the exposure of plants to HMs has on water relations, concluding that HM toxicity reduces the uptake and root-to-shoot translocation of water, by reducing the root-absorbing area, inhibiting aquaporin activity and stimulating stomatal closure, preventing transpiration (Rucińska-Sobkowiak, 2016). The growth-mediated inhibition herein reported for both cultivars was also followed by considerable reductions in the content of Chl and Car, which accompanied the observed chlorosis of leaves of both cultivars. For instance, Maivan et al. (2017) reported that *Melissa officinalis* plants only showed negative impacts on photosynthetic pigments in response to Ni stress at 500 μM , a much higher concentration than the 100 μM of Ni that were administered by Rahman et al. (2005) to barley plants or the 50 μM of Ni used in the present study on tomato plants, causing foliar chlorosis to shoots in both cases. Similarly to findings from the present study, Baccouch et al. (1998), Rahman et al. (2005), Parida et al. (2003), and others reviewed by Ameen et al. (2019), have also reported the occurrence of chlorosis, interveinal yellowing of leaves, along with reduction of Chl levels in plants under Ni stress. Some of these authors suggested that the impairment in Chl production occurred rather as an indirect effect of Ni toxicity in reducing Fe levels, given that Fe is essential for Chl biosynthesis (Marschner, 2012; Lešková et al., 2017) and the observed effects were also common symptoms of Fe deficiency.

The effects of single drought on the growth and development of *S. lycopersicum* are well-described in literature. Generally, a marked reduction of shoot and root growth occur, followed by strong disturbances in plant osmotic potential (Laxa et al., 2019; Gupta et al., 2020). Accordingly, and regarding the effects of PEG on the growth performance of GN and PC plants, the decreased growth of the shoots, and particularly the overall decrease in f. w., are in agreement with previous findings for PEG-induced stress at similar concentrations (Radhouane, 2007; Hatami et al., 2017; Hajhashemi and Sofo, 2018; Zlobin et al., 2018). Despite of that, root elongation did not suffer from PEG-induced drought in any of the tested cultivars. This finding, however, is generally accepted as a common response of plants to water deficit, in an attempt to colonize areas with a higher availability of water (Gupta et al., 2020). In agreement, a recent study conducted with several tomato cultivars exposed to water deficit conditions also revealed that root length was not hampered by the stress treatment, in opposition to shoot elongation (Kamanga, 2020). PEG-induced drought in the last 48 h caused GN and PC plants to significantly delay their biomass production and growth. Despite causing plants

to reduce their water uptake, PEG treatment did not majorly affect the relative water content of GN or PC tissues. In a similar approach, Zlobin et al. (2018), also observed that the relative water content would not fall below 85 %, even in plants under extreme PEG-induced osmotic stress. When exposed to PEG, GN and PC plants might have adjusted gas exchanges by stomatal closure, which have prevented desiccation and kept a healthy turgor pressure, according to what was further indicated by Zlobin et al. (2018). However, it is known that stomatal closure can also lead to C starvation, in which case would also contribute to plant growth reduction. Moreover, the unchanged relative water content in roots observed in PEG-exposed plants can also set some clues on the main processes behind the differences between root length and biomass. Apparently, the maintenance of root apical growth is the result of cell elongation rather than cell division, explaining the overall inhibitory effect on the biomass production (Soares et al., 2016b). Indeed, roots of drought-stressed plants might be able to translocate the water to apex cells, allowing the maintenance of cellular elongation. Besides affecting growth, drought is also frequently associated to a loss of the photosynthetic yield. The results herein obtained concerning the levels of photosynthetic pigments, on the other hand, are not identical to previous reports. Contrarily to what had been observed by Hajihashemi and Sofo (2018), who witnessed significant losses in the content of pigments in *Stevia rebaudiana*, GN tomato plants did not show changes in the levels of pigments in response to PEG, and in the shoots of PC plants, this condition even increased the levels of Chl and Car. PEG-induced growth inhibition can be a consequence of reduced water potential, and also constrained photosynthesis, and occurrence of oxidative stress (Farooq et al., 2009; Hajihashemi and Sofo, 2018). Hajihashemi and Sofo (2018) had implied that PEG exposure caused the photo-oxidation and degradation of Chl and Car, through the induction of oxidative stress. The fact that neither GN or PC plants suffered loss of photosynthetic pigments when exposed to 6 % PEG for the last 48 h of the trial, may indicate that the degree of oxidative stress induced by this treatment was not enough to affect the integrity of photosynthetic pigments and/or the defense mechanisms were efficiently activated to prevent pigment oxidation.

Besides being affected by both stress factors alone, especially Ni, GN and PC plants were also assessed to understand the consequences of the co-exposure to Ni and PEG-simulated drought. From what we could observe, shoot and root growth of GN or PC plants (both in terms of length and f. w.) were mainly inhibited by Ni stress, whether alone or in combination with drought. Although a certain tendency for aggravation of growth inhibition effects was noticed under stress combination, the exposure to 50 μ M Ni and the combination of stresses were found to be equally detrimental to the growth of plants

from both cultivars. Indeed, the combined action of both stress factors did not majorly change the inhibition values from the Ni treatment. This finding is much likely the result of the longer exposure to Ni than to drought, which only lasted 48 h. Yet, although the absence of statistical differences for growth traits between plants exposed to Ni alone or in combination with PEG, significant changes were recorded when Ni accumulation and water relations are concerned. The tested cultivars showed a distinct behavior for Ni accumulation under the joint action of Ni and PEG: while PC exhibit the same intracellular levels of Ni regardless of the co-exposure, GN increased the bioaccumulation of this metal in both roots and shoots of co-exposed plants. Nevertheless, this cultivar somehow managed to control this increase, since a not much higher growth inhibition was found, in comparison with PC. Regarding water status, GN plants only showed a decrease in water content when plants grew under the combined stress condition, but not under any of the single stresses, while in PC's plants, the relative water content in the roots was mainly affected by PEG, and in the shoots, by Ni (single or combined). The effects of combining the HM with drought-inducing conditions have not been assessed for many plant species. The few existent reports tackling this type of combination have focused on the effects of Ni, Cu, Cr, Pb or Co contamination combined with PEG-induced osmotic stress, forced drainage or suspended irrigation to simulate drought (de Silva et al., 2012; Rejeb et al., 2014; Ma et al., 2017a; Ma et al., 2017b; Cappetta et al., 2020; Wang et al., 2020). Ma et al. (2017b), and de Silva et al. (2012) observed negative additive effects on the growth and photosynthetic traits of *Trifolium arvense* and *Acer rubrum* plants, respectively, under combined drought and metal stresses, when compared to single exposure conditions. On the other hand, in a very recent study, Wang et al. (2020), noticed antagonistic effects on the growth of *Amaranthus tricolor* plants under Cu or Pb and PEG-induced drought. For instance, these authors found that the exposure to HM attenuated the negative effects induced by PEG on photosynthetic pigments and belowground growing competitiveness of *A. tricolor* (Wang et al., 2020). They hypothesized that the exposure to HM led to the induction of oxidative stress and consequently activated a signaling cascade responsible for enhancing AOX defenses that would help plants to overcome the effects caused by PEG, avoiding the aggravation of effects (Wang et al., 2020). According to Cappetta et al. (2020), and Rejeb et al. (2014), the interaction of plant responses to combined stressors indicates the existence of a crosstalk between the signaling pathways activated for each stressor. This crosstalk involves ROS and phytohormones and can lead to both synergistic or antagonistic responses in comparison to the single stress responses, and sometimes can lead to a cross-tolerance response and enhancement of plant resilience against combined stress exposure (Rejeb et al., 2014). In the present study, based on the growth performance of

plants under combined and single stresses, the overall picture is that Ni induced serious physiological disturbances to plants of both cultivars, while PEG exposure did not have such impactful effects on growth. Under combined stress, the growth and content of pigments in plants from both cultivars was not further inhibited than under the single Ni stress condition, possibly indicating that plants under Ni stress activated some mechanism for cross tolerance, preventing a further growth delay and degradation of pigments when exposed to the following PEG treatment.

Regarding only the growth performance traits, no clear distinction can be made in terms of stress tolerance for each cultivar, as both GN and PC plants were severely affected by Ni stress. As will be discussed in the following section, despite the brutal growth inhibition in response to Ni stress, GN and PC tomato plants actually showed distinctive patterns of oxidative stress induction and activation of AOXs. It is possible that under a weaker Ni contamination approach (possibly even more realistic), the observed differences in redox physiological adjustments of these two cultivars can reveal distinctive protection mechanism that could avoid (or not) such severe growth losses.

5.3. PEEKING FOR TOLERANCE TRAITS THROUGH MARKERS OF OXIDATIVE STRESS AND ANTIOXIDANT DEFENSE

As mentioned before, when plants face abiotic stress, the occurrence of oxidative stress is a very common outcome. Stress induced by drought or HM individually has been reported to induce oxidative stress, which is mainly observed by the accumulation of ROS and oxidation byproducts, such as MDA. The promptness in which a plant can activate its AOX defenses determines the degree of oxidative damages, and therefore presents an advantage for plants under abiotic stress (Soares et al., 2019a).

Aiming to assess the impacts of both stresses, either individually or in combination, the production of two of the main ROS (H_2O_2 and $O_2^{\cdot-}$) and the degree of LP were assessed in shoots and roots of both cultivars. In the present study, the accumulation of H_2O_2 in response to stress was higher in PC than in GN plants. Accordingly, the levels of $O_2^{\cdot-}$ were also more enhanced due to Ni stress in shoots of PC than in GN. Despite the Ni-induced increase of H_2O_2 levels in plants from both cultivars, no obvious oxidative damage, measurable by the degree of LP, was observed in plants exposed to single Ni stress, not even in the root tissues, where Ni concentrations were substantially higher. This opposes to the reported induction of LP that is commonly observed in plants under Ni stress (Madhava Rao and Sresty, 2000; Soares et al., 2016b; Ameen et al., 2019; Dahunsi et al., 2019). These results point out that the significantly

enhanced levels of these two ROS in response to stress, when observed, were not responsible for inducing major oxidative damage to membranes, probably due to an efficient induction of the AOX defenses. Thus, the observed inhibition in tomato plant's growth under Ni stress may have not been only related to oxidative stress, but also to the interference with other important developmental processes, including mineral nutrition and photosynthesis, as mentioned before. Ni stress has been extensively reported to cause oxidative stress to plants (Chen et al., 2009; Yusuf et al., 2011; Sachan and Lal, 2017). Toxic Ni concentrations have been reported to induce the overaccumulation of ROS by interfering with AOX enzymes (Chen et al., 2009; Ameen et al., 2019), both directly due to the high affinity of Ni to thiol groups and disulfide bonds, damaging the secondary structure of proteins and inactivating enzymes, or indirectly through competition with Fe cations, disturbing the activities of Fe-containing AOX enzymes (e.g. Fe-SOD and CAT) (Seregin and Kozhevnikova, 2006; Sachan and Lal, 2017). However, as mentioned before, data concerning the effects of Ni on the activity of AOX enzymes are rather contradictory. In some cases, the exposure of plants to Ni, mainly in relatively low levels or for a short period of time, has actually been found to activate AOX enzymes, and increase the accumulation of non-enzymatic AOXs as well, with a consequent improvement of the ROS scavenging potential (Kumar et al., 2012; Kumar et al., 2015). In the present study, tomato plants exposed to single Ni stress showed an efficient stimulation of the AOX defenses, evidenced by the increased levels of AsA and APX activity, along with the accumulation of GSH (in the shoots of PC) and Pro (in the shoots of GN). It should be noted that GN plant shoots under single Ni stress were the only tissues to reveal a prompt activation of the three AOX enzymes, suggesting a higher investment of this cultivar in the defense mechanisms to counteract Ni-induced stress. Accordingly, in shoots of this cultivar, levels of ROS remained identical to the CTL. The activity of APX was also stimulated in the roots of PC for all stress treatments and SOD's activity was enhanced in the shoots of both cultivars, more consistently in GN plants under single stress and in PC plants under combined stress. In GN and PC tomato plants, AsA and APX seemed to be the main AOX agents activated in response to these two stressors. This is different from what has been verified in a study with tomato cultivar Early Urbana Y, in which the AOX enzymes CAT and APX, but not SOD, were found to be considerably activated in the presence of Ni (Asrar et al., 2014). The overall enhancement of the AsA and DHA levels in tomato plants under Ni stress also disagree with findings by Asrar et al. (2014), Madhava Rao and Sresty (2000), and Abd_Allah et al. (2019), in which Ni exposure led to a decreased accumulation of AsA, DHA and GSH in tomato, pigeon pea and mustard plants, respectively. However, the enhanced APX activity in the roots of PC and in the shoots of GN tomato plants exposed to Ni agrees

with findings by Kumar et al. (2012) in barley plants. AsA, GSH and APX are efficient AOXs involved in the protection of important biomolecules. Besides its role as a powerful AOX, AsA also plays an important role in preserving the activity of enzymes that contain prosthetic transition metal ions (Gill and Tuteja, 2010a) and has a role in the detoxification of HM, along with GSH (Anjum et al., 2014). The levels of reduced AsA were found to be enhanced in the roots of plants from both cultivars and in PC shoots under Ni stress. Both the amounts of reduced and oxidized forms were enhanced in the roots of plants under combined stress and in GN roots exposed to Ni, which is in agreement with findings by Maheshwari and Dubey (2009) in rice seedlings. These authors also noticed that the activity of CAT remained relatively stable while the activity of APX was significantly higher in response to Ni stress, which agrees with results from the present study. As a matter of fact, CAT showed little or no induction in terms of activity in GN or PC plants in response to Ni stress. It is possible that Ni stress caused disturbances to CAT's activity by inhibiting its appropriate co-factor binding, through competition with Fe cations (Seregin and Kozhevnikova, 2006; Sachan and Lal, 2017).

Regarding the levels of Pro, a tendency for an increased accumulation of this amino acid in response to Ni stress was observed in the present study (by as much as 8-fold in GN and 15-fold in PC shoots). This agrees with findings by Uruç Parlak (2016) and Gajewska et al. (2006), in wheat plants under Ni stress. However, when comparing with the Pro increases observed in plants under combined stress (by as much as 60-fold), those variations were found to be rather insignificant, insinuating that Pro played a much more meaningful role in plants under combined stress than under single Ni stress. It is worth mentioning that besides the recognized role of Pro as a direct ROS scavenger and osmoprotectant in plants under stress, some authors have hypothesized that a high accumulation of Pro also serves as a stress signal, indicating a high sensitivity to a certain stressor (Cia et al., 2012; Soares et al., 2016b). Therefore, it is hard to discern whether a high induction in the accumulation of Pro is a sign of tolerance to stress sensitivity. Following this point of view, in the present study, the discreet, but noticeable increase in the levels of Pro in plants under single Ni stress could possibly account for its protective function (Sharma and Dietz, 2006), which together with the induction of AsA and other AOXs may have been responsible for the absence of major oxidative damages. Overall, the observed accumulation of such AOXs was more noticeable in GN tomato plants exposed to Ni, despite the higher accumulation of this HM in root tissues of this cultivar. This efficient activation of the AOX system may have accounted for the low degree of LP, and for the relatively lower levels of ROS, when compared to the plants of the PC cultivar.

The exposure to PEG-induced drought did not have an equal effect in plants from both cultivars. PC plants showed an overall little variation in the levels of H_2O_2 , while in GN plants, these were found to be slightly increased in shoots and decreased in the roots. The levels of $O_2^{\cdot-}$ were also enhanced in response to PEG in shoots of both cultivars, but not in the roots, with GN plants even presenting lower values of this ROS in relation to the respective CTL. The occurrence of oxidative damage, measured by MDA content, was only observed in the roots of PC, although ROS levels remained identical to the CTL in these tissues. In a study with summer maize plants, Ge et al. (2006) observed that MDA accumulation followed the severity of the water stress imposed by controlling irrigation, and that LP was always higher in the leaves than in the roots of these plants. Türkan et al. (2005) reported an increased accumulation of MDA in common bean plants under PEG-exposure, which was aggravated with age as well. In the present study, PEG-induced drought led to the enhancement in the activity of SOD in shoots of GN, possibly as a response to the $O_2^{\cdot-}$ burst, and further explaining the increased values of H_2O_2 in the green tissues of this cultivar. Enhanced AOX enzymatic activity has been described in plants under PEG exposure. For instance, Hatami et al. (2017) reported the increase of SOD's activity with increasing PEG-induced stress intensity in *Hyoscyamus niger* L. plants. The activity of APX in roots of PC was also enhanced in response to PEG exposure, while CAT's activity remained unaffected in tissues of both cultivars. This disagrees with findings of Hatami et al. (2017), who observed a decrease in the activities of these two AOX enzymes in *H. niger*. Moreover, Türkan et al. (2005) also witnessed that in drought-sensitive common bean plants, PEG treatment did not affect the activity of CAT, but increased that of SOD. However, in the same study, the constitutive levels of activity in this species were found to be lower than those of the closely related drought-tolerant *Phaseolus acutifolius* L.. In cassava, summer maize, and cotton plants under PEG-induced drought stress the activities of SOD and CAT have been reported to quickly increase as a response to this type of stress (Ge et al., 2006; Li et al., 2010; Fu et al., 2016). The concomitant increase of AsA reduced and oxidized forms in roots of both cultivars exposed to PEG, possibly accounts for the low levels of ROS in these tissues. Actually, AsA is known to directly remove some ROS, including $O_2^{\cdot-}$ (Soares et al., 2019). Thus, from what it appears, GN and PC both stimulated the production of AsA, with GN plants showing a better ROS removal, since $O_2^{\cdot-}$ further decrease from their respective CTL in roots. The levels of AsA were not as enhanced in the shoots under PEG exposure, both alone or combined, as they were in response to Ni, which may have been caused by a drought-induced C starvation, though stomata closure, which negatively affects the C metabolism dependent production of AsA (Smirnoff et al., 1996; Herbinger et al., 2002; Ünyayar et al., 2005).

Identically to Ni stress, single exposure to PEG also caused the levels of Pro to increase (by as much as 2-fold in GN and 4-fold in PC shoots) but not to a significant extent, when compared to the drastic rise of Pro levels in plants under combined stress. Indeed, besides being an efficient AOX, Pro has been firstly known as a potent osmolyte with a major role in regulating the response of plants to osmotic variations, including salinity and drought (Soares et al., 2019a). This tendency of increased accumulation of Pro in response to PEG is in agreement with the observed 1.5-fold increase in Pro levels in *Stevia* plants under PEG-induced drought (Hajihashemi and Sofo, 2018) as well as with findings of Zgallaï et al. (2005), who reported 10-fold increases of Pro content in both young and mature tomato plants. Moreover, this observed increase in Pro levels, either under PEG and/or Ni exposure, can shed some light on the overall maintenance of the water relations in GN and PC plants. Indeed, as reviewed by Hayat et al. (2012), the accumulation of Pro, either as a defense response and/or as a consequence of an exogenous application, can significantly enhance leaf water potential of metal- and drought-stressed plants.

The simultaneous exposure to Ni and PEG accounted for the induction of oxidative stress in plants of both cultivars, especially in the roots, where the levels of MDA increased. Similarly to single PEG stress, the levels of $O_2^{\cdot-}$ increased in plants under combined stress in shoots of both cultivars, but not in the roots. High levels of H_2O_2 were found in roots of both GN and PC plants, and also in shoots of PC. Nonetheless, the degree of LP did not show a direct relation with the levels of these two ROS, as tissues with higher H_2O_2 and $O_2^{\cdot-}$ levels actually showed lower LP. On a Ni and salinity combined approach, Amjad et al. (2019) found that exposure to 15 and 20 mg L⁻¹ Ni improved the activities of the AOX enzymes SOD, CAT and APX in two tomato cultivars and that the combination with 75 mM NaCl enhanced these enzymatic activities even more. Overall, the cultivar Naqeeb, which had been previously characterized as being more tolerant to both Ni and salinity, had higher levels of AOXs than the contrasting more sensitive cultivar, Nadir (Amjad et al., 2019). The drastic rise in the levels of Pro in plants of both cultivars under combined stress was accompanied by a significant fall in the protein content. Recalling the hypothesis described by Cia et al. (2012), in which Pro accumulation, in particular to such high levels, can be seen as a signal of stress sensitiveness, which seems to have been triggered in plants under combined stress, especially in those of the PC cultivar. What is debatable about this interpretation is that one would expect that higher Pro levels would account for a higher scavenging potential and less abundant ROS, and such correlation was not observed in plants under

combined stress, although very low amounts of MDA were found in the shoots, where Pro levels were also the highest.

In comparison to single Ni stress, the activities of AOX enzymes in the shoots of PC were found to be maintained or slightly enhanced when under the combined PEG and Ni stress, but in GN shoots, these enzymes' activities showed quite an antagonistic effect in response to the combined stress from that of shoots under single Ni stress. In fact, exposure to multiple stress does not necessarily induce the same responses as for each stress alone, nor the sum of them. The responses to combined stress depend on a lot of variables, including type of stresses, exposure times and intensity, species (and cultivars). Additive and aggravated effects on oxidative stress markers and AOX defenses have been reported in combined stress studies with HM and environmental changes. For instance, Bicalho et al. (2017) found that high temperatures increased *Dimorphandra wilsonii* seedlings' vulnerability to Zn-toxicity by interfering with seed respiration rate, inducing a higher accumulation of this HM in the seed tissues. Following a Ni and drought co-exposure approach, Salehi Eskandari et al. (2017) also observed additive deleterious effects on growth, LP and Pro accumulation when plants of the Ni-sensitive species *Cleome foliosa* were simultaneously exposed to Ni and PEG. Even so, Ünyayar et al. (2005) did not report additive effects in plants exposed to a combination of PEG-induced drought and Cd-stress. Most changes to growth and oxidative stress parameters in the drought- and Cd-sensitive tomato plants were found to be caused by the exposure to one of the stresses alone and maintained in the combined stress condition. For example, the accumulation of Cd in the tissues of tomato plants was higher in plants under single exposure to Cd than under combined stress. The growth of the shoots was just as inhibited by PEG-induced stress than by its combination with Cd. Moreover, the activities of the AOX enzymes SOD, CAT and APX in plants under PEG and Cd single stresses were identical to plants under the combined stress treatment (Ünyayar et al., 2005).

GN shoots revealed higher changes on the overall redox homeostasis (ROS levels and AOX performance) when exposed to the single Ni stress than under the co-exposure to PEG, indicating that the exposure to first stressor was probably enough for this cultivar to activate cross protection defenses and prevent the aggravation of oxidative stress upon the exposure to another stressor. Indeed, at least in shoots, LP even decreased in GN plants exposed to the combined stressors. On the other hand, PC plants showed higher ROS levels and a sharper stimulation of the AOX defenses when plants grew under combined stress than under each single stress. For instance, although PEG and/or

Ni exposure caused the ROS levels to increase in shoots of both cultivars, SOD's activity in PC shoots was only actually enhanced when both stressors were combined, while GN showed SOD activation in response to the single stresses. Yet, from what it appears, PC's increased effort in stimulating the AOX defenses was not enough to efficiently prevent the occurrence of oxidative disorders, inducing an overaccumulation of $O_2^{\cdot-}$, especially in shoots. Curiously, the absence of changes in LP pattern of PC and GN shoots can be probably related to the higher accumulation of Pro, which is known to be a potent inhibitor of LP given their membrane stabilizing properties (Hayat et al., 2012; Soares et al., 2019a). On the contrary, in roots, where GN plants exhibited an increase of LP in response to both stressors, the observed rise in Pro levels was much more tenue, possibly not enough to prevent LP to occur.

According to several reviews, a common observation is that plants with higher AOX power or lower levels of ROS have generally showed to be more tolerant to stress combinations (Koussevitzky et al., 2008; Suzuki et al., 2014; Zandalinas et al., 2018). Many of these studies have explored stress combinations in which plants grew under the simultaneous exposure to both stressors throughout several consecutive days or weeks (Ma et al., 2017a; Salehi Eskandari et al., 2017; Ameen et al., 2019; Wang et al., 2020). In the present study, plants from the stress combination treatment grew mostly under Ni stress and were only subjected to the PEG-induced drought in the last 48 h of the trial. The experimental design used in this study attempted to mimic real conditions that occur in Ni-polluted fields, in which the exposure to this HM is a continuous stressor and can be accompanied by occasional drought stress events. However, it goes without saying that, in the search for stress tolerant tomato cultivars, it would also be important to assess the differential effects of inducing drought, HM-stress or any other type of abiotic stresses and combinations to tomato cultivars on different plant life stages, since it is known that the effects of stress vary with plant age.

The results herein obtained seem to suggest that GN plants are better prepared to cope with the oxidative challenges induced by single Ni stress. These plants stimulated AOX defenses during the Ni exposure and could, therefore, prepare the overall redox status in advance so that the later addition of PEG-induced drought would already find plants actively responding to stress. In PC plants, in contrast, the entire AOX system was only substantially activated when plants suffered simultaneous exposure to the two stressors, demanding a much more drastic and speedy adjustment in terms of oxidative status and osmoprotectants.

It has been proposed that exposure to a combination of stresses leads to a completely unique pattern of responses (Pandey et al., 2015; Zandalinas et al., 2018). Examples of stress interactions can be seen in the updated version of Ron Mittler's Stress Matrix (Mittler, 2006; Zandalinas et al., 2018). The occurrence of additive effects in terms of metabolite profiling is not the most common scenario in plants under combined stress, given that plants usually face a rather specific metabolic demand when exposed to a combined stress condition, perceiving and signaling the simultaneous disturbances as completely dissimilar scenarios. In some other cases, as observed by Ünyayar et al. (2005), one of the stressors seems to be responsible for a particular physiological adjustment, and the other stressor may cause aggravation or attenuation of that effect. This is also the case observed in a study by Salehi Eskandari et al. (2017), in which Ni exposure to serpentine endemic *Cleome heratensis* plants under drought conditions actually increased plant's relative tolerance to drought. As previously suggested, plants exposed to the stress combination treatment may have activated a cross-tolerance response, which in terms of oxidative stress markers and AOX system, was definitely more evident in GN plants than in PC.

5.4. THE ROLE OF PAs IN GN AND PC PLANTS UNDER SINGLE AND COMBINED STRESS

As mentioned in several major reviews (cited in section 1.5.2.10), the involvement of PAs in regulating plants stress responses is a notion that has been gaining support from researchers worldwide. PAs have been included in the list of non-enzymatic AOXs given their actions as radical scavengers, membrane stabilizers and inhibitors of LP (Alcázar et al., 2006; Gill & Tuteja, 2010; Groppa & Benavides, 2008; Gupta et al., 2013; Sánchez-Rodríguez et al., 2016; Yu et al., 2019). However, one should not forget that not all PAs have an equal effect to plants under stress. In fact, Put accumulation can be quite intriguing and contribute to an even higher plant's vulnerability to stress. In contrast, an enhanced (Spm + Spd) / Put ratio has been related to a higher stress tolerance (Wang et al., 2007; Zhao and Yang, 2008; Sánchez-Rodríguez et al., 2016).

GN and PC tomato plants grown under Ni contamination showed significant adjustments to their internal PAs levels. In roots of both cultivars, despite the threatening accumulation of Ni, the exposure to this HM caused the levels of Put to decrease and of Spd to slightly increase. Curiously, the opposite was observed in shoots, where Put levels increased drastically in response to Ni, and Spd levels remained unaffected, although the internal Ni concentrations were much lower than in roots. Regardless of

stress treatment, roots of both cultivars showed higher constitutive levels of Spd than Put, while in the shoot tissues, Ni stress caused the levels of Put to surpass those of Spd.

Similarly to what was observed in shoot tissues, Put accumulation in response to HM stress is a fairly expected outcome, since it has been reported that the Put biosynthetic pathway is usually induced by metal stress (Wang et al., 2013; Yang et al., 2010). However, this PA's accumulation does not necessarily relate to an acclimation response to stress, as Put has been described to act mainly as a stress signal, accusing the presence of the stress (Groppa and Benavides, 2008; Zhao and Yang, 2008; Paul et al., 2018). In this sense, the observed increase of Put in the shoots (to levels higher than Spd), with a consequent decrease in the Spd/Put ratio may indicate a greater sensitivity of these tissues to Ni and combined stresses. The accumulation of Put in plants under stress has actually been recognized as an abiotic stress marker (Paul et al., 2018), with negative effects on cells, threatening the redox homeostasis and membrane stability. On the other hand, the ability of plant cells to maintain relatively higher Spd levels under stress conditions, and consequently a higher Spd/Put ratio, as was observed in the roots of GN and PC plants, can actually be seen as an attribute of stress tolerance, especially considering the high amounts of Ni found in these tissues (Liu et al., 2004; Sánchez-Rodríguez et al., 2016). This higher PA has several important physiological roles, which include ROS scavenging activity, protection of biomolecules, anti-senescence effects, and efficient activation of antioxidant defenses, among others (Hussain et al., 2019). In fact, the exogenous application of higher PAs like Spd and Spm has been used in combating metal toxicity, conferring a higher HM tolerance to crops (Paul et al., 2018). GN and PC plants exposed to Ni managed to maintain relatively controlled levels of ROS in the roots and stimulated their AOX defenses in these tissues, which additionally verified a greater accumulation of Spd and a decrease in Put levels. Such Spd increase was not seen in shoots of both GN and PC plants under Ni stress nor in the tissues of *Potamogeton crispus* plants under Cd stress (Yang et al., 2010). *P. crispus* tissues, as well as the shoots of GN and PC plants revealed a higher Put accumulation, in detriment of Spd, in response to the HM. These contrasting results on PAs content, as well as ROS and AOX levels seem to suggest that roots of the two tomato cultivars showed a greater tolerance to Ni stress than their own shoot tissues or than that observed by Yang et al. (2010) for *P. crispus* plants to Cd stress. Pietrini et al. (2015) also noticed that the levels of Spd remained relatively stable in shoots of *Amaranthus paniculatus* plants under Ni stress, while Put levels increased. The same was not observed in the roots of these plants, were Pietrini et al. (2015) observed a decrease in the levels of all free PAs in

response to increasing Ni concentrations. These differences in PA content between roots and shoots of the same plants could indicate that adjustments to PA metabolism might be tissue specific, possibly influencing the overall AOX system in a distinctive way as well.

PEG-induced drought only affected the levels of PAs in the shoots of GN, in which Put accumulated to a similar extent as for Ni-stress, Spd also slightly decreased and the Spd / Put ratio was markedly reduced. No substantial changes were observed in the levels of PAs in the roots of either cultivars due to PEG exposure. The fact that PEG exposure did not cause a Put peak in the roots, but enhanced these levels in the shoots, notably in GN plants, seems to suggest, once again, that tomato plant roots were more stress resilient than the shoots, where the Put signal was activated, revealing a higher stress sensitivity. The Put increase and Spd decrease registered in the shoots agree with findings by Pál et al. (2018) in wheat plants under 15 % PEG 6000. As also mentioned in this work, the stimulation of Put accumulation at the expense of Spd might have occurred as a consequence of its preferential metabolic canalization to the back conversion pathway, as proposed by Alcázar et al. (2011). Pál et al. (2018) also reported that no significant changes occurred in the levels of PAs in the roots under PEG exposure. The lack of Spd accumulation in response to PEG could also be related to its consumption in PA conjugation reactions, as suggested by Cvikrová et al. (2013).

Combined stress showed a non-aggravated effect on the levels of PAs in both GN and PC plants. Put levels in the roots of both cultivars even revealed a quite antagonistic response in response to the combined stress, as the effect of Ni on reducing Put levels was not sustained in the combined approach. On the other hand, shoots from plants under combined stress showed a Put accumulation identical to that in plants under single Ni stress and, in the case of GN shoots, also identical to PEG treated plants. The levels of Spd were only significantly affected by combined stress in the roots of GN under combined stress and of PC under single Ni-stress. The only additive effect was observed for Spd accumulation in the roots of GN, in which Spd levels increased more in response to the combination of stresses than to Ni or PEG exposures alone. A few studies have focused on the relationship between PA metabolism and stress combination (Cvikrová et al., 2013; Fu et al., 2014). For instance, Cvikrová et al. (2013) found that combining heat to drought stress did not cause additive effects on the levels of any PA, which remained similar to those in plants under single drought stress. Fu et al. (2014) reported that the exogenous application of Spd to trifoliolate orange seedlings conferred tolerance to combined drought and heat stresses. These authors reported that the applied Spd

acted as a signaling molecule that could enhance the activity of AOX enzymes, as well as the expression of important stress-related genes, even to the point where plants “seemed free of stress”. Moreover, Tsaniklidis et al. (2020) acknowledged separate roles of PAs in plants under biotic or abiotic stress. These authors investigated the expression of several genes related to PAs metabolism, having reported that in plants under abiotic stress (cold stress), the levels of free PAs would increase to act as protective molecules and enhance plant’s AOX potential, but that under biotic stress (viral infection) the catabolism of PAs would be stimulated causing a H₂O₂ burst that would mediate defenses against the infection. Although there are not many studies to prove the involvement of PAs in the acquisition of tolerance to combined abiotic stresses, there have already been suggestions for its use in chemical priming of seeds, especially of Spd, to improve the resilience of plants to multiple abiotic stresses (Minocha et al., 2014; Savvides et al., 2016).

Regarding the results from the present study, no major differences were observed in terms of adjustments to the PA metabolism between plants from the two cultivars GN and PC. The only possible distinction was that PC plants seemed to be more capable of maintaining relatively higher Spd / Put ratio under stressful conditions, but with no connection to ROS scavenging or to the activation of AOX defenses.

Figure 36 Overall physiological disturbances to Gold Nugget tomato plants caused by the exposure to PEG and Ni. Red or green arrows represent significant negative or positive alterations, respectively, in comparison to the CTL. Black symbols correspond to non-significant changes.













Gold Nugget	6% PEG 6000	50 μ M Ni	50 μ M Ni + 6% PEG 6000
<p>Growth</p> <p>Pigments</p> <p>Ni content</p> <p>ROS and LP</p> <p>Non-enzymatic AOX</p> <p>Enzymatic AOX</p> <p>PAs</p>	 <p> ↓ Length ↓ Biomass = Chl = Car = [Ni] ↑ H₂O₂ ↑ O₂^{•-} = LP ↑ Pro = GSH = AsA = DHA = CAT = APX ↑ SOD ↑ Put = Spd ↓ Spd / Put </p>	 <p> ↓↓ Length ↓↓ Biomass ↓ Chl ↓ Car ↑ [Ni] ↑ H₂O₂ = O₂^{•-} = LP ↑ Pro = GSH = AsA = DHA ↑↑ CAT ↑↑ APX ↑↑ SOD ↑ Put = Spd ↓ Spd / Put </p>	 <p> ↓↓ Length ↓↓ Biomass ↓ Chl ↓ Car ↑ [Ni] = H₂O₂ ↑ O₂^{•-} ↓ LP ↑↑ Pro = GSH = AsA = DHA = CAT ↑ APX = SOD ↑ Put = Spd ↓ Spd / Put </p>
<p>Growth</p> <p>Ni content</p> <p>ROS and LP</p> <p>Non-enzymatic AOX</p> <p>Enzymatic AOX</p> <p>PAs</p>	 <p> ↓ Biomass = [Ni] ↓ H₂O₂ ↓ O₂^{•-} = LP ↑ Pro = GSH ↑ AsA = DHA = CAT = APX ↓ SOD = Put = Spd = Spd / Put </p>	 <p> ↓↓ Length ↓↓ Biomass ↑↑ [Ni] ↑ H₂O₂ ↓↓ O₂^{•-} ↓ LP = Pro = GSH ↑↑ AsA ↑ DHA ↑ CAT ↑ APX = SOD ↓ Put ↑ Spd ↑ Spd / Put </p>	 <p> ↓↓ Length ↓↓ Biomass ↑↑ [Ni] ↑ H₂O₂ ↓ O₂^{•-} ↑ LP ↑ Pro ↑ GSH ↑↑ AsA ↑ DHA = CAT = APX = SOD = Put ↑ Spd = Spd / Put </p>

Figure 37 Overall physiological disturbances to Purple Calabash tomato plants caused by the exposure to PEG and Ni. Red or green arrows represent significant negative or positive alterations, respectively, in comparison to the CTL. Black symbols correspond to non-significant changes.

<p>Purple Calabash</p> <p>Growth Pigments Ni content ROS and LP Non-enzymatic AOX Enzymatic AOX PAs</p>	<p>6% PEG 6000</p>  <p>↓ Length ↓ Biomass ↑ Chl ↑ Car = [Ni] = H₂O₂ ↑ O₂⁻ ↓ LP ↑ Pro = GSH = AsA ↑ DHA ↓ CAT ↓ APX ↑ SOD ↑ Put = Spd ↓ Spd / Put</p>	<p>50 μM Ni</p>  <p>↓ Length ↓ Biomass ↓ Chl ↓ Car ↑ [Ni] ↑ H₂O₂ ↑ O₂⁻ = LP ↑ Pro ↑ GSH ↑ AsA ↑ DHA = CAT = APX ↑ SOD ↑ Put = Spd ↓ Spd / Put</p>	<p>50 μM Ni + 6% PEG 6000</p>  <p>↓ Length ↓ Biomass ↓ Chl ↓ Car ↑ [Ni] ↑ H₂O₂ ↑ O₂⁻ ↓ LP ↑ Pro ↑ GSH ↑ AsA ↑ DHA = CAT = APX ↑ SOD ↑ Put = Spd ↓ Spd / Put</p>
<p>Growth Ni content ROS and LP Non-enzymatic AOX Enzymatic AOX PAs</p>	 <p>↓ Biomass = [Ni] = H₂O₂ = O₂⁻ ↑ LP ↑ Pro ↑ GSH ↑ AsA ↑ DHA = CAT ↑ APX = SOD ↑ Put = Spd ↓ Spd / Put</p>	 <p>↓ Length ↓ Biomass ↑ [Ni] ↑ H₂O₂ ↓ O₂⁻ = LP ↑ Pro ↑ GSH ↑ AsA = DHA = CAT ↑ APX = SOD ↓ Put ↑ Spd ↑ Spd / Put</p>	 <p>↓ Length ↓ Biomass ↑ [Ni] ↑ H₂O₂ = O₂⁻ ↑ LP ↑ Pro ↑ GSH ↑ AsA ↑ DHA ↓ CAT ↑ APX ↓ SOD ↑ Put ↑ Spd ↓ Spd / Put</p>

5.5. EXPRESSION PROFILE AND INVOLVEMENT OF METAL TRANSPORTERS IN GN AND PC PLANTS UNDER SINGLE AND COMBINED STRESS

Transport and accumulation of HM into the vacuoles are crucial for their detoxification in higher plants. Plant tolerance to HM can be measured by its ability to compartmentalize these potentially toxic compounds inside the vacuoles (Clemens, 2001; Martinoia et al., 2007; Hasan et al., 2017; Shimada et al., 2018), especially in the root tissues and stems, preventing HM from reaching the photosynthetically active tissues (Chen et al., 2009). This is mainly accomplished by the presence and activity of tonoplast localized transporters (Clemens, 2001). Their respective encoding genes' expression is sometimes stress-inducible by the presence of high levels of the metals they transport, enabling a well-tuned production when plants need them the most (Clemens, 2001; Brunetti et al., 2015; Yokosho et al., 2016).

To enable an easier interpretation of the results to be discussed, **Fig. 38** and **39** summarize the observed effects of Ni, PEG-induced drought, and combined stress to GN and PC tomato plants, respectively, on the expression profile of genes encoding metal transporters putatively involved in Ni detoxification.

The levels of expression of *ABCC5-18* and *IREG2-like* genes were, in general, much higher in roots than in shoot tissues of both GN and PC plants; in contrast, the expression of *ABCB21* was identical in both organs from the CTL plants but increased much more drastically in shoots than in roots, as a response to PEG-induced drought; expression of *CAX3* and *MTP1*, on the other hand, was significantly higher in shoots than in roots, regardless of the stress treatment. The fact that both GN and PC tomato plants showed a preferential accumulation of Ni in root tissues indicates that some regulatory mechanism must have acted in preventing most Ni from reaching the photosynthetically active tissues. As mentioned before, Ni translocation can be “blocked” by its chelation and compartmentalization in the root apoplast or cell vacuoles (Chen et al., 2009; Mozafari et al., 2013; Ameen et al., 2019).

Proteins encoded by the genes *ABCC5-18* and *IREG2-like* are transmembrane transporters, conceivably located to the tonoplast (Bugchio et al., 2002; Schaaf et al., 2006; Yokosho et al., 2016; Ofori et al., 2018). Their constitutive levels were found to be higher in roots than in shoots of tomato plants and the expression of *ABCC16-18* and *IREG2-like* in roots of both cultivars was also significantly increased by the exposure to Ni, while that of *ABCC5* and *6* was only upregulated by Ni in PC roots, but not in GN

plants. The Ni-inducible expression of such transporters in the root tissues seems to suggest that they play a role in the confinement of Ni to the roots. Whether by shipping Ni to the root apoplast or to the vacuoles, these transporters certainly had a role in keeping such high levels of Ni restricted to the roots under single stress conditions. Regarding ABCC transporters, SIABCC6 was found to be closely related to the AtABCC1 and AtABCC2, which had been identified as ubiquitously expressed tonoplast localized transporters involved in metal tolerance in Arabidopsis plants, by transporting phytochelatin-HM complexes, as well as glutathionated and glucuronated compounds into the vacuoles. It has been stated that the one of the main roles of ABCC transporters is to carry HM conjugates with PCs and GSH into the vacuoles of plant cells (Hwang et al., 2016; Martinoia, 2018). The induction of the expression of these genes is considered an efficient stress-inducible mechanism for the detoxification of HM after their chelation in the cytosol. Accordingly, the also homologues *AtABCC3* and *AtABCC6* have been reported to be Cd-inducible and involved in the transport and detoxification of phytochelatin-Cd conjugates into the vacuoles of Arabidopsis plants exposed to Cd (Brunetti et al., 2015).

In a study with *AtIREG2*, a close homologue to *SIIREG2-like*, Schaaf et al. (2006) noticed that this metal transporter was involved in the Ni detoxification process, being mainly expressed in root tissues under HM stress. Schaaf et al. (2006) also reported that the overexpression of *AtIREG2* increased tolerance and potential for the accumulation of Ni in tissues. Another homologue, *FeIREG1*, described by Yokosho et al. (2016) in buckwheat plants, has been shown to be induced by exposure to Al, and has also been reported as mainly expressed in the roots of these plants, and to enhance the plant tolerance to Al and Ni, when overexpressed in Arabidopsis plants (Yokosho et al., 2016), agreeing with the former study and with the results herein obtained. Moreover, Merlot et al. (2014) identified *PgIREG2* as encoding a vacuolar Ni transporter in the hyperaccumulator species, suggesting that a high expression of this gene and possibly of homologous genes in other plants could confer tolerance to Ni. A more significant induction of this gene's expression in response to Ni stress was noticed in the roots of PC than in GN, although a higher Ni accumulation was observed in the root tissues of GN than PC. In fact, the absolute levels of expression of this gene were already higher in the roots of GN CTL plants, and even though the induction of this gene's expression in relation to the CTL was not as sharp as in PC roots, the levels of this transcript were much higher in GN plants. In the shoots, on the other hand, where Ni accumulation was substantially lower, GN plants were capable of inducing *IREG2-like* expression while PC

plants were not. This might suggest that, *per se*, GN can be more readily equipped with protective mechanisms when a stress situation appears.

Additionally, *MTP1*'s expression was substantially induced in the shoots of GN plants exposed to single Ni stress. These tissues also showed an enhanced expression of *ABCC5* and *IREG2-like*. It is important to note that the shoots of GN plants accumulated slightly higher levels of Ni than PC shoots. In this sense, the enhanced expression of *MTP1*, essentially, may have allowed for an improved detoxification of this HM in the shoots of GN, preventing it from damaging the photosynthetic machinery and further disturbing the redox homeostasis in GN foliar tissues. On the other hand, PC plants did not have any of these transporters' expression stimulated in the shoots of plants under Ni stress. Such inductions were only observed in the shoots of GN plants and may have been partially accountable for the relatively weaker effects of Ni, seen by the lower levels of ROS and the prompter activation of AOX in these tissues, when compared to PC shoots.

The expression of *CAX3* and *ABCB21* were oddly induced exclusively by the exposure to PEG-induced stress and not by Ni stress, particularly in the shoots. This was observed for both cultivars, although the induction of these two genes in the shoots was more noticeable in GN than in PC plants. In roots, on the other hand, PC plants had a higher induction of the *ABCB21* expression in response to the PEG treatment. Interestingly, the expression of genes encoding CAX transporters has actually been found to be highly inducible by several abiotic stressors such as salinity, cold and drought, which agrees with findings from the present study. For instance, as reviewed by Bickerton and Pittman (2015), the *SICAX3* homologues *AtCAX1*, *AtCAX3*, *AtEFCAX1*, *OsCAX2* and *OsCAX4*, from *Arabidopsis* and rice plants, were all found to be upregulated under water stress conditions. These transporters are thought to be tightly involved in the modulation of Ca signals under abiotic stress (Plieth et al., 2007), however, the mechanism by which CAX transporters regulate Ca levels are still not fully described. Although most SIABCB transporters have been indicated to be highly expressed in roots and suggested to be involved in ion and HM transport (Ofori et al., 2018) the *ABCB21* gene assessed in the present study revealed to be more expressed in response to the PEG treatment than to Ni stress, and its transcripts were mainly accumulated in shoots instead of roots. Not much has been explored in the involvement of ABCB transporters in plants exposed to drought, but the homologue gene *AtABCB14* has been described to regulate stomatal closure in *Arabidopsis* plants (Lee et al., 2008; Ofori et al., 2018). The *AtABCB14*-mediated malate uptake across the plasma

membrane has been shown to have a major effect on plant growth under drought stress conditions (Lee et al., 2008). Moreover, an ABCC homologue gene from *Arabidopsis*, *AtMRP5*, has also been described to be involved in the guard cell hormonal signaling and water use (Klein et al., 2003). However, this transporter's knockout mutant was found to be more resistant to drought stress than wild-type plants or mutants overexpressing *AtMRP5* (Klein et al., 2003).

Contrarily to the findings from this study, Mei et al. (2009) observed that the expression of the homologue gene *AtCAX4* was slightly induced by exposure to 100 μ M Ni, especially under Ca deficiency. These authors also found that this *Arabidopsis* gene was mainly expressed in root tissues, such as the root apex, lateral primordia, and primary root elongation zone, which disagrees with the much higher levels of this transcript found in shoots of both GN and PC plants, in comparison to roots. Unlike PEG-induced drought, the combined stress treatment did not trigger such an increase in the expression of *CAX3* or *ABCB21* transporters upon PEG co-exposure, and even caused the downregulation of *CAX3* in the roots of both cultivars. This is probably an effect of all the Ni-induced effects on plant physiology and transcriptional profile, which possibly caused the repression of these and many other gene's expression, preventing the later PEG stimuli from affecting transcription. As evidenced in **Fig. 38** and **39**, single PEG-induced drought caused more similar effects on the expression profile of genes encoding metal transporters between the two tomato cultivars than single Ni stress, suggesting that the differences between the two cultivars may be more related to the way they respond to Ni stress than to drought. This is further confirmed by the results obtained in the biochemical assessments, in which most differences observed regarding the redox homeostasis and AOX defenses were induced by exposure to single Ni stress instead of PEG-induced drought.

In relation to the combined stress condition, results showed once again that the effects on gene expression caused by Ni exposure prevailed over those caused by drought, reinforcing the majority of the biochemical results. Namely, the expression of *CAX3* or *ABCB21* genes, that would otherwise be upregulated in response to PEG, remained unaffected or even decreased in the combined stress condition, as in the single Ni stress. However, the effects on gene expression induced by single Ni stress were not additively exerted in plants under combined stress. The only cases in which the expression profile was exacerbated from that of plants under single Ni stress were for *ABCC5*, *CAX3* and *MTP1* expression in the roots of GN plants, in which single Ni stress tended to decrease the expression of these genes and the combined stress treatment

decreased it substantially more. This could be related to the fact that, unlike PC, GN roots and shoots accumulated more Ni when exposed to the combined stress treatment than under single Ni stress, being these effects mainly related to the higher Ni contents.

Gold Nugget	6% PEG 6000	50 μ M Ni	50 μ M Ni + 6% PEG 6000
ABCC5			=
ABCC6			=
ABCC16			=
ABCC18	=		=
ABCB21			=
CAX3		=	=
IREG2-like			=
MTP1	=		=
ABCC5			
ABCC6	=	=	
ABCC16			=
ABCC18	=		
ABCB21	=	=	
CAX3		=	
IREG2-like	=		=
MTP1			

Figure 38 Changes in expression of genes encoding metal transporters conceivably involved in the detoxification of Ni in Gold Nugget plants caused by the exposure to PEG and Ni. Red or green arrows represent significant increases or decreases in gene expression, respectively, in comparison to CTL levels. Black symbols correspond to non-significant changes.

Purple Calabash	6% PEG 6000	50 μ M Ni	50 μ M Ni + 6% PEG 6000
ABCC5			
ABCC6	=	=	=
ABCC16		=	
ABCC18			
ABCB21			=
CAX3			=
IREG2-like		=	
MTP1	=		=
ABCC5			
ABCC6	=		=
ABCC16			=
ABCC18			
ABCB21		=	=
CAX3	=	=	
IREG2-like			=
MTP1	=	=	

Figure 39 Changes in expression of genes encoding metal transporters conceivably involved in the detoxification of Ni in Purple Calabash plants caused by the exposure to PEG and Ni. Red or green arrows represent significant increases or decreases in gene expression, respectively, in comparison to CTL levels. Black symbols correspond to non-significant changes.

6. Conclusions

- **Growth and overall physiological performance**
 - Exposure of tomato plants to Ni stress led to a higher accumulation of this HM in roots than in shoots
 - Gold Nugget plants were capable of accumulating higher amounts of Ni in the roots than Purple Calabash, without showing a higher phytotoxic impact
 - Exposure to Ni inhibited growth, caused the interveinal yellowing of leaves, decreased the abundance of Chl and Car, and increased the levels of H₂O₂ in 20 day-old plants of both Gold Nugget and Purple Calabash tomato cultivars
 - PEG-induced drought hampered biomass production but did not affect root elongation or the levels of Chl and Car
 - Combined stress treatment did not cause additive effects on growth, water content, and levels of Chl and Car in plants from the two cultivars, as these were identical to those caused by single Ni-stress

- **Occurrence of oxidative stress and activation of AOX defenses**
 - Despite the lack of macroscopic differences in plant responses towards stress, Gold Nugget and Purple Calabash plants showed quite distinctive adjustments to stress at biochemical and molecular level
 - Gold Nugget plants showed a higher ROS accumulation and a quicker activation of AOX defenses in the shoots against single Ni stress than Purple Calabash plants
 - The exposure to Ni caused more notorious effects in the redox homeostasis and AOX system of both GN and PC tomato plants, than PEG-induced drought
 - PEG-induced drought stimulated the accumulation of ROS in the shoots of both cultivars, triggered the activity of SOD in the shoots of GN plants, and boosted AsA and APX in the roots of PC plants
 - Overall, GN plants seem to have had an earlier perception of Ni stress and were able to activate their AOX defenses in a prompter way than PC plants
 - Purple Calabash plants only showed a significant boost in their AOXs when facing combined Ni and drought stress
 - Put accumulation, recognized as a marker of stress sensitivity, occurred in the shoots of both cultivars in response to Ni stress, but also in response to PEG, in GN plants
 - Roots tissues showed better Spd/Put ratio than shoot tissues, especially in PC plants

- **Expression profile and involvement of metal transporters**

- The expression of genes encoding metal transporters was not only affected by exposure to Ni, but also, in some cases exclusively, in response to the single PEG treatment
- The expression of *ABCC5-18* and *IREG2-like* genes was higher in roots than in shoot tissues of both GN and PC plants, while expression of *CAX3* and *MTP1*, was higher in shoots than in roots, regardless of the stress treatment, and that of *ABCB21* was also more strongly induced in shoots than roots
- Ni stress upregulated the expression of *ABCC16-18* and *IREG2-like* in roots of both cultivars and of *ABCC5-6* only in the roots of PC
- Only GN plants had the expression of *MTP1*, *ABCC5* or *IREG2-like* upregulated in the shoots in response to Ni stress
- Expression of *CAX3* and *ABCB21* was induced in the shoots, mainly of GN plants by the exposure to PEG-induced stress, but not to Ni stress
- Ni effects on gene expression prevailed over those caused by PEG-induced drought, since plants under combined stress exposure showed similar patterns of gene expression as plants under single Ni stress
- The effects on *ABCC5*, *CAX3* and *MTP1* expression in the roots of GN plants were exacerbated in the combined treatment, possibly because these tissues accumulated even more Ni than those under single Ni-stress
- GN plants showed stronger adjustments to gene expression in response to single Ni stress and PEG-induced drought than PC plants

Overall, results seem to suggest that GN plants are more readily equipped with protective mechanisms when a stress situation appears, than PC plants, which may ease the adjustments demanded by the co-exposure to a second stressor.

7. Future Perspectives

The assessment of the genetic diversity of crops in the search for tolerance traits is a smart strategy for the improvement of important cultivars, but still requires considerable research, which hopefully plant physiologists will put through in the following years. For many crops and vegetables, stress tolerant cultivars are still to be discovered or have yet to be characterized from a metabolic and molecular point of view. Moreover, research on abiotic stress must now focus on an increasing number of stress factors and stress combinations. Plant breeding programs can effectively apply tolerance traits from certain species or varieties to more commercially interesting cultivars, making them less vulnerable to adverse conditions. However, plant breeders must first know where to look! Tolerance traits are still not widely described, much less regarding combined stress. So, plant physiologists and molecular biologists must first characterize this large panoply of crop varieties and find patterns of stress tolerance for several stress factors and combinations. Only then, can plant breeders do their magic!

This being said, this study leaves a few doors open for future research on the diversity of tomato plants in the search for stress tolerance traits, which we hope will shed some light on the development of Ni, drought and maybe even combined Ni and drought stress tolerant tomato cultivars. It would be interesting to carry out the following investigations:

- Assess the expression profile of genes encoding proteins involved in the metabolism of PAs
- Confirm the subcellular location of transporters encoded by the genes that were herein upregulated in response to Ni stress, in order to confirm the role in metal detoxification
- Explore the potential of applying exogenous PAs (mainly Spd) to increase tomato plant tolerance to stress
- Confirm the usefulness of the Ni stress tolerance markers herein suggested in future studies with different cultivars under the same stress conditions, such as higher retention of Ni in roots, activation of AOX enzymes, accumulation of Pro and AsA, maintenance of a high Spd/Put ratio and induction of the expression of genes encoding metal transporters in the roots exposed to Ni
- Confirm the usefulness of the combined stress tolerance markers herein suggested in future studies with different cultivars under the same stressors, such

as earlier activation of AOX defense and non-aggravation of effects when compared to single stresses

- Extend this type of research to other tomato cultivars or wild species
- Compare the responses of different tomato cultivars under more stress conditions and stress combinations
- Find a pattern of inducible effects in different cultivars responsible for enhancing tolerance to a certain stressor or combination of stresses

8. References

- Aazami MA, Torabi M, Jalili E** (2010) In vitro response of promising tomato genotypes for tolerance to osmotic stress. *African J Biotechnol* **9**: 4014–4017
- Abd Allah EF, Abeer A, Alam P, Ahmad P** (2019) Silicon Alleviates Nickel-Induced Oxidative Stress by Regulating Antioxidant Defense and Glyoxalase Systems in Mustard Plants. *J Plant Growth Regul* **38**: 1260–1273
- Abdelrahem A, Ahmed KZ** (2007) In vitro selection for tomato plants for drought tolerance via callus culture under polyethylene glycol (PEG) and mannitol treatments. *Proceeding 8th African Crop Sci. Soc. Conf.* 27-31 Oct. 2007, El-Minia, Egypt, pp 2027- 2032.
- Abdul-Baki AA** (1991) Tolerance of Tomato Cultivars and Selected Germplasm to Heat Stress. *J Am Soc Hortic Sci* **116**: 1113–1116
- Aebi H** (1984) Catalase in Vitro. *Methods Enzymol* **105**: 121–126
- Aghaie P, Hosseini Tafreshi SA, Ebrahimi MA, Haerinasab M** (2018) Tolerance evaluation and clustering of fourteen tomato cultivars grown under mild and severe drought conditions. *Sci Hortic (Amsterdam)* **232**: 1–12
- Ahmad MSA, Ashraf M, Hussain M** (2011) Phytotoxic effects of nickel on yield and concentration of macro- and micro-nutrients in sunflower (*Helianthus annuus* L.) achenes. *J Hazard Mater* **185**: 1295–1303
- Ahuja I, de Vos RCH, Bones AM, Hall RD** (2010) Plant molecular stress responses face climate change. *Trends Plant Sci* **15**: 664–674
- Ain Q, Akhtar J, Amjad M, Haq MA, Saqib ZA** (2016) Effect of Enhanced Nickel Levels on Wheat Plant Growth and Physiology under Salt Stress. *Commun Soil Sci Plant Anal* **47**: 2538–2546
- Ainsworth EA, Ort DR** (2010) How do we improve crop production in a warming world? *Plant Physiol* **154**: 526–530
- Akinci IE, Akinci S** (2010) Effect of chromium toxicity on germination and early seedling growth in melon (*Cucumis melo* L.). *African J Biotechnol* **9**: 4589–4594
- Albaladejo I, Plasencia FA, Meco V, Egea MI, Bolarin MC, Flores FB** (2015) Different strategies used by domesticated tomato and wild- related species to confront salt stress. *Procedia Environ Sci* **29**: 91–92
- Alcázar R, Bitrián M, Bartels D, Koncz C, Altabella T, Tiburcio AF** (2011) Polyamine metabolic canalization in response to drought stress in arabidopsis and the resurrection plant *craterostigma plantagineum*. *Plant Signal Behav* **6**: 243–250
- Alcázar R, Marco F, Cuevas JC, Patron M, Ferrando A, Carrasco P, Tiburcio AF, Altabella T** (2006) Involvement of polyamines in plant response to abiotic stress. *Biotechnol Lett* **28**: 1867–1876
- Alexieva V, Sergiev I, Mapelli S, Karanov E** (2001) The effect of drought and ultraviolet radiation on growth and stress markers in pea and wheat. *Plant, Cell Environ* **24**: 1337–1344
- Ali M., Shokrani S.** (2011) Soil and soilless cultivation influence on nutrients and heavy metals availability in soil and plant uptake. *Int J Appl Sci Technol* **1**: 154–160
- Alkan M, Doğan M** (2001) Adsorption of copper(II) onto perlite. *J Colloid Interface Sci* **243**: 280–291
- Ameen N, Amjad M, Murtaza B, Abbas G, Shahid M, Imran M, Naeem MA, Niazi NK** (2019) Biogeochemical behavior of nickel under different abiotic stresses: toxicity and detoxification mechanisms in plants. *Environ Sci Pollut Res* **26**: 10496–10514

- Amjad M, Ameen N, Murtaza B, Imran M, Shahid M, Abbas G, Naeem MA, Jacobsen S** (2019) Comparative physiological and biochemical evaluation of salt and nickel tolerance mechanisms in two contrasting tomato genotypes. *Physiol Plant*. doi: 10.1111/ppl.12930
- Amwata D, Mungai C, Radeny M, Solomon D** (2019) Review of policies and frameworks on climate change, agriculture, food and nutrition security in Kenya.
- Andolfo G, Ruocco M, Donato A Di, Frusciante L, Lorito M, Scala F** (2015) Genetic variability and evolutionary diversification of membrane ABC transporters in plants. *BMC Plant Biol* **15**: 1–15
- Anjum NA, Gill SS, Gill R, Hasanuzzaman M, Duarte AC, Pereira E, Ahmad I, Tuteja R, Tuteja N** (2014) Metal/metalloid stress tolerance in plants: role of ascorbate, its redox couple, and associated enzymes. *Protoplasma* **251**: 1265–1283
- Apel K, Hirt H** (2004) Reactive Oxygen Species: Metabolism, Oxidative Stress, and Signal Transduction. *Annu Rev Plant Biol* **55**: 373–399
- Asrar Z, Mozafari H, Rezanejad F, Pourseyedi S, Yaghoobi MM** (2014) Calcium and L-histidine effects on ascorbate-glutathione cycle components under nickel-induced oxidative stress in tomato plants. *Biol Plant* **58**: 709–716
- Atwell BJ, Wang H, Scafaro AP** (2014) Could abiotic stress tolerance in wild relatives of rice be used to improve *Oryza sativa*? *Plant Sci* **215–216**: 48–58
- Aydinalp C, Cresser MS** (2008) Agriculture Land use change (including biomass burning) The Effects of Global Climate Change on Agriculture. *Agric Environ Sci* **3**: 672–676
- Baccouch S, Chaoui A, El Ferjani E** (1998) Nickel toxicity: Effects on growth and metabolism of maize. *J Plant Nutr* **21**: 577–588
- Bai Y, Lindhout P** (2007) Domestication and breeding of tomatoes: What have we gained and what can we gain in the future? *Ann Bot* **100**: 1085–1094
- Baker AJM, Reeves RD, Hajar ASM** (1994) Heavy metal accumulation and tolerance in British populations of the metallophyte *Thlaspi caerulescens* J. & C. Presl (Brassicaceae). *New Phytol* **127**: 61–68
- Balaguer J, Almendro MB, Gómez I, Navarro Pedreño J, Mataix J** (1998) Tomato growth and yield affected by nickel presented in the nutrient solution. *Acta Hort* **458**: 269–272
- Baniasadi F, Saffari VR, Maghsoudi Moud AA** (2018) Physiological and growth responses of *Calendula officinalis* L. plants to the interaction effects of polyamines and salt stress. *Sci Hortic (Amsterdam)* **234**: 312–317
- Basha PO, Sudarsanam G, Reddy MMS, Sankar NS** (2015) Effect of Peg Induced Water Stress on Germination and Seedling Development of Tomato Germplasm. *Int J Rec Sci Res* **6**: 4044–4049
- Bates LS, Waldren RP, Teare ID** (1973) Rapid determination of free proline for water-stress studies. *Plant Soil* **39**: 205–207
- Bauchet G, Causse M** (2012) Genetic Diversity in Tomato (*Solanum lycopersicum*) and Its Wild Relatives. *Genet Divers Plants*. doi: 10.5772/33073
- Beauchamp C, Fridovich I** (1971) Superoxide Dismutase: Improved Assays and an Assay Applicable to Acrylamide Gels. *Anal Biochem* **44**: 276–287
- Benson DA, Cavanaugh M, Clark K, Karsch-Mizrachi I, Lipman DJ, Ostell J, Sayers EW** (2013) GenBank. *Nucleic Acids Res* **41**: D36–42
- Berberich T, Sagor GHM, Kusano T** (2015) Polyamines in Plant Stress Response. *In* T Kusano, H Suzuki, eds, *Polyam. A Univers. Mol. Nexus Growth, Surviv. Spec. Metab.*, 2015th ed. Springer Japan, Japan, pp 155–168
- Bhattacharjee S** (2005) Reactive oxygen species and oxidative burst: Roles in stress ,

senescence and signal transduction in plants. *Curr Sci* 1113–1121

- Bicalho EM, Gomes MP, Rodrigues-Junior AG, Oliveira TGS, Gonçalves C de A, Fonseca MB, Garcia QS** (2017) Integrative effects of zinc and temperature on germination in *Dimorphandra wilsonii* rizz.: Implications of climate changes. *Environ Toxicol Chem* **36**: 2036–2042
- Bickerton PD, Pittman JK** (2015) Role of cation/proton exchangers in abiotic stress signaling and stress tolerance in plants. *Elucidation Abiotic Stress Signal. Plants*. Springer, pp 95–117
- Bitá CE, Gerats T** (2013) Plant tolerance to high temperature in a changing environment: Scientific fundamentals and production of heat stress-tolerant crops. *Front Plant Sci* **4**: 1–18
- Bodner G, Nakhforoosh A, Kaul H** (2015) Management of crop water under drought : a review. 401–442
- Bradford MM** (1976) A Rapid and Sensitive Method for the Quantitation of Microgram Quantities of Protein Utilizing the Principle of Protein-Dye Binding. *Ana* **72**: 248–254
- Bradl H, ed** (2005) Heavy metals in the environment: origin, interaction and remediation. Elsevier
- Branco-Neves S, Soares C, de Sousa A, Martins V, Azenha M, Gerós H, Fidalgo F** (2017) An efficient antioxidant system and heavy metal exclusion from leaves make *Solanum cheesmaniae* more tolerant to Cu than its cultivated counterpart. *Food Energy Secur* **6**: 123–133
- Brdar-Jokanovic M, Zdravkovic J** (2015) Germination of tomatoes under PEG-induced drought stress. *Ratar i Povrt* **52**: 108–113
- Brunetti P, Zanella L, Paolis A De, Litta D Di, Cecchetti V, Falasca G, Barbieri M, Altamura MM, Costantino P, Cardarelli M** (2015a) Cadmium-inducible expression of the ABC-type transporter AtABCC3 increases phytochelatin-mediated cadmium tolerance in *Arabidopsis*. *J Exp Bot* **66**: 3815–3829
- Brunetti P, Zanella L, Paolis A De, Litta D Di, Cecchetti V, Falasca G, Barbieri M, Altamura MM, Costantino P, Cardarelli M** (2015b) Cadmium-inducible expression of the ABC-type transporter AtABCC3 increases phytochelatin-mediated cadmium tolerance in *Arabidopsis*. **66**: 3815–3829
- Bughio N, Yamaguchi H, Nishizawa NK, Nakanishi H** (2002) Cloning an iron-regulated metal transporter from rice. **53**: 1677–1682
- Cai HL, Zhu RH, Li H De** (2010) Determination of dansylated monoamine and amino acid neurotransmitters and their metabolites in human plasma by liquid chromatography-electrospray ionization tandem mass spectrometry. *Anal Biochem* **396**: 103–111
- Cairns JE, Crossa J, Zaidi PH, Grudloyma P, Sanchez C, Luis Araus J, Thaitad S, Makumbi D, Magorokosho C, Bänziger M, et al** (2013) Identification of drought, heat, and combined drought and heat tolerant donors in maize. *Crop Sci* **53**: 1335–1346
- Cappetta E, Andolfo G, Di Matteo A, Ercolano MR** (2020) Empowering crop resilience to environmental multiple stress through the modulation of key response components. *J Plant Physiol* **246–247**: 153134
- Carpita N, Sabularse D, Montezinos D, Delmer DP** (1979) Determination of the pore size of cell walls of living plant cells. *Science (80-)* **205**: 1144–1147
- Causse M, Desplat N, Pascual L, Le Paslier MC, Sauvage C, Bauchet G, Bérard A, Bounon R, Tchoumakov M, Brunel D, et al** (2013) Whole genome resequencing in tomato reveals variation associated with introgression and breeding events. *BMC Genomics*. doi: 10.1186/1471-2164-14-791
- Ceccarelli S, Grando S, Maatougui M, Michael M, Slash M, Haghparast R, Rahmanian M,**

- Taheri A, Al-Yassin A, Benbelkacem A, et al** (2010) Plant breeding and climate changes. *J Agric Sci* **148**: 627–637
- Çelik Ö, Ayan A, Atak Ç** (2017) Enzymatic and non-enzymatic comparison of two different industrial tomato (*Solanum lycopersicum*) varieties against drought stress. *Bot Stud*. doi: 10.1186/s40529-017-0186-6
- Chen C, Huang D, Liu J** (2009) Functions and toxicity of nickel in plants: Recent advances and future prospects. *Clean - Soil, Air, Water* **37**: 304–313
- Chen D, Shao Q, Yin L, Younis A, Zheng B** (2019) Polyamine function in plants: Metabolism, regulation on development, and roles in abiotic stress responses. *Front Plant Sci* **9**: 1–13
- Chen Z, Fujii Y, Yamaji N, Masuda S, Takemoto Y, Kamiya T, Yusuyin Y, Iwasaki K, Kato SI, Maeshima M, et al** (2013) Mn tolerance in rice is mediated by MTP8.1, a member of the cation diffusion facilitator family. *J Exp Bot* **64**: 4375–4387
- Chou K-C, Shen H-B** (2010) Plant-mPLoc: a top-down strategy to augment the power for predicting plant protein subcellular localization. *PLoS One* **5**: e11335
- Choudhury FK, Rivero RM, Blumwald E, Mittler R** (2017) Reactive oxygen species, abiotic stress and stress combination. *Plant J* **90**: 856–867
- Cia MC, Guimarães ACR, Medici LO, Chabregas SM, Azevedo RA** (2012) Antioxidant responses to water deficit by drought-tolerant and -sensitive sugarcane varieties. *Ann Appl Biol* **161**: 313–324
- Clemens S** (2001) Molecular mechanisms of plant metal tolerance and homeostasis. *Planta* **212**: 475–486
- Cui G, Zhao Y, Zhang J, Chao M, Xie K, Zhang C, Sun F, Liu S, Xi Y** (2019) Proteomic analysis of the similarities and differences of soil drought and polyethylene glycol stress responses in wheat (*Triticum aestivum* L.). *Plant Mol Biol* **100**: 391–410
- Cvikrová M, Gemperlová L, Martincová O, Vanková R** (2013) Effect of drought and combined drought and heat stress on polyamine metabolism in proline-over-producing tobacco plants. *Plant Physiol Biochem* **73**: 7–15
- Dahunsi B, Adebayo AJ, Oguntimehin I** (2019) Susceptibility of Cherry Tomato (*Lycopersicon Esculentum*) Plant to Simulated Foliar Cadmium and Nickel Exposures under Controlled Environment: Plant Health and Environmental Significances. *J. Environ. Earth Sci.* **2**:
- Das K, Roychoudhury A** (2014) Reactive oxygen species (ROS) and response of antioxidants as ROS-scavengers during environmental stress in plants. *Front Environ Sci* **2**: 1–13
- Delhaize E, Gruber BD, Pittman JK, White RG, Leung H, Miao Y, Jiang L, Ryan PR, Richardson AE** (2007) A role for the AtMTP11 gene of Arabidopsis in manganese transport and tolerance. *Plant J* **51**: 198–210
- Delhaize E, Kataoka T, Hebb DM, White RG, Ryan PR** (2003) Genes encoding proteins of the cation diffusion facilitator family that confer manganese tolerance. *Plant Cell* **15**: 1131–1142
- Dixit V, Pandey V, Shyam R** (2001) Differential antioxidative responses to cadmium in roots and leaves of pea (*Pisum sativum* L. cv. Azad). *J Exp Bot* **52**: 1101–1109
- Do PT, Degenkolbe T, Erban A, Heyer AG, Kopka J, Köhl KI, Hinch DK, Zuther E** (2013) Dissecting Rice Polyamine Metabolism under Controlled Long-Term Drought Stress. *PLoS One*. doi: 10.1371/journal.pone.0060325
- Donahue JL, Okpodu CM, Cramer CL, Grabau EA, Alischer RG** (1997) Responses of Antioxidants to Paraquat in Pea Leaves. *Plant Physiol* **113**: 249–257
- Dubey RMÆRS** (2009) Nickel-induced oxidative stress and the role of antioxidant defence in rice seedlings. 37–49

- Eckhardt U, Marques AM, Buckhout TJ** (2016) Two iron-regulated cation transporters from tomato complement metal uptake-deficient yeast mutants Two iron-regulated cation transporters from tomato complement metal uptake-deficient yeast mutants. doi: 10.1023/A
- Eide D, Broderius M, Fett J, Guerinot ML** (1996) A novel iron-regulated metal transporter from plants identified by functional expression in yeast. *Proc Natl Acad Sci* **93**: 5624 LP – 5628
- Enke RA** (2016) qPCR Primer Standard Curve Assay (wet lab)+ KEGG Pathway analysis (computational).
- Esham M, Jacobs B, Sunith H, Rosairo R, Siddighi BB** (2017) Climate change and food security : A Sri Lankan perspective perspective. *Environ Dev Sustain*. doi: 10.1007/s10668-017-9945-5
- Esquinas-Alcázar J** (2005) Protecting crop genetic diversity for food security: Political, ethical and technical challenges. *Nat Rev Genet* **6**: 946–953
- Facelli JM** (2008) Specialized strategies. I. Seedlings in stressful environments. *In* MA Leck, VT Parker, RL Simpson, RS Simpson, eds, *Seedl. Ecol. Evol.* Cambridge University Press, Cambridge, UK, pp 56–78
- FAO** (2018a) *FAO's Work on Climate Change*. United Nations Clim. Chang. Conf. 2018
- FAO** (2008) *CLIMATE CHANGE ADAPTATION AND MITIGATION IN THE FOOD AND AGRICULTURE SECTOR*. *Clim Chang energy food*. doi: 10.1126/science.1154102
- FAO** (2018b) *FAOSTAT Statistical Database*.
- Farooq M, Wahid A, Kobayashi N, Fujita D, Basra SMA** (2009) Plant Drought Stress: Effects, Mechanisms and Management. *In* E Lichtfouse, M Navarrete, P Dabaeke, C Alberola, eds, *Sustain. Agric.* Springer Science+Business Media, pp 153–188
- Fazeli F, Ghorbanli M, Niknam V** (2007) Effect of drought on biomass, protein content, lipid peroxidation and antioxidant enzymes in two sesame cultivars. *Biol Plant* **51**: 98–103
- Felsenstein J** (1985) Confidence limits on phylogenies: an approach using the bootstrap. *Evolution (N Y)* **39**: 783–791
- Fernandez-Pozo N, Menda N, Edwards JD, Saha S, Teclé IY, Strickler SR, Bombarely A, Fisher-York T, Pujar A, Foerster H, et al** (2015) The Sol Genomics Network (SGN)--from genotype to phenotype to breeding. *Nucleic Acids Res* **43**: D1036-41
- Firon N, Shaked R, Peet MM, Pharr DM, Zamski E, Rosenfeld K, Althan L, Pressman E** (2006) Pollen grains of heat tolerant tomato cultivars retain higher carbohydrate concentration under heat stress conditions. *Sci Hortic (Amsterdam)* **109**: 212–217
- Fita A, Rodríguez-Burruezo A, Boscaiu M, Prohens J, Vicente O** (2015) Breeding and domesticating crops adapted to drought and salinity: A new paradigm for increasing food production. *Front Plant Sci* **6**: 1–14
- Foolad MR** (2007) Current status of breeding tomatoes for salt and drought tolerance. *Adv. Mol. Breed. Towar. Drought Salt Toler. Crop*. pp 669–700
- Fothergill A, Scholey K, Butfield C, Lanfear S, Chapman A, Cordey H, Pearson H, Stark M, Wilson J** (2019) *Our Planet*.
- Foyer CH** (2018) Reactive oxygen species, oxidative signaling and the regulation of photosynthesis. *Environ Exp Bot* **154**: 134–142
- Foyer CH, Noctor G** (2013) Redox signaling in plants. *Antioxidants Redox Signal* **18**: 2087–2090
- Freeman JL, Persans MW, Nieman K, Albrecht C, Peer W, Pickering IJ, Salt DE** (2004) Increased glutathione biosynthesis plays a role in nickel tolerance in *Thlaspi* nickel hyperaccumulators W inside box sign. *Plant Cell* **16**: 2176–2191

- Fu L, Ding Z, Han B, Hu W, Li Y, Zhang J** (2016) Physiological investigation and transcriptome analysis of polyethylene glycol (Peg)-induced dehydration stress in Cassava. *Int J Mol Sci* **17**: 1–18
- Fu XZ, Xing F, Wang NQ, Peng LZ, Chun CP, Cao L, Ling LL, Jiang CL** (2014) Exogenous spermine pretreatment confers tolerance to combined high-temperature and drought stress in vitro in trifoliolate orange seedlings via modulation of antioxidative capacity and expression of stress-related genes. *Biotechnol Biotechnol Equip* **28**: 192–198
- Gajewska E, Skłodowska M** (2007) Effect of nickel on ROS content and antioxidative enzyme activities in wheat leaves. *BioMetals* **20**: 27–36
- Gajewska E, Skłodowska M, Słaba M, Mazur J** (2006) Effect of nickel on antioxidative enzyme activities, proline and chlorophyll contents in wheat shoots. *Biol Plant* **50**: 653–659
- Ge T, Sui F, Bai L, Lu Y, Zhou G** (2006) Effects of Water Stress on the Protective Enzyme Activities and Lipid Peroxidation in Roots and Leaves of Summer Maize. *Agric Sci China* **5**: 291–298
- George S, Ahmad Jatoi S, Uddin Siddiqui S** (2013) Genotypic differences against peg simulated drought stress in tomato. *Pakistan J Bot* **45**: 1551–1556
- Gerszberg A, Hnatuszko-Konka K, Kowalczyk T, Kononowicz AK** (2015) Tomato (*Solanum lycopersicum* L.) in the service of biotechnology. *Plant Cell Tissue Organ Cult* **120**: 881–902
- Gilbert N** (2010) How to avert a global water crisis. *Nature*
- Gill SS, Tuteja N** (2010a) Reactive oxygen species and antioxidant machinery in abiotic stress tolerance in crop plants. *Plant Physiol Biochem* **48**: 909–930
- Gill SS, Tuteja N** (2010b) Polyamines and abiotic stress tolerance in plants. *Plant Signal Behav* **5**: 26–33
- Gillespie KM, Ainsworth EA** (2007) Measurement of reduced, oxidized and total ascorbate content in plants. *Nat Protoc* **2**: 871–874
- Giordani C, Cecchi S, Zanchi C** (2005) Phytoremediation of soil polluted by nickel using agricultural crops. *Environ Manage* **36**: 675–681
- Goldberg T, Hecht M, Hamp T, Karl T, Yachdav G, Ahmed N, Altermann U, Angerer P, Ansonge S, Balasz K** (2014) LocTree3 prediction of localization. *Nucleic Acids Res* **42**: W350–W355
- Gomes-Junior RA, Moldes CA, Delite FS, Gratão PL, Mazzafera P, Lea PJ, Azevedo RA** (2006) Nickel elicits a fast antioxidant response in *Coffea arabica* cells. *Plant Physiol Biochem* **44**: 420–429
- Gore A, Guggenheim D, David L, Bender L, Burns SZ, Skoll J, Chilcott L, Richman B, Cassidy J, Swietlik D, et al** (2006) An Inconvenient Truth. Paramount, CA., United States of America
- Groppa MD, Benavides MP** (2008) Polyamines and abiotic stress: Recent advances. *Amino Acids* **34**: 35–45
- Groppa MD, Benavides MP, Tomaro ML** (2003) Polyamine metabolism in sunflower and wheat leaf discs under cadmium or copper stress. *Plant Sci* **164**: 293–299
- Guerinot M Lou** (2000) The ZIP family of metal transporters. **1465**: 190–198
- Gupta A, Rico-Medina A, Caño-Delgado AI** (2020) The physiology of plant responses to drought. *Science (80-)* **368**: 266 LP – 269
- Gupta K, Dey A, Gupta B** (2013) Plant polyamines in abiotic stress responses. *Acta Physiol Plant* **35**: 2015–2036

- Hajhashemi S, Sofo A** (2018) The effect of polyethylene glycol-induced drought stress on photosynthesis, carbohydrates and cell membrane in *Stevia rebaudiana* grown in greenhouse. *Acta Physiol Plant* **40**: 1–9
- Halliwell B** (2006) Reactive Species and Antioxidants . Redox Biology Is a Fundamental Theme of Aerobic Life. *Plant Heal Prog* **141**: 312–322
- Hanjra MA, Qureshi ME** (2010) Global water crisis and future food security in an era of climate change. *Food Policy* **35**: 365–377
- Hasan MK, Cheng Y, Kanwar MK, Chu XY, Ahammed GJ, Qi ZY** (2017) Responses of plant proteins to heavy metal stress—a review. *Front Plant Sci* **8**: 1–16
- Hasanuzzaman M, Alhaithloul HAS, Parvin K, Bhuyan MHMB, Tanveer M, Mohsin SM, Nahar K, Soliman MH, Al Mahmud J, Fujita M** (2019) Polyamine action under metal/metalloid stress: Regulation of biosynthesis, metabolism, and molecular interactions. *Int J Mol Sci*. doi: 10.3390/ijms20133215
- Hassan FAS, Ali EF, Alamer KH** (2018) Exogenous application of polyamines alleviates water stress-induced oxidative stress of *Rosa damascena* Miller var. *trigintipetala* Dieck. *South African J Bot* **116**: 96–102
- Hatami M, Hadian J, Ghorbanpour M** (2017) Mechanisms underlying toxicity and stimulatory role of single-walled carbon nanotubes in *Hyoscyamus niger* during drought stress simulated by polyethylene glycol. *J Hazard Mater* **324**: 306–320
- Hayat S, Hayat Q, Alyemeni MN, Wani AS, Pichtel J, Ahmad A** (2012) Role of proline under changing environments: A review. *Plant Signal Behav* **7**: 1456–1466
- Heath RL, Packer L** (1968) Photoperoxidation in isolated chloroplasts. *Arch Biochem Biophys* **125**: 189–198
- Herbinger K, Tausz M, Wonisch A, Soja G, Sorger A, Grill D** (2002) Complex interactive effects of drought and ozone stress on the antioxidant defence systems of two wheat cultivars. **40**: 691–696
- Hoekstra AY, Mekonnen MM** (2012) The water footprint of humanity. *Proc Natl Acad Sci U S A* **109**: 3232–3237
- Howe KL, Contreras-Moreira B, De Silva N, Maslen G, Akanni W, Allen J, Alvarez-Jarreta J, Barba M, Bolser DM, Cambell L, et al** (2020) Ensembl Genomes 2020—enabling non-vertebrate genomic research. *Nucleic Acids Res* **48**: D689–D695
- Hussain MM, Saeed A, Khan AA, Javid S, Fatima B** (2015) Differential responses of one hundred tomato genotypes grown under cadmium stress. *Genet Mol Res* **14**: 13162–13171
- Hwang JU, Song WY, Hong D, Ko D, Yamaoka Y, Jang S, Yim S, Lee E, Khare D, Kim K, et al** (2016) Plant ABC Transporters Enable Many Unique Aspects of a Terrestrial Plant's Lifestyle. *Mol Plant* **9**: 338–355
- Iannelli MA, Pietrini F, Fiore L, Petrilli L, Massacci A** (2002) Antioxidant response to cadmium in *Phragmites australis* plants. *Plant Physiol Biochem* **40**: 977–982
- IPCC** (2007) *Climate Change 2007: Impacts, Adaptation and Vulnerability*. Cambridge University Press, Cambridge, UK
- IPCC** (2014) *Climate Change 2014: Impacts, Adaptation, and Vulnerability*. Cambridge University Press
- Jaleel CA, Riadh K, Gopi R, Manivannan P, Inès J, Al-Juburi HJ, Chang-Xing Z, Hong-Bo S, Panneerselvam R** (2009) Antioxidant defense responses: physiological plasticity in higher plants under abiotic constraints. *Acta Physiol Plant* **31**: 427–436
- Jing J, Guo S, Li Y, Li W** (2020) The alleviating effect of exogenous polyamines on heat stress susceptibility of different heat resistant wheat (*Triticum aestivum* L.) varieties. *Sci Rep* **10**:

1–12

- Jones DT, Taylor WR, Thornton JM** (1992) The rapid generation of mutation data matrices from protein sequences. *Bioinformatics* **8**: 275–282
- Joseph B, Jini D** (2011) Development of salt stress-tolerant plants by gene manipulation of antioxidant enzymes. *Asian J Agric Res* **5**: 17–27
- Kamanga RM** (2020) Screening and differential physiological responses of tomato (*Solanum lycopersicum* L.) to drought stress. *Plant Physiol Reports* **25**: 472–482
- Kang J, Park J, Choi H, Burla B, Kretzschmar T, Lee Y, Martinoia E** (2011) Plant ABC Transporters. *Arab B.* doi: 10.1199/tab.0153
- Klein M, Perfus-Barbeoch L, Frelet A, Gaedeke N, Reinhardt D, Mueller-Roeber B, Martinoia E, Forestier C** (2003) The plant multidrug resistance ABC transporter AtMRP5 is involved in guard cell hormonal signalling and water use. *Plant J* **33**: 119–129
- Koussevitzky S, Suzuki N, Huntington S, Armijo L, Sha W, Cortes D, Shulaev V, Mittler R** (2008) Ascorbate Peroxidase 1 Plays a Key Role in the Response of *Arabidopsis thaliana* to Stress Combination. *J Biol Chem* **283**: 34197–34203
- Krämer U, Cotter-Howells JD, Charnock JM, Baker AJM, Smith JAC** (1996) Free histidine as a metal chelator in plants that accumulate nickel. *Nature* **379**: 635–638
- Krämer U, Pickering IJ, Prince RC, Raskin I, Salt DE** (2000) Subcellular localization and speciation of nickel in hyperaccumulator and non-accumulator *Thlaspi* species. *Plant Physiol* **122**: 1343–1353
- Krämer U, Talke IN, Hanikenne M** (2007) Transition metal transport. *FEBS Lett* **581**: 2263–2272
- Kulkarni M, Deshpande U** (2007) In vitro screening of tomato genotypes for drought resistance using polyethylene glycol. *African J Biotechnol* **6**: 691–696
- Kumar H, Sharma D, Kumar V** (2012) Nickel-induced oxidative stress and role of antioxidant defence in Barley roots and leaves. *Int J Environ Biol* **2**: 121–128
- Kumar P, Rouphael Y, Cardarelli M, Colla G** (2015) Effect of nickel and grafting combination on yield, fruit quality, antioxidative enzyme activities, lipid peroxidation, and mineral composition of tomato. *J Plant Nutr Soil Sci* **178**: 848–860
- Kumar PA, Reddy NN, Lakshmi NJ** (2017) PEG Induced Screening for Drought Tolerance in Tomato Genotypes. *Int J Curr Microbiol Appl Sci* **6**: 168–181
- Kumar S, Stecher G, Li M, Knyaz C, Tamura K** (2018) MEGA X: Molecular Evolutionary Genetics Analysis across Computing Platforms. *Mol Biol Evol* **35**: 1547–1549
- Kusano T, Berberich T, Tateda C, Takahashi Y** (2008) Polyamines: Essential factors for growth and survival. *Planta* **228**: 367–381
- de la Peña R, Hughes J** (2007) Improving Vegetable Productivity in a Variable and Changing Climate. *Int Crop Res Inst Semi-Arid Trop* **4**: 1–22
- Laxa M, Liebthal M, Telman W, Chibani K, Dietz K** (2019) The Role of the Plant Antioxidant System in Drought Tolerance. *Antioxidants* **8**: 1–31
- Lee M, Choi Y, Burla B, Kim YY, Jeon B, Maeshima M, Yoo JY, Martinoia E, Lee Y** (2008) The ABC transporter AtABCB14 is a malate importer and modulates stomatal response to CO₂. *Nat Cell Biol* **10**: 1217–1223
- Lešková A, Giehl RFH, Hartmann A, Fargašová A, von Wirén N** (2017) Heavy metals induce iron deficiency responses at different hierarchic and regulatory levels. *Plant Physiol* **174**: 1648–1668
- Li D, Li C, Sun H, Wang W, Liu L, Zhang Y** (2010) Effects of drought on soluble protein

content and protective enzyme system in cotton leaves. **4**: 56–62

- Lichtenthaler HK** (1987) Chlorophylls and Carotenoids: Pigments of Photosynthetic Biomembranes. *Methods Enzymol* **148**: 350–382
- Lipper L, Thornton P, Campbell BM, Baedeker T, Braimoh A, Bwalya M, Caron P, Cattaneo A, Garrity D, Henry K, et al** (2014) Climate-smart agriculture for food security. *Nat Clim Chang* **4**: 1068–1072
- Liu HP, Dong BH, Zhang YY, Liu ZP, Liu YL** (2004) Relationship between osmotic stress and the levels of free, conjugated and bound polyamines in leaves of wheat seedlings. *Plant Sci* **166**: 1261–1267
- Ma T, Duan XH, Yang YY, Yao J, Gao TP** (2017a) Zinc-alleviating effects on iron-induced phytotoxicity in roots of *Triticum aestivum*. *Biol Plant* **61**: 733–740
- Ma Y, Rajkumar M, Zhang C, Freitas H** (2017b) Serpentine endophytic bacterium *Pseudomonas azotoformans* ASS1 accelerates phytoremediation of soil metals under drought stress. *Chemosphere* **185**: 75–85
- Madhava Rao K V., Sresty TVS** (2000) Antioxidative parameters in the seedlings of pigeonpea (*Cajanus cajan* (L.) Millspaugh) in response to Zn and Ni stresses. *Plant Sci* **157**: 113–128
- Maggio A, Saccardo F** (2008) Functional biology of abiotic stress tolerance in tomato. *Acta Hort* **789**: 75–86
- Maksimović I, Kastori R, Krstić L, Luković J** (2007) Steady presence of cadmium and nickel affects root anatomy, accumulation and distribution of essential ions in maize seedlings. *Biol Plant* **51**: 589–592
- Marschner H** (2012) *Marschner's Mineral Nutrition of Higher Plants*, 3rd ed. Academic Press, San Diego, CA
- Martinoia E** (2018) Vacuolar transporters – Companions on a longtime journey. *Plant Physiol* **176**: 1384–1407
- Martinoia E, Maeshima M, Neuhaus HE** (2007) Vacuolar transporters and their essential role in plant metabolism. *J Exp Bot* **58**: 83–102
- Martins V, Bassil E, Hanana M, Blumwald E, Gerós H** (2014a) Copper homeostasis in grapevine: Functional characterization of the *Vitis vinifera* copper transporter 1. *Planta* **240**: 91–101
- Martins V, Teixeira A, Bassil E, Hanana M, Blumwald E, Gerós H** (2014b) Copper-based fungicide Bordeaux mixture regulates the expression of *Vitis vinifera* copper transporters. *Aust J Grape Wine Res* **20**: 451–458
- Mäser P, Thomine S, Schroeder JI, Ward JM, Hirschi K, Sze H, Talke IN, Amtmann A, Maathuis FJM, Sanders D, et al** (2001) Phylogenetic relationships within cation transporter families of *Arabidopsis*. *Plant Physiol* **126**: 1646–1667
- Mathialagan T, Viraraghavan T** (2002) Adsorption of cadmium from aqueous solutions by perlite. *J Hazard Mater* **94**: 291–303
- Mei H, Cheng NH, Zhao J, Park S, Escareno RA, Pittman JK, Hirschi KD** (2009) Root development under metal stress in *Arabidopsis thaliana* requires the H⁺ / cation antiporter CAX4. *New Phytol* **183**: 95–105
- Meng S, Zhang C, Su L, Li Y, Zhao Z** (2016) Nitrogen uptake and metabolism of *Populus simonii* in response to PEG-induced drought stress. *Environ Exp Bot* **123**: 78–87
- Merlot S, Hannibal L, Martins S, Martinelli L, Amir H, Lebrun M** (2014) The metal transporter PglREG1 from the hyperaccumulator *Psychotria gabriellae* is a candidate gene for nickel tolerance and accumulation. **65**: 1551–1564
- Mersha F, Leta A** (2019) *Climate Change and Its Impact on Agricultural Production* : An

Empirical Review from Sub-Saharan African Perspective. *J Agric Econ Rural Dev* **5**: 627–633

- Mignolet-Spruyt L, Xu E, Idänheimo N, Hoerberichts FA, Mühlenbock P, Brosche M, Van Breusegem F, Kangasjärvi J** (2016) Spreading the news: Subcellular and organellar reactive oxygen species production and signalling. *J Exp Bot* **67**: 3831–3844
- Miller G, Suzuki N, Ciftci-Yilmaz S, Mittler R** (2010) Reactive oxygen species homeostasis and signalling during drought and salinity stresses. *Plant, Cell Environ* **33**: 453–467
- Minhas PS, Rane J, Pasala RK** (2017) Abiotic Stress Management for Resilient Agriculture. *Abiotic Stress Manag Resilient Agric* 1–517
- Minocha R, Majumdar R, Minocha SC** (2014) Polyamines and abiotic stress in plants: A complex relationship. *Front Plant Sci* **5**: 1–17
- Mittler R** (2006) Abiotic stress, the field environment and stress combination. *Trends Plant Sci* **11**: 15–19
- Mittler R** (2017) ROS Are Good. *Trends Plant Sci* **22**: 11–19
- Mittler R** (2002) Oxidative stress, antioxidants and stress tolerance. *Trends Plant Sci* **7**: 405–410
- Mittler R, Vanderauwera S, Suzuki N, Miller G, Tognetti VB, Vandepoele K, Gollery M, Shulaev V, Van Breusegem F** (2011) ROS signaling: The new wave? *Trends Plant Sci* **16**: 300–309
- Morrissey J, Baxter IR, Lee J, Li L, Lahner B, Grotz N, Kaplan J, Salt DE, Lou M** (2009) The Ferroportin Metal Efflux Proteins Function in Iron and Cobalt Homeostasis in Arabidopsis. *21*: 3326–3338
- Mozafari H, Asrar Z, Rezanejad F, Pourseyedi S** (2013) Calcium and L-histidine interaction on growth improvement of three tomato cultivars under nickel stress. **57**: 131–144
- Munné-Bosch S, Alegre L** (2003) Drought-induced changes in the redox state of α -tocopherol, ascorbate, and the diterpene carnosic acid in chloroplasts of Labiatae species differing in carnosic acid contents. *Plant Physiol* **131**: 1816–1825
- Munné-Bosch S, Alegre L** (2002) The Function of Tocopherols and Tocotrienols in Plants The Function of Tocopherols and Tocotrienols in. *CRC Crit Rev Plant Sci* **21**: 31–57
- Murshed R, Lopez-Lauri F, Sallanon H** (2008) Microplate quantification of enzymes of the plant ascorbate-glutathione cycle. *Anal Biochem* **383**: 320–322
- Nagajyoti PC, Lee KD, Sreekanth TVM** (2010) Heavy metals, occurrence and toxicity for plants: A review. *Environ Chem Lett* **8**: 199–216
- Nasibi F, Heidari T, Asrar Z, Mansoori H** (2013) Effect of arginine pre-treatment on nickel accumulation and alleviation of the oxidative stress in *Hyoscyamus niger*. *J Soil Sci Plant Nutr* **13**: 680–689
- Nazir F, Salim R, Hameed O Bin** (2017) Effect of Climate Change on Food Safety and Quality : A Review. *Int. J. Adv. Res. Sceince Eng.* **06**:
- Nguyen TPL, Mula L, Cortignani R, Seddaiu G, Dono G, Viridis SGP, Pasqui M, Roggero PP** (2016) Perceptions of Present and Future Climate Change Impacts on Water Availability for Agricultural Systems in the Western Mediterranean Region. *Water*. doi: 10.3390/w8110523
- Nishida S, Aisu A, Mizuno T** (2012) Induction of IRT1 by the nickel-induced iron-deficient response in Arabidopsis. *Plant Signal Behav* **7**: 1–4
- Ofori PA, Mizuno A, Suzuki M, Martinoia E, Reuscher S, Aoki K, Shibata D, Otagaki S, Matsumoto S, Shiratake K** (2018) Genome-wide analysis of ATP binding cassette (ABC) transporters in tomato. *PLoS One* **13**: 1–26

- Olesen JE, Trnka M, Kersebaum KC, Skjelvåg AO, Seguin B, Peltonen-Sainio P, Rossi F, Kozyra J, Micale F** (2011) Impacts and adaptation of European crop production systems to climate change. *Eur J Agron* **34**: 96–112
- Osmolovskaya N, Shumilina J, Kim A, Didio A, Grishina T, Bilova T, Keltsieva OA, Zhukov V, Tikhonovich I, Tarakhovskaya E, et al** (2018) Methodology of drought stress research: Experimental setup and physiological characterization. *Int J Mol Sci*. doi: 10.3390/ijms19124089
- Pál M, Tajti J, Szalai G, Peeva V, Végh B, Janda T** (2018) Interaction of polyamines, abscisic acid and proline under osmotic stress in the leaves of wheat plants. *Sci Rep* **8**: 1–12
- Palacios G, Gómez I, Carbonell-Barrachina A, Navarro Pedreño J, Mataix J** (1998) Effect of nickel concentration on tomato plant nutrition and dry matter yield. *J Plant Nutr* **21**: 2179–2191
- Pandey P, Ramegowda V, Senthil-kumar M** (2015) Shared and unique responses of plants to multiple individual stresses and stress combinations : physiological and molecular mechanisms. *Front Plnt Sci* **6**: 1–14
- Pang K, Li Y, Liu M, Meng Z, Yu Y** (2013) Inventory and general analysis of the ATP-binding cassette (ABC) gene superfamily in maize (*Zea mays* L .). *Gene* **526**: 411–428
- Parida BK, Chhibba IM, Nayyar VK** (2003) Influence of nickel-contaminated soils on fenugreek (*Trigonella corniculata* L.) growth and mineral composition. *Sci Hortic (Amsterdam)* **98**: 113–119
- Pathak S** (2018) Polyamines: the curtailment of cadmium toxicity in plants. *Adv Plants Agric Res* **8**: 472–474
- Paul S, Banerjee A, Roychoudhury A** (2018) Role of Polyamines in Mediating Antioxidant Defense and Epigenetic Regulation in Plants Exposed to Heavy Metal Toxicity. *In M Hasanuzzaman, ed, Plants Under Met. Met. Stress*. Springer Nature Singapore Pte Ltd., pp 229–247
- Persans MW, Nieman K, Salt DE** (2001) Functional activity and role of cation-efflux family members in Ni hyperaccumulation in *Thlaspi goesingense*. *Proc Natl Acad Sci U S A* **98**: 9995–10000
- Pietrini F, Iori V, Cheremisina A, Shevyakova NI, Radyukina N, Kuznetsov V V., Zacchini M** (2015) Evaluation of nickel tolerance in amaranthus paniculatus | Plants by measuring photosynthesis oxidative status antioxidative response and metal-binding molecule content. *Environ Sci Pollut Res* **22**: 482–494
- Pittman JK, Bonza MC, De Michelis MI** (2011) Ca²⁺ Pumps and Ca²⁺ Antiporters in Plant Development. *In M Geisler, K Venema, eds, Transp. Pumps Plant Signaling, Signal. Commun. Plants*, 7th ed. pp 39–64
- Pittman JK, Hirschi KD** (2016) CAX-ing a wide net: Cation/H(+) transporters in metal remediation and abiotic stress signalling. *Plant Biol (Stuttg)* **18**: 741–749
- Plieth C, Gao D, Knight MR, Trewavas AJ, Sattelmacher B** (2007) Self-reporting Arabidopsis thaliana expressing pH- and [Ca²⁺]-indicators unveil apoplastic ion dynamics. *In B Sattelmacher, WJ Horst, eds, Apoplast High. Plants Compart. Storage, Transp. React. Significance Apoplast Miner. Nutr. High. Plants*. Springer, Hannover, Germany, pp 373–394
- Radhouane L** (2007) Response of Tunisian autochthonous pearl millet (*Pennisetum glaucum* (L.) R. Br.) to drought stress induced by polyethylene glycol (PEG) 6000. *African J Biotechnol* **6**: 1102–1105
- Ragab R, Prudhomme C** (2002) Climate change and water resources management in arid and semi-arid regions: Prospective and challenges for the 21st century. *Biosyst Eng* **81**: 3–34
- Rahman H, Sabreen S, Alam S, Kawai S** (2005) Effects of nickel on growth and composition of

- metal micronutrients in barley plants grown in nutrient solution. *J Plant Nutr* **28**: 393–404
- Rangan P, Subramani R, Kumar R, Singh AK, Singh R** (2014) Recent advances in polyamine metabolism and abiotic stress tolerance. *Biomed Res Int*. doi: 10.1155/2014/239621
- Rasmussen S, Barah P, Suarez-Rodriguez MC, Bressendorff S, Friis P, Costantino P, Bones AM, Nielsen HB, Mundy J** (2013) Transcriptome responses to combinations of stresses in *Arabidopsis*. *Plant Physiol* **161**: 1783–1794
- Rees DC, Johnson E, Lewinson O** (2009) ABC transporters: the power to change. *Nat Rev Mol Cell Biol* **10**: 218–227
- Rejeb I Ben, Pastor V, Mauch-Mani B** (2014) Plant responses to simultaneous biotic and abiotic stress: Molecular mechanisms. *Plants* **3**: 458–475
- Ricachenevsky FK, Menguer PK, Sperotto RA, Williams LE, Gong J, Institutes S** (2013) Roles of plant metal tolerance proteins (MTP) in metal storage and potential use in biofortification strategies. *Front Plant Sci* **4**: 1–16
- Rivero RM, Mestre TC, Mittler R, Rubio F, Garcia-Sanchez F, Martinez V** (2014) The combined effect of salinity and heat reveals a specific physiological, biochemical and molecular response in tomato plants. *Plant, Cell Environ* **37**: 1059–1073
- Rizhsky L, Liang H, Mittler R** (2002) The combined effect of drought stress and heat shock on gene expression in tobacco. *Plant Physiol* **130**: 1143–1151
- Rizhsky L, Liang H, Shuman J, Shulaev V, Davletova S, Mittler R** (2004) When Defense Pathways Collide. The Response of *Arabidopsis* to a Combination of Drought and Heat Stress. *Plant Physiol* **134**: 1683–1696
- Rosenzweig C, Iglesias A, Yang XB, Epstein PR, Chivian E** (2001) Climate change and extreme weather events Implications for food production, plant diseases, and pests. *Glob Chang Hum Heal* **2**: 90–104
- Rucińska-Sobkowiak R** (2016) Water relations in plants subjected to heavy metal stresses. *Acta Physiol Plant*. doi: 10.1007/s11738-016-2277-5
- Sachan P, Lal N** (2017) An Overview of Nickel (Ni²⁺) Essentiality, Toxicity and Tolerance Strategies in Plants. *Asian J Biol* **2**: 1–15
- Sachan P, Lal N** (2019) Molecular Mechanisms of Nickel (Ni²⁺) Homeostasis in Plants: Uptake, Tolerance and Hyperaccumulation. *Environ. Toxicol. Bioremediation*. pp 178–196
- Safriel U, Adeel Z** (2005) Ecosystems and human well-being: Current State and Trends, Chapter 22: Dryland Systems. *Ecosyst Hum Well-Being Curr State Trends Find Cond Trends Work Gr* 625–662
- Saint-Claire PM** (1976) Germination of *Sorghum Bicolor* Under Polyethylene Glycol-Induced Stress. *Can J Plant Sci* **56**: 21–24
- Saito A, Saito M, Ichikawa Y, Yoshiba M, Tadano T, Miwa E, Higuchi K** (2010) Difference in the distribution and speciation of cellular nickel between nickel-tolerant and non-tolerant *Nicotiana tabacum* L. cv. BY-2 cells. *Plant, Cell Environ* **33**: 174–187
- Salehi Eskandari B, Ghaderian SM, Schat H** (2017) The role of nickel (Ni) and drought in serpentine adaptation: contrasting effects of Ni on osmoprotectants and oxidative stress markers in the serpentine endemic, *Cleome heratensis*, and the related non-serpentinophyte, *Cleome foliolosa*. *Plant Soil* **417**: 183–195
- Sánchez-Rodríguez E, Romero L, Ruiz JM** (2016) Accumulation on free polyamines enhanced antioxidant response in fruit of grafting tomato plants under water stress. *J Plant Physiol* **190**: 72–78
- Sánchez-Rodríguez E, Rubio-Wilhelmi Mm, Cervilla LM, Blasco B, Rios JJ, Rosales MA, Romero L, Ruiz JM** (2010) Genotypic differences in some physiological parameters symptomatic for oxidative stress under moderate drought in tomato plants. *Plant Sci* **178**:

30–40

- Sari A, Tuzen M, Citak D, Soylak M** (2007) Adsorption characteristics of Cu(II) and Pb(II) onto expanded perlite from aqueous solution. *J Hazard Mater* **148**: 387–394
- Savvides A, Ali S, Tester M, Fotopoulos V** (2016) Chemical Priming of Plants Against Multiple Abiotic Stresses: Mission Possible? *Trends Plant Sci* **21**: 329–340
- Schaaf G, Honsbein A, Meda AR, Kirchner S, Wipf D, Wire N Von** (2006) AtIREG2 Encodes a Tonoplast Transport Protein Involved in Iron-dependent Nickel Detoxification in *Arabidopsis thaliana* Roots. *J Biol Chem* **281**: 25532–25540
- Seregin I V., Kozhevnikova AD** (2006) Physiological role of nickel and its toxic effects on higher plants. *Russ J Plant Physiol* **53**: 257–277
- Sethy SK, Ghosh S** (2013) Effect of heavy metals on germination of seeds. *J Nat Sci Biol Med* **4**: 272–275
- Shah K, Nongkynrih JM** (2007) Metal hyperaccumulation and bioremediation. *Biol Plant* **51**: 618–634
- Shahid MA, Balal RM, Khan N, Rossi L, Rathinasabapathi B, Liu G, Khan J, Cámara-Zapata JM, Martínez-Nicolas JJ, García-Sánchez F** (2018) Polyamines provide new insights into the biochemical basis of Cr-tolerance in Kinnow mandarin grafted on diploid and double-diploid rootstocks. *Environ Exp Bot* **156**: 248–260
- Shamim F, Saqlan SM, Athar H, Waheed A** (2014) Screening and selection of tomato genotypes / cultivars for drought tolerance using multivariate analysis. **46**: 1165–1178
- Sharma P, Jha AB, Dubey RS, Pessarakli M** (2012) Reactive Oxygen Species, Oxidative Damage, and Antioxidative Defense Mechanism in Plants under Stressful Conditions. *J Bot* **2012**: 1–26
- Sharma SS, Dietz K** (2006) The significance of amino acids and amino acid-derived molecules in plant responses and adaptation to heavy metal stress. *J Exp Bot* **57**: 711–726
- Shevyakova NI, Il'ina EN, Kuznetsov V V.** (2008) Polyamines increase plant potential for phytoremediation of soils polluted with heavy metals. *Dokl Biol Sci* **423**: 457–460
- Shigaki T, Pittman JK, Hirschi KD** (2003) Manganese specificity determinants in the *Arabidopsis* metal/H⁺ antiporter CAX2. *J Biol Chem* **278**: 6610–6617
- Shimada T, Takagi J, Ichino T, Shirakawa M, Hara-Nishimura I** (2018) Plant Vacuoles. *Annu Rev Plant Biol*. doi: 10.1146/annurev-arplant-042817-040508
- Silber A, Bar-Yosef B, Suryano S, Levkovitch I** (2012) Zinc adsorption by perlite: Effects of pH, ionic strength, temperature, and pre-use as growth substrate. *Geoderma* **170**: 159–167
- de Silva NDG, Cholewa E, Ryser P** (2012) Effects of combined drought and heavy metal stresses on methylation and chromatin patterning xylem structure and hydraulic conductivity in red maple (*Acer rubrum* L.). *J Exp Bot* **63**: 5957–5966
- Smirnoff N, Sciences B, Laboratories H, Road W** (1996) The Function and Metabolism of Ascorbic Acid in Plants. 661–669
- Smith P, Gregory PJ** (2013) Climate change and sustainable food production. *Proc. Nutr. Soc. Aberdeen*, pp 21–22
- Soares C, Branco-Neves S, de Sousa A, Pereira R, Fidalgo F** (2016a) Ecotoxicological relevance of nano-NiO and acetaminophen to *Hordeum vulgare* L.: Combining standardized procedures and physiological endpoints. *Chemosphere* **165**: 442–452
- Soares C, Carvalho MEA, Azevedo RA, Fidalgo F** (2019a) Plants facing oxidative challenges—A little help from the antioxidant networks. *Environ Exp Bot* **161**: 4–25

- Soares C, Cunha A, Soares C, Branco-neves S, Sousa A De, Azenha M, Cunha A** (2018) SiO₂ nanomaterial as a tool to improve *Hordeum vulgare* L. tolerance to nano-NiO stress. *Science of the Total Environment* SiO₂ nanomaterial as a tool to improve *Hordeum vulgare* L. tolerance to nano-NiO stress. *Sci Total Environ.* doi: 10.1016/j.scitotenv.2017.12.002
- Soares C, Pereira R, Spormann S, Fidalgo F** (2019b) Is soil contamination by a glyphosate commercial formulation truly harmless to non-target plants? – Evaluation of oxidative damage and antioxidant responses in tomato. *Environ Pollut* **247**: 256–265
- Soares C, de Sousa A, Pinto A, Azenha M, Teixeira J, Azevedo RA, Fidalgo F** (2016b) Effect of 24-epibrassinolide on ROS content, antioxidant system, lipid peroxidation and Ni uptake in *Solanum nigrum* L. under Ni stress. *Environ Exp Bot* **122**: 115–125
- Soltani Maivan E, Radjabian T, Abrishamchi P, Talei D** (2017) Physiological and biochemical responses of *Melissa officinalis* L. to nickel stress and the protective role of salicylic acid. *Arch Agron Soil Sci* **63**: 330–343
- Stevens F, DiCaprio L, Davidoski T, Killoran JD, Ratner B, Packer J, Monroe M** (2016) *Before the Flood*. Twentieth Century Fox Home Entertainment, Inc., CA., United States of America
- Stocker TF, Clarke GKC, Le Treut H, Lindzen RS, Meleshko VP, Mugara RK, Palmer TN, Pierrehumbert RT, Sellers PJ, Trenberth KE, et al** (2001) Physical Climate Processes and Feedbacks. *Clim. Chang.* 2001 Sci. Bases. Contrib. Work. Gr. I to Third Assess. Rep. Intergov. Panel Clim. Chang. p 881
- Suzuki N, Rivero RM, Shulaev V, Blumwald E, Mittler R** (2014) Abiotic and biotic stress combinations. *New Phytol* **203**: 32–43
- Tahi H, Wahbi S, El Modafar C, Aganchich A, Serraj R** (2008) Changes in antioxidant activities and phenol content in tomato plants subjected to partial root drying and regulated deficit irrigation. *Plant Biosyst* **142**: 550–562
- Taiz L, Zeiger E** (2012) *Responses and Adaptations to Abiotic Stress*. *Plant Physiol.*, Fifth Edit. Sinauer Associates Inc., pp 755–778
- Taiz L, Zeiger E, Møller IM, Murphy A** (2014) *Plant Physiology and Development*. Sinauer
- Tajti J, Janda T, Majláth I, Szalai G, Pál M** (2018) Comparative study on the effects of putrescine and spermidine pre-treatment on cadmium stress in wheat. *Ecotoxicol Environ Saf* **148**: 546–554
- Take E, Hofstrand D** (2015) Global warming - impact of climate change on global agriculture. *Ag Decis. Mak. Newsl.* 12:
- The UniProt Consortium** (2019) UniProt: a worldwide hub of protein knowledge. *Nucleic Acids Res* **47**: D506–D515
- Todorova D, Katerova Z, Sergiev I, Alexieva V** (2014) Polyamines - involvement in plant stress tolerance and adaptation. *Plant Adapt to Environ Chang significance Amin acids their Deriv* 194–221
- La Torre GL, Saitta M, Giorgia Potorti A, Di Bella G, Dugo G** (2010) High performance liquid chromatography coupled with atmospheric pressure chemical ionization mass spectrometry for sensitive determination of bioactive amines in donkey milk. *J Chromatogr A* **1217**: 5215–5224
- Treviño MB, O'Connell MAO** (1998) Three Drought-Responsive Members of the Nonspecific Lipid-Transfer Protein Gene Family in *Lycopersicon pennellii* Show Different Developmental Patterns of Expression. *Plant Physiol* **116**: 1461–1468
- Tsaniklidis G, Pappi P, Tsafouros A, Charova SN, Nikoloudakis N, Roussos PA, Paschalidis KA, Delis C** (2020) Polyamine homeostasis in tomato biotic/abiotic stress cross-tolerance. *Gene* **727**: 144230

- Türkan I, Bor M, Özdemir F, Koca H** (2005) Differential responses of lipid peroxidation and antioxidants in the leaves of drought-tolerant *P. acutifolius* Gray and drought-sensitive *P. vulgare* L. subjected to polyethylene glycol mediated water stress. *Plant Sci* **168**: 223–231
- Ünyayar S, Keles Y, Cekic F** (2005) The antioxidative response of two tomato species with different drought tolerances as a result of drought and cadmium stress combinations. *Plant Soil Environm* 57–64
- Uruç Parlak K** (2016) Effect of nickel on growth and biochemical characteristics of wheat (*Triticum aestivum* L.) seedlings. *NJAS - Wageningen J Life Sci* **76**: 1–5
- Verma G, Srivastava D, Tiwari P, Chakrabarty D** (2019) ROS Modulation in Crop Plants Under Drought Stress. *React Oxyg Nitrogen Sulfur Species Plants* **1**: 311–336
- Verslues PE, Ober ES, Sharp RE** (1998) Root Growth and Oxygen Relations at Low Water Potentials. Impact of Oxygen Availability in Polyethylene Glycol Solutions. *Plant Physiol* **116**: 1403–1412
- Vinocur B, Altman A** (2005) Recent advances in engineering plant tolerance to abiotic stress: Achievements and limitations. *Curr Opin Biotechnol* **16**: 123–132
- Wang H, Liang W, Huang J** (2013) Putrescine mediates aluminum tolerance in red kidney bean by modulating aluminum-induced oxidative stress. *Crop Sci* **53**: 2120–2128
- Wang S, Wei M, Cheng H, Wu B, Du D, Wang C** (2020) Indigenous plant species and invasive alien species tend to diverge functionally under heavy metal pollution and drought stress. *Ecotoxicol Environ Saf* **205**: 111160
- Wang W, Paschalidis K, Feng JC, Song J, Liu JH** (2019) Polyamine catabolism in plants: A universal process with diverse functions. *Front Plant Sci*. doi: 10.3389/fpls.2019.00561
- Wang X, Shi G, Xu Q, Hu J** (2007) Exogenous polyamines enhance copper tolerance of *Nymphoides peltatum*. *J Plant Physiol* **164**: 1062–1070
- Wassmann R, Jagadish SVK, Sumfleth K, Pathak H, Howell G, Ismail A, Serraj R, Redona E, Singh RK, Heuer S** (2009) Chapter 3 Regional Vulnerability of Climate Change Impacts on Asian Rice Production and Scope for Adaptation. *Adv Agron*. doi: 10.1016/S0065-2113(09)01003-7
- Wechsler M, Speicher A** (2016) Sustainable. Hourglass Films LLC, IL., United States of America
- Yang H, Shi G, Wang H, Xu Q** (2010) Involvement of polyamines in adaptation of *Potamogeton crispus* L. to cadmium stress. *Aquat Toxicol* **100**: 282–288
- Yokosho K, Yamaji N, Mitani-ueno N, Shen RF, Ma JF** (2016) An Aluminum-Inducible IREG Gene is Required for Internal Detoxification of Aluminum in Buckwheat. **57**: 1169–1178
- Yordanov I, Velikova V, Tsonev T** (2000) Plant responses to drought, acclimation, and stress tolerance. *Photosynthetica* **38**: 171–186
- Yu Y, Zhou W, Zhou K, Liu W, Liang X, Chen Y, Sun D, Lin X** (2018) Polyamines modulate aluminum-induced oxidative stress differently by inducing or reducing H₂O₂ production in wheat. *Chemosphere* **212**: 645–653
- Yu Z, Jia D, Liu T** (2019) Polyamine Oxidases Play Various Roles in Plant Development and Abiotic Stress Tolerance. *Plants* **8**: 184
- Yusuf M, Fariduddin Q, Hayat S, Ahmad A** (2011) Nickel: An overview of uptake, essentiality and toxicity in plants. *Bull Environ Contam Toxicol* **86**: 1–17
- Zamir D** (2001) Improving plant breeding with exotic genetic libraries. *Nat Rev Genet* **2**: 983–989
- Zandalinas SI, Mittler R, Balfagón D, Arbona V, Gómez-Cadenas A** (2018) Plant adaptations to the combination of drought and high temperatures. *Physiol Plant* **162**: 2–12

- Zgallaï H, Steppe K, Lemeur R** (2005) Photosynthetic, physiological and biochemical responses of tomato plants to polyethylene glycol-induced water deficit. *J Integr Plant Biol* **47**: 1470–1478
- Zhang S, Fan X, Fu Y, Wang Q, McAvoy E, Seal DR** (2019) Field Evaluation of Tomato Cultivars for Tolerance to Tomato Chlorotic Spot Tosspovirus. *Plant Heal Prog* **20**: 77–82
- Zhao H, Yang H** (2008) Exogenous polyamines alleviate the lipid peroxidation induced by cadmium chloride stress in *Malus hupehensis* Rehd. *Sci Hortic (Amsterdam)* **116**: 442–447
- Zhao J, Shi G, Yuan Q** (2008) Polyamines content and physiological and biochemical responses to ladder concentration of nickel stress in *Hydrocharis dubia* (Bl.) Backer leaves. *BioMetals* **21**: 665–674
- Zhou R, Kong L, Yu X, Ottosen CO, Zhao T, Jiang F, Wu Z** (2019) Oxidative damage and antioxidant mechanism in tomatoes responding to drought and heat stress. *Acta Physiol Plant* **41**: 0
- Zlobin IE, Ivanov Y V., Kartashov A V., Kuznetsov V V.** (2018) Impact of drought stress induced by polyethylene glycol on growth, water relations and cell viability of Norway spruce seedlings. *Environ Sci Pollut Res* **25**: 8951–8962